

COMPARATIVE ANATOMY OF THE INSECT
TRACHEAL SYSTEM
PART 1: INTRODUCTION, APTERYGOTES,
PALEOPTERA, POLYNEOPTERA

HOLLISTER W. HERHOLD

Richard Gilder Graduate School and Division of Invertebrate Zoology,
American Museum of Natural History, New York

STEVEN R. DAVIS

Division of Invertebrate Zoology, American Museum of Natural History;
Laboratory of Developmental Neurobiology, Kanazawa University, Kanazawa, Japan

SAMUEL P. DEGREY

Kimberly Research and Extension Center, University of Idaho, Kimberly

DAVID A. GRIMALDI

Division of Invertebrate Zoology, American Museum of Natural History, New York

BULLETIN OF THE AMERICAN MUSEUM OF NATURAL HISTORY

Number 459, 184 pp., 127 figures, 5 tables, 78 plates

Issued March 10, 2023

CONTENTS

Abstract.....	4
Introduction.....	4
History of Tracheal Research.....	5
Tracheae of Individual Species.....	7
Insect Respiration – A Shift in Thinking.....	10
Micro-CT Scanning for Insect Morphology.....	11
Goals of This Study.....	13
The Complexity of Insect Breathing.....	14
Methods and Materials.....	15
Specimen Collection and Storage.....	15
Specimen Selection and Taxonomic Coverage.....	16
Micro-CT Scanning – Techniques and Parameters.....	16
Volume Reconstruction, Postprocessing, Segmentation, and Visualization.....	17
Tracheal Nomenclature.....	21
Homology.....	23
A Uniform Tracheal Nomenclature System.....	23
Results.....	27
Tracheal Visualizations.....	27
Availability of Digital Data.....	27
Class Insecta.....	28
Order Archaeognatha.....	28
Family Machilidae.....	28
Order Zygentoma.....	31
Family Lepidotrichidae.....	33
Family Lepismatidae.....	38
Order Ephemeroptera.....	41
Family Ephemeridae.....	45
Family Baetidae.....	45
Order Odonata.....	47
Family Aeshnidae.....	52
Family Calopterygidae.....	54
Order Zoraptera.....	62
Family Zorotypidae.....	62
Order Dermaptera.....	62
Family Anisolabididae.....	69
Family Forficulidae.....	70
Order Plecoptera.....	77
Family Perlodidae.....	80
Family Nemouridae.....	83
Order Orthoptera.....	86
Family Gryllidae.....	88
Family Romaleidae.....	94
Family Raphidophoridae.....	94
Family Tettigoniidae.....	99

Order Grylloblattodea	102
Family Grylloblattidae	102
Order Embioptera	108
Family Oligotomidae	108
Order Phasmatodea	113
Family Timematidae	113
Family Phasmatidae	121
Superorder Dictyoptera	129
Order Mantodea	129
Family Mantidae	133
Family Empusidae	134
Order Blattodea	134
Family Blattidae	136
Family Blaberidae	142
Infraorder Isoptera	143
Family Archotermopsidae	143
Family Rhinotermitidae	151
Discussion	153
Phylogenetic Patterns	153
Longitudinal Connections	154
Wing-leg Tracheae and Chapman's Triangle	161
Basal Relationships	170
Networked Head Tracheae	172
Homoplasy	172
Flight and Wing Tracheae	172
Weight Relief	173
Auditory Adaptations	174
Differences in Metamorphic Development	175
Other Variations in Tracheal Morphology	175
Conclusions and Future Work	175
Acknowledgments	176
References	176
List of Plates	183

ABSTRACT

A broad comparative study of insect respiratory morphology is presented. Tracheae, epidermal invaginations extending into the body in branching networks of tubes, supply tissues with direct access to air for gas exchange. While previous tracheal studies focused on a handful of taxa and lacked in consistency, here a unified system of tracheal nomenclature is established using visualizations from micro-CT scanning of representatives from apterygotes, Paleoptera, and Polyneoptera, totaling 29 species, 29 genera, and 26 families in 13 insect orders. Three-dimensional visualizations of named tracheal branches establish robust assessments of homology and provide a framework for further studies across class Insecta. Patterns in respiratory architecture are presented along with a discussion of future investigations into phylogenetic and physiological questions.

INTRODUCTION

The respiratory system of terrestrial arthropods is a defining characteristic of this highly successful group. Unlike their aquatic counterparts, who possess external gills, for many terrestrial arthropods their respiratory structures are essentially internal gills, such as the book lungs in certain arachnids and pleopodal “lungs” in oniscoid isopods (Schmidt and Wägele, 2001). The vast majority, however, have tracheae: an intricate network of thin-walled, ectodermally derived, chitinous branching tubules that transport respiratory gases to and from tissues and the surrounding air. Tracheae occur in myriapods (Hilken et al., 2021), some arachnids (Acarì (Richard et al., 1990), Opiliones, Ricinulei, some Araneae), solifuges (Franz-Guess et al., 2016; Franz-Guess and Starck, 2016), and throughout hexapods (Snodgrass, 1935). With a few exceptions (i.e., some Protura, some Collembola, and chironomid larvae with high concentrations of hemoglobin) all insects that have been examined thus far possess tracheae. In fact, because of the widespread occurrence of insects in nearly every terrestrial habitat, it could be said that the majority of all land-dwelling animals use tracheae for respiration.

As the tracheal system has likely been present in insects since their establishment on land, perhaps sometime in the Silurian (Grimaldi and Engel, 2005), it has also been adapted over evolutionary time for a surprising variety of functions. Air sacs, common across a wide range of insects,

are enlarged tracheae (Snodgrass, 1935) and appear to have several functions. Pumping of abdominal air sacs is a form of active ventilation (Weis-Fogh, 1967; Wasserthal, 1996; Harrison et al., 2013; Heinrich et al., 2013) also seen during discontinuous gas exchange (Lighton, 1996). Tracheae themselves have also been shown to be an active component in ventilation via periodic compression (Westneat et al., 2003; Socha et al., 2008; Greenlee et al., 2013; Waters et al., 2013; Pendar et al., 2015; Hochgraf et al., 2018). Air circulation may also be involved in thermoregulation, although it has been shown (at least in bees) that movement of hemolymph may contribute more to heat exchange (Heinrich, 1976).

Tracheae have also been coopted in insects for both hearing and sound production. Ears, typically in the form of a tympanal membrane backed by a tracheal sac and a chordotonal organ, have evolved an astounding 20 times or more in insects (Yager, 1999; Gopfert and Hennig, 2016) in various parts of the body, including the legs of katydids (Rössler, 1992); the abdomen, thorax, and even wings of Lepidoptera (Yager, 1999); and the thorax of mantises (Yager and Hoy, 1987). (It has also been observed that the sides of the insect head are one of the few places where auditory organs are absent.) Likewise, tracheal modifications also form sound-producing structures, most notably (and audibly) in cicadas, the loudest insect known (Nelson, 1979; Fonseca and Popov, 1994). Contact with a tracheal air sac serves to amplify sounds either produced (e.g., a resonance chamber) or received.

Auditory signaling is not the only use of tracheae for communication. Bioluminescence in lampyrids relies on intricate tracheal structures that provide oxygen to the abdominal lantern, one of the most energy-efficient light sources known (Tsai et al., 2014; Dunn et al., 2022).

The ability to fly is perhaps the most significant adaptation to the ecological and evolutionary success of insects. Flight allows vastly increased dispersal and tracking of resources and mates, escape from predators, and opens ecological niches unavailable to ground-dwelling organisms. Air sacs likely provide buoyancy and weight relief (Wigglesworth, 1963), and thoracic (and possibly abdominal) tracheal structures operate as active bellows to increase airflow to the flight motor (Wasserthal et al., 2018), the most metabolically active tissue in the animal kingdom (Klowden, 2013).

The tracheal system is not the only respiratory mode in insects. Certain insects are well known for their use of hemoglobins either in poorly oxygenated environments (e.g., chironomid midges, stomach bot flies), or for buoyancy (e.g., notonectids). But it had long been held that the efficiency of the tracheal system removed the requirement for respiratory proteins. Recent transcriptome-based studies have uncovered insectahemoglobins, a distinctive type of hemoglobin, throughout insects (Burmester and Hankeln, 2007; Herhold et al., 2020). However, not all of these proteins are necessarily respiratory in nature, and further research is needed to uncover specific functions.

HISTORY OF TRACHEAL RESEARCH

First Steps – Optical Microscopy

The works of Aristotle are often cited as some of the first inquiries into the natural history of insects. His insights into insect respiration were based on his observations that insects are highly resistant to asphyxia. It was believed that the purpose of breathing in humans (and animals) was to cool the blood and thereby the heart,

thought to be the source of heat in the body. As insects were seemingly solid in composition, and therefore bloodless (and apparently heartless), they had no need for respiration (Lee, 1929; Weiss, 1929). It was not until the invention of the microscope and essential refinements by van Leeuwenhoek in the 15th century that scientists could undertake investigations of insect anatomy and physiology. Armed with these new tools, 17th-century physician and biologist Marcelo Malpighi made numerous discoveries in insects, including of both tracheae and spiracles, their associated openings in the insect body wall (Malpighi, 1669). Figure 1 is a plate drawn by Malpighi's contemporary, entomologist Jan Swammerdam, sometime in the late 1600s from his famous *Bybel der Natuure*, published posthumously (Swammerdam, 1737). The locations of spiracles and the arrangement of longitudinal tracheal trunks is rendered in detail, along with reproductive structures and the alimentary canal. The study of freshly dissected specimens is facilitated by air in the tracheae, which contrast silvery against other soft internal tissues. Dissections are still very tedious, however, given the delicate nature and intricacy of tracheae, and the fact that they quickly fill with fluid.

Throughout the 19th century, European researchers set the standard for insect morphological research, and of insect respiratory systems as well. In 1836, George Newport produced what for the time was a comprehensive summary of insect respiration, including detailed descriptions not only of tracheae but also their innervation, musculature, and other organs and tissues they serve (Newport, 1836). Newport even included physiological data such as the survival time of insects immersed in various media.

The earliest modern comparative study of insect respiratory morphology was conducted in 1877 by Finnish zoologist Johan Axel Palmén. Although primarily known through his work on birds, Palmén was the first to discuss the differences in tracheal architecture across multiple orders, including Ephemeroptera, Odonata, Diptera, Hymenoptera, Lepidoptera, and Coleoptera

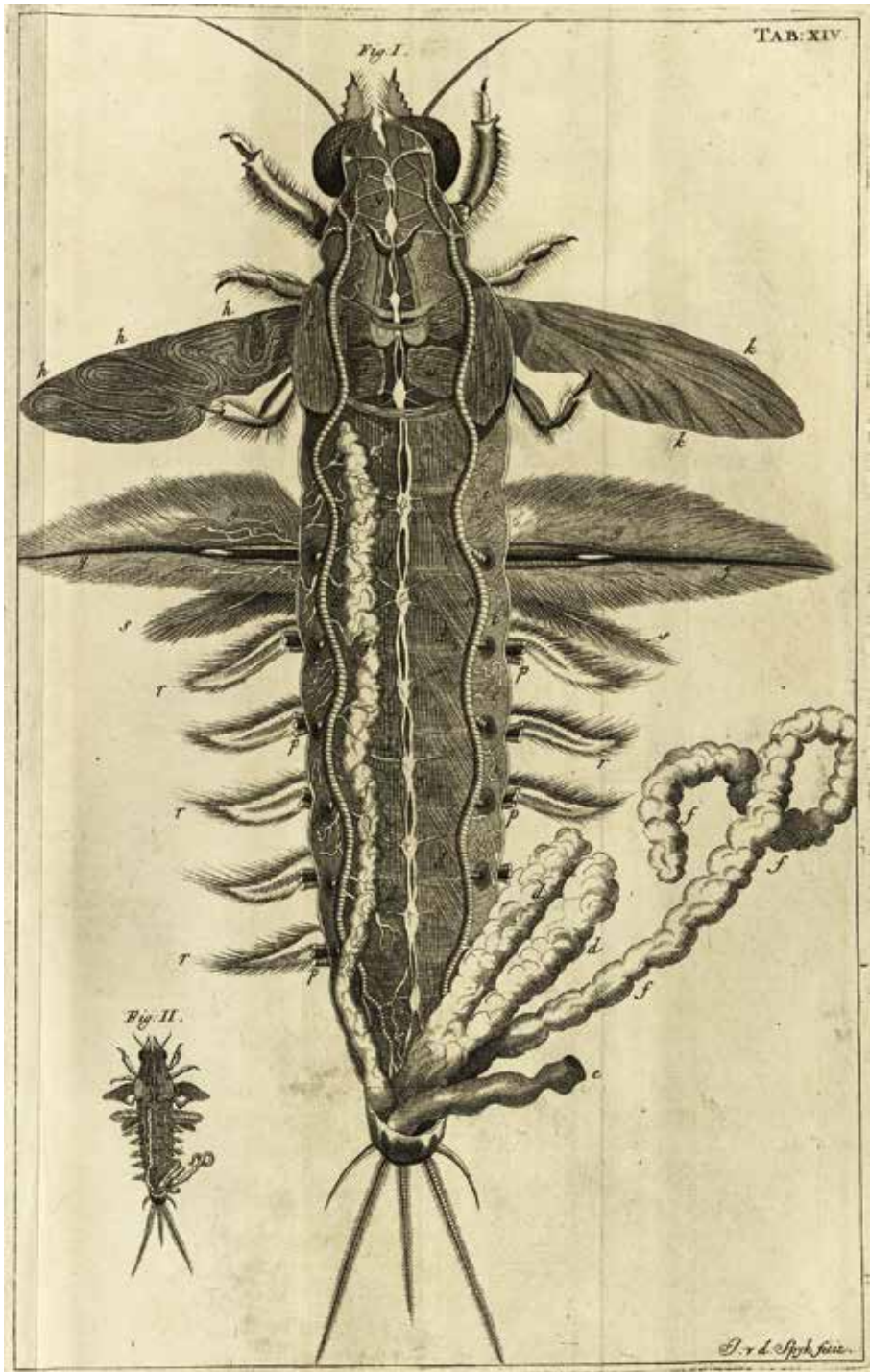


FIGURE 1. Mayfly nymph internal anatomy by Swammerdam, 17th century. Published posthumously (Swammerdam, 1737).

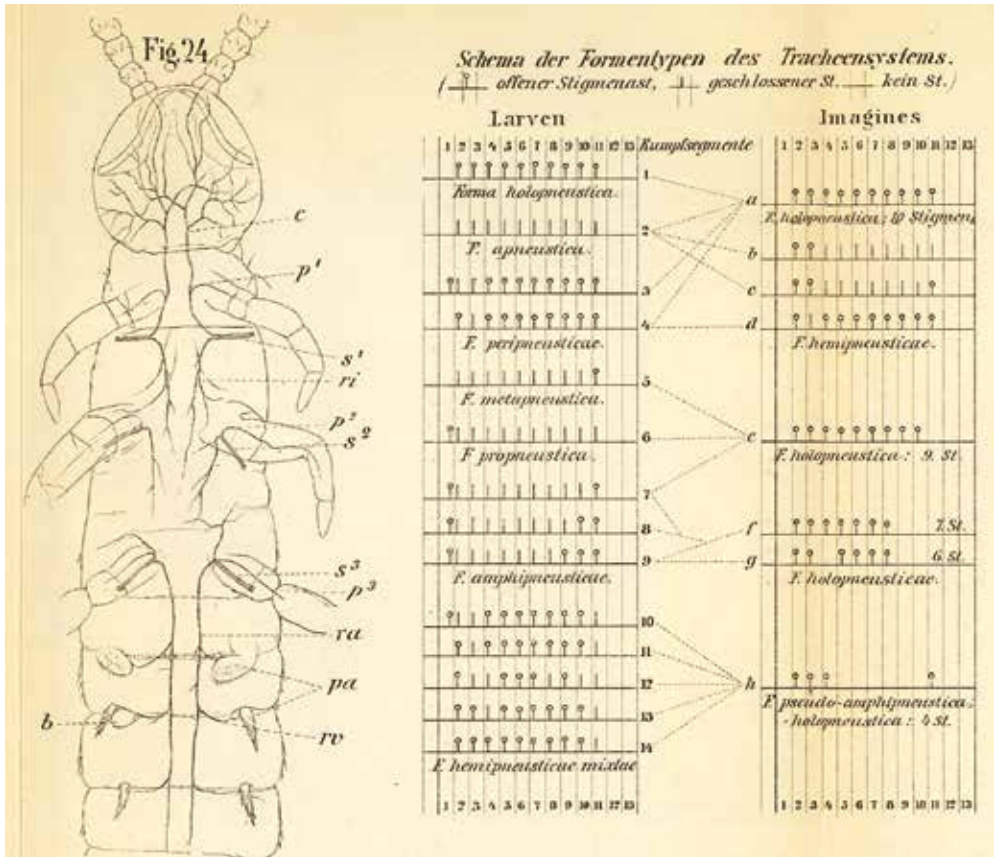


FIGURE 2. Palmén's (1877) "Scheme of the Types and Shapes of the Tracheal System," along with a representative diagram of the dipluran *Campodea fragilis*.

(Palmén, 1877). Figure 2 shows his categorization of different types of tracheal arrangements, sorted by spiracle presence and "pneumatic" arrangements of tracheae.

Giovanni Battista Grassi, in his work on myriapods, hypothesized that the ancestral tracheal system in myriapods and insects consisted of a series of disconnected, but possibly serially homologous segmental regions that later combined into a longitudinally (and laterally) interconnected system (Grassi, 1885; Kennedy, 1922). It should be noted that this hypothesis was based on what was thought to be a close relationship between Myriapoda and Insecta (forming the "Tracheata") that has since been revised. It is now generally agreed that Myriapoda is a sister

group to Crustacea, and that insects are closely related to terrestrial crustaceans (Grimaldi, 2010; Koenemann et al., 2010; Giribet and Edgecombe, 2019).

TRACHEAE OF INDIVIDUAL SPECIES

Owing in part to incremental advances in microscopy, the first part of the 20th century saw work on insect respiratory morphology that became references for decades. The first and perhaps most innovative work was from Karl Šulc, known primarily for his work on scale insects. He introduced an illustration technique where a full outline of the insect is drawn with a vertical dividing line showing the dorsal side on the left

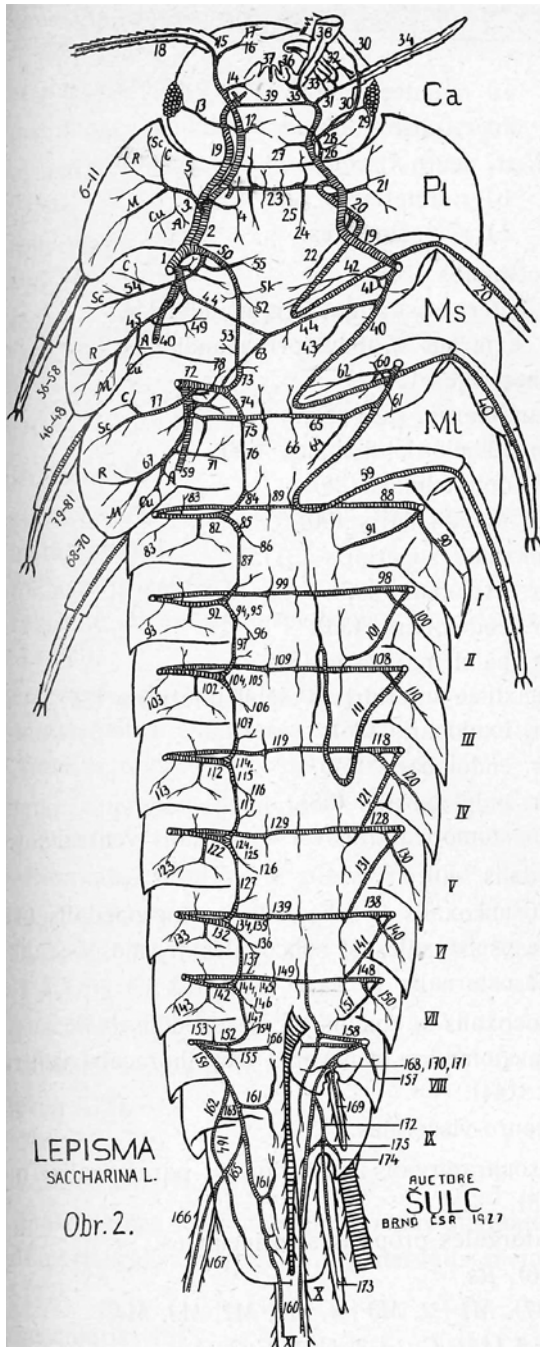


FIGURE 3. Illustration of the tracheal system of *Lepisma saccharina* by Šulc (1927). Note dorsal side on left half and venter on right.

and the venter on the right (Kondo et al., 2008), still a standard technique in scale insect work. His early illustration of the tracheal system of the spittlebug *Philaneus lineatus* (Šulc, 1912) and a more refined diagram of the silverfish *Lepisma saccharina* (Šulc, 1927), shown in figure 3, are both demonstrations of these state-of-the-art visualizations of tracheal anatomy. Around the same time, Willy Alt's 1912 works on *Dytiscus marginalis* diving beetles featured the tracheal system of both larval (Alt, 1912b) and adult (Alt, 1912a) stages. Subsequent works on the tracheal anatomy of individual species or small groups of closely related taxa featured locusts (Vinal, 1919), termites (Fuller, 1919), and stick insect immatures (Lehmann, 1925). Entognaths were not completely ignored in these early investigations: Maldwyn Davies's 1927 study of *Sminthurus viridis* was the first (and remains one of the only) investigations of collembolan tracheae.

Toward the middle of the 20th century, techniques for investigating insect physiology improved, including work on respiration and in particular adaptations for flight. The famed insect physiologist Torkel Weis-Fogh produced a massive body of work regarding flight in locusts (Weis-Fogh, 1956a, 1956b, 1964; Weis-Fogh and Jensen, 1956). Parasitism requires adaptations to survive in a host, and in a fascinating study on dipteran larvae, Keilin (1944) detailed a variety of morphological (tracheae) and molecular (hemoglobins) respiratory adaptations in fly parasites of arthropods, amphibians, and mammals. Vladimír Landa, one of the most prominent researchers of Ephemeroptera, published a comprehensive study of the tracheal architecture of mayfly larvae (Landa, 1948). His colleague Tomáš Soldán investigated changes in *Doliana americana* (Ephemeroptera: Behningiidae) tracheae during development, comparing both naiads and adults (Soldán, 1979). In his 1958 dissertation work, Clyde Sterling Barnhart extensively documented *Lepisma saccharium* anatomy in a study that echoed Šulc from 1927 (Barnhart, 1958, 1961). Beetles, the most speciose order of insects, were also a focus, such as L.K. Vats's (1972) work on

synthetic account, but it lacks an in-depth comparative analysis across many orders.

Comparative studies of respiratory structures were not entirely absent. In addition to studies on specific taxa, researchers also focused on particular body regions, such as R.N. Chapman's (1918) dissertation on the basal connections of tracheae to insect wings. This early comparative study included specific exemplars from Blattodea (termed Orthoptera in 1918), Plecoptera, Neuroptera, Lepidoptera, Hemiptera, Coleoptera, Trichoptera, Ephemeroptera, and Hymenoptera. Clarence Kennedy (1922) and Loren Steiner (1929) attempted to homologize the insect tracheal system using odonates, but, as we demonstrate here, two taxa from a single order are insufficient to accomplish such a task. F. Carpentier (1927) attempted serial homologization of thoracic and abdominal tracheae, work that was ambitious and likely hampered because of the use of only a single taxon, *Phasgonura viridissima* (Orthoptera: Tettigoniidae). In his comprehensive comparative study of Ensifera, Swedish entomologist Kjell Ander (1939) incorporated (and critiqued) much of the literature on respiratory morphology up to that point, including homologies and terminology of Stuart Vinal (1919) (whose work he largely discarded), Kennedy (1922), Carpentier (1927), as well as foundational work by Šulc (1927).

Some of the few comprehensive comparative studies were conducted by Joan M. Whitten in the 1950s through 1970s (Whitten, 1955, 1956, 1957, 1959, 1960, 1962, 1972). Her work on comparative anatomy of larval Diptera was facilitated by the relative ease of observation of major tracheae through the thin cuticle, but this should not diminish the impressive scope of the work involved.

INSECT RESPIRATION – A SHIFT IN THINKING

There are substantial differences between vertebrate and insect respiratory systems. Vertebrate respiratory and circulatory systems are linked, in

that active ventilation of the lungs by muscles is coupled with pumping of red blood cells throughout a closed vascular system to provide respiratory gases and nutrients to organs. The insect respiratory (tracheal) system is not coordinated with the circulatory system, in which organs are surrounded by hemolymph that is not actively circulated. This division, combined with the extension of tracheae deep into the insect body, has led to the impression that partial pressure gradients and simple diffusion were sufficient for respiratory gas exchange. Studies beginning in the mid-20th century focusing on flight physiology only strengthened this line of thought. Insect physiologists such as Weis-Fogh began to compare flying insects with birds, their vertebrate counterparts also highly adapted for flight, to investigate phenomena such as unidirectional airflow and active ventilation of flight musculature (Weis-Fogh, 1964, 1967).

In his 1985 synopsis of the history of insect respiratory research, Müller (1985) chronicled the progression toward a deeper understanding of insect respiration, including the hypothesis that insect respiration was likely not due to simple passive diffusion. Beginning with Aristotle, Müller's review includes a comprehensive summary of insect respiratory study since the advent of microscopy, including the discovery of tracheoles and the beginnings of insect respiratory physiology. Modern insect physiology texts such as those by Chapman (2013) and Klowden (2013) now present insect respiration is a complex process that varies widely across the over two dozen recognized insect orders.

The study of tracheal structures, however, has remained reliant on techniques unchanged for hundreds of years, namely tedious dissection and manual illustration or photography. As noted, this approach has hindered a broad comparative approach. A recent review of apterygote hexapod tracheal systems by Dittrich and Wipfler (2021), for example, relies almost exclusively on methods hundreds of years old. These techniques would soon be augmented, or even replaced, by a superior method—micro-CT scanning.

MICRO-CT SCANNING FOR INSECT MORPHOLOGY

Optical microscopy and dissection remained the primary means of study for insect internal morphology for centuries and is still performed, even for tracheal studies (Strauss, 2021). The development of microcomputed X-ray tomography in the late 20th century (Flannery et al., 1987), however, helped usher in a renaissance in insect morphology (Friedrich and Beutel, 2008). Micrometer-sized anatomical features can be visualized in a nondestructive manner, enabling in situ analysis of internal structures. Micro-CT is particularly useful for determining respiratory structures such as tracheae. As volumetric datasets from micro-CT are three-dimensional grids of X-ray absorbance in the sample, differentiating tissue from air is a relatively straightforward process (Iwan et al., 2015). Micro-CT datasets also allow interactive visualization of 3D structures with a wide array of tools for “virtual dissection,” allowing for more effective study and comparisons of insect internal anatomy, particularly delicate and intricate ones like a tracheal network.

While early development of micro-CT techniques for imaging respiratory structures used specimens from a few orders (Socha and De Carlo, 2008), most micro-CT work to date has primarily focused on a single taxon or a certain group (as was common with research using traditional techniques). Tenebrionid beetles have been used in several of the original CT scan studies, including Kaiser and colleagues’s quantitative methods to compare the tracheal volume (estimated using stereological point counting from 2D projections) in a study of insect gigantism (Kaiser et al., 2007) and Raś and colleagues quantification of *Tenebrio molitor* tracheal volume and architecture across developmental stages (Raś et al., 2018). Live-scanning beetles using high-power X-rays from a synchrotron has shown active ventilation in the passalid beetle *Odontotaenius disjunctus* (Waters et al., 2013), and several studies (Iwan

et al., 2015; Raś et al., 2018; Alba-Tercedor et al., 2019) have detailed the tracheal anatomy of both adult and immature beetles.

Individual species in other orders of insects (and arthropods) have been the subject of micro-CT techniques, including certain flies (Wasserthal et al., 2018), locusts (Harrison et al., 2013; Greco et al., 2014), bees (Greco et al., 2008; Gonzalez et al., 2019; Herhold et al., 2019), and even centipedes (Hilken et al., 2021). Studies have also focused on tracheal compression using high-resolution synchrotron imaging (Westneat et al., 2003), including hypoxia-induced compression (Greenlee et al., 2013); 3D printing of tracheal structures (Greco et al., 2014); quantitative analysis of the distribution of air spaces (Shaha et al., 2013); and even capturing insects during a variety of behaviors (Alba-Tercedor et al., 2021).

The insect flight motor has been studied for decades, and micro-CT analyses are providing new insights into the biomechanics of insect flight. Synchrotron studies enable detailed visualizations of the flight motor in motion (Walker et al., 2014), views of the tracheal system in real-time (Socha et al., 2010; Mokso et al., 2015; Pendar et al., 2015; Pendar et al., 2019), and reveal intricate morphology of flow-directing valves (Wasserthal et al., 2018).

It is clear that micro-CT has led to a renaissance in insect morphology (Friedrich and Beutel, 2008), of particular importance here is Iwan et al. (2015) using micro-CT to investigate insect tracheal architecture. In large part, the impetus for the current study was to investigate patterns in insect tracheal architecture using the application of Iwan et al.’s techniques in a comparative approach across multiple orders. As described in this summary, several studies have focused on insect tracheal morphology using both traditional and advanced methods (see table 1), but here we present a comprehensively comparative analysis of insect respiratory structures using high-resolution micro-CT methods with representatives from nearly all non-holometabolous orders.

TABLE 1

Insect Trachea Studies

Methods: D, dissection; M, micro-CT; LA, lactic acid.

Stage: L, larva; N, nymph; P, pupa; A, adult

Order	Family	Genus	Stage	Method	Reference
Lepidoptera	Bombycidae			D	Malpighi, 1669
Ephemeroptera			L, A	D	Swammerdam, 1737
Various				D	Newport, 1836
Various				D	Palmén, 1877
Myriapoda	Several			D	Grassi, 1885
Odonata	Libellulidae	<i>Plathemis Lydia</i>	L	D	Scott, 1905
Coleoptera	Dytiscidae	<i>Dytiscus marginalis</i>		D	Alt, 1912a, 1912b
Odonata	Several			D	Tillyard, 1914, 1917
Various				D	Chapman, 1918
Orthoptera	Acrididae	<i>Dissosteria carolina</i>		D	Vinal, 1919
Blattodea (Isoptera)	Several			D	Fuller, 1919
Odonata	Lestidae, Coenagrionidae	<i>Lestes</i> sp., <i>Paripatus</i> sp.	L	D	Kennedy, 1922
Phasmatodea	Lonchodidae	<i>Carausius morosus</i>	L	D	Lehmann, 1925
Zygentoma	Lepismatidae	<i>Lepisma saccharinum</i>	A	D	Šulc, 1927; Barnhart, 1958, 1961
Orthoptera	Tettigoniidae	<i>Phasgonura viridissima</i>		D	Carpentier, 1927
Odonata	Aeshnidae	<i>Anax junius</i>	N	D	Steiner, 1929
Various			L, P, N, A	D	Snodgrass, 1935
Hymenoptera	Apididae	<i>Apis mellifera</i>	A	D	Snodgrass, 1936
Orthoptera	Several (Ensifera)			D	Ander, 1939
Diptera	Several		L, P	D	Keilin, 1944
Ephemeroptera	Several		L	D	Landa, 1948
Diptera	Several		L	D	Whitten, 1955, 1956, 1957, 1959, 1960
Embioptera	Embiidae	<i>Embolynta baetsi</i>	A	D	Lacombe, 1958, 1971
Coleoptera	Passalidae	<i>Popilius disjunctus</i>	A	D	Robertson, 1962
Coleoptera	Bruchidae	Several		D	Vats, 1972
Coleoptera	Gyrinidae	<i>Dineutes indicus</i>	A	D	Tonapi, 1977
Ephemeroptera	Behningiidae	<i>Doliana americana</i>	L, A	D	Soldán, 1979
Orthoptera	Acrididae	<i>Schistocerca americana</i>	A	D	Burrows, 1980
Mantodea	Mantidae	<i>Hierodula membranacea</i>	A	D	Kerry and Mill, 1997
Phasmatodea	Lonchodidae	<i>Carausius morosus</i>	A	D	Schmitz and Perry, 1999; Strauss, 2021
Isopoda	Oniscidea	Several	Various	D	Schmidt and Wägele, 2001
Various				M	Socha and De Carlo, 2008
Coleoptera		<i>Odontotaenius disjunctus</i>	A	M	Waters et al., 2013

TABLE 1 *continued*

Order	Family	Genus	Stage	Method	Reference
Orthoptera	Acrididae	<i>Schistocerca americana</i>	A	M	Shaha et al., 2013
Diptera	Calliphoridae	<i>Calliphora vicina</i>	A	M	Walker et al., 2014; Wasserthal et al., 2018
Coleoptera	Tenebrionidae	<i>Tenebrio molitor</i>	L, P, A	M	Iwan et al., 2015; Raś et al., 2018
Several			Various	LA	Ruan et al., 2018
Coleoptera	Curculionidae	<i>Hypothenemus hampei</i>	A	M	Alba-Tercedor et al., 2019
Phasmatodea	Phasmatidae, Diapheromeridae	<i>Ramulus artemis</i> , <i>Siypolidea sipylus</i>	A	D	Strauss, 2021

Major studies on insect tracheae. Note that some recent studies occasionally use dissection.

GOALS OF THIS STUDY

The challenge presented in assessing homology in the insect tracheal system was best summarized by Snodgrass (1935: 431):

Kennedy [1922] and Steiner [1929] have attempted, from a study of the Zygoptera, to deduce a more detailed concept of the primitive tracheation springing from each primary tracheal invagination, from which might be evolved the basic pattern of the tracheal system in each of the insect orders. Kennedy observes, however, that the ‘readiness of the tracheal system to develop new branches has been one of the things which has made homologization of the branches seem such a hopeless task.’ We may add that the same condition still prevails to such an extent that it would be useless to present here any attempt at a comparative study of the tracheal system.

What was not possible toward the end of the 20th century is now achievable with current methods. The goals of this study include the following:

1. documenting the tracheal systems across Insecta
2. establishing homologies and a uniform terminology for insect tracheae
3. determining synapomorphic features of tracheae both among and within orders

4. determining adaptive patterns in tracheal system structure, such as those that may be correlated with flight or locomotion abilities.

To date, documentation and naming of tracheal structures has been done piecemeal, with common terminology used infrequently, if at all. The lack of a common terminology is part of what has made it difficult to assess homology in insect tracheal architecture. The aforementioned table 1 lists the major studies to date of insect tracheal systems, and there is little if any consistency in nomenclature. Most detailed tracheal studies focus on specific species (or occasionally groups). This often results in long lists of terminology applicable to only a few taxa (or even just one taxon), such as Raś “main posterior mesoleg trachea” in the beetle *T. molitor* (Raś et al., 2018), a structure that may not be present in any other order. Other terms are nonspecific and could apply to a number of body regions, such as “ventral abdominal commissure” (Alba-Tercedor et al., 2019) or “posterior dorsal connective” (Barnhart, 1958, 1961).

Tracheae common to multiple taxa suffer from inconsistent naming as well. Using the trachea that extends into the foreleg as an example, a structure very likely present in insects from every order, Snodgrass’s “basal wing trachea” (described by Alba-Tercedor, Snodgrass’s account is more descriptive in nature than actually apply-

ing nomenclature) is referred to as “trachea propedalis” by Šulc (1927), simply “leg trachea” by Barnhart (1961), the “main proleg trachea” by Raś et al. (2018), and the “prothoracic leg trunk” by Alba-Tercedor et al. (2019). Abbreviations applied to these tracheae in figures are equally inconsistent. For example, this “leg trachea,” or “LT” of Barnhart, has no specific abbreviation other than a simple ‘*i*’ in Snodgrass’s figure 225, and is labeled “malt” by Raś and “PtLt” by Alba-Tercedor. Studies to date have incorporated tables that indicate terms previously used and their updated counterparts (Iwan et al., 2015; Raś et al., 2018; Alba-Tercedor et al., 2019; Strauss, 2021), but these updates are more applications of seemingly appropriate terminology to newly studied taxa rather than an attempt to standardize naming conventions or assess homology. Notable exceptions include locusts, for which Strauss referred to Burrows’s nomenclature from nearly 30 years previous (Burrows, 1980; Strauss, 2021), and beetles, for which Raś and colleagues applied established Coleoptera nomenclature for those few beetle tracheae that were named (Crowson, 1981; Raś et al., 2018). Other authors appear to apply established morphological terms from Snodgrass (1935); however, the lack of coverage on tracheal morphology in this landmark work hinders these efforts.

The application of comparative methods to micro-CT data across multiple orders and within families permits assessment of homology to establish a uniform terminology for insect tracheae. Although CT provides unprecedented detail, it can provide almost too much data, in that it can be difficult to identify tracheal homology due to the proliferation of branches in some taxa. The situation is similar in other micro-CT studies, such as those involving insect musculature (Friedrich and Beutel, 2008; Blanke et al., 2014). The effectiveness of the comparative method, when complemented with observational methods such as micro-CT, uniquely allows for assessment of homology (Harvey and Pagel, 1991). Raś et al. (2018) sought a similar goal in their study on develop-

mental stages of *Tenebrio molitor* beetles; our work here expands on this foundation by incorporating data from multiple orders.

Apterygote hexapods serve as an important basis for assessing tracheal homology, as their respiratory systems are more generalized and unaffected by wing development or flight musculature. Given their phylogenetic positions, branching patterns established in these basal orders form the basis for the ground-plan of topological identity necessary for determining connectivity in more complex tracheal systems.

THE COMPLEXITY OF INSECT BREATHING

While modern methods have assisted in revealing the previously hidden aspects of the insect tracheal system, this is only the first step in the process. Insect respiratory systems are deceptively complex, with a web of adaptations developed over evolutionary time for this diverse group of organisms.

Differences in spiracular morphology and physiology have been studied since the development of the microscope (Malpighi, 1669; Swammerdam, 1737), and more recent treatments have used comparative methods to infer evolutionary patterns, albeit on a limited scale (Nikam and Khole, 1989). As with tracheal systems, most studies focus on particular taxa, such as hissing cockroaches (Nelson, 1979; Nelson and Fraser, 1980) and locusts (Weis-Fogh, 1967). Table 2 presents a summary of some of the available information regarding spiracle types in some of the groups presented here. Abdominal pumping produces pressure that leads to tracheal compression, which may be used for active ventilation, indicating that passive diffusion is very likely not the only gas exchange mechanism (Heinrich, 1976; Westneat et al., 2003; Socha et al., 2008; Waters et al., 2013; Pendar et al., 2015; Pendar et al., 2019). Wigglesworth’s landmark *The Principles of Insect Physiology* discusses insect respiration in some detail, including tracheal development, differences in spiracular control, fluid filling of tra-

TABLE 2

Spiracle Types

Spiracular opening and closing mechanisms for various orders (where known).

|| denotes musculature for opening and closing; O indicates always open.

Question marks indicate uncertainty in results from the referenced study.

Group	Representative	T2	T3	A1	A2	A3	A4	A5	A6	A7	A8	References
Zygentoma	<i>Tricholepidion</i>	?	?							?	?	Malpighi, 1669
Ephemeroptera		O?	O?									Swammerdam, 1737
Dermaptera	<i>Forficula</i>			?	?	?	?	?	?	?	?	
Plecoptera	<i>Pteronarcys</i> spp., <i>Taniopteryx</i> spp.	?	?	?	?	?	?	?	?	?	?	Nelson and Hanson, 1968
Orthoptera	<i>Neduba</i> spp.											Snodgrass, 1935
Grylloblattodea	<i>Galloidiana yuasai</i> , <i>Grylloblatta</i> spp.			O?	Fujita and Machida, 2017							
Mantophasmatodea	<i>Mantophasma</i> spp., <i>Austrophasma caledonensis</i>											Klass et al., 2002; Wipfler et al., 2015
Embioptera		O?	O?									
Phasmatodea	<i>Timema</i> spp., <i>Diapheromera femorata</i>			?	?	?	?	?	?	?	?	Tilgner et al., 2008
Mantodea	<i>Mantis religiosa</i>			?	?	?	?	?	?	?	?	Brannoch et al., 2017
Blattodea	<i>Blatta</i> spp.											Snodgrass, 1935
Isoptera	<i>Zootermopsis</i> spp., <i>Hodotermes mossambicus</i>											Inder and Duncan, 2015

cheoles, water loss, and even respiration in endoparasitic insects (Wigglesworth, 1972). Numerous studies have investigated directional airflow, primarily related to insect flight and even including valve mechanisms (Vinal, 1919; Weis-Fogh and Jensen, 1956; Weis-Fogh, 1967; Harrison et al., 2013; Wasserthal, 2015; Wasserthal and Frohlich, 2017; Wasserthal et al., 2018). Additionally, the assumption that insects do not require respiratory proteins was recently shown to be invalid, with the discovery of the expression of hemoglobins in all insect orders (Herhold et al., 2020). Obviously, respiration involves many variables, but we begin with virtual road maps of the tracheal networks, hopefully serving as a morphological scaffold and the basis for future investigations.

METHODS AND MATERIALS

SPECIMEN COLLECTION AND STORAGE

All specimens were collected live. Pinned specimens are inappropriate for the study of tracheae as desiccation distorts internal structures. Specimens preserved in alcohol are also unsuitable, as alcohol fills air spaces with fluid, making determination of tracheal and air-sac morphology via micro-CT difficult. Most specimens were field-collected in the New York City metropolitan area (New York, New Jersey) and Black Rock Forest (Cornwall, NY) by the authors. *Neocloeon triangulifer* (Ephemeroptera), *Extatosoma tiaratum* (Phasmatodea), *Medauroidea extradentata* (Phasmatodea), *Idolomantis diabolica* (Mantodea), and *Gromphadorinha portentosa* (Blatto-

dea) were obtained from laboratory cultures of the American Museum of Natural History (AMNH). *Grylloblatta* sp. (Grylloblattodea), *Tricholepidion gertschi* (Zygentoma), and *Timema* cf. *californicum* (Phasmatodea) were collected in California. *Zorotypus hubbardi* (Zoraptera) was collected in Gainesville, Florida.

As soon as possible after capture, specimens were stored in tight vials with moist tissue to reduce sublimation and desiccation and frozen to -80°C to allow long-term preservation of tracheae and air sacs. Freezing of live specimens for storage and subsequent thawing just prior to scanning allows determination of tracheal structures via micro-CT with a minimum of preservational artifacts. Early in the study, a handful of specimens were frozen to -20°C , and it was found that smaller tracheae experienced fluid filling over time but freezing to -80°C eliminated these events. After scanning, specimens were deposited as vouchers in the collections of the AMNH Division of Invertebrate Zoology.

SPECIMEN SELECTION AND TAXONOMIC COVERAGE

As insects thrive in nearly every terrestrial habitat, their diversity is nearly ubiquitous. As such, collecting common, local species in the New York City metropolitan area yielded a broad swath of insect orders. Particular efforts were made to obtain phylogenetically critical or basal taxa not available locally, such as *Tricholepidion gertschi* (Zygentoma), *Grylloblatta* sp. (Grylloblattodea), *Oligotoma negra* (Embiop-tera), specimens from Phasmatodea, the Madagascar hissing cockroach *Gromphadorhina portentosa* (Blattodea), and the lubber grasshopper *Romalea microptera* (Orthoptera). In all, the study includes representatives from 13 orders of insects, including representatives from nearly all Polyneopteran orders (except for Mantophasmatodea) and the important apterous basal orders Archaeognatha and Zygentoma.

As noted above, micro-CT scanning is a powerful technique that allows unparalleled access to

the study of internal structures of insects. Micro-CT datasets are commonly well over 1 GB for a single file and can reach over 50 GB for high-resolution synchrotron scans; datasets for this study range from 1 to 4 GB for a single volume. Polygon counts for tracheal models routinely reach 10 million triangles and occasionally exceed 100 million polygons. It is certain that these benchmarks will one day seem “quaint”, but at the time of this study the effort expended in postprocessing, segmentation, rendering, and labeling of a single-digit gigabyte file of a single specimen was substantial. Consequently, while the addition of certain taxa or specimens would certainly assist in the investigation of certain questions, the issue of practicality was often in the forefront of the study, and taxon sampling and order selection were considered carefully to achieve useful and meaningful results. Additionally, as no two specimens included are from the same genus, generic names are used herein.

MICRO-CT SCANNING – TECHNIQUES AND PARAMETERS

All specimens were scanned at the AMNH Microscopy and Imaging Facility using a GE v|tome|x s240 micro-CT scanner equipped with a 180 kV X-ray source. Over the course of the study—spanning more than four years of collection and scanning—the hardware and software of the system was upgraded several times, including two different detectors. The first was a DXR-250RT Real Time amorphous silicon 14-bit flat-panel detector, composed of a 20.62 cm square 1024×1024 pixel array at 200 micrometer pixel pitch. During the study, the system was upgraded to larger DXR-250 featuring a 41 cm square, 2048×2048 pixel array at 200 μm pitch. No significant differences in data quality were observed between the two detectors for determining tracheal architecture.

As the s240 is a cone-beam scanner, where the specimen is rotated in the beam while projections are captured on the stationary detector, the resolution that can be achieved is a function of

how close the specimen can be placed to the X-ray source. Consequently, specimen size has a direct impact on scan resolution. The size disparity in the range of specimens examined resulted in a wide range of voxel sizes, from 2.2 μm for the zorapteran to 44.7 μm for the Chinese mantis. While scanning at lower resolution is suboptimal for locating extremely small architectures such as tracheoles, all scans were found to have sufficient resolution for determination of tracheal homology.

Specimens were mounted vertically to allow positioning of the insect as close as possible to the X-ray source to maximize scan resolution. A wide array of vials and containers were used for mounting, with immobilization of the insect being paramount, as movement of structures, either internal or external, can cause reconstruction artifacts that may necessitate repeating a scan. Specimens were placed in the vial for best fit, with some oriented with the head up and some with head down. Gravity has been shown to cause shifts in hydraulic pressure downward changing the size of respiratory structures (Harrison et al., 2020), especially in larger specimens. This effect appears to be particularly relevant for air sacs and smaller tracheae, which are not studied here. While hydraulic pressure likely collapsed smaller tracheae in some specimens, the presence of homologous major branches across orders was still observed.

Insects were mounted with moistened cotton batting or paper towels and sealed with clay or plastic tape as desiccation during the scan process causes movement, resulting in blurred scans. Except for the aeshnid dragonfly, where the wings were removed and scanned separately, all specimens were scanned whole and a variety of techniques were used to immobilize and mount insects for scanning. As the length of some scans could increase the temperature of the specimen well above room temperature, insects were often “braced” with a variety of materials to prevent movement during the scan. Loose cotton and both open- and closed-cell foam were typically used. Air cells in closed-cell foam can expand

slightly during longer scans due to the elevated temperature in the scanning chamber, and this can cause undesirable micrometer-scale movement of the specimen during the scan. For shorter duration or larger resolution scans, this movement was irrelevant, but for longer-term (greater than 1 hour), high-resolution (voxel sizes smaller than 5 μm) scans, closed-cell foam was avoided. Scanning parameters for all specimens, including voxel size, beam energy, current, and exposure times can be found in table 3.

VOLUME RECONSTRUCTION, POSTPROCESSING, SEGMENTATION, AND VISUALIZATION

For all scans, volume reconstruction from raw projections was performed using GE/Phoenix datos|x reconstruction software v.2.3.2. A combination of manual and semiautomatic geometry correction in datos|x was used for each specimen. Reconstructed volumes were exported as 16 bit .tif stacks for postprocessing. Multiscanned stacks, more than one scan tall, were stitched into a single volume using FIJI after export as separate .tif stacks (Preibisch et al., 2009; Schindelin et al., 2012). Specimens were cropped when appropriate using FIJI (Schindelin et al., 2012) and exported as .nrrd (Nearly Raw Raster Data) files, an open-source and widely used volume file format, prior to segmentation and rendering. Postprocessing and analysis of all specimens was done using 3D Slicer (Fedorov et al., 2012).

Typically, the first step in the visualization process is “vial removal.” The vial and packing material used to hold the specimen immobile during the scanning process is often of similar density to insect cuticle, and consequently, of similar X-ray absorbance. These materials appear in the scan dataset and obscure visualization of the specimen, making removal of this material necessary for effective analysis. (Researchers seeking high-resolution scans of Eppendorf tubes and other containers are welcome to contact the authors.) Removal of the regions containing packing materials was achieved using a “fill

TABLE 3

Scanned Specimens

Specimens micro-CT scanned for the study at AMNH Microscopy and Imaging Facility GE v|tomex|s240 scanner, with scanning parameters.

Order	Family	Taxon	Resolution (mm)	Beam (kV)	Current (μA)	Averaged frames	Frame Skip	Exposure (msec)
Archaeognatha	Machilidae	<i>Trigoniophthalmus alternatus</i>	0.0060	60	210	3	1	400
Zygentoma	Lepidotrichidae	<i>Tricholepidion gertschi</i>	0.0066	70	400	3	1	333
Zygentoma	Lepismatidae	<i>Thermobia domestica</i>	0.0072	70	290	3	1	333
Zygentoma	Lepismatidae	<i>Lepisma saccharina</i>	0.0048	70	220	4	1	333
Ephemeroptera	Baetidae	<i>Neocloeon triangulifer</i> (subimago)	0.0041	80	250	4	1	400
Ephemeroptera	Baetidae	<i>Neocloeon triangulifer</i> (adult)	0.0023	90	170	4	1	400
Ephemeroptera	Ephemeridae	<i>Ephemera</i> sp.	0.0131	60	200	2	1	333
Odonata	Aeshnidae	Adult	0.0210	90	220	4	1	200
Odonata	Aeshnidae	Immature	0.0302	60	480	3	1	333
Odonata	Calopterygidae		0.0194	60	280	2	1	333
Zoraptera	Zorotypidae	<i>Zorotypus hubbardi</i>	0.0022	80	250	4	1	400
Dermaptera	Forficulidae	<i>Forficula auricularia</i>	0.0135	60	240	2	1	333
Dermaptera	Anisolabididae	<i>Anisolabis maritima</i>	0.0116	80	290	3	1	333
Plecoptera	Perlodidae		0.0060	60	400	3	1	333
Plecoptera	Nemouridae		0.0030	60	200	2	1	333
Orthoptera	Gryllidae	<i>Gryllus</i> sp.	0.0121	100	180	4	1	200
Orthoptera	Raphidophoridae	<i>Tachycines asynamorosus</i>	0.0188	70	285	3	1	333
Orthoptera	Tettigoniidae	<i>Meconema thalassinum</i>	0.0179	60	400	3	1	333
Orthoptera	Romaleidae	<i>Romalea microptera</i>	0.0270	70	285	3	1	333
Grylloblattodea	Grylloblattidae	<i>Grylloblatta</i> sp.	0.0129	70	220	3	1	333
Embioptera	Oligotomidae	<i>Oligotoma negra</i>	0.0053	90	180	3	0	400
Phasmatodea	Timematidae	<i>Timema</i> cf. <i>californicum</i>	0.0051	60	200	3	1	333
Phasmatodea	Phasmatidae	<i>Extatosoma tiaratum</i>	0.0422	80	250	3	1	333
Phasmatodea	Phasmatidae	<i>Medauroidea extradentata</i>	0.0351	60	230	3	1	500
Mantodea	Mantidae	<i>Tenodera sinensis</i>	0.0447	90	170	3	0	400
Mantodea	Empusidae	<i>Idolomantis diabolica</i>	0.0305	80	250	3	1	333
Blattodea	Blattidae	<i>Periplaneta americana</i>	0.0386	60	440	3	1	333
Blattodea	Blaberidae	<i>Blaptica dubia</i>	0.0214	70	290	3	1	333
Blattodea	Blaberidae	<i>Gromphadorhina portentosa</i>	0.0311	70	210	4	1	400
Isoptera	Rhinotermitidae	<i>Reticulitermes flavipes</i>	0.0050	60	200	3	1	333
Isoptera	Archotermopsidae	<i>Zootermopsis angusticollis</i>	0.0053	95	170	4	1	200

between slices” technique, where the desired sample area was marked at representative slices spaced throughout the volume along the posterior-anterior axis of the specimen. A masking volume was then created by interpolating across these slices using a morphological contour interpolation method (Zukić et al., 2016). When applied against the original volume, the Mask Scalar Volume function in 3D Slicer removed the unwanted vial and packing material, leaving only the insect.

For most scans, the difference in absorption values for air vs. insect was such that no post-processing was necessary to improve differentiation between the two areas. For a handful of scans, however, insect and air were close enough in absorption values that segmentation was difficult. For these scans, automatic Window/Level was used in FIJI to remap intensity values and “spread out” the histogram of the scan to facilitate segmentation (Schindelin et al., 2012).

Image segmentation is an extensive area of research in the field of machine vision, but can be summarized as the process of selecting and separating areas of interest in digital images. In medical imaging, segmentation is used to isolate areas of human anatomy or pathologies, such as bone, blood, muscle, tumor, and other tissues of interest. As medical CT scanners use precisely calibrated dosages to limit the amount of radiation exposure to the patient, standardized X-ray absorption measurements known as Hounsfield units (HU) are used to easily select and segment desired anatomy. Some examples include air, standardized at -1000 HU, water at 0 HU, unclotted blood between +13 and +50 HU, and cancellous (spongy) bone from +300 to +400 HU.

Micro-CT scans in a research setting, however, use a range of beam energies and exposure times, resulting in a lack of standardized X-ray absorption values. Scanning parameters are customized for each specimen to optimize resolution, dynamic range, and overall image quality; settings suitable for a given specimen may not be optimal for the next. A short scan of a cicada at 90 kV, for example, will have a different absorp-

tion value for air (and everything else) than a long scan of a dragonfly at 60 kV. Segmentation of anatomy requires manual determination of absorbance values of the desired areas, followed by a combination of manual and semiautomated methods to separate desired structures into independent segments to be visualized in 3D. For determining insect respiratory architectures, only two segments are of interest—air and body. Determining the absorbance of air is achieved by manually sampling the values outside the insect using FIJI or 3D Slicer, and the range of absorbance values for the insect body is determined by a simple thresholding technique within 3D Slicer to select the maximum and minimum values. For some scans, absorbance values for air were close enough to those for tissue, such that occasional adjustment of threshold values was required during segmentation to achieve the desired quality.

Labeling of tracheal structures was performed in 3D Slicer using a variety of techniques, depending on the complexity of the specimen. The Markups module was used to place named points corresponding to various structures, and data files with these points are available for all specimens in the online supplementary digital data (<https://doi.org/10.5531/sd.sp.55>). Points were typically placed interactively in the 3D view, or where necessary, on 2D slices through careful observation of anatomy along with viewing slice position in the 3D view. Interactive use of the 3D paintbrush in both 2D and 3D views was often useful in locating small or occluded structures. Clipping of segmentation models was successful in exposing internal trachea obscured by large structures. Manual back-and-forth rotation of tracheal models in the 3D view, using either perspective or orthographic projections, was a useful method for exploiting motion parallax to determine the relative position of deeply nested structures. Volume rendering of the specimen overlaid on top of segmented tracheal structures was also found to be an effective method, especially when viewed side by side with a 3D

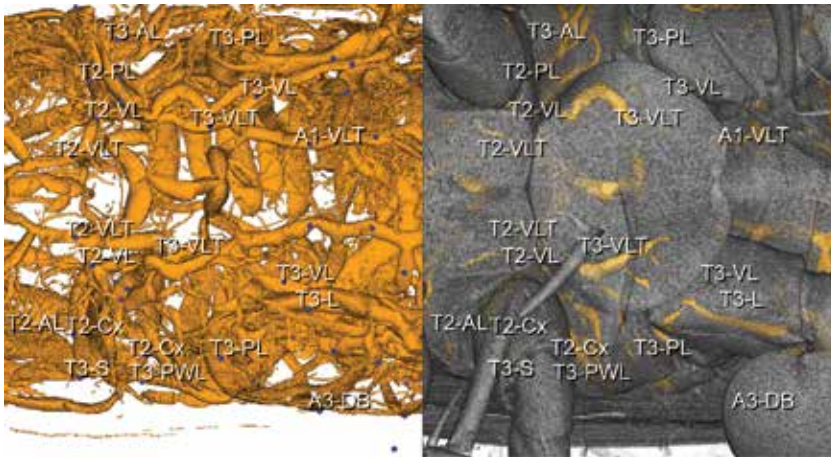


FIGURE 5. Placement of tracheal labels in 3D Slicer. In this ventral view of *Gryllus*, the left side of the window is trachea only, while the right side is trachea with the body volume rendered. Split views like this, especially when including the body alongside the trachea, were especially effective when mapping complex tracheal architectures.

view of just trachea, as seen in figure 5. The effective use of lighting and shadows, in particular environment map lighting and ambient occlusion, was also useful in judging the relative position of complex tracheal architectures. These techniques are common to a range of visualization applications but may have slightly different names than used in 3D Slicer.

The 3D models of the air and body structures were smoothed in 3D Slicer's Segment Editor module with a smoothing factor of 0.1 prior to export in Stanford PLY format for rendering of publication-quality images. Application of minimal smoothing reduces the "stair-stepping" effect caused by conversion to a 3D mesh while preserving high-resolution morphological detail, and a value of 0.1 was empirically determined across all scans to be a generally suitable value. A handful of specimen models with very high polygon counts (over 90 million triangles) were decimated in Slicer's Surface Toolbox module with a decimation factor of 0.7. Decimated models were carefully checked by eye to ensure preservation of small morphological details. The open-source animation software Blender (versions 2.92, 3.0) was used for scene layout and surfacing, and Pixar Photorealistic RenderMan

(version 24) was used for 3D rendering (Blender Online Community, 2018; Pixar Animation Studios, 2021). Imported models were smooth shaded (interpolated normals) to reduce faceting and surfaced with a provided preset specular phenolic plastic material. Although modern rendering software provides essentially limitless lighting and surfacing options, colors and materials were chosen to provide as much information as possible concerning morphology without becoming distracting. Lighting was identical for all figures and plates, with two rectangular area lights used, one behind the camera and one above the model, placed at about a 45° angle. (Sample scene files are available from the authors upon request.) Still images used to compose figures and plates were typically rendered at an image size of 6900 × 9600 pixels in Blender to preserve detail of structures less than ten micrometers in size during printing. Test renders of specimens with features below 2.0 μm in size were performed to ensure preservation of exceedingly small details, and specimens were rendered at higher resolution when necessary (such as especially long and narrow Odonata). Images of tracheae and body were rendered separately to high-dynamic range 32 bit per channel

floating point .tif files and then composited in Adobe Photoshop using a simple overlay technique, placing the 3D rendering of the air spaces above that of the rendered image of the body. The opacity of the body was set at approximately 30% to facilitate visualization of tracheal structures and their locations in situ. Composite images were converted to 8 bit per channel RGBA at 600 dpi for publication. Plates were composed, labeled, and annotated in Adobe Illustrator. While all plates and most figures are rendered output from Blender and RenderMan, certain figures in the text are direct screen-captures from 3D Slicer before composition and annotation in Adobe Illustrator.

Some specimens, such as *Forficula auriculara* (Dermoptera: Forficulidae) possess single tracheae that extend anteriorly or posteriorly for a substantial distance, in this case the very long cerci (forceps). To present as much detail as possible in the plates, such specimens were cropped slightly to allow greater enlargement of tracheal detail in the rest of the image. In these instances, the full specimen is shown as an inset with the cropped region shown (see pls. 26–28 for examples).

TRACHEAL NOMENCLATURE

“The Master said, ‘If something has to be put first, it is, perhaps, the rectification of names.’” This advice from Confucius (*Analects*, Book 13, Chapter 3, translated by James Legge) could not be more essential for morphology/comparative anatomy, as well as taxonomy, and indeed any science. A primary goal of this work is to present a uniform nomenclature for insect tracheal morphology. As reviewed in the Introduction, comparative analyses of tracheae across multiple orders of insects are lacking, as is a common terminology for insect tracheae. In the interest of preserving as much foundational work as possible, the proposed nomenclature here seeks to incorporate and extend commonly used terms. As the earliest study to label the tracheal system of an entire organism, Šulc (1927) was used as a

scaffold and starting point. Specifically, nomenclature from substantial contributions to tracheal research by Chapman (1918) on pterygotes, Šulc (1927) on *Lepisma*, Snodgrass (1935) on insect morphology in general, Ander (1939) on Ensifera, Barnhart (1961) on *Ctenolepisma*, Raš et al. (2018) on *Tenebrio*, and Alba-Tercedor et al. (2019) on *Hypothenemus hampei* were collated to create the system presented. Although this study does not include holometabolous taxa, dozens of specimens across virtually all orders not presented here have been scanned and examined, along with the studies mentioned, to verify the utility of the system presented. To assist in the use of this system, table S1 in the online supplement (<https://doi.org/10.5531/sd.sp.55>) presents the list of terms and abbreviations from these significant contributors, often overlapping and some conflicting, along with the uniform terminology introduced here. The complete tracheal nomenclature system, with abbreviations and descriptions, is shown in table 4.

While as much nomenclature was preserved as possible, some modifications were required. Most notably, the relative positions of “anterior” and “posterior” tracheae conflict among studies. For example, Raš et al. (2018) refer to the trachea leading from the mesothoracic spiracle to the midleg as “posterior,” whereas Chapman (1918), Kennedy (1922), Šulc (1927), and Ander (1939) all refer to this as an “anterior” leg trachea. The difference is presumably based on the point of view of the observer—is the direction of the trachea relative to the leg or to the segment? The trachea is located in the posterior region of the segment, but anterior to the leg. For consistency with the earliest and most numerous studies, the convention of relative to the leg is applied here, where we use *-AL* and *-PL* to denote anterior and posterior branches feeding into leg trachea, *positioned relative to the leg trachea in question* rather than the “source” of the trachea. Other tracheae not leading to appendages use position relative to the segment in question, as established by Carpentier (1927) and used by Ander (1939) for supraventral tracheae. Several

TABLE 4

AMNH Trachea Terminology

Terminology and abbreviations for nomenclature presented. For thoracic and abdominal tracheal abbreviations, 'n' refers to the segment number and bracketed letters denote optional prefixes (D, dorsal; M, medial; V, ventral).

Example: A2-DB-VVi refers to second abdominal segment, dorsal branch ventral visceral trachea.

Head Tracheae Term	Abbrev.	Thoracic Tracheae Term	Abbrev	Abdominal Tracheae Term	Abbrev.
Dorsal cephalic trunk	H-DCT	Prothoracic cephalic trunk	T2-CT	Abdominal typmanum	A-Ty
Cephalic dorsal intersection	H-DX	Prothorax proparanotal	T1-Pn	abdominal spiracle	An-S
Intercalary	H-Ic	leg	Tn-L	dorsal branch	An-DB
Dorsal cephalic commissure	H-DC	coxa	Tn-Cx	ventral branch	An-VB
Ocelli	H-Ocel	femoral	Tn-Fm	dorsal commissure	An-DC
Ocular	H-Oc	thoracic dorsal commissure	Tn-DC	ventral commissure	An-VC
Frontal	H-Ft	thoracic ventral commissure	Tn-VC	abdominal spiracular branch	An-SB
Frontal commissure	H-FtC	thoracic dorsal longitudinal trunk	Tn-DLT	dorsal longitudinal trunk	An-DLT
Clypeal	H-Cl	thoracic ventral intersection	Tn-VX	ventral longitudinal trunk	An-VLT
Labrum	H-Lbr	thoracic ventral longitudinal trunk	Tn-VLT	medial longitudinal Trunk	An-MLT
Antennal	H-Ant	thoracic auditory trachea	Tn-Aud	visceral longitudinal trunk	An-ViLT
Cephalic ventral trunk	H-VCT	thoracic auditory septum	Tn-Sept	ventral commissure	An-VC
Mandible	H-Md	thoracic dorsal branch	Tn-DB	ganglion	An-Ga
Maxilla	H-Mx	thoracic ventral branch	Tn-VB	gill	An-Gi
Maxillary palpus	H-MxPlp	thoracic spiracle	Tn-S	abdominal visceral	An-Vi
Labial	H-Lbm	ventral spiracle (when split)	Tn-VS	abdominal ventral visceral	An-VVi
Labial palpus	H-LbmPlp	spiracular atrium	Tn-SATR	abdominal dorsal visceral	An-DVi
Cephalic ventral commissure	H-VC	anterior leg	Tn-AL	abdominal dorsal branch visceral	An-DB-[D,M,V]Vi
Cephalic ventral intersection	H-VX	posterior leg	Tn-PL	abdominal ventral branch visceral	An-VB-[D,M,V]Vi
Cephalic dorsal-ventral branch	H-DVB	ventral leg	Tn-VL	abdominal DLA visceral	An-DLA-Vi
		wing bridge	Tn-Wbr	terminal filament	A-TF
		anterior wing base	Tn-AWba	cercus	A-Cr
		posterior wing base	Tn-PWba		
		costal-radial wing	Tn-W-c-r		
		cubital-anal wing	Tn-W-cu-a		
		flight muscle	Tn-FM		
		spiracular branch	Tn-SB		
		visceral	Tn-Vi		
		asymmetric commissure	Tn-AsymC		

tracheae named by Ander (1939) are exclusive to Orthoptera and for consistency his terminology is retained herein for those taxa.

Some readers may note that the abbreviations for several terms, particularly for cephalic tracheae, are slightly redundant. For example, H-VCT, the ventral cephalic trachea, is obviously cephalic as it is prefixed with H- to denote that tagma. We felt that it was more advantageous to retain VCT, similar or identical to previous studies, and prepend H- for clarity than to rename this trachea H-VT.

HOMOLOGY

Application of terms to features across multiple orders requires a robust assessment of homology (de Pinna, 1991; Brower and Schawaroch, 1996). Broad comparative studies are essential as insects feature unparalleled diversity in form and disparity in size. Tracheal morphology lends itself well to this task, as all insects possess a common set of morphological traits that serve as a starting point for mapping tracheae: spiracles. Branching patterns from spiracular openings were used as the landmarks for assessing tracheal homology (and serve as primary homology, *sensu de Pinna, 1991*), albeit with a few notable exceptions, detailed in the Discussion section. As position and size of tracheae can vary across taxa based on physiological constraints, connectivity and branching patterns across tagma and segments were used next (serial, or secondary homology). Relative position and orientation were also observed and compared with related taxa; however, this can result in some apparent inconsistencies. For example, T2-DB (mesothoracic dorsal branch) is oriented dorsally in the majority of taxa but is distinctly horizontal or even ventrally located in select specimens; it is the connectivity pattern and relative position that defines tracheal homology rather than similarity of form. Lastly, the arrangement of finer branches in specific areas can help inform as to what organs or tissues are tracheated. However, the scans used here were

targeted for determining air spaces from integument, rather than differentiating tissue types. As a result, visceral branch designations should not be interpreted as homologous across taxa.

Insect head morphology features a wide array of morphological diversity, including (but not limited to) reduction or great modification of mouthparts, absence or presence of eyes, position and length of antennae, and many other adaptations. These differences in head morphology make determination of homologies in the head rather challenging, especially in taxa with tracheal networks and loops. As head appendages are discernible in nearly all taxa included and are all supplied by T2-S, head tracheae are named according to the appendages supplied by a given tracheae (the “destination”), rather than the spiracle supplying that trachea (the “source”). Where multiple appendages are fed by a single trachea, these are included in the name. As these branches commonly supply more than one appendage and head morphology is diverse, labels containing multiple names may not indicate true homologies. Tracheae supplying antennae and eyes, for example, exhibit a wide array of morphologies and should not be considered homologous. Also, many head tracheae supply muscles that, although extensively studied in many taxa, are not mapped here; tracheae where the appendage supplied cannot be determined are designated “visceral” and should not be interpreted as homologous. In short, all indications are that insect head respiratory morphology is a vast topic and further research is needed.

A UNIFORM TRACHEAL NOMENCLATURE SYSTEM

The descriptions of tracheal morphology in this section primarily use abbreviations for tracheal names in the interest of readability and brevity. The nomenclature is defined with a small set of terms and consistent rules in the hope that the reader is able to gain familiarity with minimal effort. Figure 6 is a schematic representation of the insect tracheal system for reference.

1. **A trachea is prefaced by H, T, A, followed (for T and A) by a segment number.** Tagma and segments are referred to as one of H (head), T (thorax), or A (abdomen) followed by the segment number (as appropriate) as numerals. For example, T2 refers to thoracic segment 2 (mesothorax), and A4 refers to abdominal segment 4. For tracheae that may span multiple segments or a range of segments a comma (,) is used to specify a list of segments and double points (..) is used to specify a range. Thus, A3..5 refers to abdominal segments 3 through 5, A4,7 refers to abdominal segments 4 and 7, and A2,5..8 refers to abdominal segments 2, 5, 6, 7, and 8. Descriptions for generalized segment morphology use *n* to denote any segment number, as in *An-DB* to broadly refer to abdominal dorsal branches.
2. **Trachea names begin with the location of the origin of the trachea.** The trachea origin is defined as the segment with the spiracle that directly leads to the trachea in question, using spiracles as the primary landmarks in the tracheal system. Abbreviations for tracheae used in all plates and figures begin with this location, followed by a dash. For example, the prefix T2- refers to a trachea supplied by the spiracle of thoracic segment 2 (mesothorax), and A6- denotes tracheae beginning from one of the spiracles of abdominal segment 6. Head tracheae are all prefaced with H- and prothoracic tracheae are prefaced with T1- even though they are supplied by the mesothoracic spiracle T2-S. While this is a slight departure from the convention of using the source spiracle for a given trachea name, the head and prothorax are exceptions as they do not possess spiracles, and all head and prothoracic tracheae originate with T2-S.
3. **Orientation is relative to the trachea being described and are noted using prefixed capital letters A for anterior, P for posterior, D for dorsal, M for medial, and V for ventral.** Directions are used to differentiate multiple tracheae that may branch from a particular location or are similar to other tracheae except for relative location. For example, T2-AL and T2-PL denote branches anterior and posterior to T2-L that both feed into T2-L, *positioned relative to the leg trachea in question* rather than the “source” of the trachea. When a trachea splits into several branches that all share the same direction and morphology, these may be numbered for clarity, such as the flight muscles T2-FM1 and T2-FM2 in Ephemeroptera.
4. **Longitudinal trunks, designated LT, are tracheae that link spiracles along the anterior-posterior length of the insect.** The location in the body is prepended, e.g., DLT for dorsal longitudinal trunk, especially for insects with multiple longitudinal trunks. As noted, the spiracular origin of the trachea is always prefixed, so A4-DLT would be the section of the dorsal longitudinal trunk supplied by the spiracle of abdominal segment 4.
5. **Branches, designated B, are tracheae that subdivide into smaller tracheae and lead to other branches, or tracheae that extend into the viscera, designated Vi.** Branches may also link with commissures that connect spiracles laterally, such as ventral commissures VC or dorsal commissures DC.
6. **Visceral tracheae refer to the many small branches that supply various organs and tissues, especially in the abdomen.** While “viscera” has typically implied digestive tissues, here we refer to any tissues whose function cannot be immediately determined. Occasionally, multiple visceral tracheae may branch from a given larger trachea, and when this occurs, the relative direction (A, P, D,

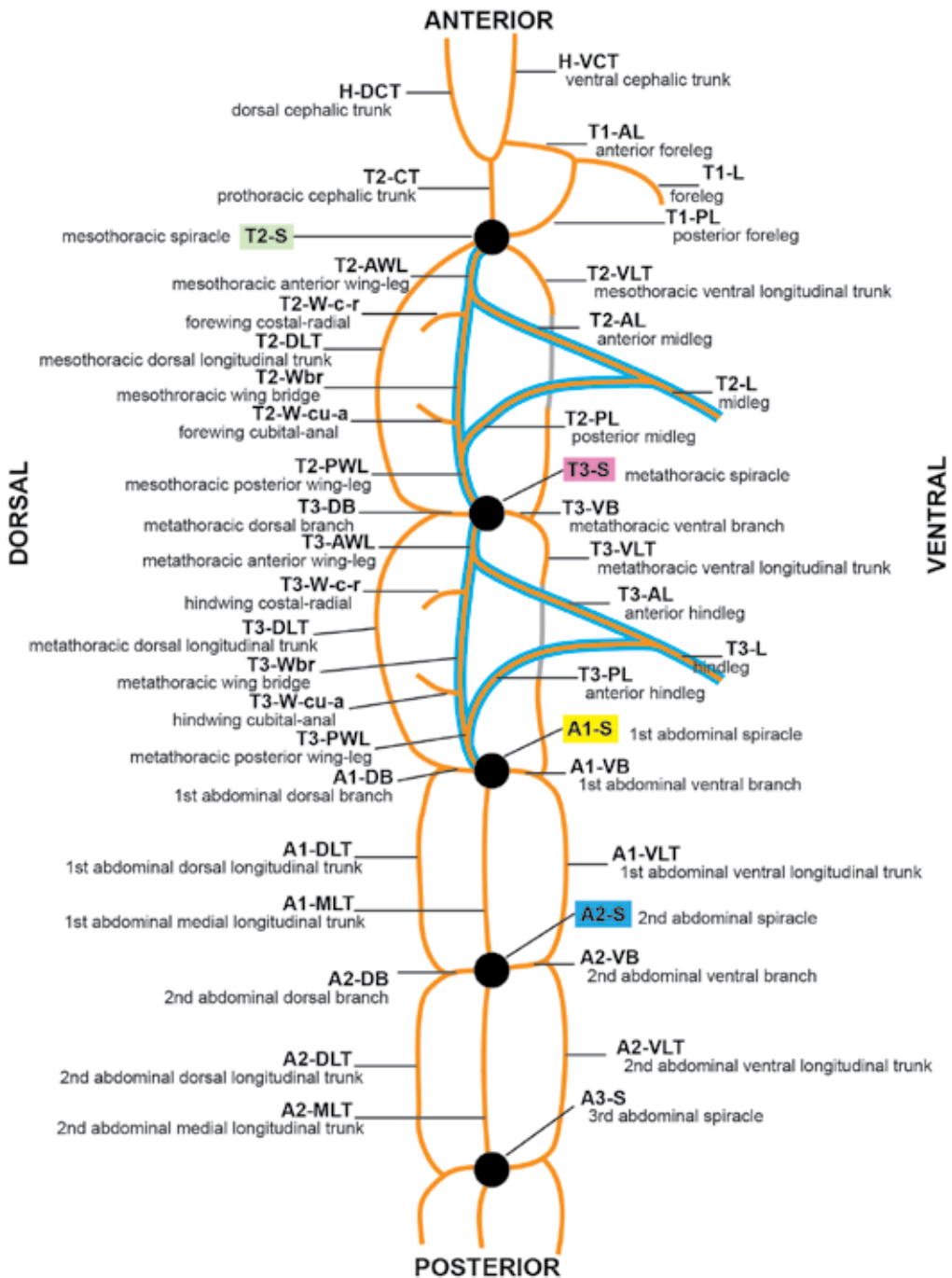


FIGURE 6. Schematic diagram of insect tracheal architecture, with nomenclature. Note that this is a representative diagram; not all insects possess all tracheae shown. Chapman's Triangle is highlighted in blue (see Discussion section).

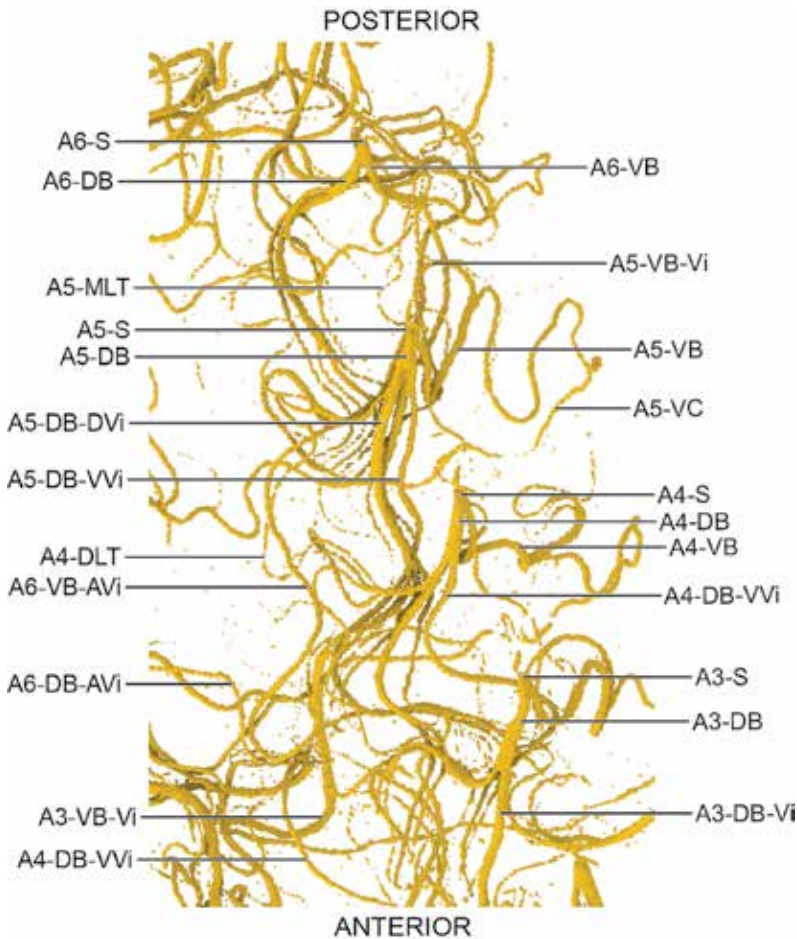


FIGURE 7. Detail of several abdominal visceral tracheae in the termite *Reticulatermes*. Note labeling of relative positions to assist in differentiating various visceral tracheae.

M, or V) of the visceral tracheae may pre-pended so they can be more easily differentiated. Multiple visceral tracheae with similar direction are numbered, such as A4-DLT-VVi1 and so on. Figure 7 is an example of several visceral tracheae branching in various directions from A5-DB of *Reticulatermes flavipes* (Isoptera: Rhinotermitidae). It is important to note that assessing homology in visceral tracheae is challenging and is not done here—visceral tracheae are annotated with direction and numbering to assist in following branches, and similar-

ity in numbering and direction across taxa does not imply homology.

7. **Head tracheal branches that divide to supply multiple head appendages or areas are designated by the trachea supplying that branch.** As noted above, head tracheae are named based on the appendage supplied rather than the spiracle that supplies that trachea. For example, the head trachea that divides into branches leading to the ocular and antennal tracheae is designated H-Oc-Ant. To reiterate, Insecta feature a vast array of diversity in form and disparity in size in heads,

and assessment of homology in head tracheal branches is not as rigorous as in the thorax or abdomen.

RESULTS

Thirty specimens from 13 insect orders and 26 families were scanned to determine tracheal architectures. Phylogenetic relationships among major groups discussed herein generally follow Misof et al. (2014) and Wipfler et al. (2019). The following descriptions use the nomenclature established above; readers are directed to the section A Uniform Tracheal Nomenclature System, above, for guidance.

Most specimens are described individually; however, certain orders (such as Ephemeroptera and Plecoptera) possess many common elements. These are described below as ordinal-level descriptions, followed by family-level sections that highlight important differences. Not all species are described in detail, especially ones in which there is an extensive, anastomosing tracheal system, like *Romalea* (Orthoptera: Romaleidae) and *Extatosoma* (Phasmatodea: Phasmatidae). In these cases, images are provided along with some identifications of obvious tracheal trunks and branches, with commentary on major aspects of modifications.

Common names, while avoided by most entomologists (especially in scientific communications), are included below for nonentomologists. These names should not be considered stable and are only for convenience.

TRACHEAL VISUALIZATIONS

For all figures and plates, tracheae are displayed in 3D in orange with the exterior of the insect shown in the background to provide context. Colors were chosen for high contrast that would also not conflict with established color schemes, such as in medical imaging (red and blue for venous structures, yellow for nerves, etc.). Tracheae are rendered in orthographic projection: features “behind” are the same dimensions as those in

the foreground and not perspective-projected for depth foreshortening. Lateral images are shown with the head to the right and the dorsal side up, and labels are generally applied to features on the right side of the insect such that they indicate features in the foreground of the image. For dorsal images, features toward the dorsal side of the insect are typically labeled, and likewise for ventral images. Head tracheae vary widely in morphology, and occasionally both foreground and background tracheae are labeled for ease of interpretation. Dorsal and ventral images are positioned to achieve clarity in tracheal structures and not necessarily rotated 180° (relative to each other) about the anterior-posterior axis of the insect.

It is important to note that the visualizations are of the air-filled tracheal lumen, and not the trachea itself. Insect trachea tissue is thin, invaginated endocuticle reinforced with taenidia and is difficult to differentiate in micro-CT scans from other internal structures without staining or other contrast-enhancement techniques. These processes can require drying and the introduction of materials and techniques that may distort tracheal morphology. The tracheal lumen, as air space inside the insect body, is far simpler to differentiate, and the techniques here are designed to incur a minimum of interference with internal anatomy. The morphological differences between trachea and tracheal lumen are largely insignificant, except in cases where a trachea has collapsed or filled with fluid, when these areas appear as gaps or missing sections. This is noted in the results where appropriate. The ends of tracheal branches toward the tracheoles may also fill with fluid, but at sub-micrometer diameters these features were too small to be captured at the scan resolutions used even if not filled with fluid.

AVAILABILITY OF DIGITAL DATA

Unbound large-format prints of all plates are provided with the printed publication for ease of comparative analyses and for greater resolution of the scans. Although great effort has been taken

to provide visualizations that confer as much information as possible, the three-dimensional nature of tracheal systems often does not lend itself well to two-dimensional projections, even when multiple views are used (as they are here). Consequently, files containing labeled 3D models of tracheae for all taxa in the study are available as supplementary digital information (<https://doi.org/10.5531/sd.sp.55>), allowing researchers to interactively explore the tracheal systems presented here. Included project files can be opened and viewed with the popular open-source application 3D Slicer, available as of writing at <http://www.slicer.org> (Fedorov et al., 2012), and all tracheae are labeled using the Markups module within 3D Slicer. While 3D Slicer was used for all the analyses herein, the files provided are in established, nonproprietary formats for import into any chosen application. Additionally, full-resolution .pdf files for all plates are available with the 3D model files.

The raw reconstructed volumes used to complete segmentations of the tracheal system are prohibitively large for perpetual online storage but are available from the authors on request.

CLASS INSECTA

ORDER ARCHAEOGNATHA

Family Machilidae

Trigoniophthalmus alternatus

“Jumping bristletail”

Figures 8 (lateral), 9 (dorsal, ventral)

Plates 1 (lateral), 2 (dorsal), 3 (ventral)

Trigoniophthalmus, as the representative of the most basal order in Class Insecta, is notable in its tracheal architecture by a complete lack of longitudinal connections between spiracles. This taxon is critical to understanding the apparent insect ground-plan tracheal structure.

The thoracic tracheae of most taxa are supplied by both T2-S and T3-S, with T2-DLT connecting longitudinally. In *Trigoniophthalmus*,

however, T3-S appears to only supply T3-L and its associated coxa. Branches from T2-S extend posteriorly into the metathorax, nominally supplied by T3-S, including an apparent T3-DLT. The naming of T3-DLT here is an instance of using the positional criterion in homology (sensu Remane, 1952), in that the connectivity of this trachea is not consistent with other taxa; however the position suggests its identification as T3-DLT (de Pinna, 1991). T2-VB extends posterior, almost in the opposite direction of the anterior-reaching cephalic branches. While the position of T2-VB may not appear to be “ventral” in nature, a comparison of its relative position in the hump-backed *Trigoniophthalmus* and in particular its connection to T2-L with apterygote taxa from Zygentoma and Dermaptera demonstrates its homology as a ventral branch. Several tracheae range anteriorly or posteriorly beyond segment boundaries, most prominently A5-DB-DVi, which extends posteriorly past A6-S, reaching A7-S; and A7-Cr, which likewise extends posteriorly from A7-S into both the cerci and terminal filament. However, tracheae for most segments, particularly in the abdomen, remain restricted to their individual segment, placing *Trigoniophthalmus* among the simplest tracheal body plans in this study and unique in its lack of longitudinal connections. This corroborates observations made by Palmén (1877) and reviewed by Dittrich and Wipfler (2021).

DESCRIPTION: HEAD: Characteristically arched thorax, pronotum covering much of head, making boundary between thoracic tracheae and head tracheae rather indistinct. T2-S at anteriormost margin of mesothorax, covered by overhanging tergum, shown in figure 10. H-DCT very thick, with three branches: H-Ic, extending anteriorly and dorsad; H-Oc-Ant anterior and medially before dividing into H-Oc toward midline and H-Ant laterally; H-Mx proceeds antieriad with H-MxPlp branching ventrally and antieriad. H-VCT very thick, with two branches: H-Lbm ventrad, extending into H-LbmPlp; H-Md antieriad,

crossing over H-Md from opposite side of head but not connecting.

THORAX: T2-S present, with five tracheae: H-DCT and H-VCT leading anteriad directly into head, beginning at T2-S and running parallel for length of prothorax; T2-DB leading dorsad; T2-VB and T2-L directly posteriad. H-DCT with no thoracic branches; H-VCT with T1-L branching ventrally; T1-VC present, extending from T1-L. T2-DB-Vi branches just dorsal of T2-S, extending anteriorly; T2-DB continuing dorsad, dividing into what appear to be anterior T1-DLT and posterior T2-DLT near midline; T1-DLT and T2-DLT extend into viscera with no connections to neighboring spiracles. T2-L running posteriad and ventrally, into midleg; large T2-L-Vi and smaller T2-VC divide from T2-L posterior from T2-S. T2-VC joins with anterior-arching T3-VC to form T2-VX intersection. T2-L-Vi extends posteriad into metathorax, with apparent dorsal T3-DLT, T3-Cx ventral, and numerous small visceral tracheae. T3-S ventral to and much smaller than T2-S, with two tracheae: T3-L and T3-VB. T3-L extending dorsad with small T3-L-Vi before arcing ventrad into hind leg; T3-VB directly toward midline with small T3-VC branch that arcs anteriorly to join T2-VC at T2-VX.

ABDOMEN: A1..7-S present, all located ventrally. No longitudinal connections present; figure 11 with representative abdominal segment. An-S with An-DB running dorsad along arc of body wall, turning inward toward midline of body but not forming DC; An-VB branching dorsally for a short distance before arcing ventrad toward midline. An-VC absent. An-DB with visceral tracheae An-DB-MVi, branching anterior and medially halfway up body; An-DB-DVi branches dorsally toward tergal wall. A5-DB-DVi extends posteriorly to 8th abdominal segment; A7-DB-DVi extends posteriorly past 8th abdominal segment,

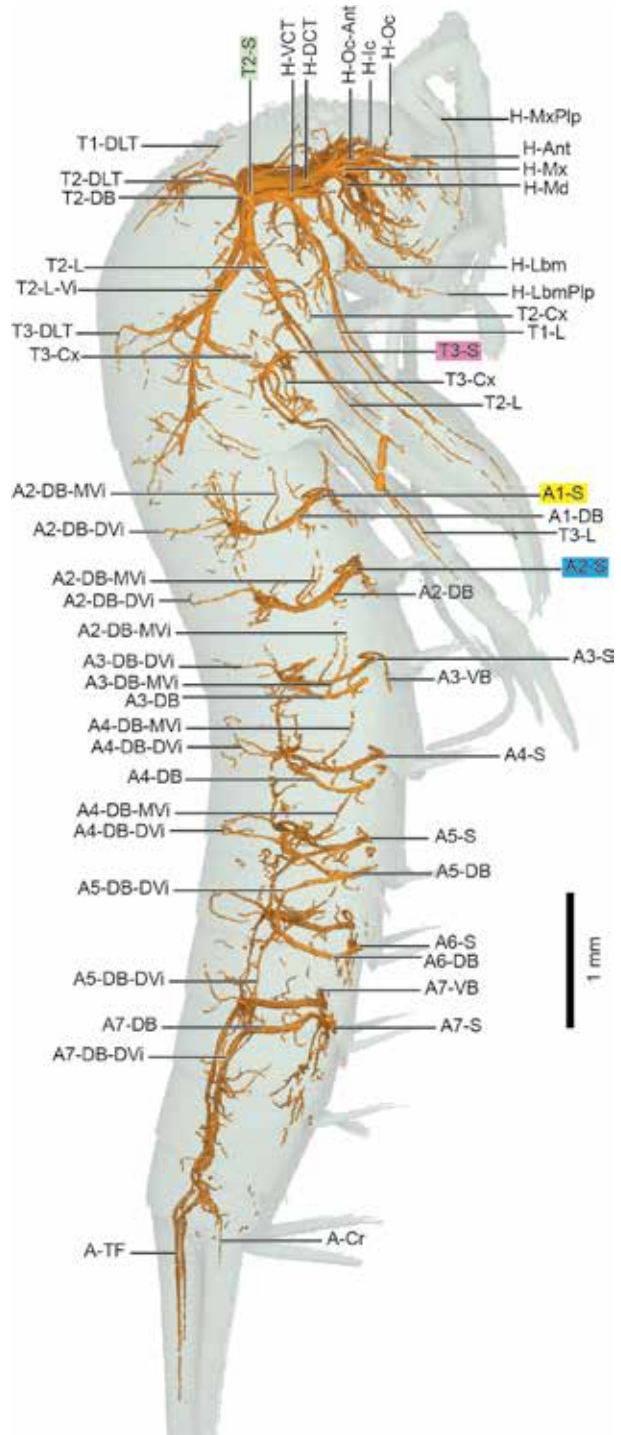


FIGURE 8. *Trigoniophthalmus alternatus* (Archaeognatha: Machilidae), lateral view.

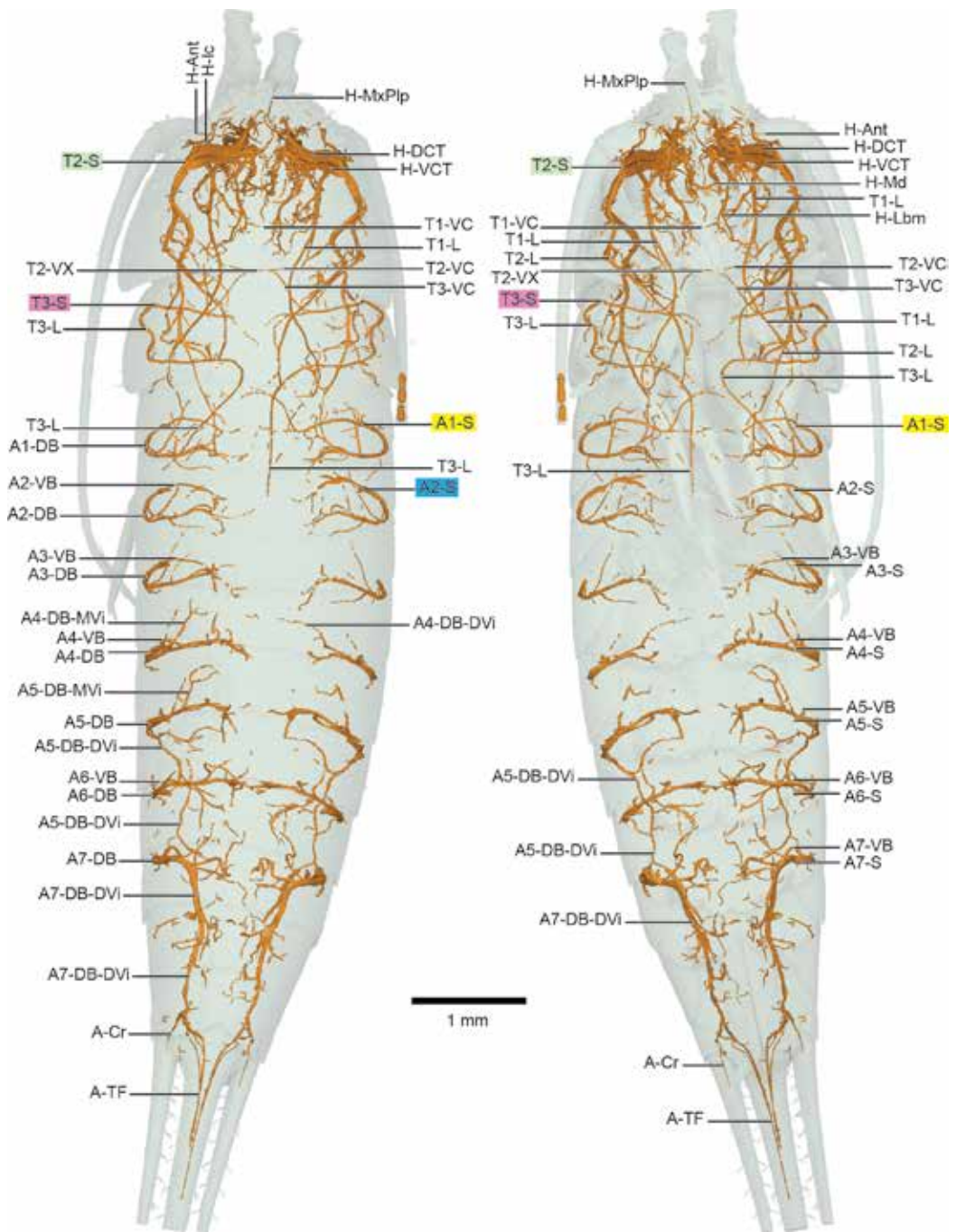


FIGURE 9. *Trigoniphthalmus alternatus* (Archaeognatha: Machilidae), dorsal (left) and ventral (right) views.

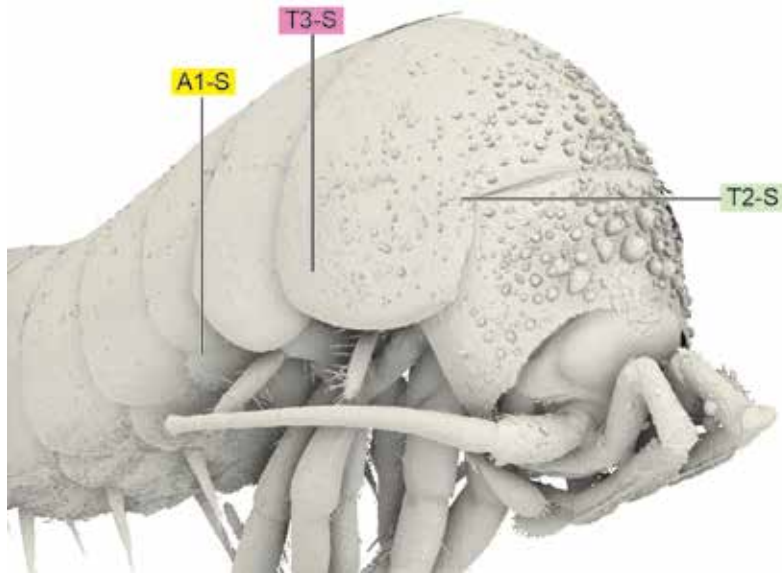


FIGURE 10. *Trigoniphthalmus* (Archaeognatha) head detail front-right view, showing location of T2-S, anterior and under mesothoracic tergum. Positions of T3-S and A1-S, likewise under tergites, also shown. Direct screen capture from 3D Slicer.

dividing into A-TF and A-Cr; neither A5-DB-DVi nor A7-DB-DVi connect to spiracles of other segments. A-TF with two tracheae per side (4 total); A-Cr single trachea per cercus.

ORDER ZYGENTOMA

There are very few micro-CT studies of *Zygentoma* to date; most notably, synchrotron radiation micro-CT of *Tricholepidion gertschi* heads has been used to investigate *Zygentoma* morphology for systematic study (Blanke et al., 2014), but not tracheae. This genus is particularly significant given the disputed placements within and near *Zygentoma* (Engel, 2006; Blanke et al., 2014). *Zygentoma* are relevant in general as a sister group to the pterygotes, and indeed they share several tracheal synapomorphies. Three specimens from two orders were scanned here: *Thermobia domestica* and *Lepisma saccharinum* from Lepismatidae, and the relict silverfish *Tricholepidion gertschi* from Lepidotrichidae. Scan resolutions were within a $2.4 \mu\text{m}^3/\text{voxel}$ range, with

Lepisma at the highest resolution of $4.8 \mu\text{m}^3/\text{voxel}$ and *Thermobia* with the lowest resolution at $7.2 \mu\text{m}^3/\text{voxel}$. Resolving the smallest tracheae at these resolutions tends to be more a function of specimen preservation rather than scanning parameters. Although the level of detail varies slightly between these scans, sufficient resolution was achieved to locate small visceral tracheae in all three specimens, indicating suitability for comparative purposes. Although the zygentoman head morphology is similar among the specimens, in the sections below Lepidotrichidae thoracic and abdominal detail are described separately due to substantial differences.

Tricholepidion appears to possess only two pairs of functional abdominal spiracles, A7-S and A8-S. The elongate, sinusoidal trunks beginning at A7-S and extending anteriorly to the thorax are not present in the two lepismatid specimens. If *Tricholepidion* is indeed basal to Lepismatidae, it is possible that these trunks are plesiomorphic, and a loss of these tracheae in *Thermobia* and *Lepisma* could be derived.

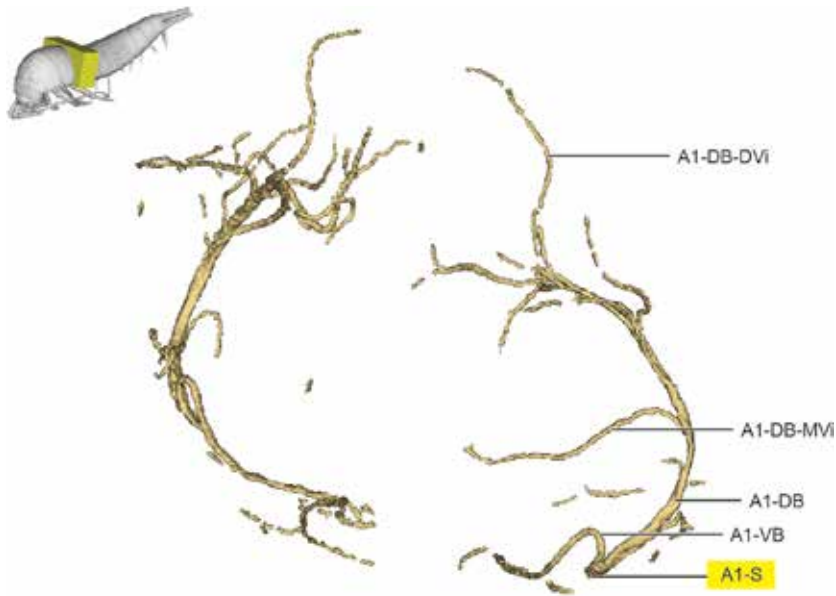


FIGURE 11. *Trigoniphthalmus alternatus* (Archaeognatha: Machilidae) abdominal tracheal detail, abdominal segment 1.

In both species scanned from Lepismatidae, leg tracheae branch from T2-S and T3-S in an arc leading posteriorly into the legs, each with a small branch extending dorsad. Here we interpret these as T2-AWL and T3-AWL, with T2-AWba and T3-AWba branching dorsad. An alternative pattern is to designate these dorsal branches as simply T2,3-L-DVi, but the similarity of the branching pattern with both apterous and winged taxa included herein (e.g., *Grylloblatta*) strongly suggests homology with these wing base tracheae; Šulc (1927) interpreted these as possible wing tracheae.

DESCRIPTION: HEAD: H-DCT with two branches: H-Ft dorsal; H-Ant-Lbr anteriad and slightly ventral, dividing into H-Ant and H-Lbr close to base of antenna. H-VCT with three branches, dividing at approximately same location: small H-Lbm extends ventrally; H-Mx continues anteriorly before proceeding ventrad; larger H-Oc-Md extends anteriorly. H-VC absent in *T. gertschi* but present in both Lepismatidae. H-Oc branching dorsally, H-Md continues anteriorly and ventrad, following shape of mandibular sclerite.

THORAX: *Tricholepidion* with significant differences among *Zygentoma*, notably T2-DLT and T3-DLT elongate, with dorsal visceral branches similar to T2-DB and T3-DB; a complete description of the thorax of *Tricholepidion* thorax is below. For both Lepismatidae: T2-S with three branches: T2-CT, T2-AWL, and T2-VB. T2-CT very thick, running directly anteriad with T2-DB just anterior to T2-S; T2-CT dividing into H-DCT and H-VCT in prothorax. Thinner T2-AWL arcing posteriorly, slightly dorsad, with thin but prominent dorsad and posteriorly arcing T2-AWba. T2-ACx present with T2-VC, remainder of T2-AWL extending into midleg as T2-L. T2-DB dividing into T2-DLT, extending in posterior arc and T1-DLT, ending blind in prothorax. Small T1-Pn present just anterior of H-DCT/H-VCT split. T1-L branching ventrally from H-VCT; T1-L with T1-VC branch present; T1-ACx from T1-VC; T1-PCx from T1-L. Small T2-VB with T2-VB-Vi. T2-L two branches: prominent, dorsad and posteriorly arcing T2-L-DVi. *Thermobia* with T2-PCx from T2-L, note that T2-PCx is from T2-VB in *Lepisma*. T2-VC

with connection from T3-AsymC medially, originating from left side in *Thermobia* and right side in *L. saccharinum*. T3-S with three branches: T3-DB, T3-AWL, and T3-VB. T3-DB directly dorsal with Y-shaped bifurcation to T2-DLT from anterior and T3-DLT toward A1-S. T3-AWL posteriad with T3-AWba, longer in *Lepisma* than *Thermobia*. T3-PCx from T3-L in *T. domestica*, T3-VC in *L. saccharinum*. T3-VB ventral and slightly inward with AsymC from left side of *T. domestica*, right side of *L. saccharinum*, anterior to connect with T2-VC.

ABDOMEN: *T. gertschi* with significant differences to other *Zygentoma*, including apparent lack of functional abdominal spiracles (except A7-S and A8-S), and a sinusoidal A7-VLT extending anteriorly over several segments; a complete description of abdomen is below. For Lepismatidae: A1.8-S present, all located laterally. *An-SB* present for segments in middle of abdomen but variable; see detailed descriptions. *An-S* (or *An-SB*) with *An-DB* and *An-VB* present. *An-DB* running dorsad, bifurcating into Y-shaped junction with *An-DLT* anterior and posteriad; all abdominal segments connected via dorsal trunk. *An-VB* running ventrad, connecting with opposite side via thin *An-VC*; A1.7-VC present in *T. domestica*, A4.7-VC not visible in *L. saccharinum* scan but likely present; A8-VC absent. *An-DB-Vi* and *An-VB-Vi* numerous, see sections below for details. A8-DB and A8-VB large, curving medially before proceeding posteriad; A8-DB with A-TF and A-Cr in *T. domestica* but not visible in *L. saccharinum* scan (presence/absence ambiguous).

FAMILY LEPIDOTRICHIDAE

Tricholepidion gertschi

“Relic Silverfish”

Figures 12 (lateral), 13 (dorsal, ventral)

Plates 4 (lateral), 5 (dorsal, ventral)

The sole extant member of Lepidotrichidae, *T. gertschi* features some unusual tracheal mor-

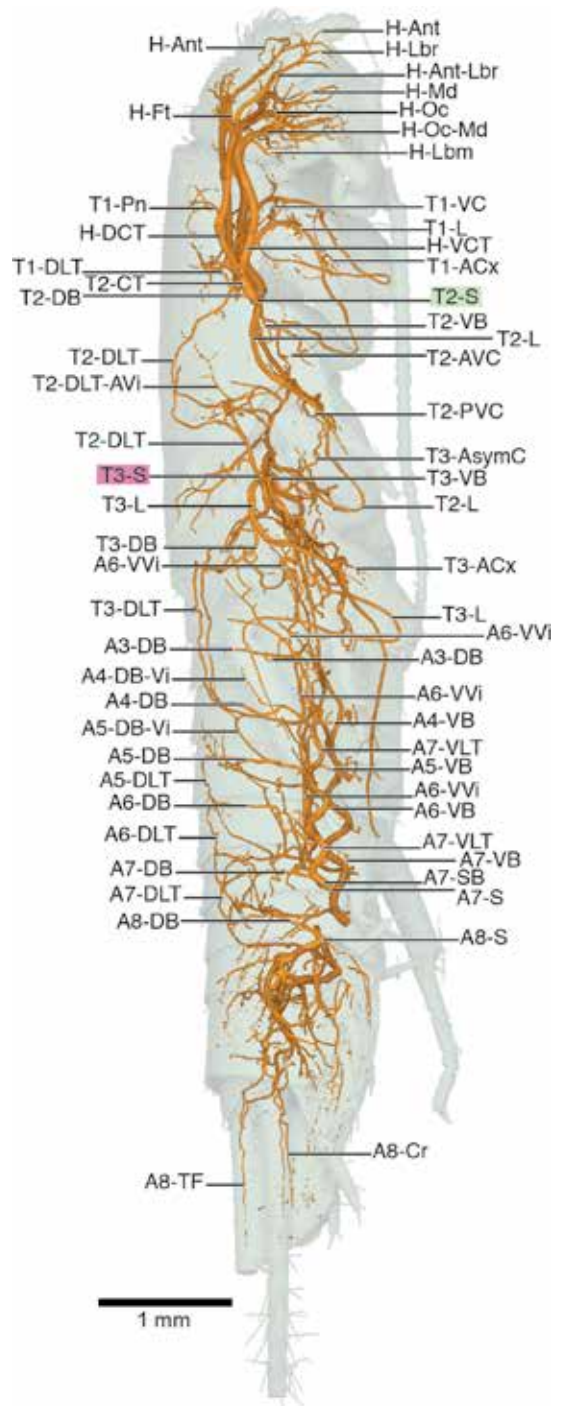


FIGURE 12. *Tricholepidion gertschi* (*Zygentoma*: Lepidotrichidae), lateral view.

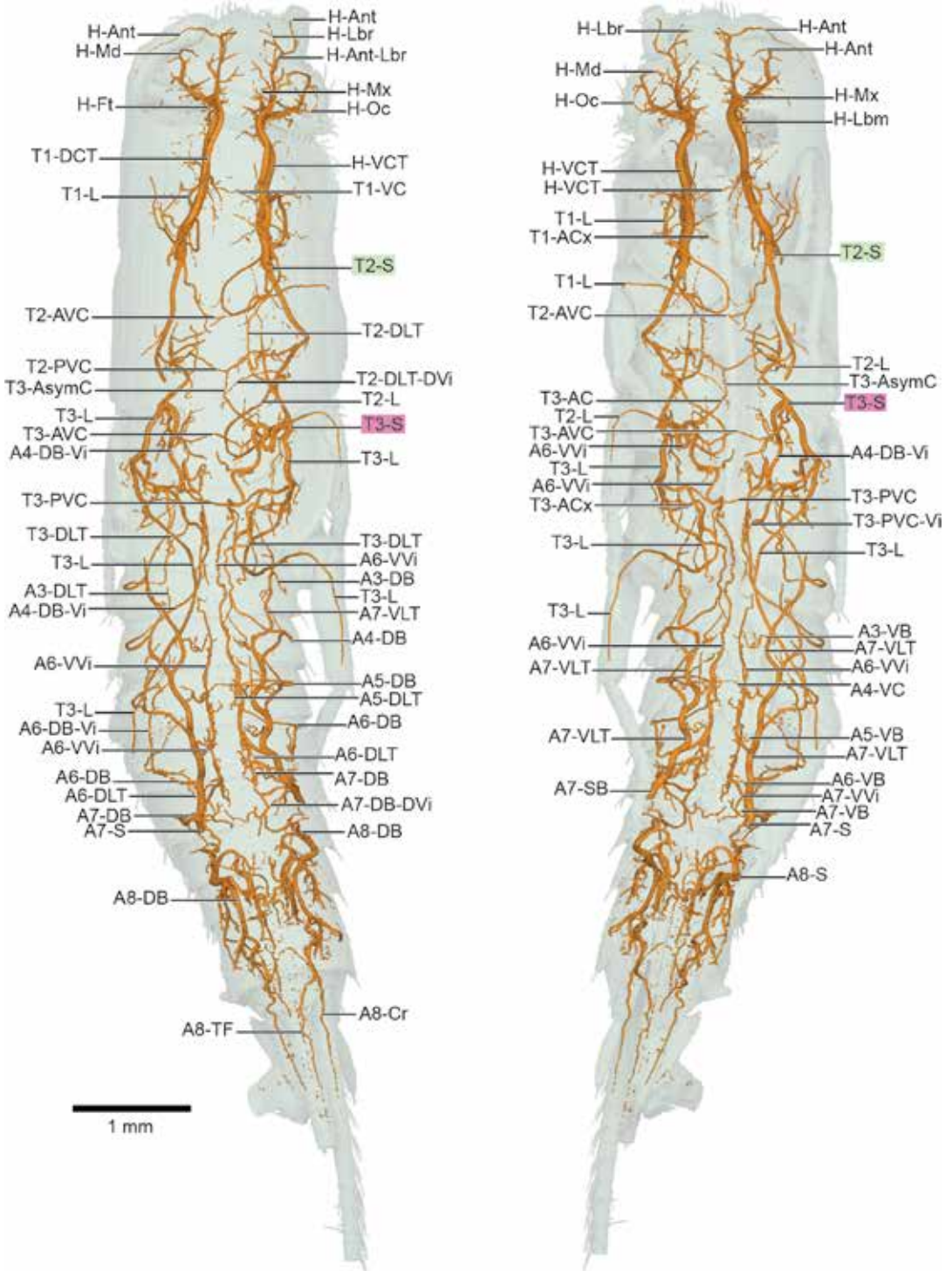


FIGURE 13. *Tricholepidion gertschi* (Zygentoma: Lepidotrichidae), dorsal (left) and ventral (right) views.

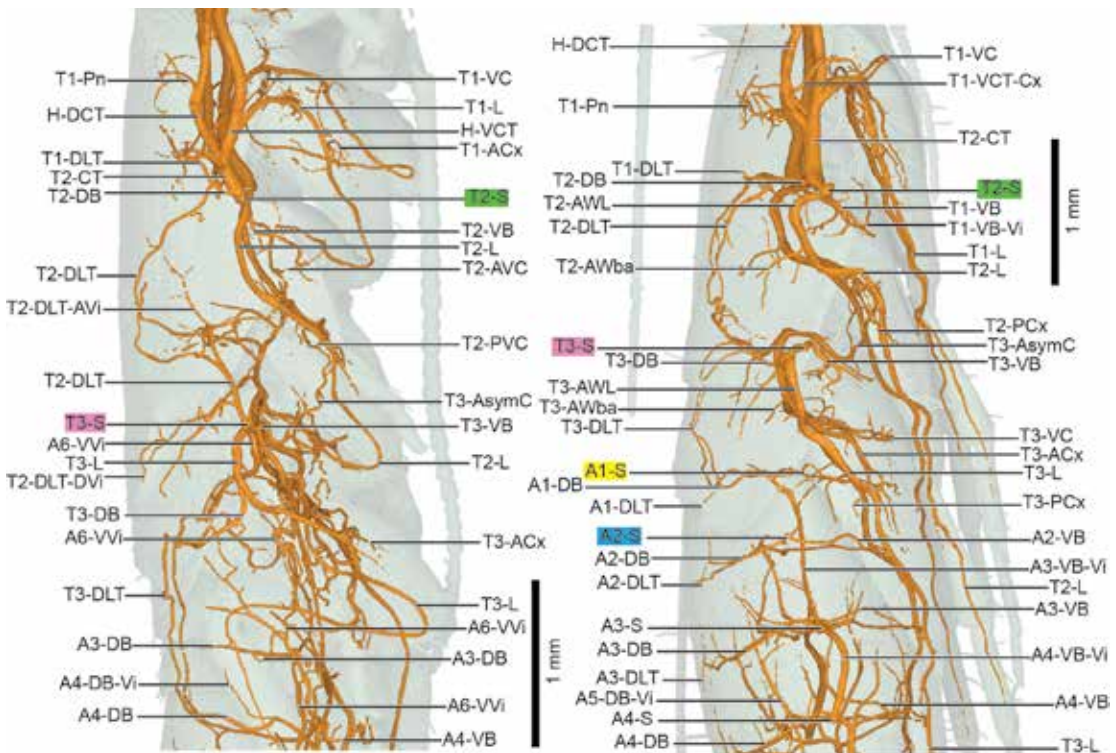


FIGURE 14. *Tricholepidion gertschi* (left) and *Thermobia domestica* (right) thoracic tracheae detail. Note T2-Wba and T3-Wba in *Thermobia* but absent in *Tricholepidion*, and unusual T2-DLT and T3-DLT in *Tricholepidion*.

phology. While the head tracheae are quite similar to the two Lepismatidae, the thorax and abdomen are described separately here because of their distinctiveness.

Mentioned above in the ordinal-level overview, the sinusoidal VLT beginning at A7 and proceeding anteriorly is interpreted here as a VLT. However, this trunk does not connect spiracles along the length of the insect, and it may not be truly homologous to *An*-VLT in other groups. As this *An*-VLT is also not present in other Zygentoma, it could be an apomorphy of *Tricholepidion* or, as mentioned above, represent a range of plesiomorphies in abdominal trunk development that appeared in the early lineages leading to the Pterygota. In the thorax, T3-DLT is asymmetric, and is interpreted differently based on the right or left side, in that T3-DB-Vi connects as expected relative

to the spiracle on one side, but not the other. Scanning of additional specimens would indicate if this morphology is a “teratology” unique to this particular specimen or a condition found in all *Tricholepidion*.

DESCRIPTION: HEAD: H-DCT slightly smaller in diameter (approx. 55 μm) than H-VCT (approx. 80 μm) at entry into head capsule. H-VCT with small H-VCT-DVi running dorsad prior to division into H-Lbm, H-Hx, and H-Oc-Ant. H-VC absent.

THORAX: Meso- and metathorax with substantial differences from Lepismatidae, see figure 14. T2-S with three branches, very thick T2-CT directly anterior; smaller T2-L arcing posteriorly and slightly dorsad then ventrally; small T2-VB. T2-AWba absent. T2-CT with T2-DB just anterior of T2-S; T2-CT dividing into H-DCT and H-VCT in prothorax. T1-Pn

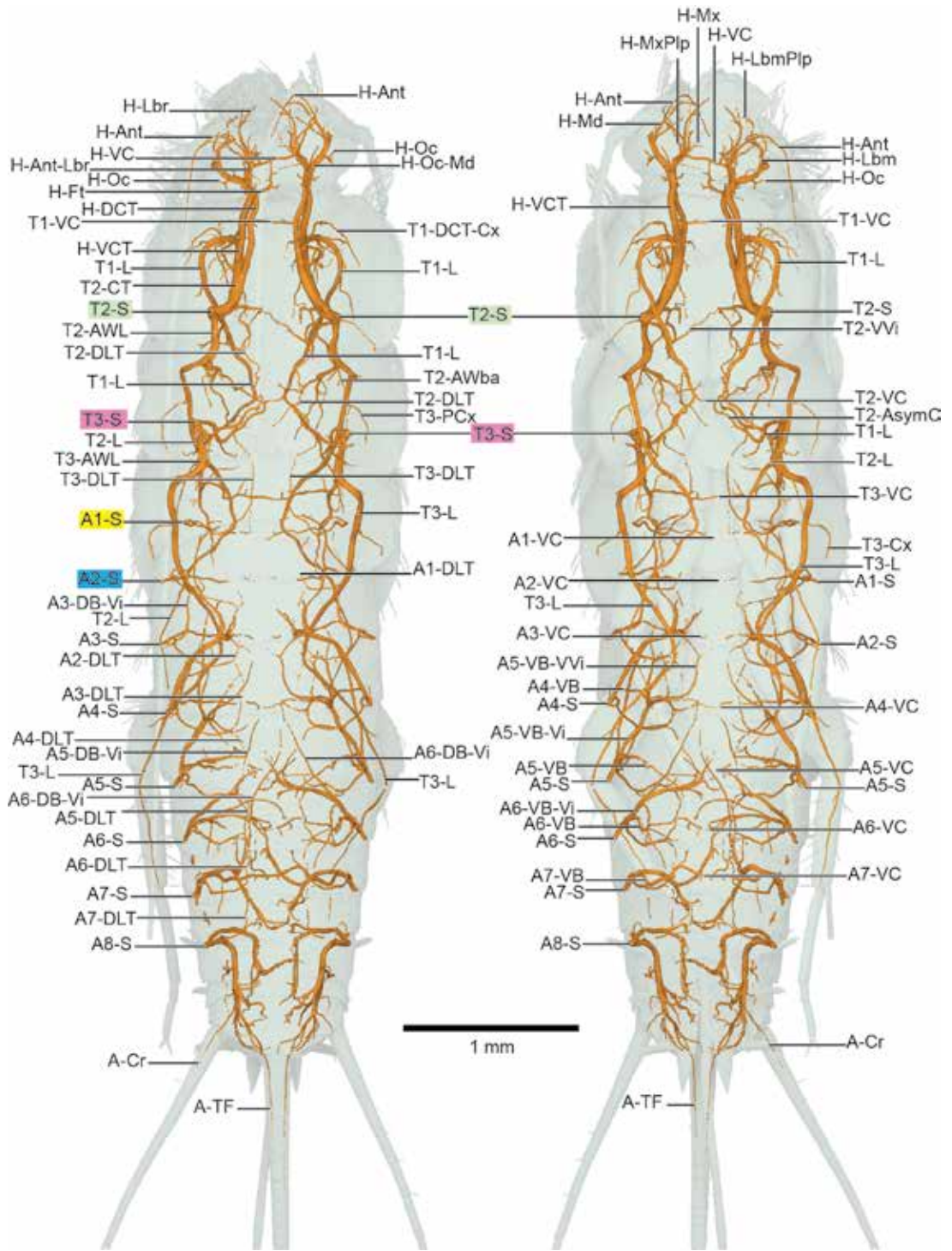


FIGURE 16. *Thermobia domestica* (Zygentoma: Lepismatidae), dorsal (left) and ventral (right) views.

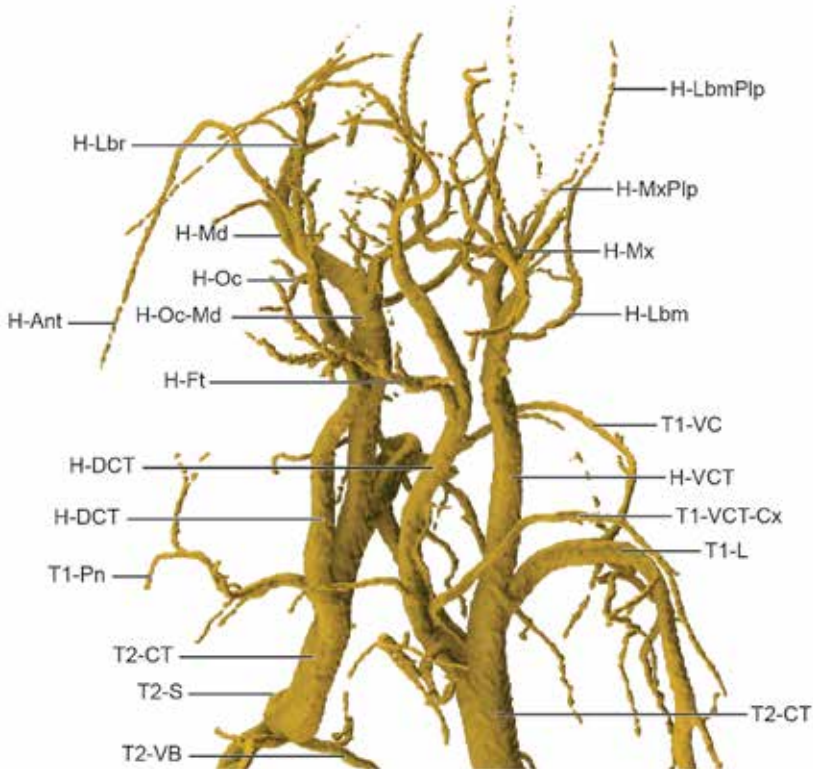


FIGURE 17. Detail of *Thermobia* head tracheae, quarter-dorsal view (rotated axially).

ABDOMEN: A1..6-S absent, A7-S and A8-S present. A7-S with short A7-SB, continuing anteriorly as sinusoidal A7-VLT, terminating in metathorax. A7-VLT with A3..7-DB dorsally, generally linking with respective *An*-DLT sections with the exception of short A3-DB on right side. A2-DB not present. Several visceral tracheae anterior to A3..7-DB and A7-VLT, two with notable morphology: A6-VVi on right side, extending anteriorly to connect with T3-S; A4-DB-Vi, likewise connecting with T3-S on left side. A6-VVi also prominent on left side, extending anteriorly, ending blind near third abdominal segment. A4-DB-Vi on right side short. A4-DB connecting with T3-DLT. Short A3..6-VB present, extending from A7-VLT; A4-VC visible. A7-DB splits into three tracheae on right side, all connecting to A7-DLT.

FAMILY LEPISMATIDAE

Thermobia domestica

“Firebrat”

Figures 15 (lateral), 16 (dorsal, ventral)

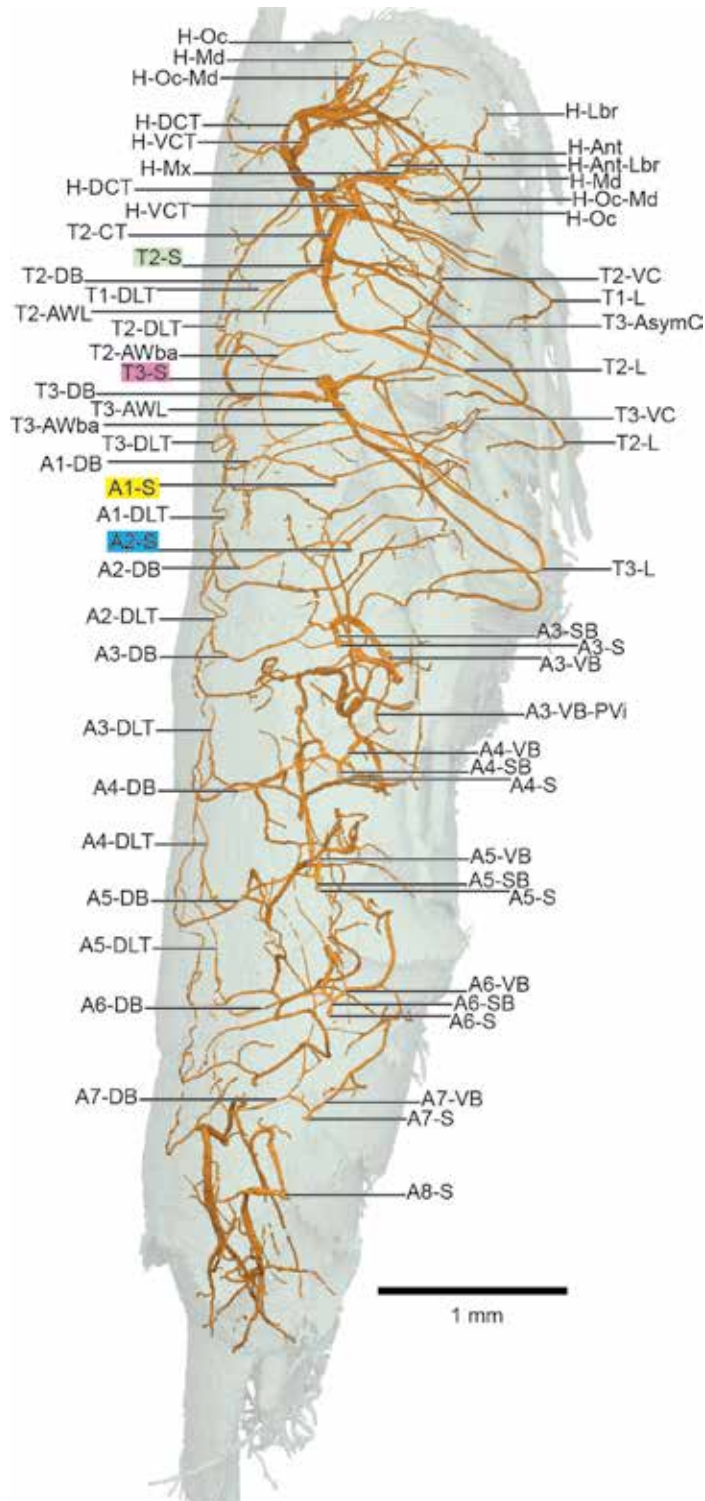
Plates 6 (lateral), 7 (dorsal, ventral)

DESCRIPTION: HEAD: H-LbmPlp and H-MxPlp discernible. H-VC present, branching from H-Mx. Head detail, figure 17.

THORAX: H-VCT with T1-VCT-Cx on right side only. T2-DB long, extending dorsad before splitting into T1-DLT and T2-DLT. Short T3-SB present. T3-PCx extending from T3-L.

ABDOMEN: A2..6-SB present on specimen left side, A5-SB and A6-SB prominent; A5-SB and

FIGURE 18. *Lepisma saccharinum* (*Zygentoma*: Lepismatidae) lateral view.



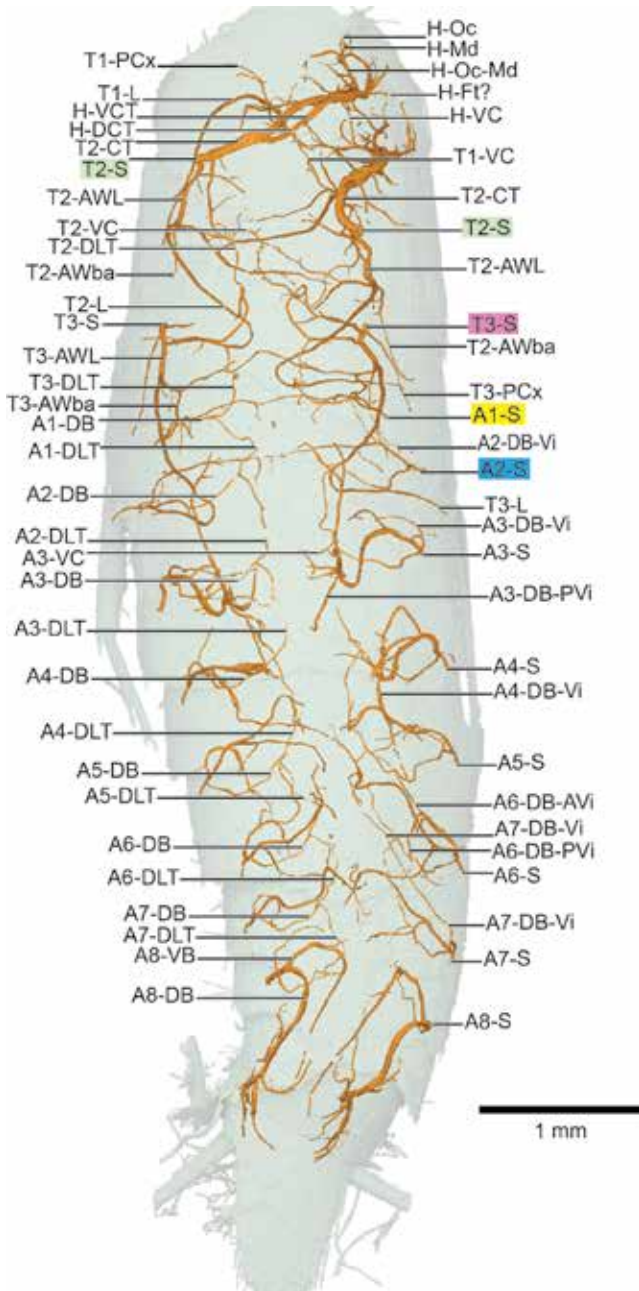


FIGURE 19. *Lepisma saccharinum* (Zygentoma: Lepismatidae) dorsal view.

A6-SB present on right side. *An*-DB antieriad, with visceral tracheae branching anteriorly before dorsal branch divides into Y-shaped connection with *An*-DLT anteriorly and posteriad. A4..7-VB-Vi large and branching antieriad, typically spanning multiple segments, with smaller A4..7-VB continuing ventrad, connecting to opposing side via A4..7-VC; A4-VB-Vi, A5-VB-Vi larger, each dividing into several smaller visceral tracheae and spanning several segments; A6-VB-Vi large but extending anteriorly just past A5-S; A7-VB-Vi similar, with several visceral tracheal branches, extending both antieriad and posteriorly. A8-DB running toward midline before turning posteriad, dividing into several smaller tracheae and A-TF, A-Cr. A8-VB running dorsally along body wall, turning sharply posteriorly.

Lepisma saccharinum

“Silverfish”

Figures 18 (lateral), 19 (dorsal), 20 (ventral)

Plates 8 (lateral), 9 (dorsal), 10 (ventral)

The tracheal system of *Lepisma saccharinum* was first detailed by Šulc (1927), and his terminology from this study can be found in supplementary table S1.

DESCRIPTION: HEAD. H-VC present, branching from H-Mx.

THORAX: T2-PCx extending laterally from T2-VB. T3-SB absent; T3-VB extending directly from T3-S. T3-SB present. T3-PCx branching from T3-VC.

ABDOMEN: A1..7-SB present; A3..6-SB more prominent. *An*-DB extending antieriad, several segments with visceral tracheae branching before dorsal branch that divides into Y-shaped con-

nection with *An*-DLT anterior and posterior. A4-DB-Vi prominent and asymmetric, right side extending anteriorly briefly before sharp turn toward posterior, reaching as far as A5-S; left side smaller, extending posteriorly and ventrad. A6-DB with A6-DB-AVi, A6-DB-PVi not extending beyond segment. A7-DB-Vi asymmetric, with short left side but elongate right, extending anteriorly past A5-S. A1-VB and A2-VB extending to form A1-VC, A2-VC. A3-VB similar, extending toward position of (not visible but likely present) A3-VC; larger A3-VB-Vi branching toward midline. A3-VB-Vi subdivides into A3-VB-AVi, extending anteriorly to metathorax, A3-VB-PVi running posteriorly but not crossing into following segment. A4.6-VB-Vi similar, larger than A4.6-VB and branching toward midline, extending anteriorly as far as neighboring segment. A7-VB-Vi asymmetric; left side beginning ventrally before curving dorsad, ending near A7-DLT; right side shorter and ending ventrad near midline. A8-DB, A8-VB large and ventrad toward terminalia; A-TF and A-Cr not discernible in this scan.

ORDER EPHEMEROPTERA

Ephemeroptera are unique in having a winged subimago developmental stage; all other pterygotes have lost this molt as winged individuals. Additionally (and relevant to tracheation), Ephemeroptera, like Odonata, possess direct flight muscles, where the wing muscles insert directly at the wing bases. Mayfly tracheae were first described in detail by Swammerdam (1737; see fig. 1), and modern treatments include Needham et al. (1935), Landa (1948, 1969), and Soldán (1979). Chapman (1918) included a discussion of wing tracheae of mayflies in his early comparative analysis.

For this study, three mayfly specimens were scanned: an adult *Ephemera* sp. (Ephemeridae) and *Neocloeon triangulifer* subimago and adult (Baetidae). The *Neocloeon* specimens afforded the opportunity to compare tracheal architecture

between the winged stages. Although scan resolution ranged from 13 μm for *Ephemera* sp. to 2 μm for the adult *Neocloeon*, sufficient detail was achieved to determine that all three specimens of both taxa are remarkably similar in tracheal architecture, the primary difference being the morphology of the air sac. Adult Ephemeroptera do not feed, and the alimentary canal forms a large, central air sac (Soldán, 1979), perhaps aiding the emergence of the alate subimago from the water, with visceral trachea either reduced or displaced. While not complete until the adult stage, the subimago possesses smaller but substantial air spaces that fuse to form the single adult air sac (see fig. 21). As air sacs in tracheal visualizations can obscure details of smaller branches, all air sacs are omitted from the Ephemeroptera plates. Due to the size of the wings, Ephemeroptera plates are shown with the wings cropped to show as much detail as possible without scaling the image to fit the page. Other minor differences between specimens are described in their respective sections below.

T2-S is the start point of the longitudinal trunk, which arcs toward the midline of the body for a short distance before turning posteriorly and proceeding all the way to the terminalia. While similar structures have been noted in the larvae of many insect orders (Snodgrass, 1935; Whitten, 1960; Wigglesworth, 1972), the presence of a large, nearly linear longitudinal trunk in an adult that spans the length of the body appears to be unique to Ephemeroptera. This structure is likely homologous with the dorsal longitudinal trunk seen in other taxa, and individual segments of the trachea are referred as such, beginning with T2-DLT as the start. The thoracic portion of the DLT in *Ephemera* appears to be two tracheae, arranged dorsoventrally. This is the result of compression in the thorax—distention of the air-filled alimentary canal, compression by packing material for CT scanning, or postmortem settling of tissues can all contribute to deformation of tracheae in soft-bodied insects such as mayflies.

Noted by Chapman (1918), Ephemeroptera possess only anterior wing base tracheae (T2,3-

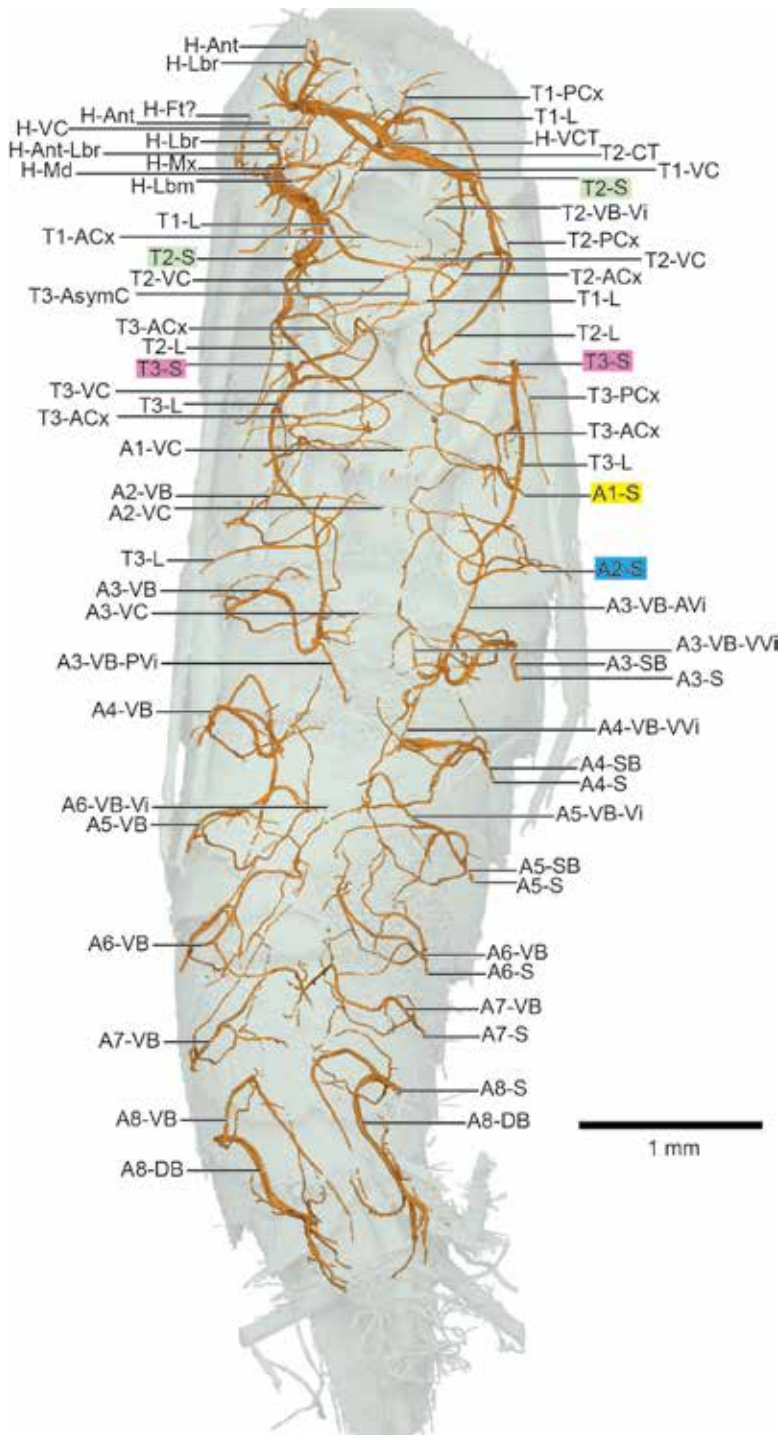


FIGURE 20. *Lepisma saccharinum* (Zygentoma: Lepismatidae) ventral view.

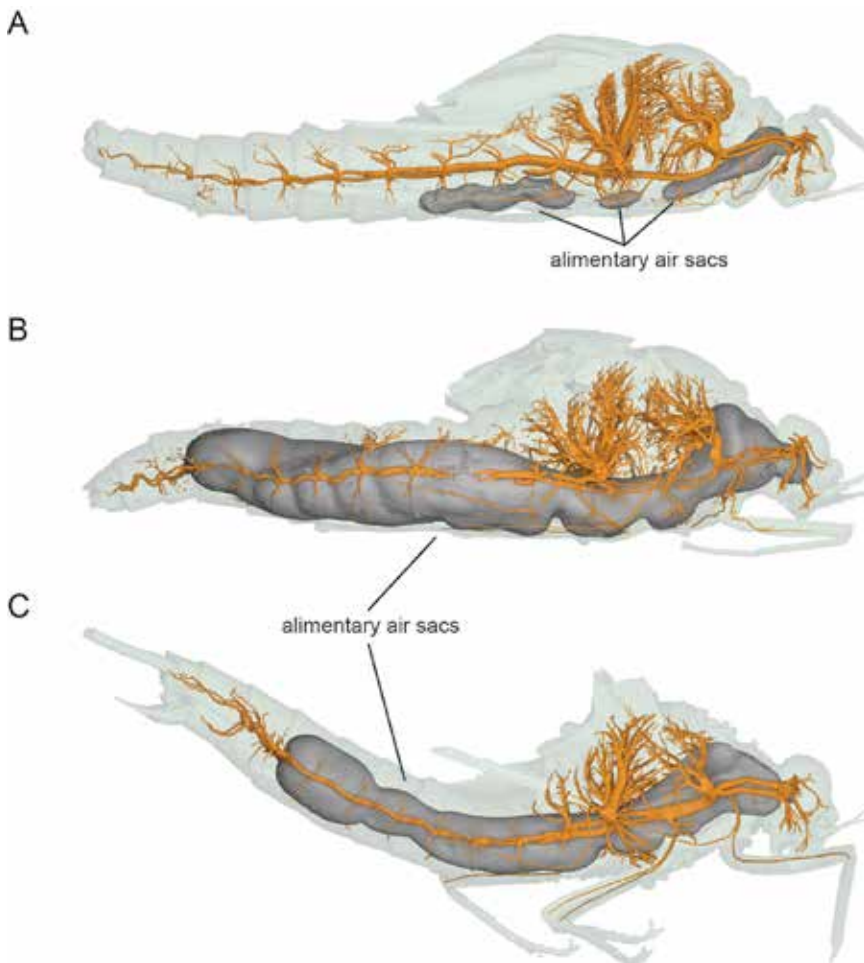


FIGURE 21. Air sacs formed from alimentary canal in subimago and adult Ephemeroptera, shown in lateral views. **A.** *Neocloeon triangulifer* subimago; **B.** *N. triangulifer* adult; **C.** *Ephemerella* sp. adult. Specimens not to same scale.

AWba), extending into the wing as T2,3-W-c-r with the corresponding PWba and W-cu-a tracheae absent. This lack of a branch leading to the trailing-edge wing tracheae is a condition apparently unique to mayflies.

The three ephemeropteran specimens display some disparity in the origins of H-Oc branches. These appear to be developmental variations, as larger trunks may supply different regions as smaller tracheae “sprout” from them during ontogeny.

It remains unclear whether all abdominal spiracles are functional. Needham et al. (1935)

indicates that abdominal spiracles may be continuously open, but close examination of the spiracular openings via CT cross section suggests that A2-S through A7-S may be closed or unused.

DESCRIPTION: BODY: Adults with long central air sac formed from modified alimentary canal, extending from head capsule to end of 7th abdominal segment; subimago with individual air sacs that fuse in the imago (see fig. 21).

HEAD: Tracheal morphology largely from Landa (1948), but with unified nomenclature here. Palmen’s organ (H-PO) prominent and

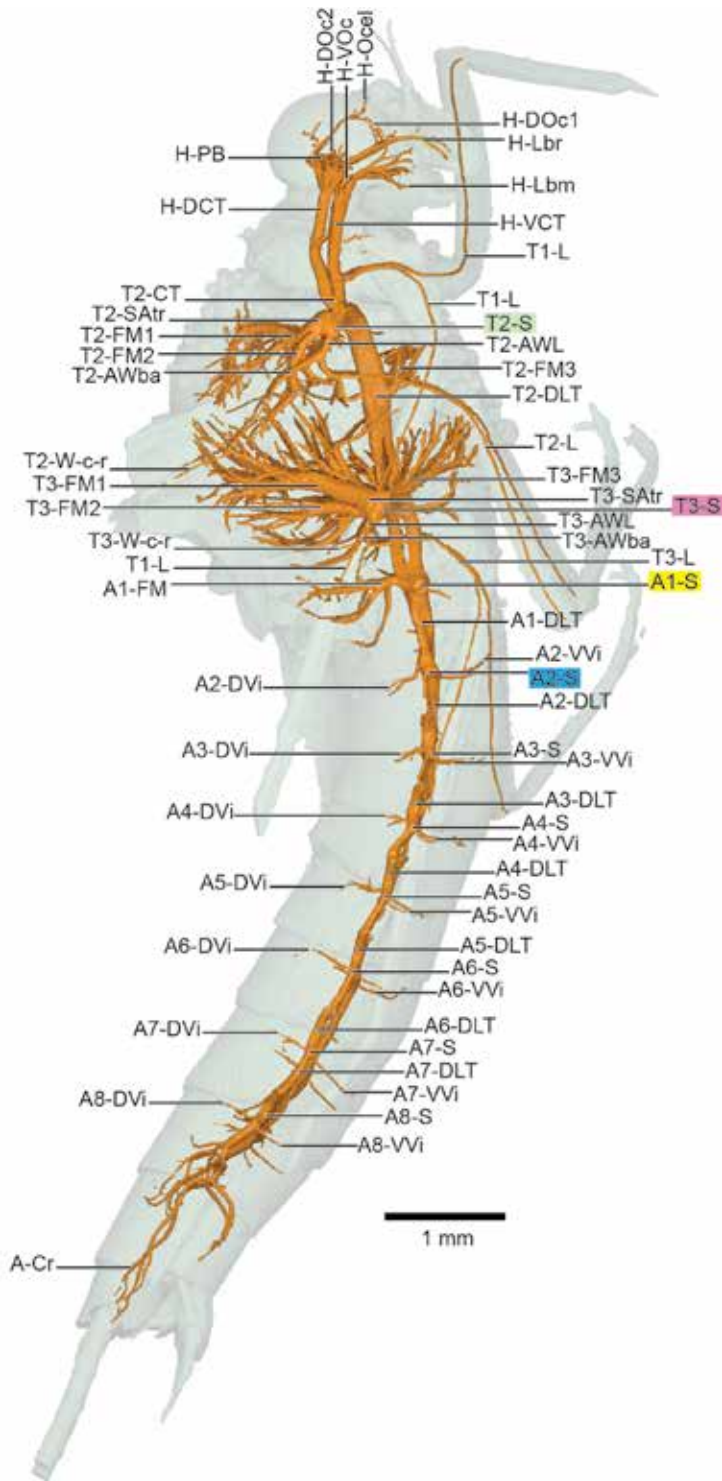


FIGURE 22. *Ephemera* (Ephemeroptera: Ephemeridae) lateral view.

centrally located. Just after entry into head capsule, thick H-DCT bifurcates into two tracheae; dorsal one of these proceeds anteriorly a short distance before dividing into H-Ocel and dorsal branch to H-PO; ventrally H-Lbr branches anteriorly shortly with H-DOc branch before remaining trachea turns directly ventrad; H-Lbr continues toward reduced mouthparts with small H-Ant branch at base of antennae. H-VCT thick, splits into three branches at base of head capsule: H-VOc, extending laterally toward eye; H-Lbm directly ventrad, and ventrally supplying H-PO.

THORAX: T2-S with three branches: T2-CT, T2-SAttr, and T2-DLT. T2-CT very short, before bifurcating into anterior H-DCT and H-VCT at posterior margin of prothorax. T1-L branching directly ventrad from T2-VCT anterior of H-DCT/H-VCT split from T2-CT. T2-SAttr dorsal, with T2-AWL posteriad and multiple T2-FM dorsad: thick T2-FM1 splitting dorsally and subdividing into smaller tracheae that supply flight muscles, thinner T2-FM2 running dorsad and slightly posteriad; T2-AWL arcing briefly dorsad and posteriad before proceeding ventrad into midleg as T2-L, with T2-AWba branching near dorsal apex of arc and continuing to T2-W-c-r. T2-PWba absent. T2-DLT very thick, beginning mediad before arcing directly posteriad and continuing to the terminalia. Small T2-FM3 extends ventrally from T2-DLT midway between T2-S and T3-S. T3-S opens into very thick T3-SAttr, with (effectively) five branches: T3-DB, T3-AWL, and three T3-FM. T3-DB runs directly mediad, linking with T2-DLT from anterior, continuing directly posteriad as T3-DLT. T3-AWL arcing briefly dorsad and then posteriad, similar to T2-AWL, with T3-Wba branching near apex of arc while T3-L continues into hindleg; T3-Wba continues as T3-W-c-r into wing. T3-PWba absent. T3-FM1 very thick, extends directly dorsad and T2-FM2 posteriad and slightly ventrad into flight muscle; T3-FM3 runs ventrad in fanlike extension into flight muscle.

ABDOMEN: A1-S, A8-S functional; unclear if A2..7-S connect through body wall. A1-S modified, with large A1-FM dorsally; T3-DLT from anterior, continuing posteriad as A1-DLT. Remaining abdominal segments similar, with *An-S* linked with neighboring segments via *An-DLT* extending linearly through abdomen past A8-S. A8-DLT extending into terminalia as A-Cr. All *An-S* with various visceral tracheae extending dorsad and posteriad from *An-S*, dorsal and ventral commissures absent.

FAMILY EPHEMERIDAE

Ephemera sp.

“Burrowing mayflies”

Figures 22 (lateral), 23 (dorsal, ventral)

Plates 11 (lateral), 12 (dorsal), 13 (ventral)

Ephemera sp., a much larger species at approximately 1 cm body length, was scanned at 13.1 μm voxel size, lower resolution than the two baetid specimens at 2.3 μm and 4.1 μm . Smaller abdominal visceral tracheae visible in the baetid scans are likely present in *Ephemera* but not visible at the scanned resolution.

DESCRIPTION: HEAD: Two H-DOc: H-DOc1 extending from H-Ocel, H-DOc2 from H-DCT. H-Ant barely visible in this scan, likely due to lower resolution.

THORAX: T1-VVi originating from H-DCT on left side; T1-VVi1 from H-DCT and T1-VVi2 from H-VCT on right side.

FAMILY BAETIDAE

Two baetids were scanned to investigate developmental changes. These are two separate specimens, not the same specimen scanned twice, as done in beetles by Lehmann et al. (2021). Tracheal morphology between subimago and adult is strikingly consistent, apart from the single alimentary air sac in the adult (vs. divided in subimago), indicating that tracheal development is essentially complete by the subimago stage.

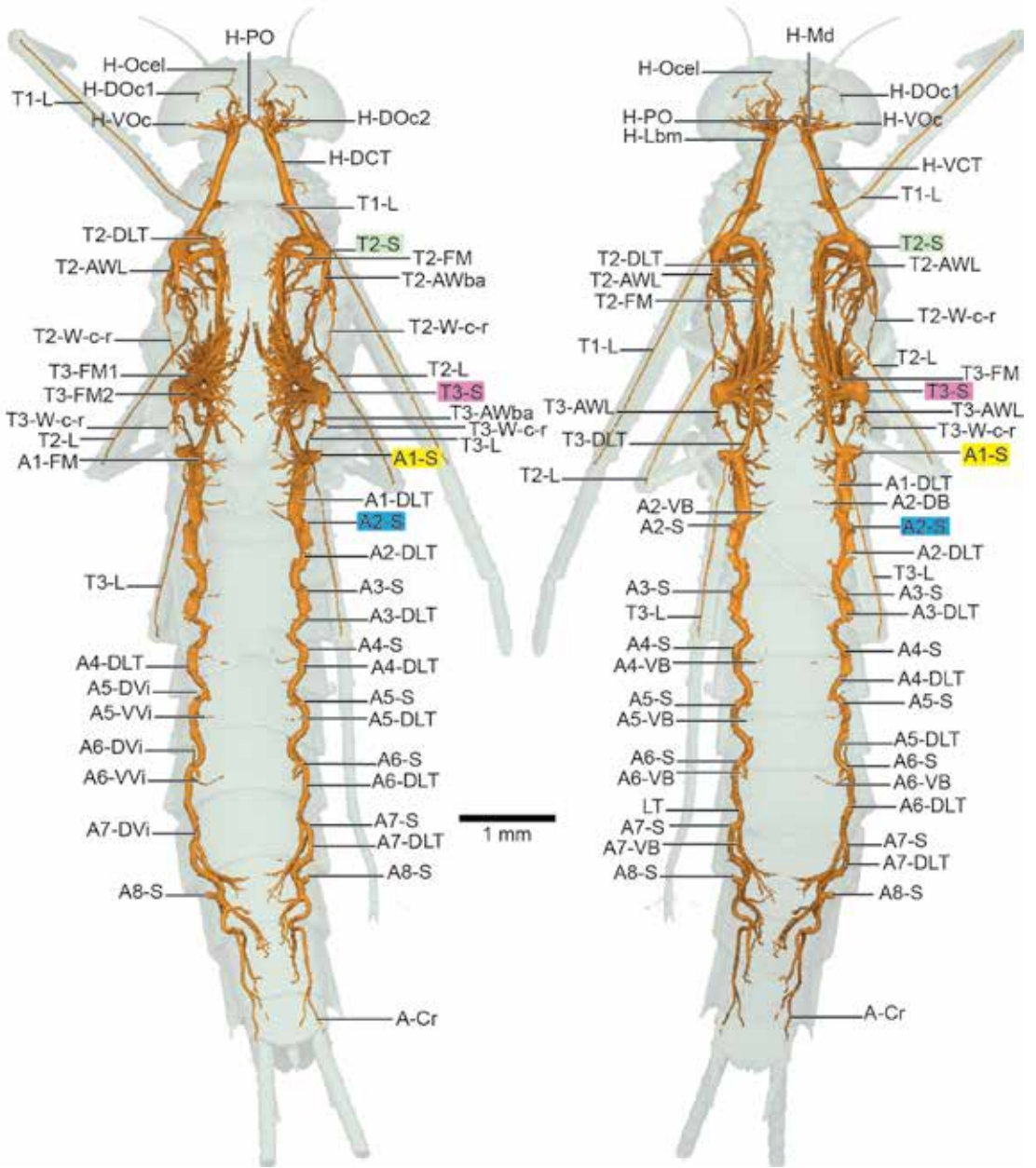


FIGURE 23. *Ephemera* (Ephemeroptera: Ephemeridae) dorsal (left) and ventral (right) views.

Neocloeon triangulifer subimago

“Triangle small minnow mayfly”

Figures 24 (lateral), 25 (dorsal, ventral)

Plates 14 (lateral), 15 (dorsal, ventral)

DESCRIPTION: BODY: Several alimentary canal air spaces present, fusing into single one in adult.

HEAD: H-DCT and H-VCT similar in size, extend into head capsule from prothorax.

THORAX: T1-DVi branches from H-VCT on left side, H-DCT on right.

ABDOMEN: A2..7-Gi gill attachments visible laterally on *An-DLT*, midway between spiracles; A1-Gi on posteroventral extension from A1-S, reduced in adult (no other vestiges of gill attachment sites present in adults). Several dorsal visceral tracheae extend anteriorly beyond segment boundaries; ventral Vi (retained) within segment.

Neocloeon triangulifer adult

“Triangle small minnow mayfly”

Figures 26 (lateral), 27 (dorsal, ventral)

Plates 16 (lateral), 17 (dorsal, ventral)

DESCRIPTION: H-DCT, H-VCT, T_n-DLT, *An-DLT*, and several T_n-FM compressed laterally along some sections; since subimago maintains these as broad tracheal lumina, this is likely a preservation artifact in the adult.

BODY: Single air sac, coopted from alimentary canal, extending from head capsule to end of 7th abdominal segment (see fig. 21).

HEAD: As above, but with H-DOc extending from trachea leading to H-PO.

THORAX: T1-DVi from H-VCT.

ORDER ODONATA

Respiration in Odonata, especially aquatic naiad immatures, has been the subject of investigation for some time, although much of the morphological work was performed more than a century ago. Scott (1905) presented one of the

earliest detailed studies on dragonfly tracheae using a libellulid immature, highlighting notable characteristics such as the crossover of longitudinal trunks leading from the thorax to the abdomen, a trait retained in the adult. Tillyard (1917) remains the standard for dragonfly morphology, and he carefully diagrammed the tracheal architecture via dissection, although also with an emphasis on immatures. Chapman (1918) included both *Anax* and *Lestes* in his comparative study of leg-wing tracheal morphology. Kennedy (1922) built on Chapman's work, extending it to abdominal tracheae; his extension to multiple orders insects using only odonate specimens is shown here to be insufficient. Recent studies have investigated physiological aspects, including active tracheal compression (likely related to respiration) in Odonata observed through synchrotron imaging by Westneat et al. (2003). For this study, three odonates were scanned, an aeshnid dragonfly larva at 30 μm resolution, an adult aeshnid at 21 μm resolution, and a calopterygid damselfly at 19 μm. As noted above, the wings of the adult aeshnid were removed and scanned separately; wing scans are not included here, though wing-base tracheae are retained and labeled.

Tillyard (1917) identified three pairs of longitudinal trunks in his figure 75 (included here as fig. 28), whereas the aeshnid and calopterygid specimens here possess four, a condition not seen in any other order. *An-DLT* is comprised of elongated and compartmentalized air-sac-like tracheae connected segmentally or perhaps intermittently by regular tubular tracheae, and these were likely misidentified by Tillyard as air sacs rather than tracheae, which were discernible as such with micro-CT.

Scott (1905) indicated several tracheae present in the mid and hind legs of immatures but absent in adults, also noted by Chapman (1918), although with his own terminology. It is possible that these extra tracheae develop into the air-sac tracheae, which seem to be largely absent overall in immatures (otherwise they would have difficulty swimming underwater). Future studies

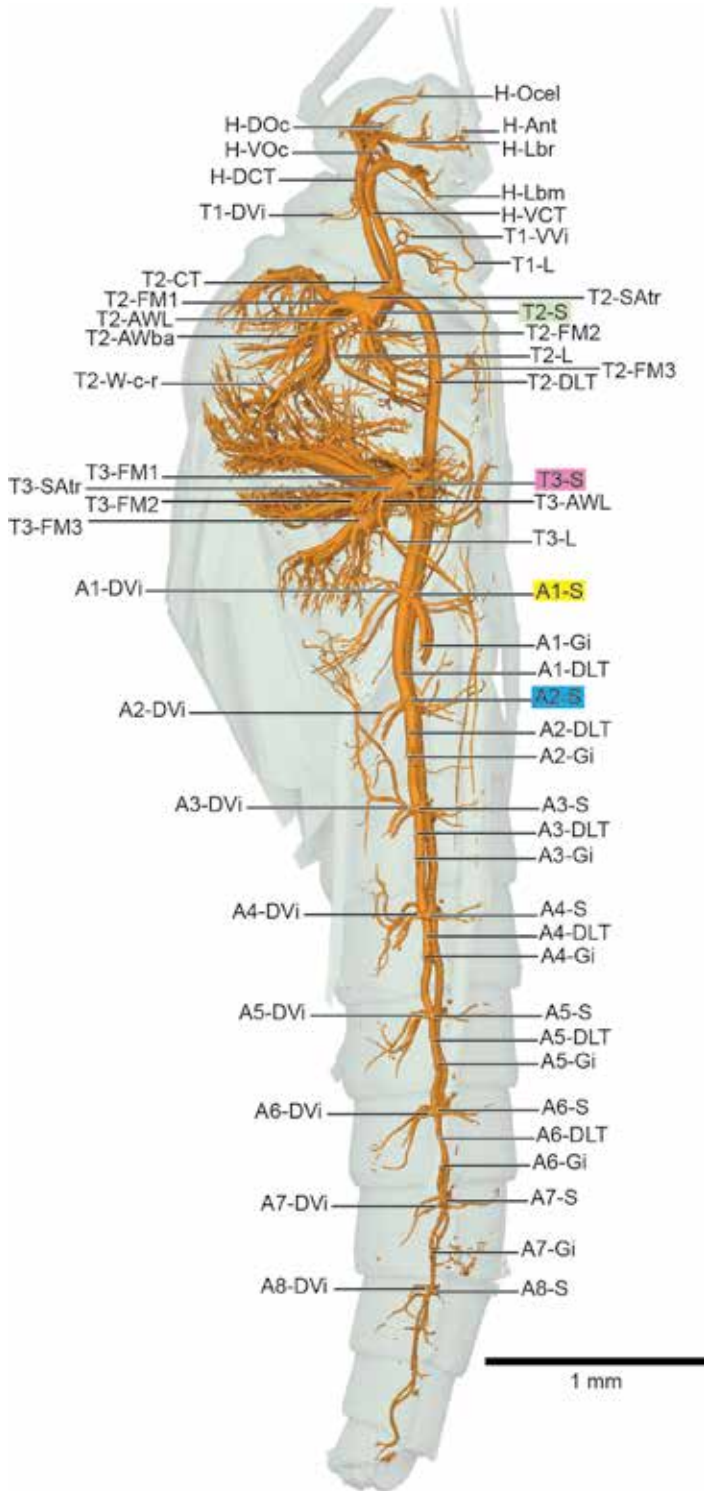


FIGURE 24. *Neocloeon triangulifer* (Ephemeroptera: Baetidae) subimago lateral view.

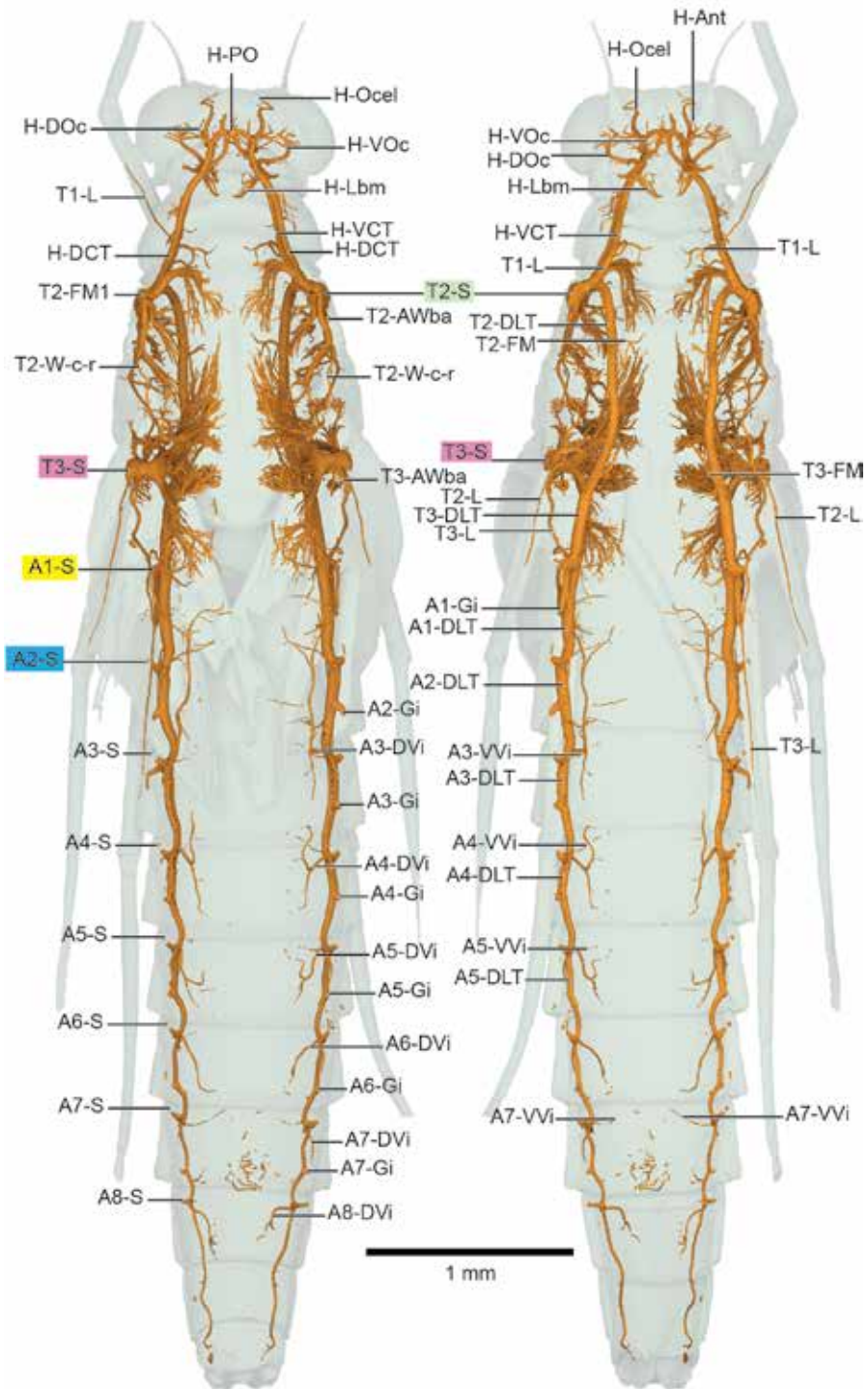


FIGURE 25. *Neocloeon triangulifer* (Ephemeroptera: Baetidae) subimago dorsal (left) and ventral (right) views.

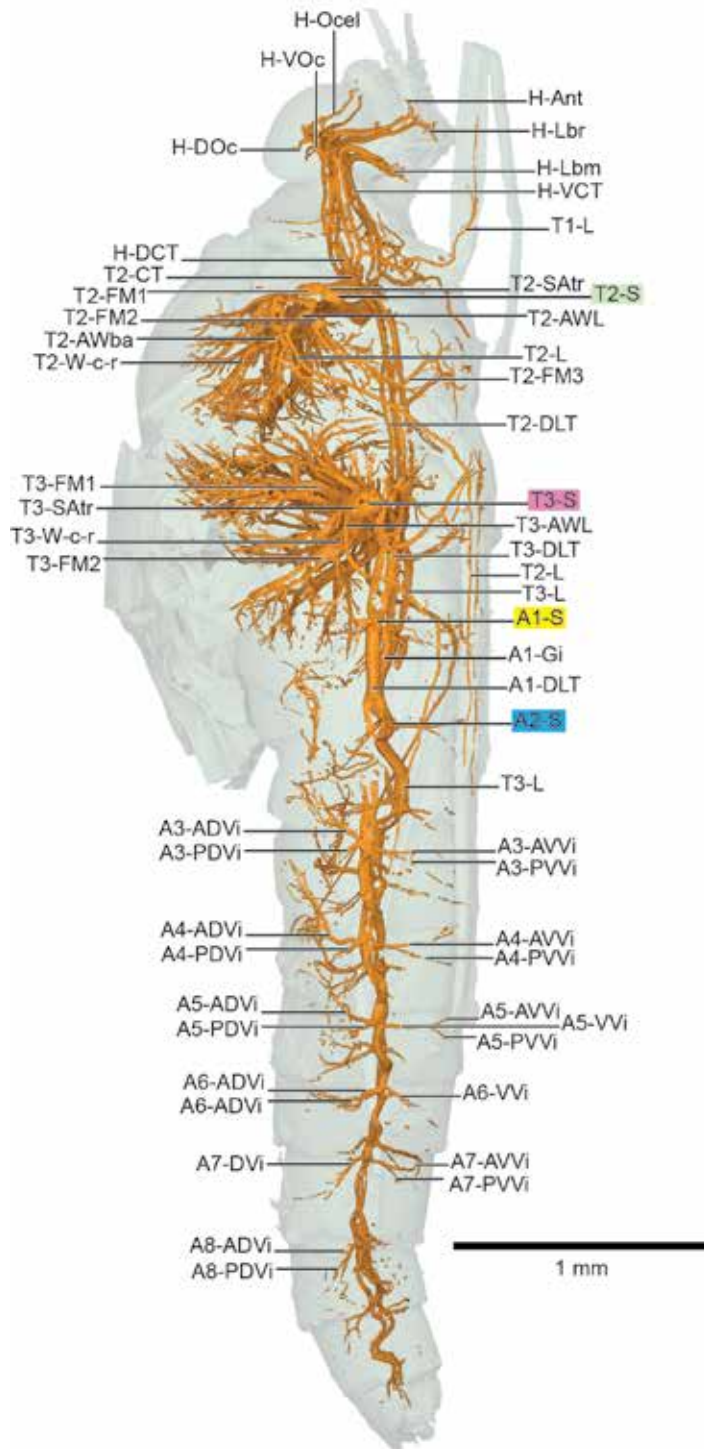


FIGURE 26. *Neocloeon triangulifer* (Ephemeroptera: Baetidae) adult lateral view.

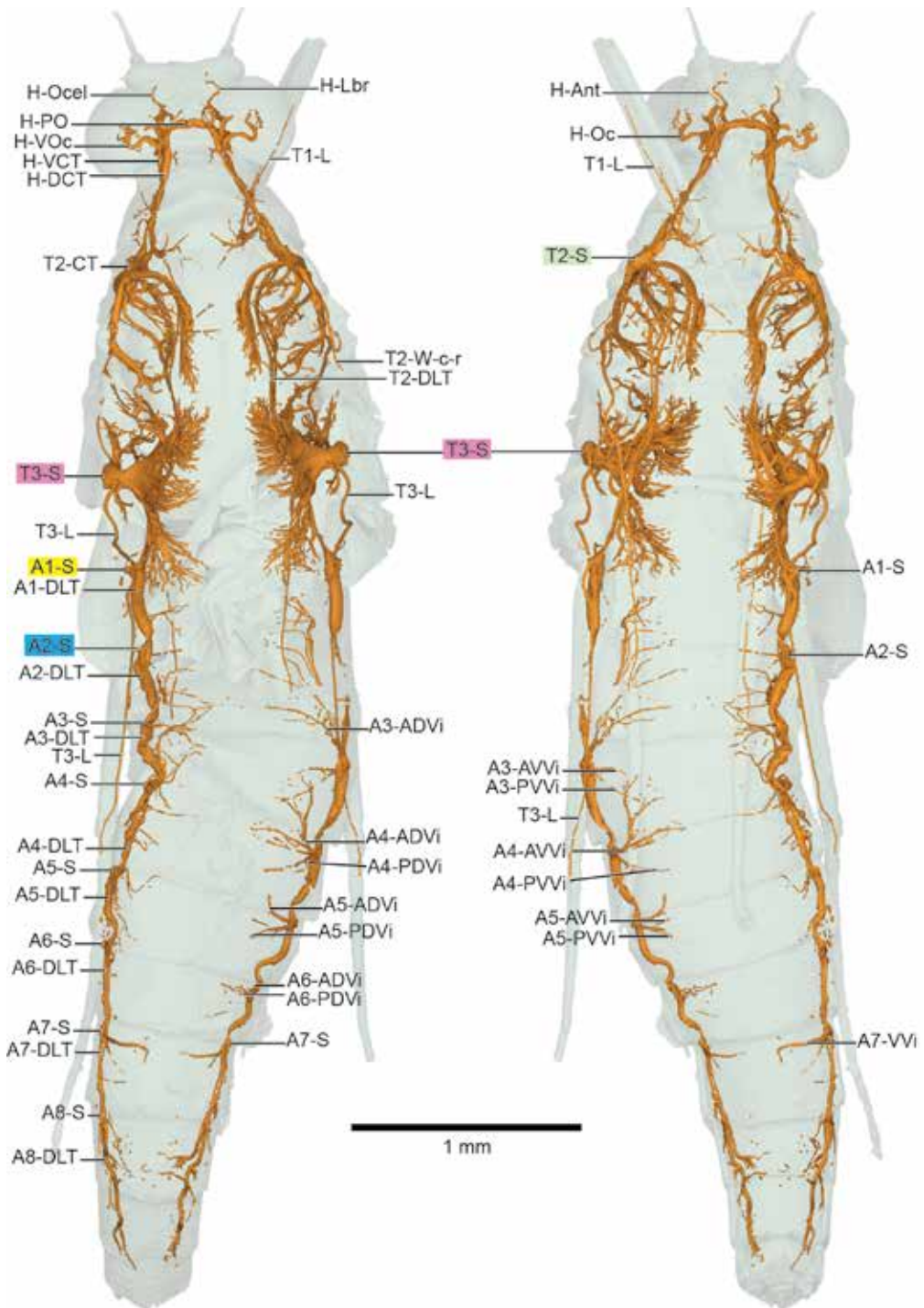


FIGURE 27. *Neocloeon triangulifer* (Ephemeroptera: Baetidae) adult dorsal (left) and ventral (right) views.

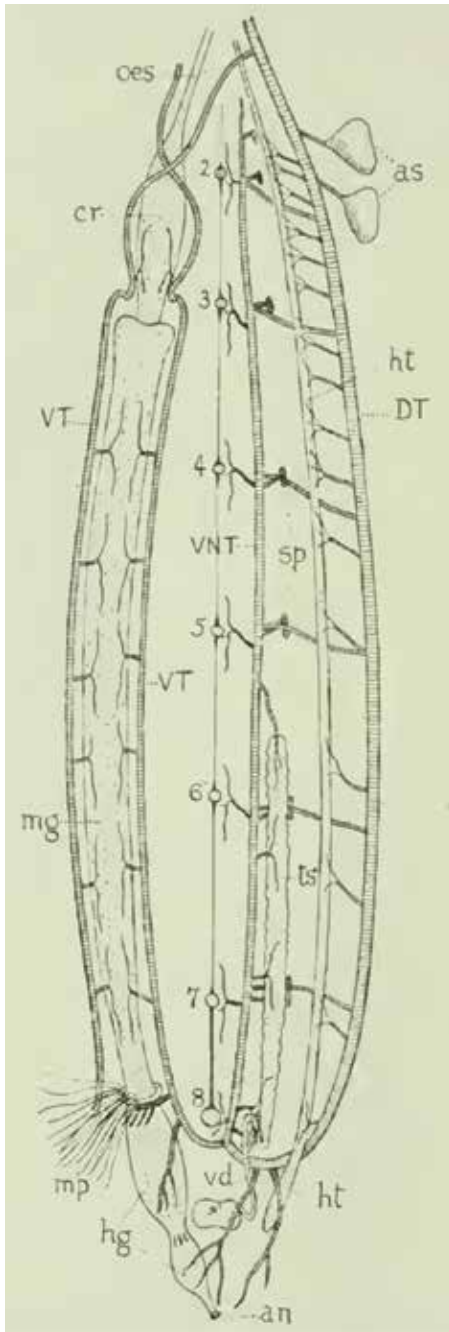


FIGURE 28. Tillyard's (1917) figure 75, showing three longitudinal trunks: dorsal trunk DT, visceral trunk VT, and ventral trunk VNT.

should investigate this proliferation of tracheae and their possible development into the numerous air-sac tracheae.

The thorax of both specimens features a large number of air spaces. The flight musculature of odonates is thought to grow substantially during maturation of the adult (Marden, 1989; Anholt et al., 1991; Marden, 2000). It could be that these air spaces allow expansion of flight muscle—as the adult exoskeleton is fixed in size, empty volume must be allocated in advance to allow for an increase in flight muscle mass. Interestingly, this would be the inverse of the “gas bag in the gut” phenomenon (see Discussion), where the alimentary canal is coopted into a large air space in the adult.

FAMILY AESHNIDAE

“Hawkers” or “Darners”

The adult Aeshnidae has many air sacs arranged throughout the body, with many thoracic air spaces likely for muscle growth. Preliminary estimates indicate that over 50% of the volume of the specimen is air, either tracheal or in air sacs (Herhold et al., in prep.). Many major tracheae lead into and out of large air sacs, both in the thorax and abdomen, such that determining tracheal pathways and assessing homology is challenging. Most notably, the abdomen possesses four paired longitudinal trunks, a condition not seen in any other insect in this study. This unusual morphology of the adult relative to other winged insects suggested that some of these features may be holdovers from the aquatic immature stage, so a naiad was collected and scanned.

To facilitate differentiation of tracheae and tracheated air sacs in the plates and figures for the adult, a subset of the air sacs that serve as tracheal pathways are shown in orange and tubular tracheae are shown in yellow, and the specimen body outline in transparent gray (as in other plates and figures). Although the tracheae are presented as if “on top” of the air sacs, they

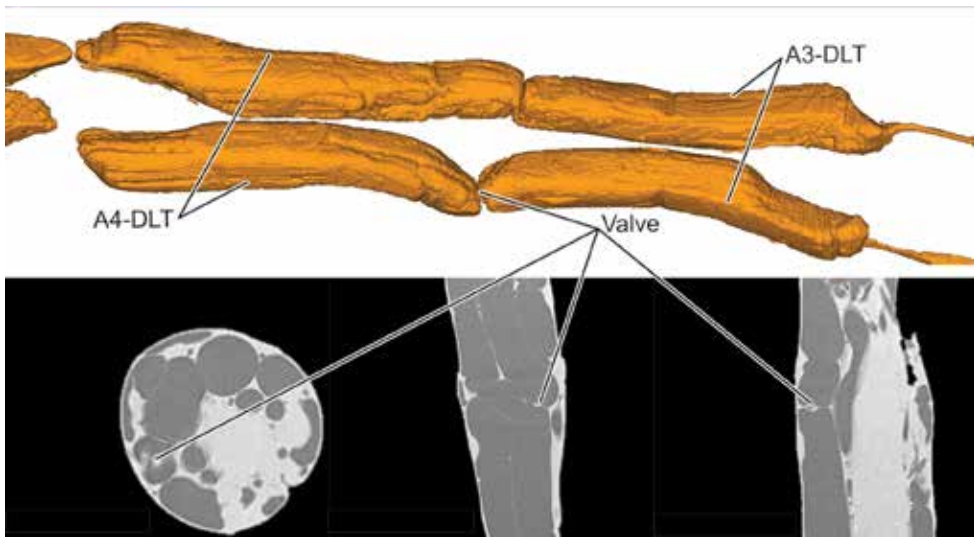


FIGURE 29. Apparent valve between abdominal segments, between A3-DLT and A4-DLT.

are located deeper inside the body. The inset image in the plates shows all air spaces (tracheae and air sacs) in gray; readers are encouraged to refer to the 3D models in the supplementary digital data, where air sacs, tracheae, and tracheated air sacs can be viewed separately or together interactively.

X-ray cross sections from CT scan data indicate the likely presence of flow-directing valves between some air sacs and tracheae in the adult, particularly in the thorax and abdomen (see fig. 29). Air-sac flow-control valves have been documented in Diptera by Wasserthal et al. (2018), and further research into these structures is needed in Odonata.

Aeshna sp. immature

Figure 30 (lateral, dorsal, ventral)

Determining the correct placement and assessment of homology of the longitudinal trunks in the aeshnid adult required the scanning of an aquatic immature. The closed tracheal system of the naiad dragonfly is built around the rectal gills,

and was first detailed by Scott (1905) and Tillyard (1917), whose terminology we adapt here.

The aeshnid naiad possesses four paired longitudinal trunks in the abdomen, one more than determined by Tillyard (1917). His Dorsal Trunk DT is our *An*-DLT, and we adapt his Visceral Trunk VT as Visceral Longitudinal Trunk *An*-VLT. However, Tillyard's Ventral Trunk VNT is actually homologous to the Medial Longitudinal Trunk *An*-MLT, as it follows the spiracles along the lateral body wall (see description for adult, below). The abdominal *An*-VLT is depicted as shorter ventral branches (but not labeled) by Tillyard in his fig. 75 (fig. 28). In figure 30 here it is barely visible in the ventral view but likely present as a longitudinal trunk. This specimen was collected early in the study and frozen to -20°C rather than -80°C , possibly causing smaller structures to be infilled with fluid, and the $30\ \mu\text{m}$ scan resolution is not ideal for capturing smaller details such as these fine tracheae. Regardless, the presence of the branches leading to these more linear, ventrally located tracheae indicates that these are indeed *An*-VLT.

Aeshna sp. adult

Figures 31, 32 (lateral, anterior, posterior); 33, 34 (dorsal, anterior, posterior), 35, 36 (ventral, anterior, posterior)

Plates 18 (lateral), 19 (dorsal), 20 (ventral)

DESCRIPTION: HEAD: Numerous air sacs throughout most of the head, creating a complex, interlocking network of tracheae and air sacs. Larger, discernible features outlined here. H-DCT running anteriorly, leading to large, nearly hemispherical air sacs that feed numerous H-Oc anteriorly. H-VCT similar, supplying a network of ventral air sacs that connect dorsoventrally; H-Lbm ventral to this network.

THORAX: Odonate thoracic morphology, adapted for synchronous (direct) flight musculature, is substantially different from Neoptera. Consequently, assessment of homology for thoracic tracheal morphology is tenuous at best. Several tracheae, particularly those supplying the wings, appear to be homologous, including T2,3-Wbr and T2,3-W-c-r, but the homology of structures found in other winged insects such as T2,3-AWL and T2,3-PWL are not as clear. Many dorsal-ventral tracheae branch from leg tracheae and extend into the flight muscles throughout the pterothorax; it is likely these do not have homologs with Neoptera. T2,3-DLT is differentiable based on homologous connections to spiracles and extension into the abdomen, though the air-sac-based morphology is substantially different from other taxa. As mentioned previously, many tracheae also enter and exit large thoracic air sacs, and apparent valves between these spaces likely facilitate active ventilation. Further research is indicated to accurately locate and effectively visualize these structures.

ABDOMEN: Tillyard's "visceral" trunk ViLT extending from thorax posteriorly to end at A8-S; ViLT is unsegmented but is numbered An-ViLT in areas for convenience. ViLT crossing laterally at anterior end of abdomen; this cross-over migrating posteriorly from immature (see fig. 30). A2-ViLT with several ventral branches into

viscera, including A2-ViLT-VB. A1..8-S present, with A1..8-SB present. A1-SB long, extending mediad and dorsad from A1-S. A2-SB much shorter; subsequent A3..8-SB present but short. A1-SB dividing into A1-DB, A1-VB, and joining with A1-MLT anteriorly and posteriorly. A1-DB running dorsad and anteriorly, extending into network of leg/wing thoracic tracheae; A1-VB proceeding ventrad and mediad along body wall, joining with T3-VLT anteriorly and A1-VLT posteriorly in T-shaped junction. A2-S with similar morphology but A2-SB shorter and more dorsal and slightly posterior to A2-DB; subsequent A3..8-S similar to A2-S with very short An-SB and An-DB dorsal and posterior. All An-DB supplying air-sac-like An-DLT, extending from thorax through abdomen as far as A6-DLT; apparent gap between A6-DLT and A7-DLT, followed by narrow, more trachealike A8-DLT extending posteriorly. As noted, valvelike structures discernible between adjacent air sacs (see fig. 37). An-MLT extending through abdomen, beginning at thorax and terminating posteriorly of A8-S. An-VLT small and nearly linear, likewise beginning in thorax, connecting with each An-S via An-DB and terminating posteriorly of A8-S.

FAMILY CALOPTERYGIDAE

Calopteryx maculata

"Ebony jewelwing"

Figures 38, 39 (lateral, anterior, posterior), 40 (dorsal), 41 (ventral)

Plates 21 (lateral), 22 (dorsal), 23 (ventral)

A single damselfly was scanned at 19 μm , which should have been sufficient to capture details of abdominal tracheae; however, this specimen was frozen to -20°C early in the study. As small tracheae were likely infilled, this specimen is not described in detail, but three-dimensional models are included in the online supplementary digital data.

The thoracic tracheae appear to be very similar to the aeshnid, along with extensive air sacs.

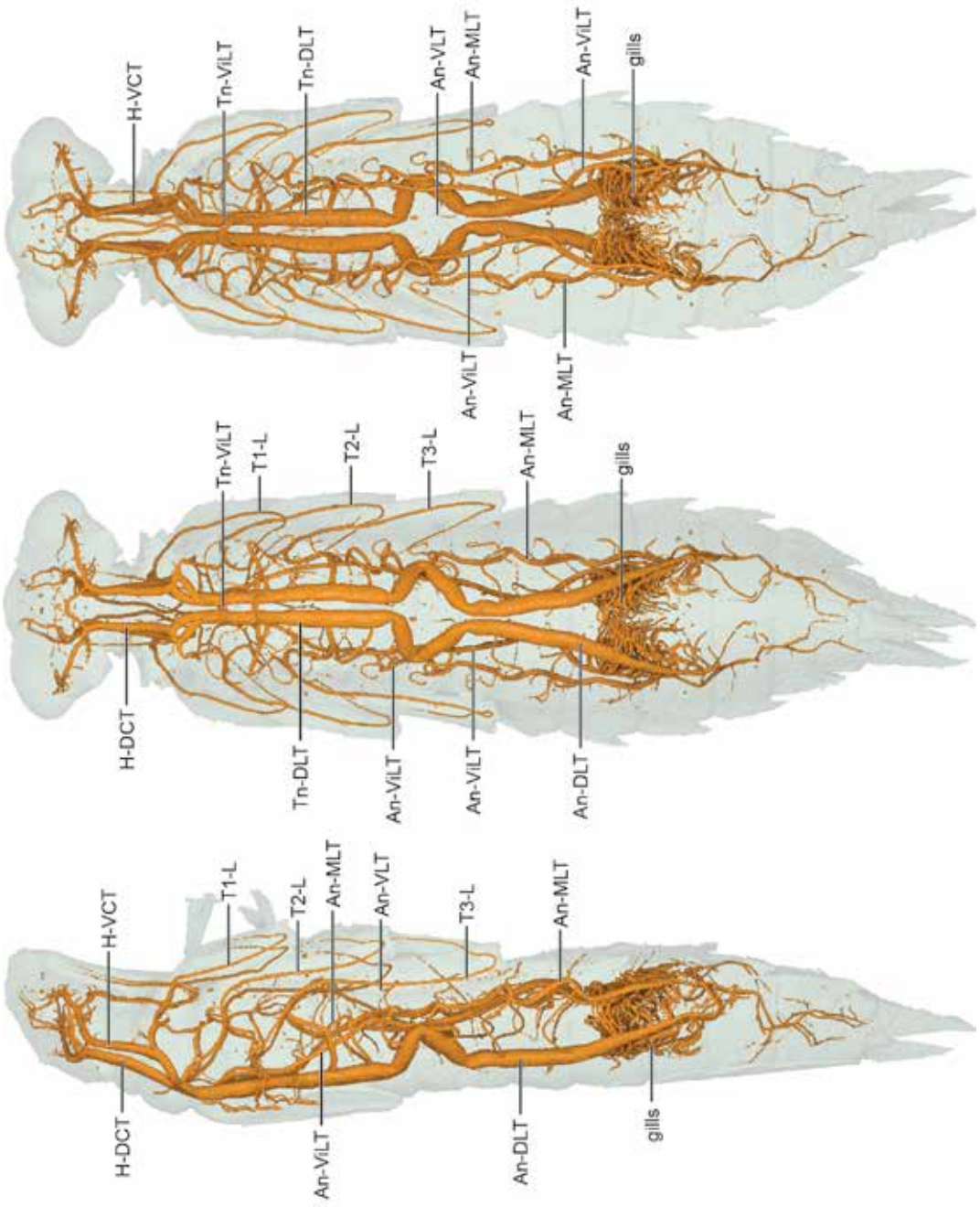


FIGURE 30. Aeshnid immature with longitudinal trunks labeled. Lateral (left), dorsal (middle), and ventral (right) views.

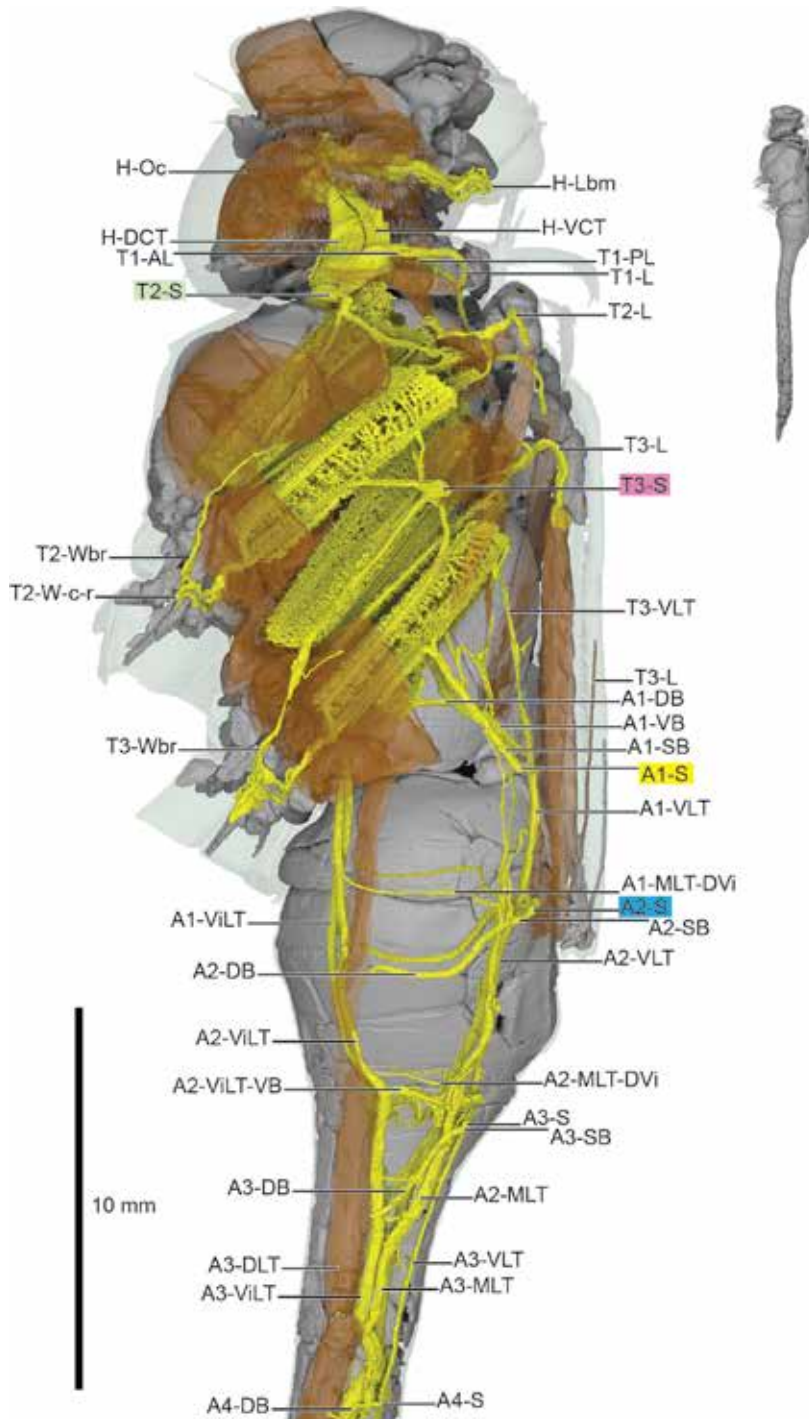


FIGURE 31. Odonata: Aeshnidae anterolateral view.

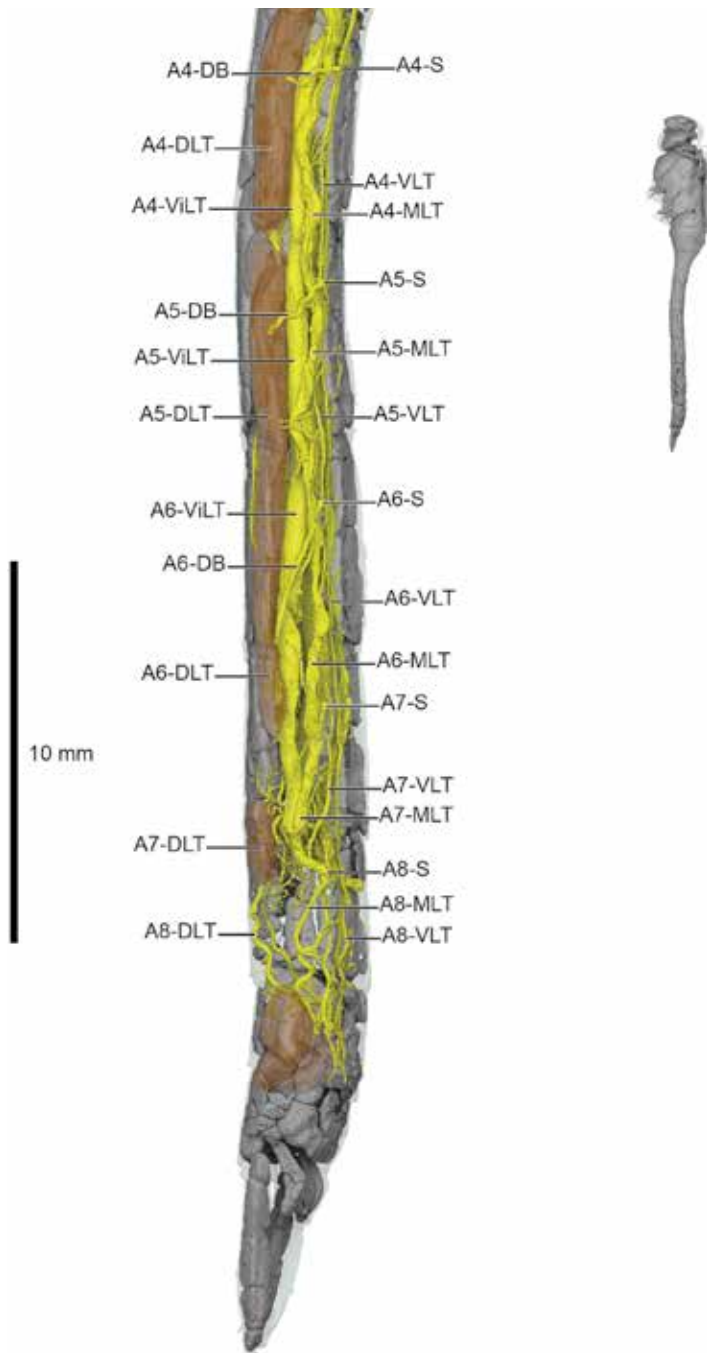


FIGURE 32. Odonata: Aeshnidae posterolateral view.

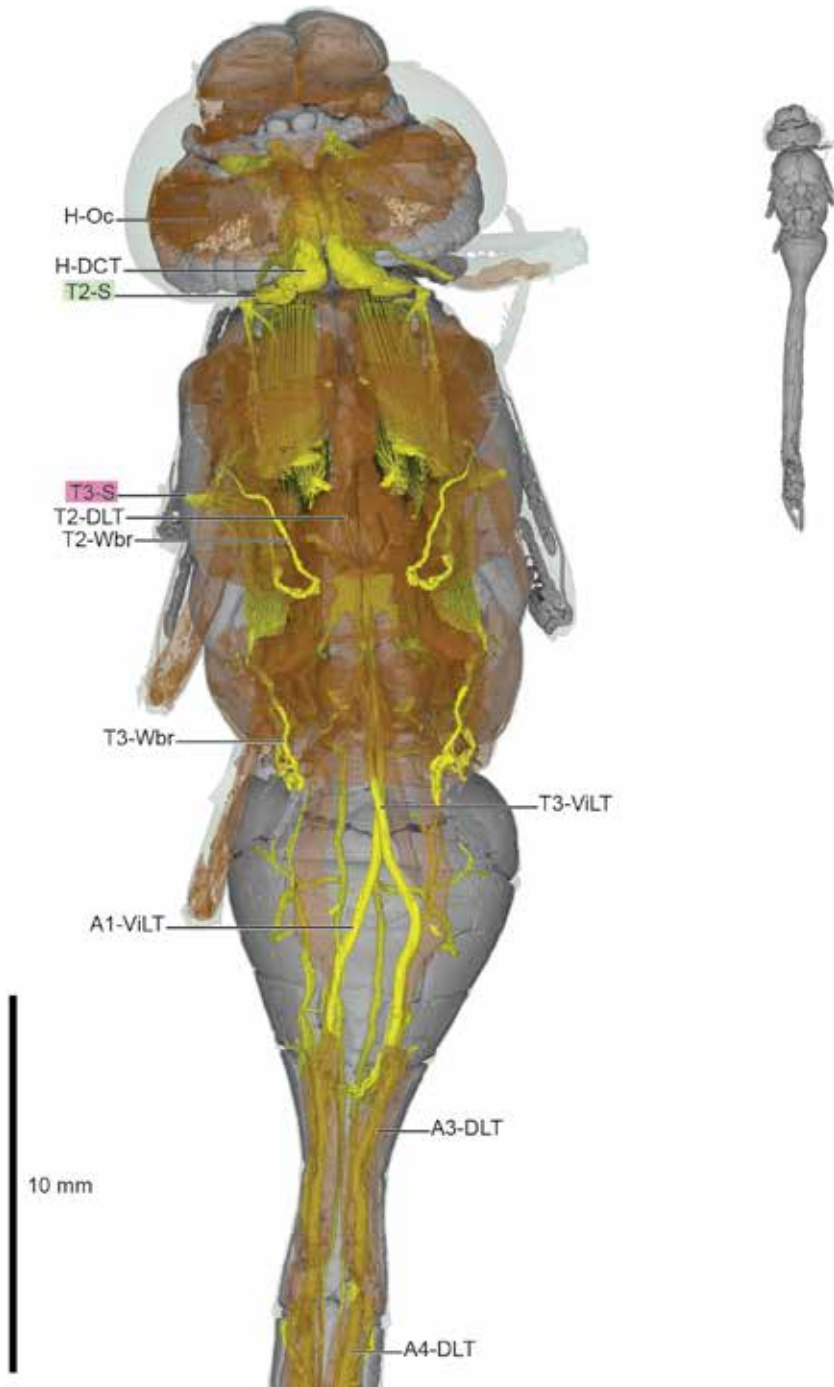


FIGURE 33. Odonata: Aeshnidae anterodorsal view.

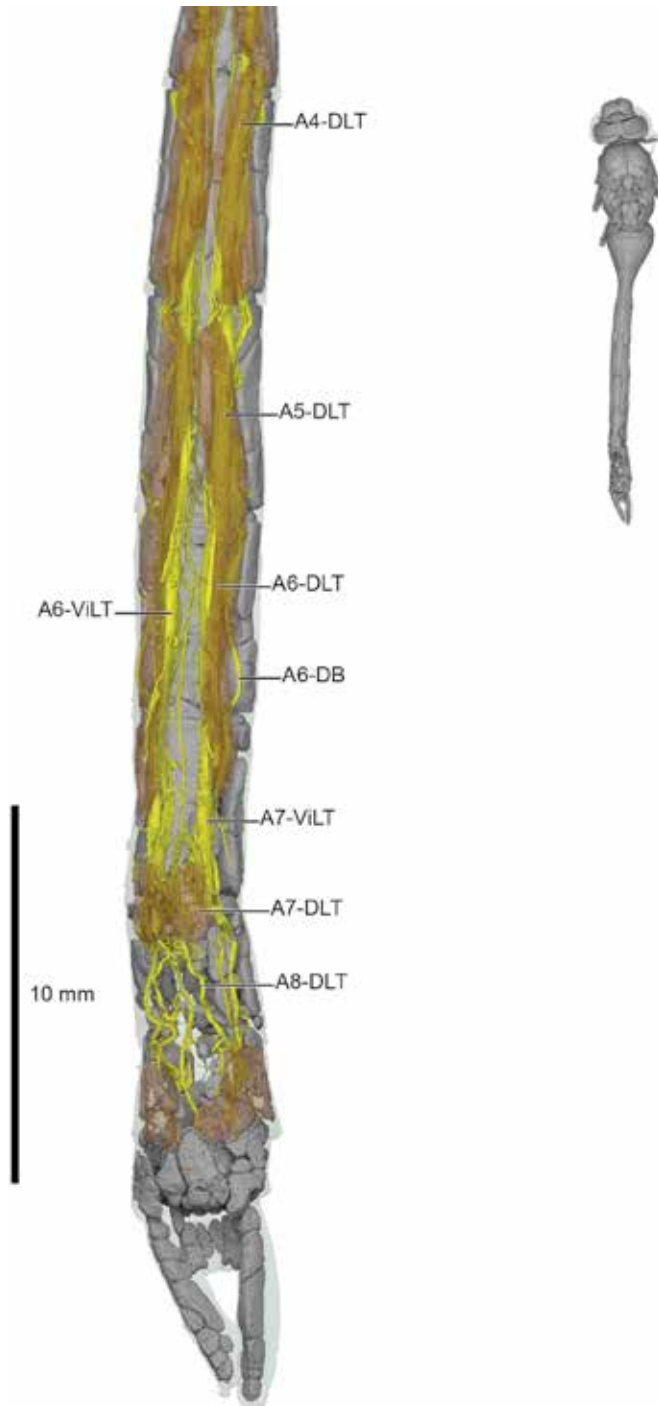


FIGURE 34. Odonata: Aeshnidae posterodorsal view.

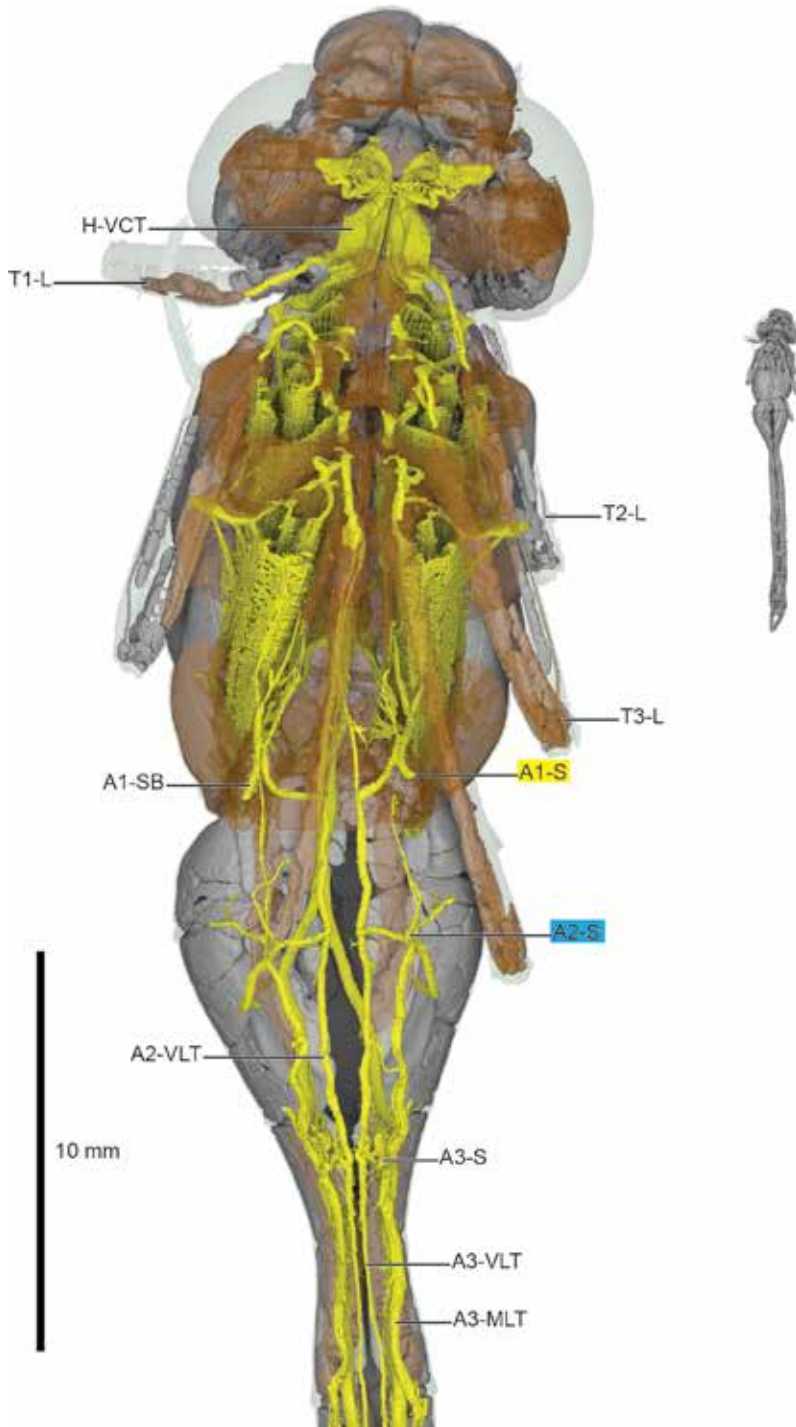


FIGURE 35. Odonata: Aeshnidae anteroventral view.

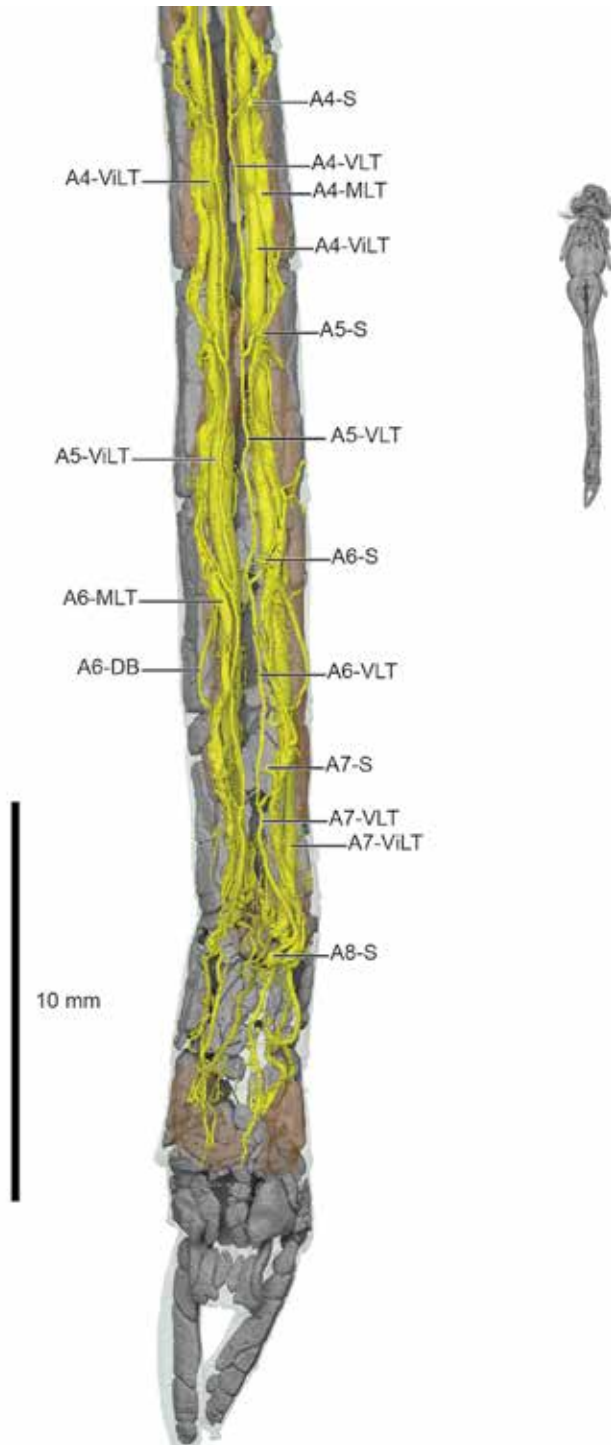


FIGURE 36. Odonata: Aeshnidae posteroventral view.

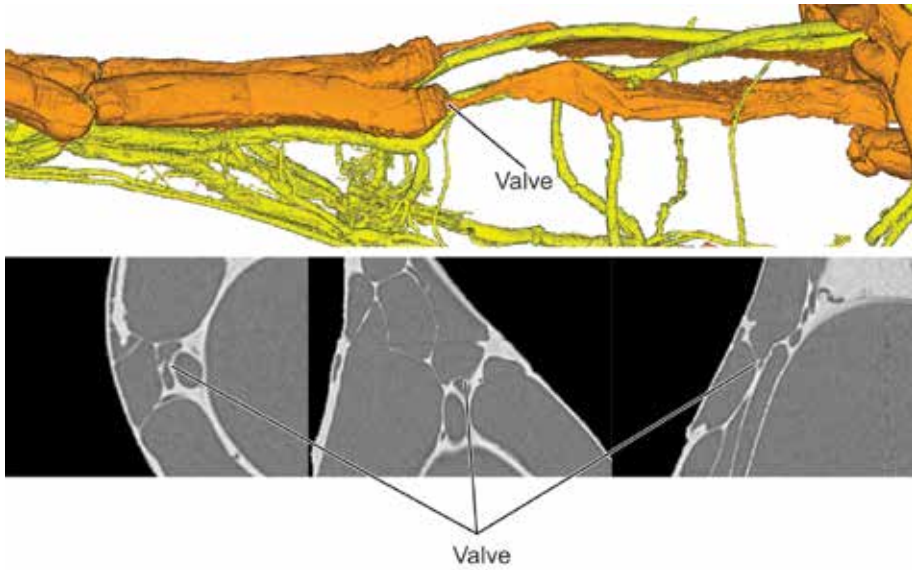


FIGURE 37. Aeshnidae with valve. Direct screen capture from 3D Slicer.

It is unclear whether there are four paired abdominal trunks as in the dragonfly, but it seems likely. Further studies should focus on *Zygoptera* in addition to more dragonfly specimens to verify and solidify tracheal patterns in the flight motor and abdomen.

ORDER ZORAPTERA

FAMILY ZOROTYPIDAE

Zorotypus hubbardi

“Hubbard’s angel insect”

Figure 42 (lateral, dorsal)

Several *Z. hubbardi* specimens were collected from Florida. Unlike the other taxa, where specimens were frozen alive, these specimens died during transport and were frozen upon arrival. Likely due to their untimely demise, tracheae suffered from fluid infilling before scanning, resulting in obscured morphology. Several specimens were scanned, and the best example was chosen for inclusion here. Zoraptera are an excellent candidate for further micro-CT study of better-preserved specimens.

DESCRIPTION: HEAD: H-DCT and H-VCT in close contact, proceeding anteriorly. H-Ant off H-DCT, no other head tracheae visible in this scan.

THORAX: T2-S with several branches visible on specimen right side but only two determinable: T2-VB and T2-CT. T2-VB ventrad; T2-VC present. T3-S visible with T3-DLT extending dorsad and posteriorly to link with A1-S. Other thoracic tracheae partial, determined from examining volume cross sections to establish position in the body.

ABDOMEN: A1..7-S discernible.

ORDER DERMAPTERA

Dermaptera have been the subject of recent micro-CT studies, including the discovery of active tracheal compression via synchrotron imaging (Westneat et al., 2003) as well as a detailed analysis of the head of *Forficula auricularia* (Neubert et al., 2017). Dermaptera phylogeny is considered to be generally unresolved, with distinctions between lower Dermaptera and higher Dermaptera considered somewhat arbitrary (Haas, 2018). Recent transcriptomic and

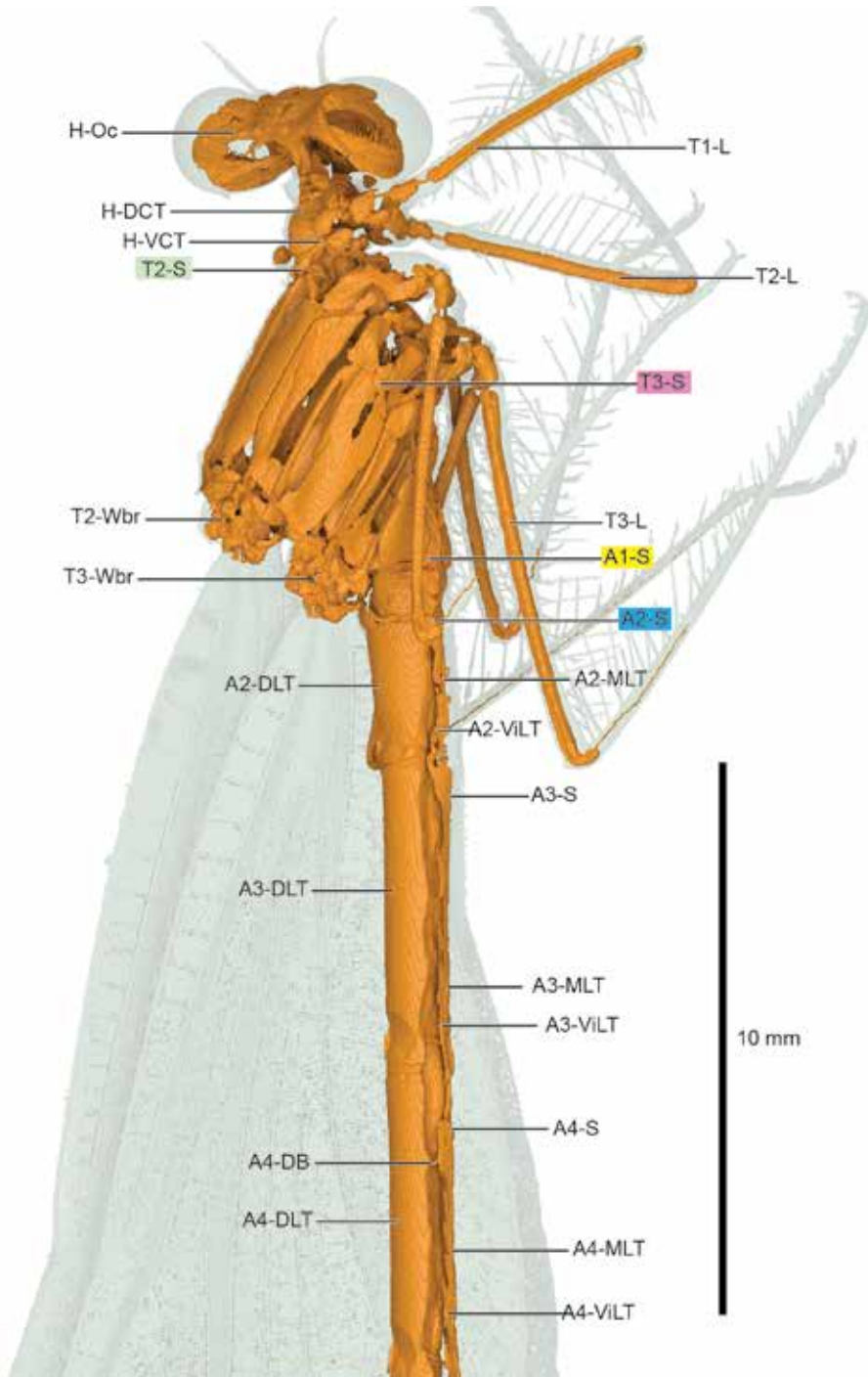


FIGURE 38. Calopterygidae anterolateral view.

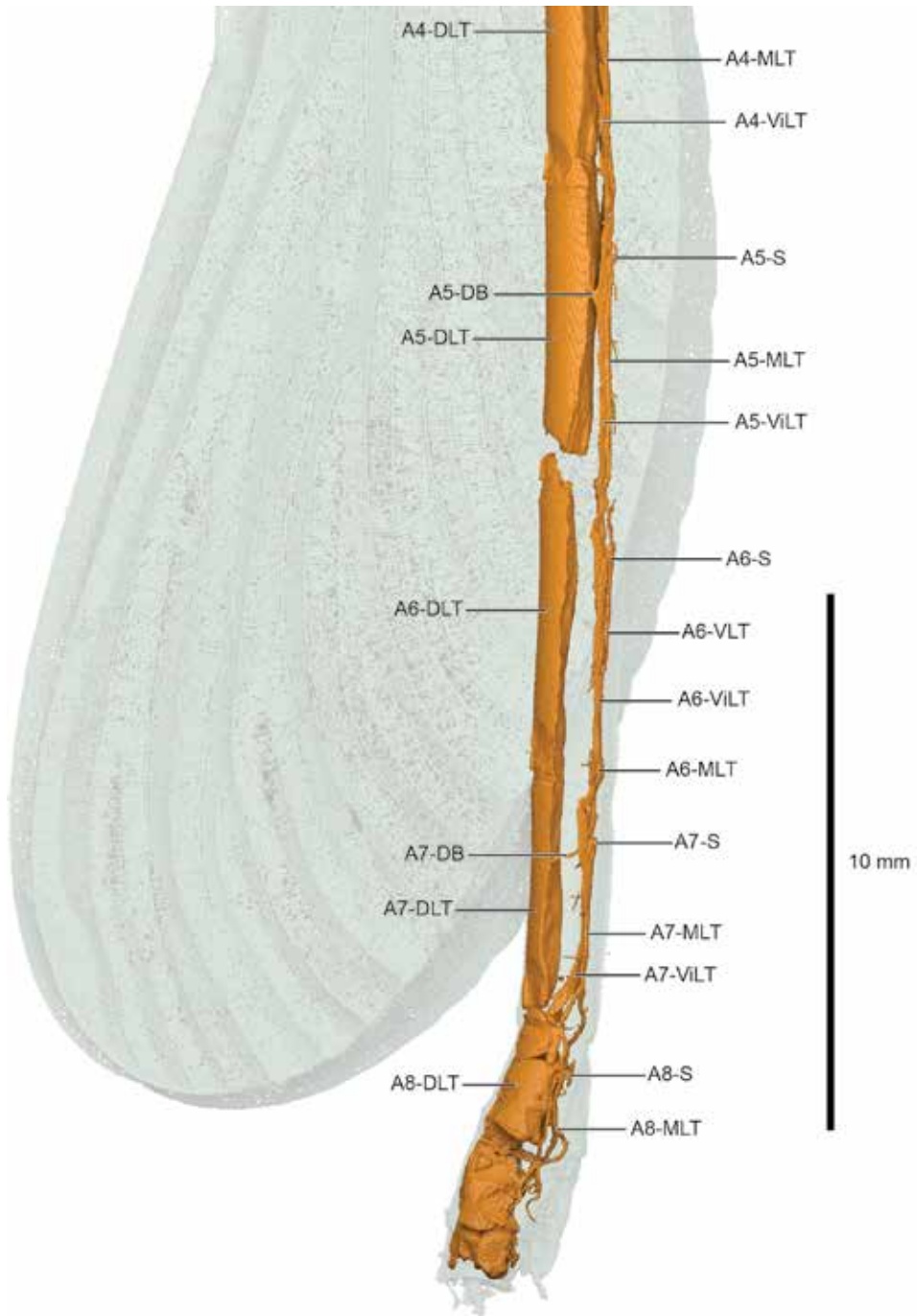


FIGURE 39. Calopterygidae posterolateral view.

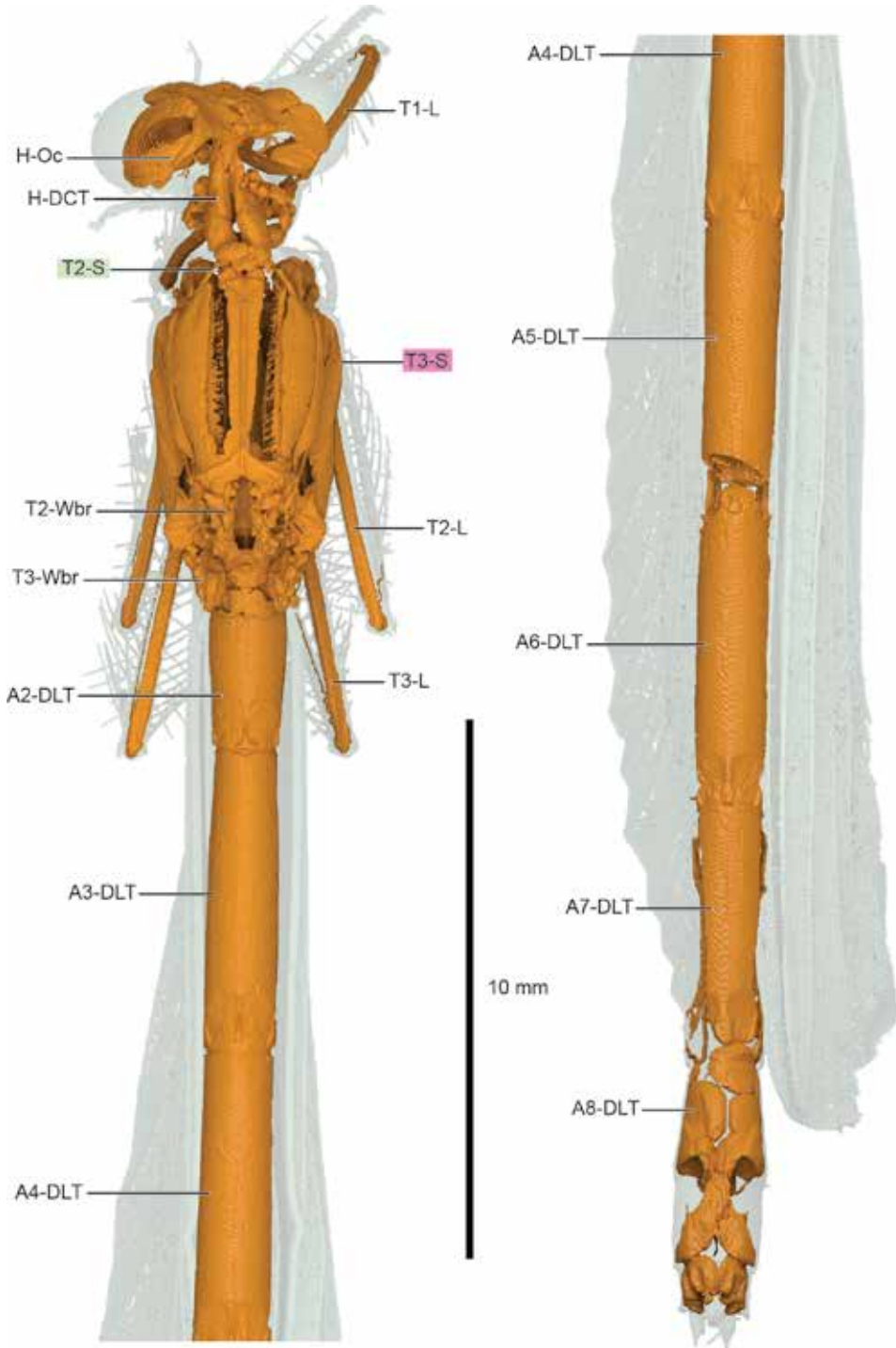


FIGURE 40. Calopterygidae dorsal.

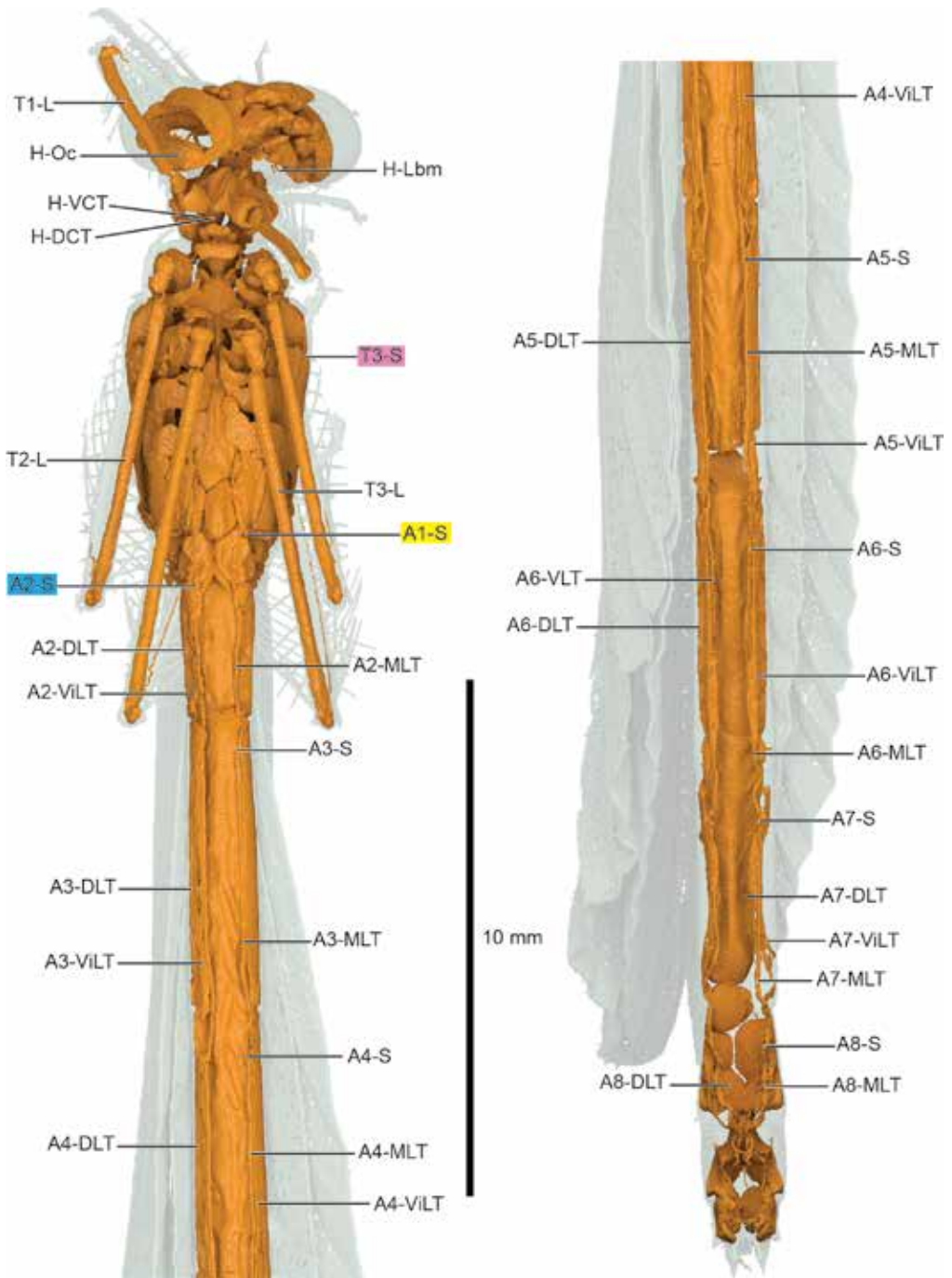


FIGURE 41. Calopterygidae ventral.

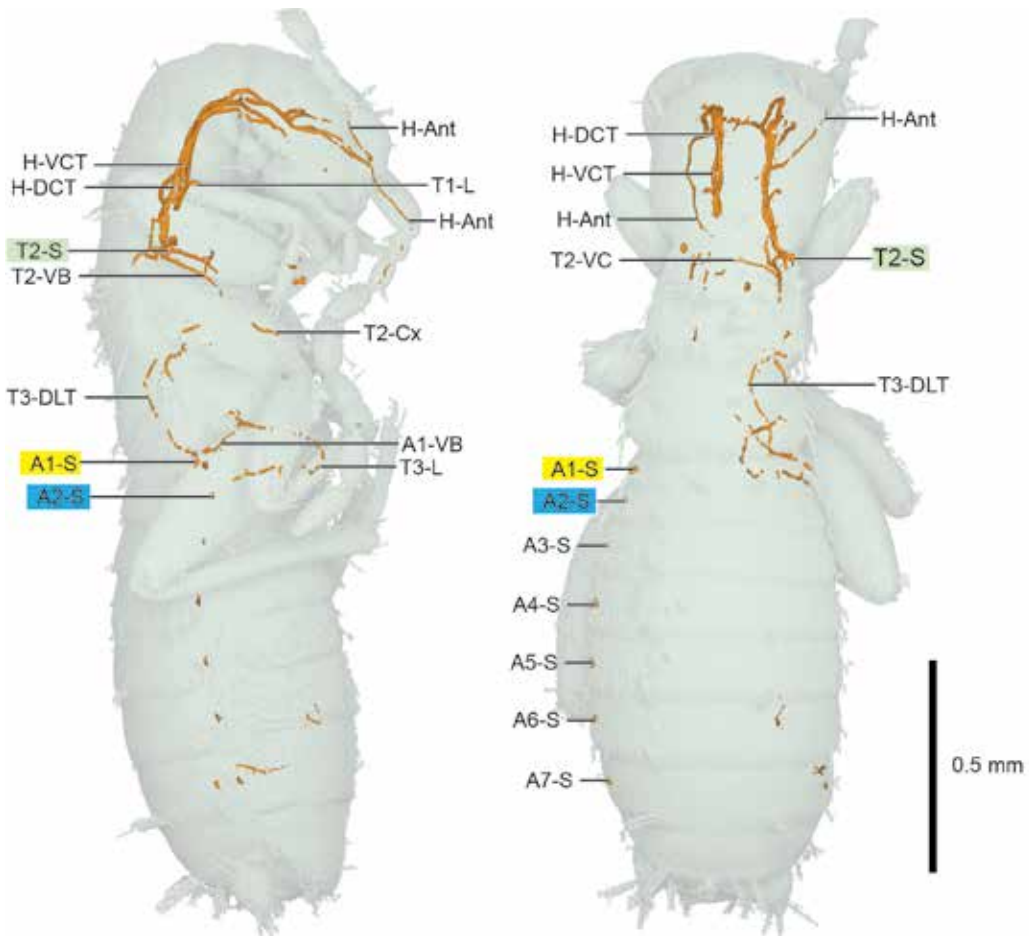


FIGURE 42. *Zorotypus hubbardi* (Zoraptera: Zorotypidae) lateral (left) and dorsal (right) views.

morphological studies have refined relationships within Dermaptera (Wipfler et al., 2020); however, these analyses omit the fossil record (Tihelka et al., in prep). The taxa here consist of one “lower” dermapteran (*Anisolabis maritima*, Anisolabidae, female) and one “higher” (*Forficula auricularia*, Forficulidae, male), and although *Anisolabis* lacks wings, they are alike in tracheal architecture. Sex was determined for both species based on sexual dimorphism of the cerci. While the specimens were scanned at similar resolutions, 11.6 mm³/voxel for *Anisolabis* and 13.5 mm³/voxel for *Forficula* (see table 3 for all scan parameters), substantially more visceral tracheae are visible in the *Anisolabis* scan. This may

be the result of slightly higher resolution, but also possibly due to different scanning parameters or preservation artifacts (fluid filling of small tracheae postmortem). Regardless, sufficient detail is present in both specimens to assess tracheal homology.

The two dermapteran specimens are similar in their overall tracheal layout, with most differences in the heads. Wing base tracheae T2,3-Wbr are well-developed in *Anisolabis*, even though apterous; however, wing tracheae T2,3-W-c-r and T2,3-W-cu-a are absent. A1-S is positioned dorsally in both specimens, unlike the remaining abdominal spiracles, possibly a modification for the ability of earwigs to raise the abdomen dorsally and forward to

use the forceps for predation and defense. Additionally, the *An-VLT-Vi* in *Anisolabis* all proceed anteriorly, whereas in *Forficula*, there appears to be a "split" where *An-VLT* proceeds anteriorly for *A2..5-VLT-Vi..5*, but posteriorly for *A6..7-VLT-Vi*.

DESCRIPTION: HEAD: Majority of tracheal structures similar between *Anisolabis* and *Forficula*, differences described here for comparative clarity. H-DCT and H-VCT of similar diameter; H-DCTs curve inward slightly such that left and right tracheae nearly touch before turning laterally outward on entry to head capsule; H-VCT proceeds straight into head. H-DCT with several branches just anterior of cervix: H-DCC, H-DCT-DVi, H-Oc, and H-Ant. H-DCC present. H-DCT-Dvi running laterally and dorsad. H-Oc arcing laterally, with several small tracheae extending into eye, then continuing anteriorly and ventrad via H-Oc-Md to link with ventral H-Md; H-Oc-Ant branches off H-Oc in *Anisolabis* into antenna. H-Ant extends anteriorly through head into antenna; left side of *Forficula* as H-Ant-Ft with H-Ft branching off H-Ant near base of antenna. H-Ant with multiple tracheae in *Anisolabis*; likely present in *Forficula* but not visible in this scan. H-VCT likewise with several branches just anterior of cervix: H-VCT-Vi, H-Ft-Lbr (absent in *Forficula*), H-VC (off H-Ft-Lbr in *Anisolabis*), and H-Mx-Md. H-VCT-Vi runs laterally and ventrad, like dorsal trachea. In *Anisolabis*, H-Ft-Lbr runs anteriorly, with H-VC extending medially to link left and right sides; H-Ft branching laterally and anteriorly with H-Lbr directly anteriorly. In *Forficula*, H-VC branching directly from H-VCT. Both H-VC with H-VC-Dvi running directly anteriorly, extending as far as frontal area in *Forficula*. H-Ft-Lbr (absent in *Forficula*) running anteriorly, with small H-Ft splitting laterally and anteriorly, remaining H-Lbr anteriorly. H-Mx-Md runs anteriorly and slightly laterally, with several branches: H-Lbm running ventrad, with short H-LbmPlp; H-Mx ventrad, with short H-MxPlp. Remaining H-Md branch runs anteriorly, with H-Oc-Md connection from H-DCT; H-Md-Ant branching dorsally (absent in *Forficula* left side) to join H-Ant from H-DCT.

THORAX: Although the thoraces of *Anisolabis* and *Forficula* differ substantially in overall exte-

rior morphology, as seen in figure 43, the tracheal topology of the thorax is retained between the two taxa. T2-S with four tracheae: H-DCT, H-VCT, T2-AWL, T2-DB; T2-CT absent. H-DCT arcs mediad before proceeding anteriorly; T1-Dvi branching close to T2-S, extending anteriorly with several smaller branches; T1-DC present. H-VCT similar to H-DCT, arcing medially then anteriorly toward head. T1-AWL branching dorsoventrally; T1-VC present, separating from T1-AL while remainder of T1-AL continues into foreleg. T2-AWL extending posteriorly and slightly dorsad, bifurcating into T2-AL and T2-Wbr; T2-AL continues ventrad and posteriorly into midleg; T2-Wbr running dorsad and laterally, connecting directly with T2-S. T2-DB extending medially, ventrad and slightly anteriorly, with three branches: T1-PL, T2-DLT, T2-VT. T1-PL extending through coxae before joining with T1-AL and continuing into proleg; T1-Fm visible. T2-DLT proceeds anteriorly to connect directly with T3-S via T3-DB. T2-VLT ventrad and posteriorly, following mesothoracic sternite before arcing anteriorly to link with T3-S. T3-S with four branches: T2-Wbr, T3-AWL, T3-DB, T3-VB. T2-Wbr extends from T2-S linking directly to T3-S. T3-AWL extending slightly dorsad before turning ventrad and laterally, bifurcating into T3-AL and T3-Wbr; T3-AL continues posteriorly into hindleg; T3-Wbr extending posteriorly to connect directly to T3-S. T3-DB running mediad, linking with T2-DLT from anterior and T3-DLT continuing posteriorly. T3-VB runs mediad and posteriorly, with T3-VLT branching posteriorly; T3-VB subsequently bifurcates into T2-PL and T2-VLT connection from T2-S. T2-PL runs anteriorly from T3-S, joining with T2-AL from T2-S, continuing into midleg; several T2-Fm present. T3-VLT with T3-VL into hindleg femur.

ABDOMEN: A1..8-S present. A1-S highly modified from subsequent segments, placed dorsally with four branches: T3-Wbr, A1-DB, A1-VB, T3-PL. T3-Wbr connecting directly from T3-S; small T3-Wbr-Vi extends dorsad and medially along metathoracic tergite. A1-DB mediad, linking with T3-DLT from anterior and A1-DLT con-

tinuing posteriad. A1-VB ventrad, with A1-VLT branching directly posteriad; A1-VB continues ventrally, bifurcating into T3-Fm, extending laterally into hind leg, and A1-VC; T3-VLT connects with A1-VC. T3-PL runs ventrad and posteriad, joining with T3-AL before extending into hindleg. Tracheae from A2..6-S similar, A4-S described here as example. A4-S with three branches: A3-VLT, A4-DB, and A4-VLT. A3-VLT runs anterior, extending from A3-S. A4-VLT branches medially and dorsad before curving posteriad and laterally toward A5.S. At apex of this arc A4-VLT-Vi extends anteriorly, spanning several segments. *An*-VLT-Vi variable, see taxon descriptions below. Midway between A4-S and A5-S, A4-VC branches ventrad at right angle, following abdominal sternite. A4-DB directly dorsad; A3-DLT connecting from anterior and A4-DLT from posterior to form Y-shaped junction. Visceral tracheae extend from either end of A4-DB: A4-DB-Mvi extends laterally and dorsad from start (ventral end) of A4-DB; A4-DB-Dvi from base of Y-shaped junction with A3-DLT and A4-DLT. A4-DLT-Dvi present but A4-DC absent. *An*-DLT-Vi numerous and highly variable, see descriptions below. A7-S connections like previous segments but distance between A7-S and A8-S greatly shortened. A8-DB with three tracheae: A7-VLT, A8-DB, and A8-VLT, but with posterior branching varying between taxa, see descriptions below. Extensive tracheation in A7 and A8 in both genera, no doubt for large muscles that control the forceps.

FAMILY ANISOLABIDIDAE

Anisolabis maritima

“Maritime earwig”

Figures 44 (lateral), 45 (dorsal, ventral)

Plates 24 (lateral), 25 (dorsal, ventral)

A greater number of smaller tracheae are visible in the *Anisolabis* scan than the *Forficula* scan. As the CT scans for this study specifically targeted tracheal morphology, visualization of internal morphology of organs and internal

structures was generally not possible. Therefore, determining the specific tissues supplied by a given trachea is challenging. However, some structures appear to have a particular tracheal morphology, such as muscle fibers and some other structures, and the detail afforded in the *Anisolabis* scan allows for some possibilities. For example, A3-VLT-Vi begins by branching from A3-VLT and proceeding anteriorly. Just before reaching the anterior end of the abdomen; however, A3-VLT-Vi splits into several smaller tracheae that turn posteriorly to form a cone, most likely the tracheation of a portion of the alimentary canal, possibly the proventriculus. Additional detail is observable in the terminalia, specifically the cerci. As mentioned previously, extensive tracheation of A7 and A8 is for musculature controlling the forceps, and two tracheae are seen extending into the cerci. A8-DLT-Cr is supplied by A8-DLT, which arcs ventrad and posteriorly into each side of the forceps, and a second trachea A8-VLT-Cr from A8-VLT, reaching basically straight posteriad to cross over A8-DLT-Cr into the cerci.

DESCRIPTION: HEAD: H-DCT and H-VCT similar diameter; H-DCTs curve inward slightly such that left and right tracheae nearly touch before turning laterally outward on entry to head capsule; H-VCTs both proceed straight into head. H-DCT with several branches just anterior of cervix: H-DCC, H-DCT-Dvi, H-Oc, and H-Ant. H-DCC present, with several small H-DCC-Dvi fanning laterally and anterior along head capsule. H-DCT-Dvi runs laterally and dorsad, branching off H-Oc. H-Oc arcing laterally, with several small tracheae extending into eye, then continuing anteriorly and ventrad via H-Oc-Md to link with ventral H-Md; H-Oc-Ant branches off H-Oc into antenna. H-Ant extends anteriorly through head into antenna; H-Ant with multiple tracheae in *Anisolabis* (H-Md-Ant, below). H-VCT likewise with several branches just anterior of cervix: H-VCT-Vi, H-Ft-Lbr, H-VC, and H-Mx-Md. H-VCT-Vi laterally and dorsad, like dorsal trachea. H-Ft-Lbr anterior, with H-VC extending medially to link left and

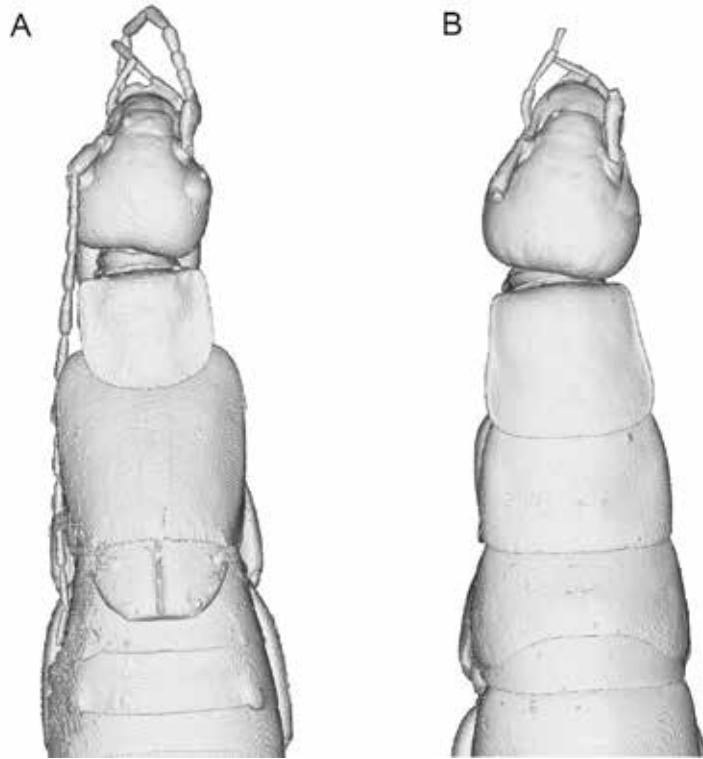


FIGURE 43. Dermaptera thoraxes, dorsal view: A. *Forficula*, B. *Anisolabis*.

right sides; H-Ft branching laterally and anterior with H-Lbr running directly anterior. Both H-VC with H-VC-Dvi running directly anterior. H-Ft-Lbr runs anterior, with small H-Ft splitting laterally and anterior, remaining H-Lbr running anterior. H-Mx-Md runs anterior and slightly laterally, with several branches: H-Lbm run ventrad, with short H-LbmPlp; H-Mx running ventrad, with short H-MxPlp. Remaining H-Md branch runs anterior, with H-Oc-Md connection from H-DCT; H-Md-Ant branching dorsally to parallel H-Ant from H-DCT.

THORAX: T1-DVi branching from H-DCT closer to T2-S than in *Forficula*. T1-MVi visible. Several T1-Fm visible. T3-VL with connection to VLT near A1-VB connection, forming X-shaped chiasma.

ABDOMEN: A4-DLT-Mvi branching from interior side of A4-DLT, slightly posterior to junction with A4-DB on right side of the body but nearly

at Y-shaped junction on the left side. Branching of An-DLT-Mvi from interior side of the dorsal longitudinal trunk varies between left and right side, but general anterior-posterior direction of tracheae is consistent for each segment (see fig. 46). A4-VLT-Vi anterior, extending through nearly two body segments. Anterior direction of An-VLT-Vi consistent for *Anisolabis*. A8-VLT-Cr and A8-DLT-Cr extending into forceps.

FAMILY FORFICULIDAE

Forficula auricularia

“Common earwig”

Figures 47 (lateral), 48 (dorsal), 49 (ventral)

Plates 26 (lateral), 27 (dorsal), 28 (ventral)

DESCRIPTION: HEAD: H-DCT and H-VCT thick, of similar diameter; H-DCTs curve inward

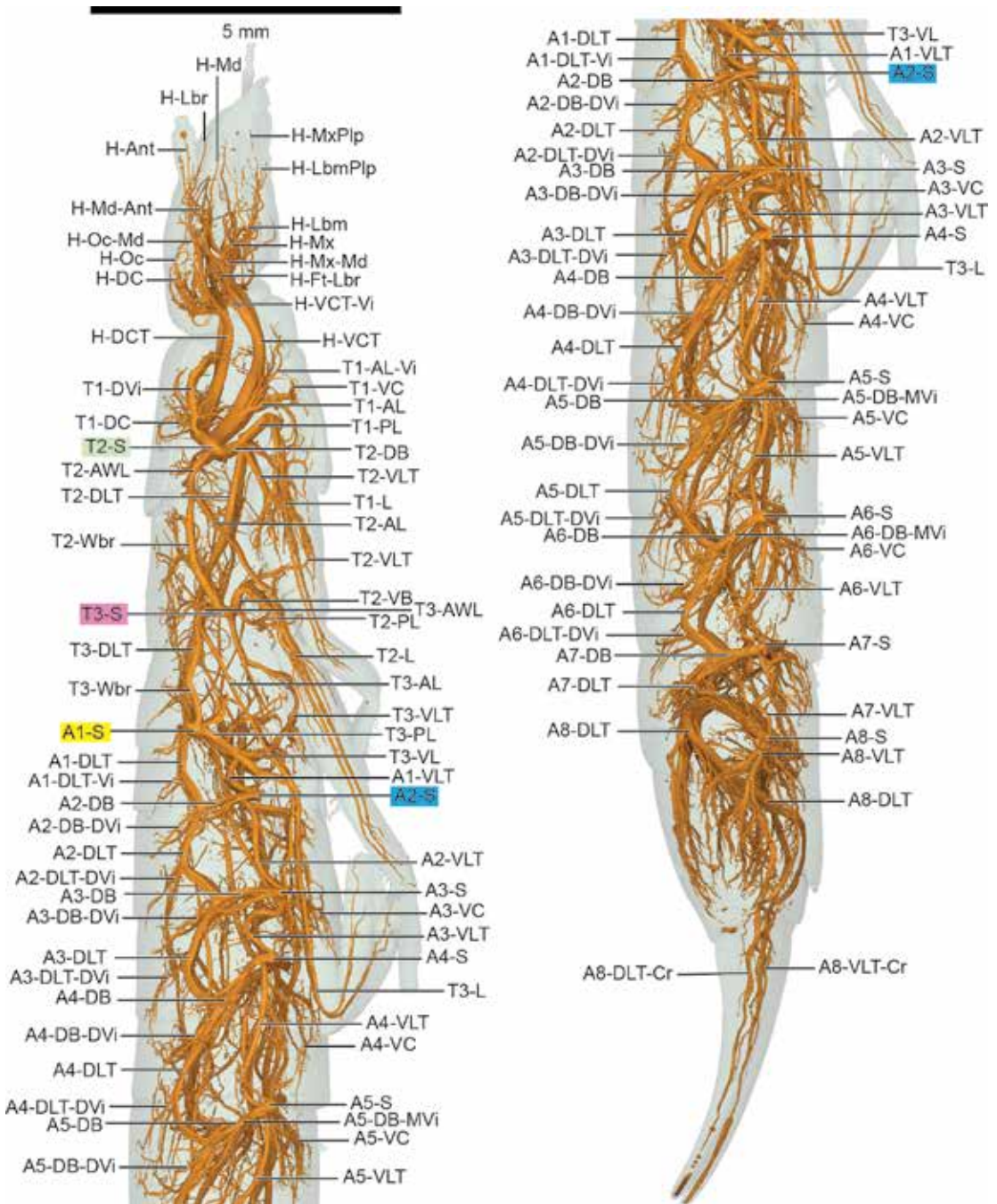


FIGURE 44. *Anisolabis maritima* (Dermaptera: Anisolabididae) lateral view.

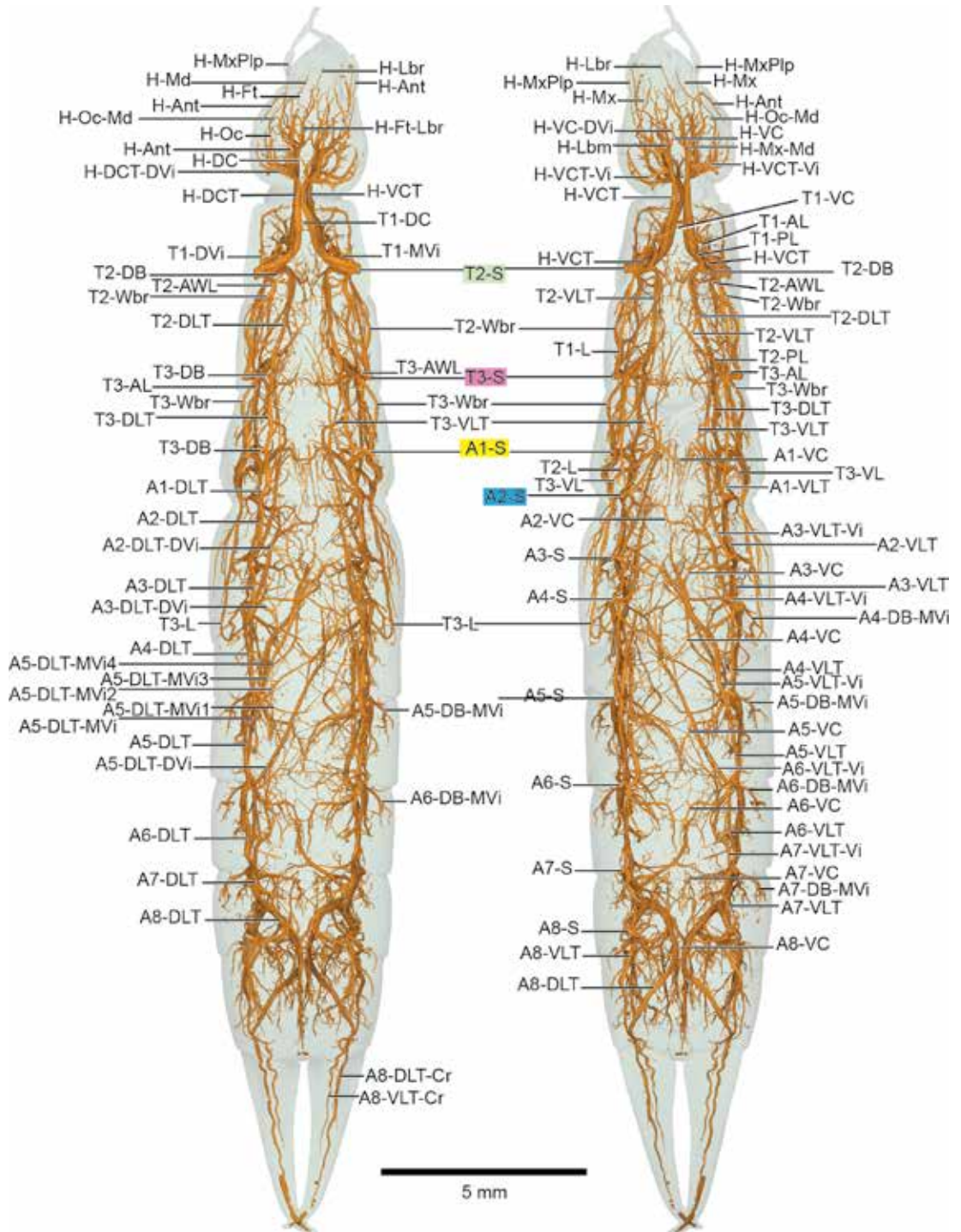


FIGURE 45. *Anisolabis maritima* (Dermaptera: Anisolabididae) dorsal (left) and ventral (right) views.

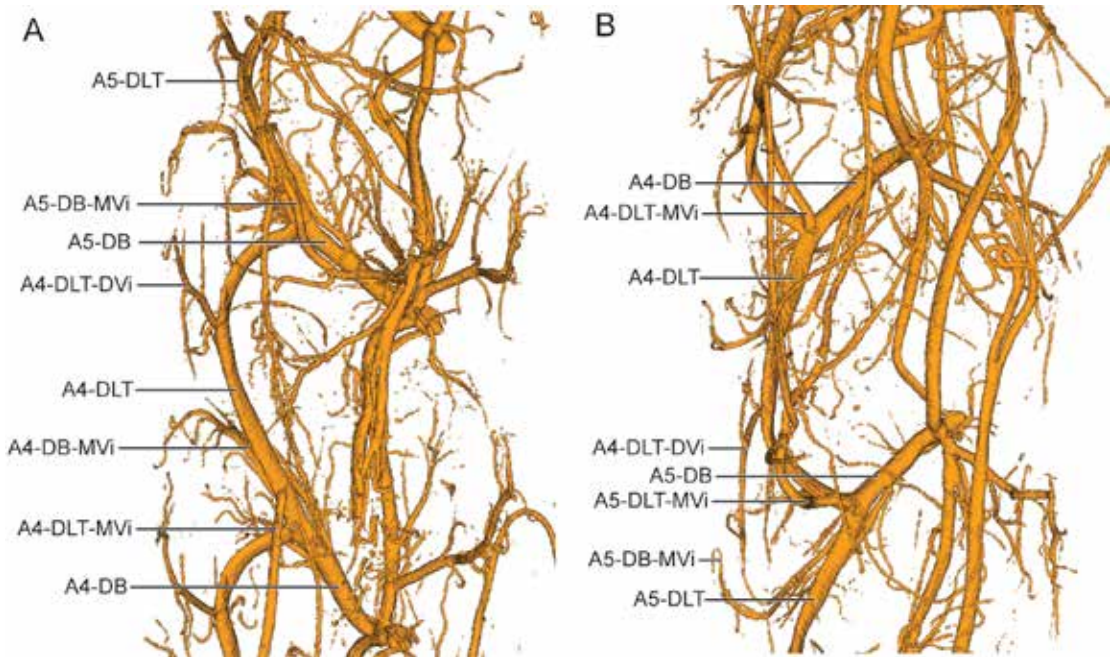


FIGURE 46. Internal views of *Anisolabis*, showing variation between left and right side in origin of visceral tracheae along dorsal longitudinal trunk. **A.** Right side. **B.** Left side.

slightly such that left and right tracheae nearly touch before turning laterally outward on entry to head capsule; H-VCTs both proceed straight into head. H-DCT with several branches just anterior of cervix: H-DCC, H-DCT-Dvi, H-Oc, and H-Ant. H-DCC present. H-DCT-Dvi running laterally and dorsad. H-Oc arcing laterally, with several small tracheae extending into eye, then continuing anteriorly and ventrad via H-Oc-Md to link with ventral H-Md. H-Ant extends anteriorly through head into antenna; left side of *Forficula* as H-Ant-Ft with H-Ft branching off H-Ant near base of antenna; H-Ft branches off H-VCT-sourced H-Md on right side. H-Ant with multiple tracheae in *Anisolabis*; likely present in *Forficula* but not visible in this scan. H-VCT likewise with several branches just anterior of cervix: H-VCT-Vi, H-VC, and H-Mx-Md. H-VCT-Vi running laterally and ventrad, like dorsal trachea. H-VC branches directly from H-VCT. Both H-VC with H-VC-Dvi run directly anteriad, extending as far as frontal area. H-Ft-Lbr absent. H-Mx-Md run-

ning anteriad and slightly laterally, with several branches: H-Lbm runs ventrad, with short H-LbmPlp; H-Mx running ventrad, with short H-MxPlp. Remaining H-Md branch runs anteriad, with H-Oc-Md connection from H-DCT; H-Md-Ant branching dorsally on right side to join H-Ant from H-DCT; H-Ft branching from H-Md on right side.

THORAX: Distance between T2-S and T3-S much shorter in *F. auricularia* (See fig. 43).

ABDOMEN: Abdominal tracheae of *F. auricularia* consistent with description of overall dermapteran tracheae above except for direction of visceral tracheae. A6..7-VLT-Vi similar to their anterior counterparts, except A6..7-VLT-Vi extend posteriorly rather than anteriorly, and do not extend beyond segment boundaries; A5-A6 appears to be dividing line for visceral tracheae from median longitudinal trunk, where A2..5-VLT-Vi tracheae extend anteriorly and A6..7-VLT-Vi extend posteriorly. A2..7-VLT-Vi not bilaterally symmetric; right side tracheae larger in

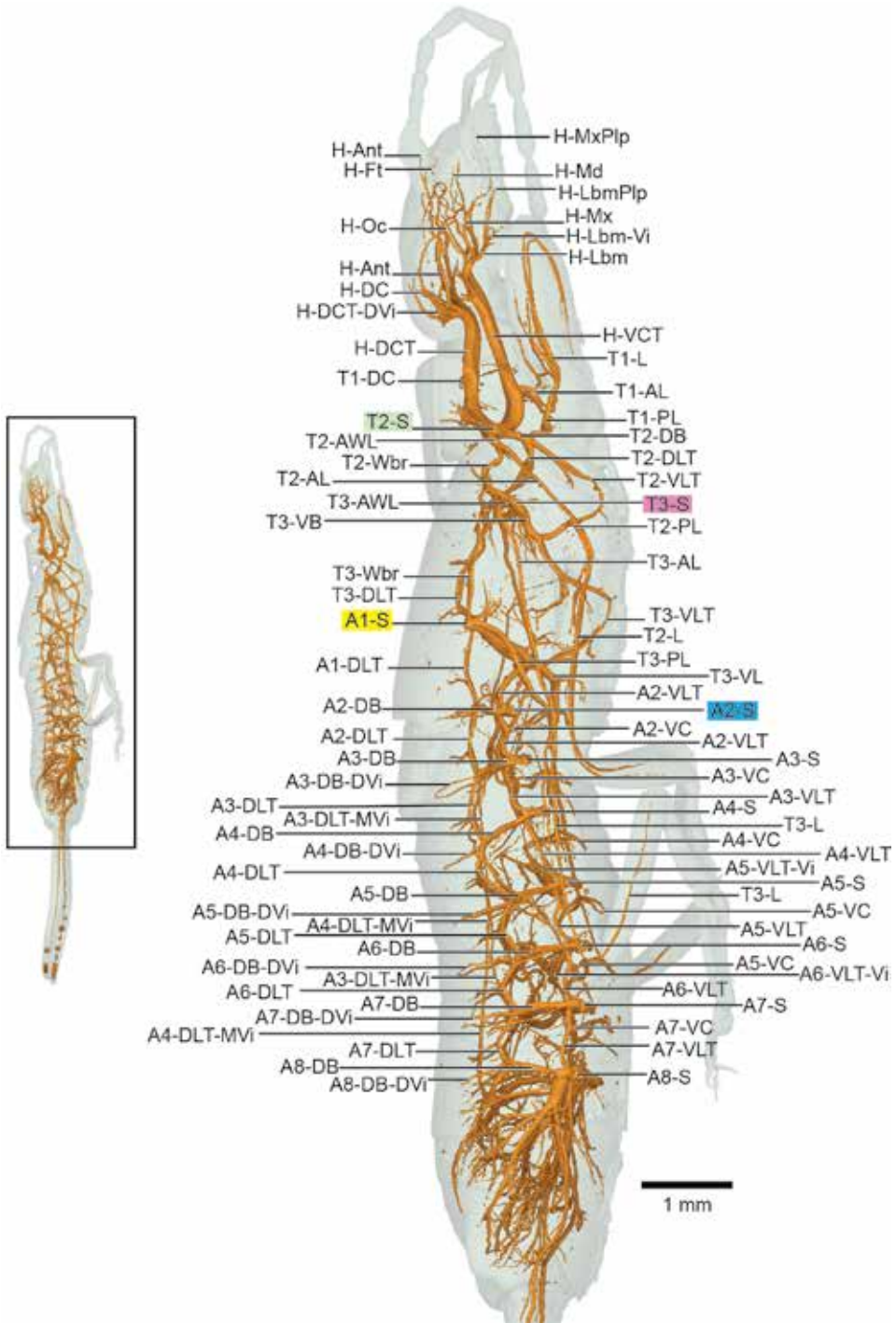


FIGURE 47. *Forficula auricularia* (Dermaptera: Forficulidae), lateral view.

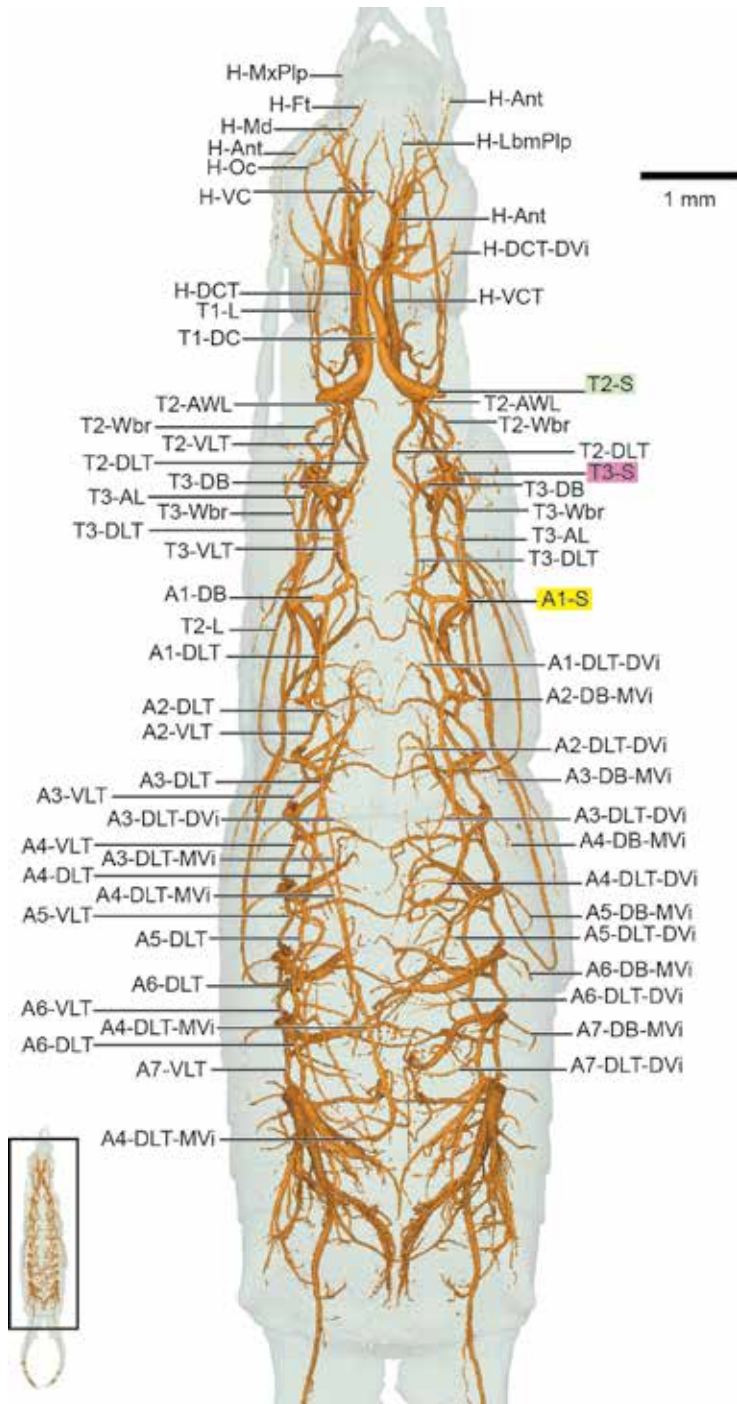


FIGURE 48. *Forficula auricularia* (Dermaptera: Forficulidae), dorsal view.

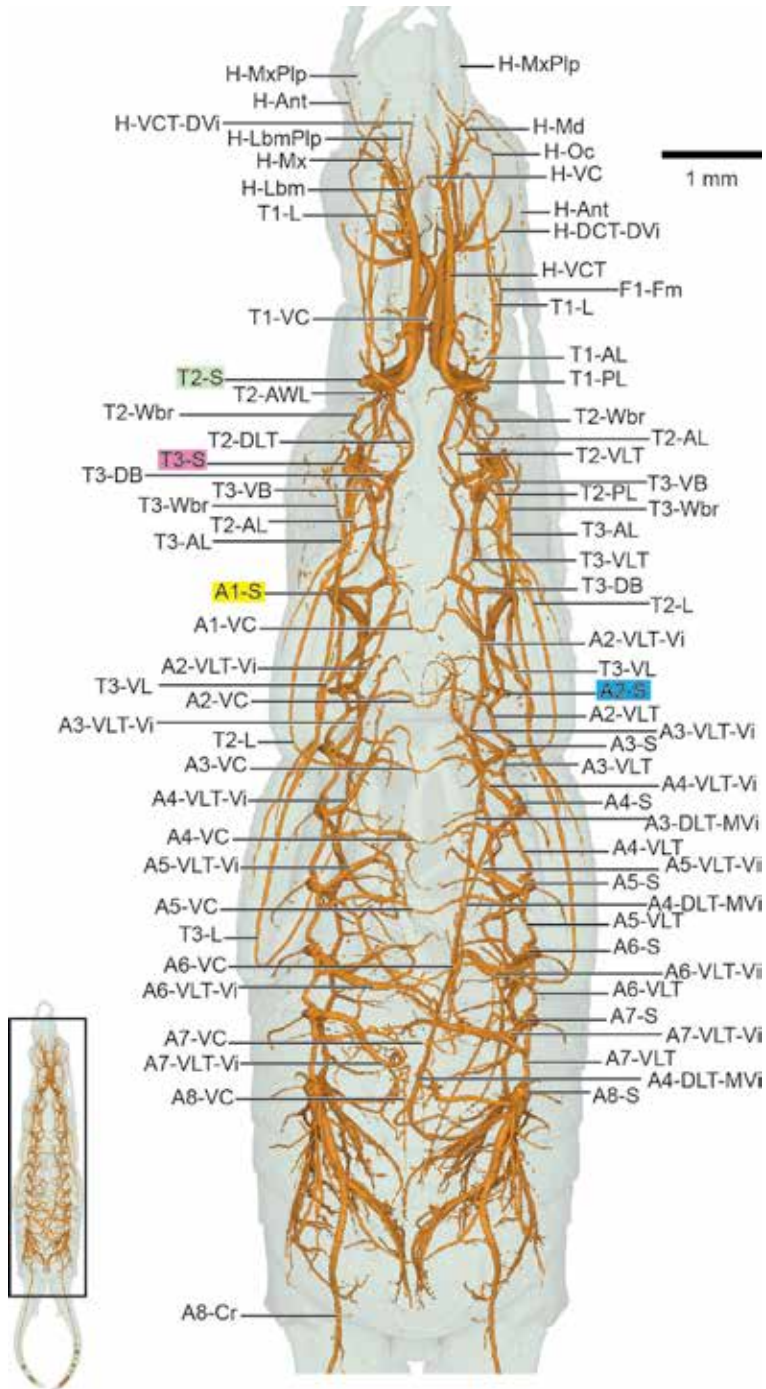


FIGURE 49. *Forficula auricularia* (Dermaptera: Forficulidae), ventral view.

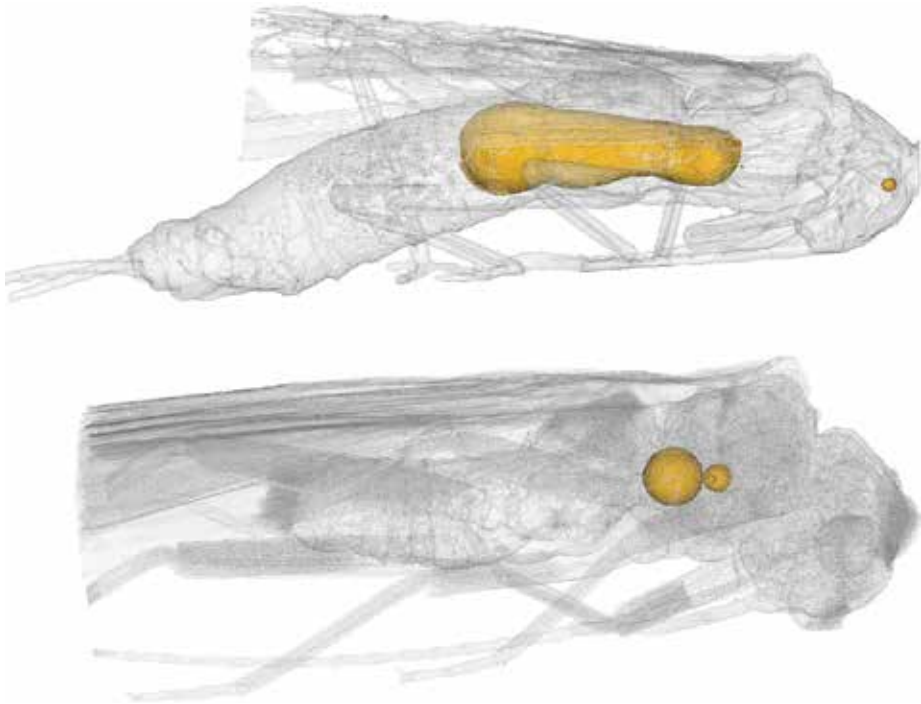


FIGURE 50. Alimentary canal air space position in Plecoptera: Perlodidae (top), Nemouridae (bottom).

cross-sectional area than left. Right side tracheae, while extending into body, also do not supply exact same areas/organs as those from left side. A3-DLT-Mvi and A4-DLT-Mvi on left side extend directly toward the posterior, with A3-DLT-Mvi ending near A7-DB. A3-DLT-Mvi on right side much reduced from left side counterpart, extending posteriorly as far as A4. A4-DLT-Mvi highly modified; after extending toward the middle of the body, continues well into A8 and A9, where it turns toward body wall in large arc that results in trachea pointing anteriorly. A4-DLT-Mvi with similar loop on right as on left, but much shorter, with apex of loop reaching as far as A5-DB. Extensive branching/tracheation in A7 and A8 for cercal (forceps) muscles.

ORDER PLECOPTERA

Respiration in stonefly naiads via gills has been studied for decades, partly because of the significance of stoneflies as indicators of water

quality. Two plecopteran specimens were scanned, one from Perlodidae and one from Nemouridae. The Nemouridae scan, at 3 μm resolution, shows substantially more smaller tracheae than the Perlodidae, scanned at 6 μm . Cromulent detail is present in both specimens to assess homology.

Numerous visceral tracheae branch from A4-DLT-Dvi and extend throughout the abdomen. Tracheae from A4-DLT-Dvi are pervasive throughout the abdomen, leading to the question of why this particular spiracle is so important. Other insects have adaptations for individual spiracles, such as the single abdominal “hissing” spiracle in *Gromphadorhina* (Nelson, 1979; Nelson and Fraser, 1980; Heinrich et al., 2013), but the presence of tracheae throughout the abdomen indicates a likely respiratory function. Future studies should investigate O_2 input versus CO_2 output, for example.

The perlodid specimen scanned here is another example of cooption of the gut as an air

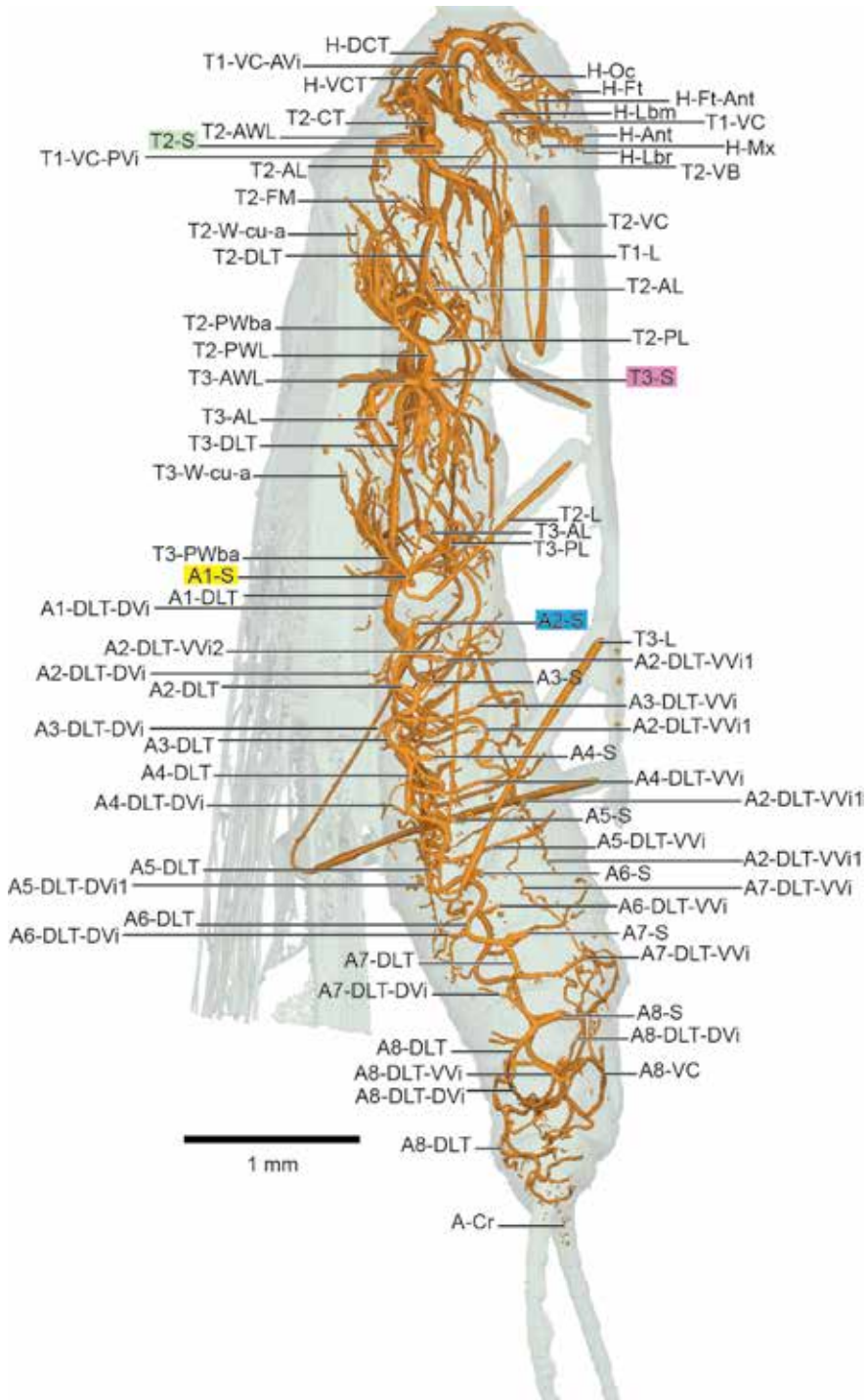


FIGURE 51. Perlodidae (Plecoptera) lateral.

space in nonfeeding adults. Likely for weight reduction, this condition also seen in mayflies and male Embioptera.

Other notable open issues include ventral visceral VVi tracheae in Perlodidae that are likely VC, as these are present in Nemouridae. Additionally, T2,3-VLT are present in Nemouridae but not Perlodidae. It is possible that the absence of T2,3-VLT in Perlodidae is a preservational artifact and scanning of further specimens is indicated to verify these features.

DESCRIPTION: HEAD: The two specimens differ in life history: adult Nemouridae, in the Group Euholognatha, have functional mouthparts adapted for feeding on algae, lichens, or soft pollen; while Perlodidae, in Systellognatha, is known to have adults with reduced mouth parts that typically do not feed. Consequently, head morphology is different enough to describe each family in the sections below.

THORAX: Thoracic tracheal morphology is largely similar between the two species scanned but with substantive differences; thoraces for both are described here for comparative clarity and also detailed in family sections below. Large thoracic air spaces present in both species, but spherical nature of air spaces in Nemouridae indicates possibility of preservational artifact (see fig. 50). Putative air sac in Perlodidae begins in thorax, extending into abdomen. T2-S with four tracheae: T2-CT, T2-DB, T2-VB, T2-AWL. T2-CT very thick, proceeding anteriorly in sinusoidal curve; Nemouridae with two branches off T2-CT: T1-L extending ventrad, and T1-Gi just posteriad of cervix. T1-Vi present. T1-L with tibial trachea greatly enlarged relative to femoral trachea. T2-DB running directly mediad, arcing posteriorly to continue as T2-DLT, with a number of T2-DLT-Dvi branching dorsally, likely into flight muscle; Nemouridae with large T2-FM extending dorsad close to T2-S; T2-Fm arcs medially to connect to opposing side as T2-DC; T2-FM off T2-DLT and T2-DC not visible in Perlodidae. T2-VB posteriad and ventrad; in Perlodidae, blind ending near mesocoxae; T2-VC present, positioned approximately halfway

between procoxae and mesocoxae. T2-VB asymmetric in Nemouridae; on right side, extending ventrad and posteriad, arcing dorsally just anterior to mesocoxae to link with T3-S via T2-DLT, while on left side, T2-VB mirrors right side but turns abruptly mediad to link with T2-VB on left side, forming T2-VC. T2-VB in Nemouridae with multiple T2-VB-Vi that likely supply flight muscle; single large T2-VB-Vi extending directly from T2-S on left side but mirroring similar T2-VB-Vi from T2-VB on right side. T2-VB-Vi not visible in Perlodidae scan. T2-AWL begins dorsally, turning posteriorly and ventrad toward midleg, joining T2-PL ventrally from T3-S; T2-AWL with a sharp turn posteriad in Perlodidae, likely where T2-AL and T2-Awba (or T2-W-c-r) would split but not visible in this scan; in Nemouridae T2-AWL short, with T2-AL and T2-W-c-r bifurcating just dorsal to T2-S. T2-AL tracheal lumen not visible and likely fluid filled in right side of Perlodidae; left side of same specimen with short gap and smaller trachea connecting. T2-AL complete in Nemouridae. T2-W-c-r extending dorsally and posteriad into wing. T2-W-c-r not visible in Perlodidae. T3-S with four connections: T3-DB, T3-VB, T2-PWL, T3-AWL. T3-DB short and directed inward, linking with T2-DLT anteriorly and T3-DLT posteriorly; large T3-FM runs dorsad where T3-DB joins T2-DLT and T3-DLT. T3-FM running dorsad with several tracheae extending into flight muscles; T3-FM continues dorsad, arcing medially to join with opposite side via T3-DC; T3-DC not visible in Perlodidae but likely present. T3-VB runs ventrad and posteriad, with numerous branches extending into flight muscle; T3-VB with T3-VC branch inward, meeting opposite side, near ventral sternite. In Nemouridae, T3-VB on left side continues as T3-VLT, linking with A1-S; T3-VLT absent on right side. T3-VLT not visible in Perlodidae. T2-PWL running directly anteriorly, bifurcating into T2-Pwba extending dorsally and anteriorly and T2-PL, mediad. T2-PwBa continues dorsally, with several branches into flight muscle and single, small T2-W-cu-a extending into trailing edge of fore-

wing. T2-PL arcing medially and ventral before turning laterally, joining with T2-AL from anterior and extending posteriorly into T2-L. T2-L with tibial trachea greatly enlarged relative to femoral trachea. T3-AWL running ventrad, just medial from T3-S, with small T3-W-c-r branching dorsally where remaining trachea turns posteriorly into T3-AL. T3-W-c-r not visible in *Perlodidae* but likely present.

ABDOMEN: Abdominal morphology largely similar between *Perlodidae* and *Nemouridae*, with overall structure described here and specific differences given below. Air sac in *Perlodidae* extends as far as A3-S (fig. 50). A[1..8]-S present. A1-S branching modified from remaining abdominal segments, with slight differences between *Perlodidae* and *Nemouridae*. Both specimens with A1-DB and A1-VB; *Perlodidae* with T3-Pwba directly from A1-S, *Nemouridae* with T3-Pwba from A1-VB slightly ventrad from A1-S. Both T3-Pwba anteriorly and slightly dorsad, splitting into several smaller visceral tracheae likely supplying flight muscle and single T3-W-cu-a into trailing edge of hind wing. A[1..8]-DB and A[1..8]-DLT present in both taxa, with numerous visceral tracheae from DLT detailed in sections below. A[1..8]-VB, A[2..8]-SB, A[1..8]-VC present in *Nemouridae* but absent (or not visible) in *Perlodidae*. See family-level sections for descriptions of visceral tracheae.

FAMILY PERLODIDAE

“Stripetails” or “Springflies”

Figures 51 (lateral), 52 (dorsal), 53 (ventral)

Plates 29 (lateral), 30 (dorsal), 31 (ventral)

The scanned perlotid is a gravid female specimen, with numerous eggs visible (see section on abdomen). These have been omitted from visualizations for clarity; visceral tracheae anastomose among eggs. Large central air sac begins in mesothorax and extends as far as A3-S in abdomen (also omitted from visualizations for clarity, see fig. 50). As mentioned above, adult perlotids have

reduced mouthparts and generally do not feed; the head tracheal system is described in full here.

DESCRIPTION: HEAD: H-DCT and H-VCT elongate and winding through prothorax, bifurcating from T2-CT well posteriorly of cervix. H-DCT begins straight on entry to head capsule with short H-DVT-DVi before turning medially toward eye, with three branches: H-Oc, H-Ft-Ant, and H-Ft. H-Oc short, extending laterally into eye. H-Ft-Ant dorsoventral, linking H-DCT with H-Ant from H-VCT. H-DCT blind ending at H-Ft. H-DCC absent. H-VCT generally straight and running anteriorly, with anterodorsal H-VCT-DVi and ventral H-Lbm before continuing anteriorly to split into H-Ant, H-VC, and H-Md-Lbr. H-Ant lateral, with connection to H-DCT via H-Ft-Ant. H-VC running directly medially, linking with opposite side of head. H-Md-Lbr continues anteriorly, arcing medially with branch into H-Md before continuing anteriorly and blind ending at H-Lbr.

THORAX: T2-S with four tracheae: T2-CT, T2-DB, T2-VB, T2-AWL. T2-CT large in diameter, proceeding anteriorly in sinusoidal curve, much shorter than in *Nemouridae*, dividing into H-DCT and H-VCT in mid-prothorax. Single T1-Vi present. T1-L running ventrad from H-VCT, with tibial trachea greatly thickened relative to femoral trachea. T1-VC present, extending medially from each T1-L to connect with opposite side; T1-VC-Avi extending anteriorly toward head, looping posteriorly near cervix; T1-VC-Pvi running directly posteriorly. T2-DB running directly medially, arcing posteriorly to continue as T2-DLT, with several T2-DLT-Dvi branching dorsally, likely into flight muscle; T2-FM off T2-DLT and T2-DC not visible but likely present. T2-VB posteriorly and ventrad, ending blind near mesocoxae; T2-VC present, positioned approximately halfway between forecoxae and mesocoxae; continuation of T2-VB as T2-VLT toward T3-S (as in *Nemouridae*) likely present but not visible in this scan. T2-VB-Vi not visible but likely present. T2-AWL begins dorsally, turning posteriorly and ventrad toward midleg, joining T2-PL ventrally from T3-S;

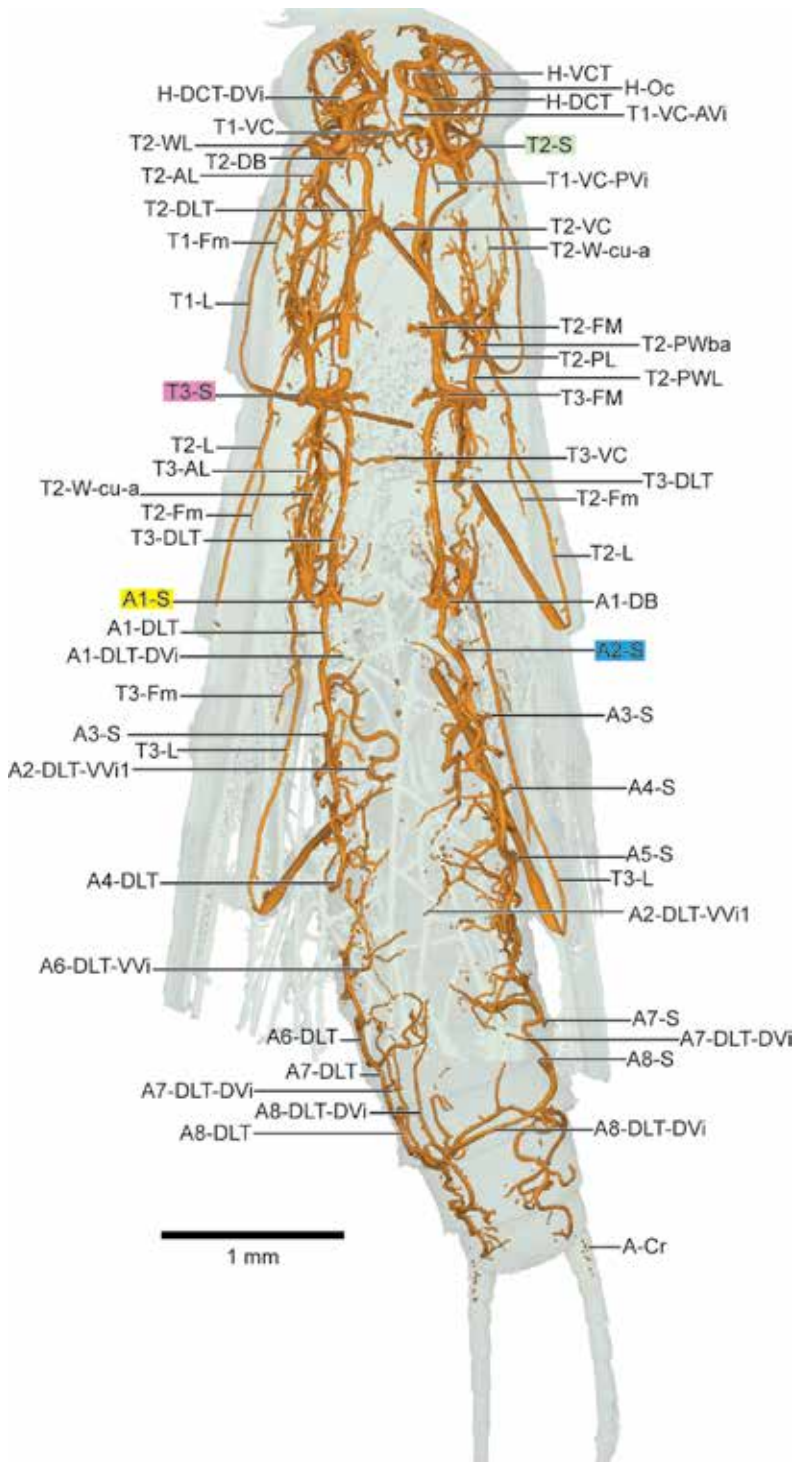


FIGURE 52. Perlodidae (Plecoptera) dorsal.

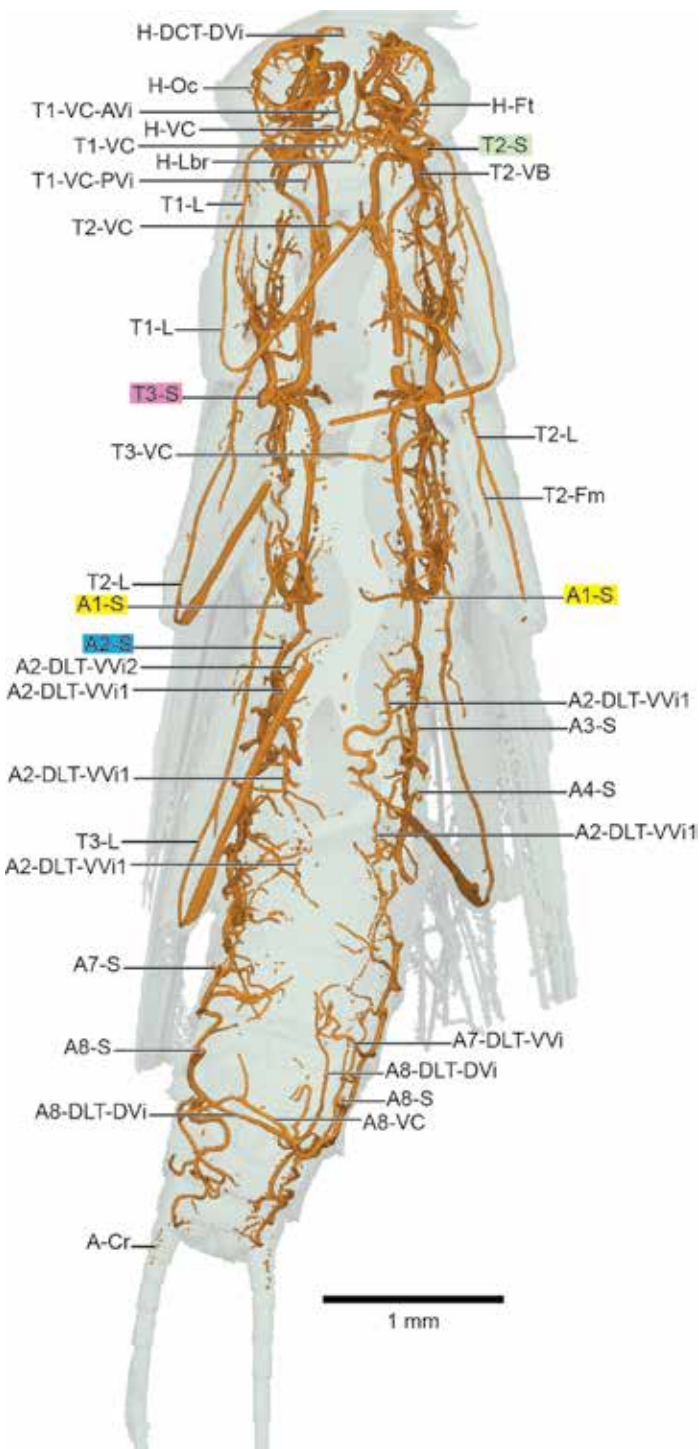


FIGURE 53. Perlodidae (Plecoptera) ventral.

T2-AWL with a sharp turn posteriad, likely where T2-AL and T2-Awba (or T2-W-c-r) would split but not visible in this scan; T2-AL tracheal lumen not visible and likely fluid filled in right side; left side of same specimen with gap and smaller trachea connecting. T2-W-c-r not visible but likely present. T3-S with four connections: T3-DB, T3-VB, T2-PWL, T3-AWL. T3-DB short and running directly inward, linking with T2-DLT running anterior and T3-DLT posteriad; large T3-FM dorsad where T3-DB joins T2-DLT and T3-DLT. T3-FM running dorsad with several tracheae extending into flight muscles; T3-FM continues dorsad, arcing medially to join with opposite side via T3-DC, not visible but likely present. T3-VB running ventrad and posteriad, with numerous branches extending into flight muscle; T3-VB with T3-VC branching inward, meeting opposite side, near ventral sternite. T3-VLT not visible but likely present. T2-PWL running directly anterior, bifurcating into T2-Pwba extending dorsally and anterior and T2-PL, medial. T2-PWba continues dorsally, with several branches into flight muscle and single, small T2-W-cu-a extending into trailing edge of forewing. T2-PL arcing medially and ventral before turning laterally, joining with T2-AL anteriorly and extending posteriorly into T2-L. T2-L with tibial trachea greatly thickened relative to femoral trachea. T3-AWL running ventrad, just medial from T3-S, with small T3-W-c-r branching dorsally where remaining trachea turns posteriad as T3-AL. T3-W-c-r not visible but likely present.

ABDOMEN: Numerous eggs present, see figure 54. T3-Pwba branching directly from A1-S. *An*-VB, *An*-SB, A[1..7]-VC absent (or not visible), A8-VC present. A[1..8]-DLT-Dvi present, possibly supplying dorsal vessel. Several segments with elongate visceral tracheae, spanning several segments, including: A2-DLT-Vvi2, extending posteriorly past A5-S; A7-DLT-Vvi, extending anteriorly past A5-S; A6-DLT-Dvi, extending dorsad and anteriorly past A4-S on left side only. Remaining visceral tracheae elongate but winding, often extending past segment boundary before reversing direction, occasionally several times; visceral tracheae often with asymmetric left/right branching patterns. Noticeable lack of left-right commissures with exception of A8-S and right side A8-DLT-Dvi extending mediad, crossing center line and proceeding anteriorly on left side toward A7-S; A8-DLT-Dvi on left side extending anteriorly, not crossing to opposite side.

FAMILY NEMOURIDAE

“Spring stoneflies” or “Brown stoneflies”

Figures 55 (lateral), 56 (dorsal), 57 (ventral)

Plates 32 (lateral), 33 (dorsal), 34 (ventral)

DESCRIPTION: HEAD: T2-CT elongate and winding, with H-VCT and H-DCT bifurcating immediately after entry into head capsule. H-DCT short and running directly anteriad, dividing into H-Oc laterally and H-DCC mediad. H-DCC with several small visceral tracheae, dorsally and ventrally. H-VCT running directly ventrad, proceeding anteriorly in a J-shaped arc; H-VCT-Dvi running dorsad/antieriad and H-VC ventrad/posteriad before H-VCT continues ventrad and arcs anteriorly, dividing into H-Ant laterally and H-Md-Ft-Lbr. Along this second branch, H-Md branches ventrad, with H-Ft-Lbr

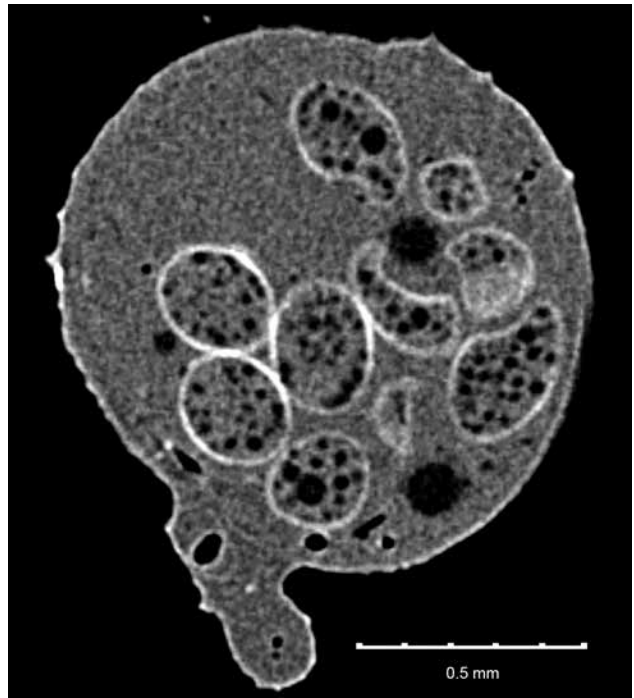


FIGURE 54. Perlodidae lateral cross section of abdomen, showing eggs.

extending anteriorly a short distance before bifurcating into H-Ft dorsally and H-Lbr ventrally. No connections between H-DCT and H-VCT (unlike Perlodidae).

THORAX: Air space present in mesothorax (see fig. 50), but likely a preservational artifact rather than an air sac due to spherical nature. T2-S with four tracheae: T2-CT, T2-DB, T2-VB, T2-AWL. T2-CT large, elongate, and S-shaped, with T1-L running ventrad near prothoracic coxae (rather than typical configuration of T1-L from H-VCT, as in Perlodidae); T1-Gi running ventrad just posterior to neck; each side with two T1-Gi visible. T1-VC present, extending mediad from T1-L. Two T1-Vi present, on either side (longitudinally) of T1-L. T1-L with tibial portion greatly enlarged relative to femoral portion. T2-DB directly mediad, arcing posteriorly to continue as T2-DLT, with several T2-DLT-Dvi branching dorsally, likely into flight muscle; large T2-FM

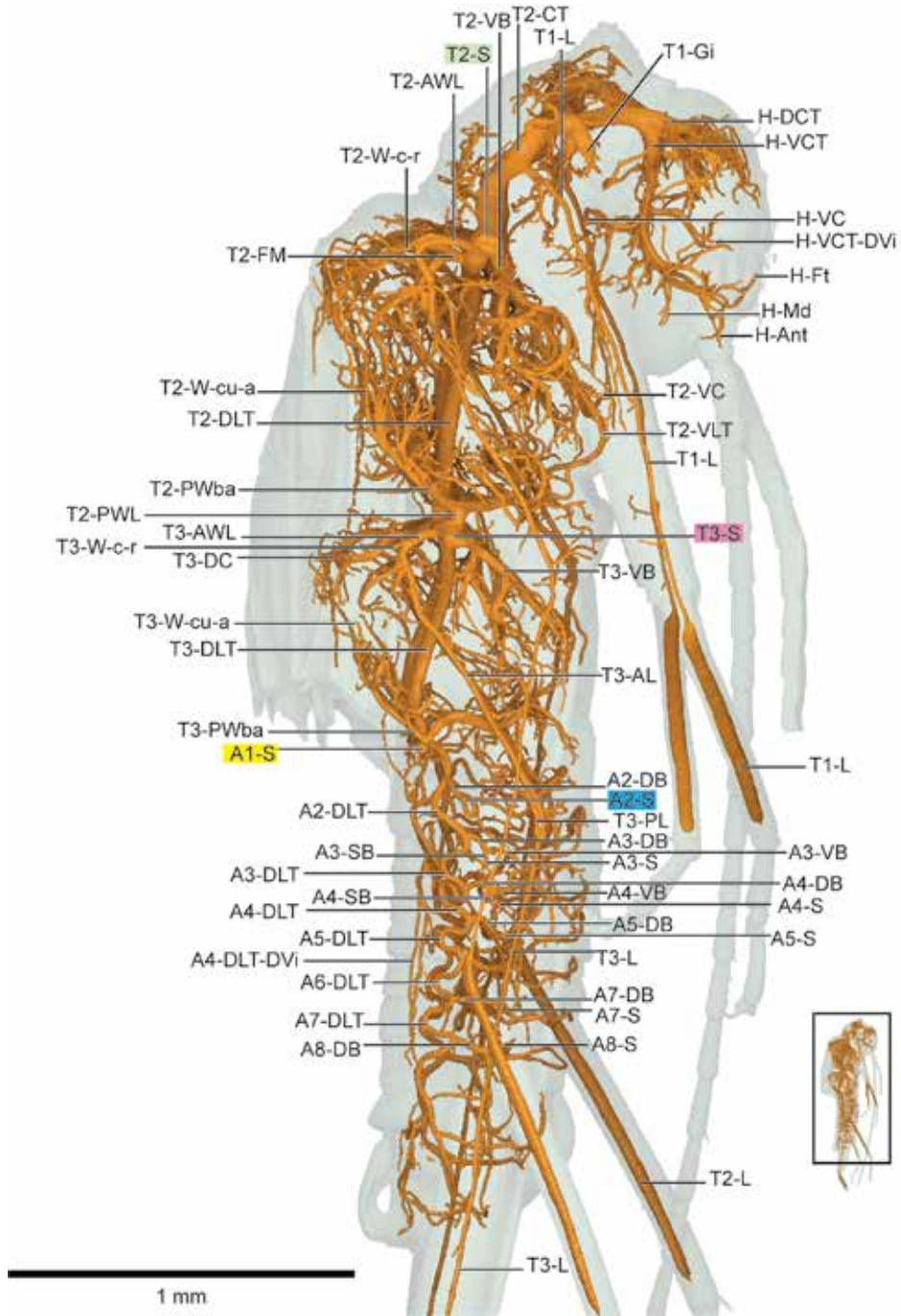


FIGURE 55. Nemouridae (Plecoptera) lateral.

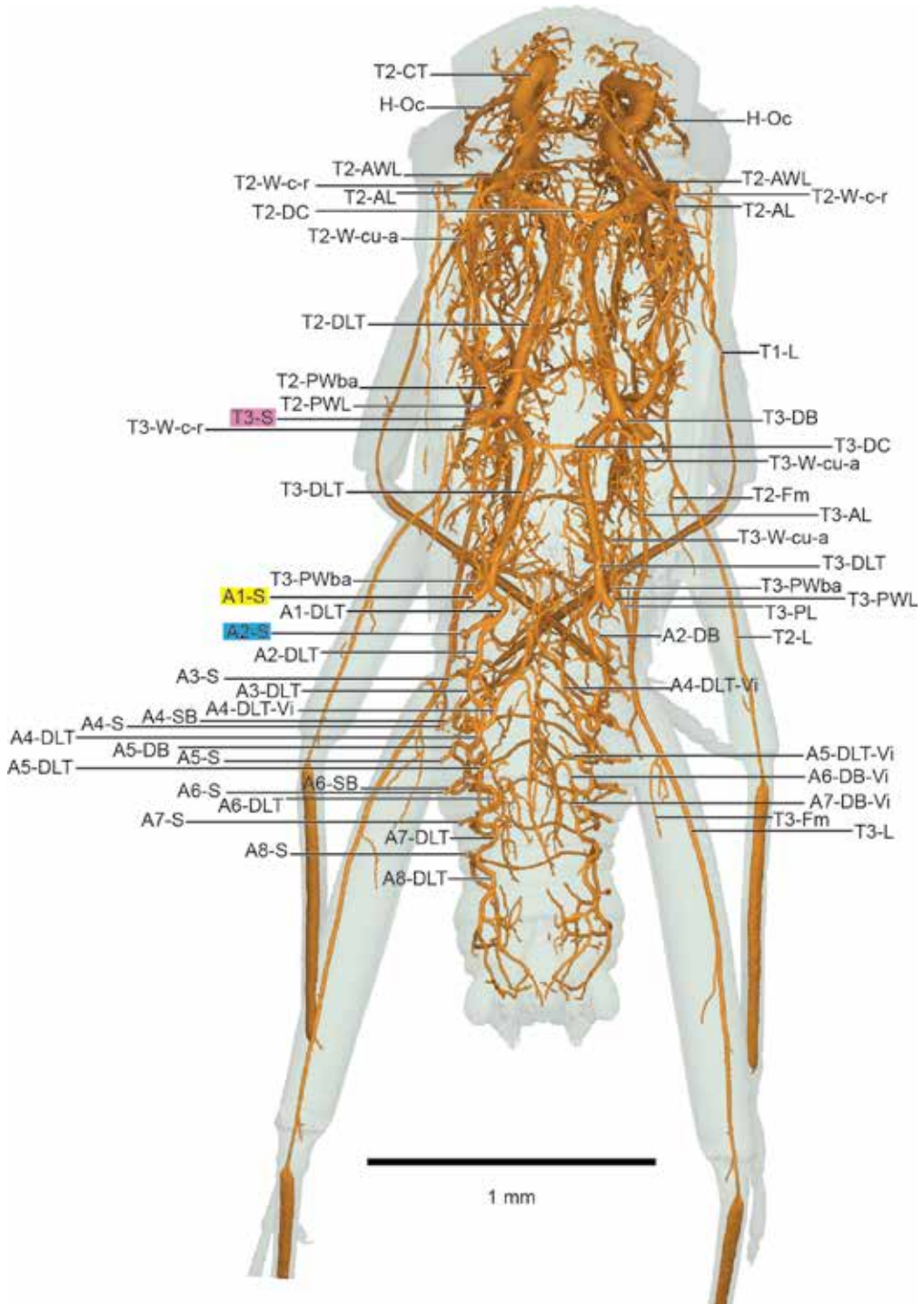


FIGURE 56. Nemouridae (Plecoptera) dorsal.

branching ventrally from T2-DLT just medial to T2-S, extending dorsad and medially to form T2-DC. T2-VB running posteriad and ventrad; in Perlodidae, ending blind near mesocoxae; T2-VC present, positioned approximately halfway between forecoxae and mesocoxae. T2-VB asymmetric: on right side, extending ventrad and posteriad, arcing dorsally just anterior to mesocoxae to link with T3-S via T2-DLT, while on left side, T2-VB mirrors right side but turns abruptly medially to link with T2-VB on left side, forming T2-VC. T2-VB in Nemouridae with multiple T2-VB-Vi that likely supply flight muscle; single large T2-VB-Vi extending directly from T2-S on left side but mirroring similar T2-VB-Vi from T2-VB on right side. T2-AWL short, with T2-AL and T2-W-c-r bifurcating just dorsal of T2-S. T3-S with four connections: T3-DB, T3-VB, T2-PWL, T3-AWL. T3-DB short and directed inward, linking with T2-DLT anteriorly and T3-DLT posteriad; large T3-FM running dorsad where T3-DB joins T2-DLT and T3-DLT. T3-FM runs dorsad with several tracheae extending into flight muscles; T3-FM continues dorsad, arcing medially to join with opposite side via T3-DC. T3-VB running ventrad and posteriad, with numerous branches extending into flight muscle; T3-VB with T3-VC branch inward, meeting opposite side near ventral sternite. T3-VB on left side continues as T3-VLT, linking with A1-S; T3-VLT absent on right side. T2-PWL running directly anteriorly, bifurcating into T2-Pwba dorsally and anteriorly into T2-PL, medially. T3-AsymC from T2-PL on left side, crossing midline to connect with T2-VLT on right side. T3-AsymC like T3-VLT, except with modification to link with T2-VLT on right side. T2-PWBa continues dorsally, with several branches into flight muscle and single, small T2-W-cu-a extending into trailing edge of forewing. T2-PL arcing medially and ventrally before turning laterally, joining with T2-AL from anterior and extending posteriorly into T2-L. T2-L with tibial portion greatly enlarged

relative to femoral portion. T3-AWL ventrad, just medial from T3-S, with small T3-W-c-r branching dorsally where remaining trachea turns posteriad as T3-AL.

ABDOMEN: T3-Pwba branching from A1-VB slightly ventral to A1-S. A[1..8]-VB, A[2..8]-SB, A[1..8]-VC present. Many segments with elongate visceral tracheae spanning several segments, most notably A4-DLT-Dvi, beginning directly dorsad before branching into several long tracheae that extend anteriorly and posteriad, spanning the entire length of the abdomen with many ventral branches throughout; and A4-VB-Vi, with similar branches running anteriorly and posteriad. A6-DB-Vi branching similar but not as extensive as A4; connection between A4-DLT-Vi and A6-VB-Vi possible but could be scanning artifact. Due to the complexity of the visceral branching, readers are directed to the online supplementary digital data, available for downloading and interactive visualization for this specimen.

ORDER ORTHOPTERA

Orthopteran anatomy (and some tracheae) has been diagrammed in classic works, but the first proper treatments of respiratory systems were by Vinal (1919: for *Dissosteria carolina*), Carpentier (1927: for *Phasgonura viridissima*), and Ander (1939: for Ensifera in general). Several tracheal terms were introduced using Orthoptera, particularly those involving auditory adaptations and saltatorial legs, and the work of these researchers (particularly Ander) was instrumental in mapping the tracheae here. More modern studies have focused on physiology, including ventilation in *Schistocera gregaria* in influential experimental works by Miller (1960a, 1960b, 1960c), active tracheal compression in Orthoptera observed via synchrotron imaging by Westneat et al. (2003), and the distribution of air spaces in *Schistocera americana* by Shaha et al. (2013).

Four orthopteran specimens were scanned: *Gryllus* sp. (Gryllidae), *Romalea microptera*

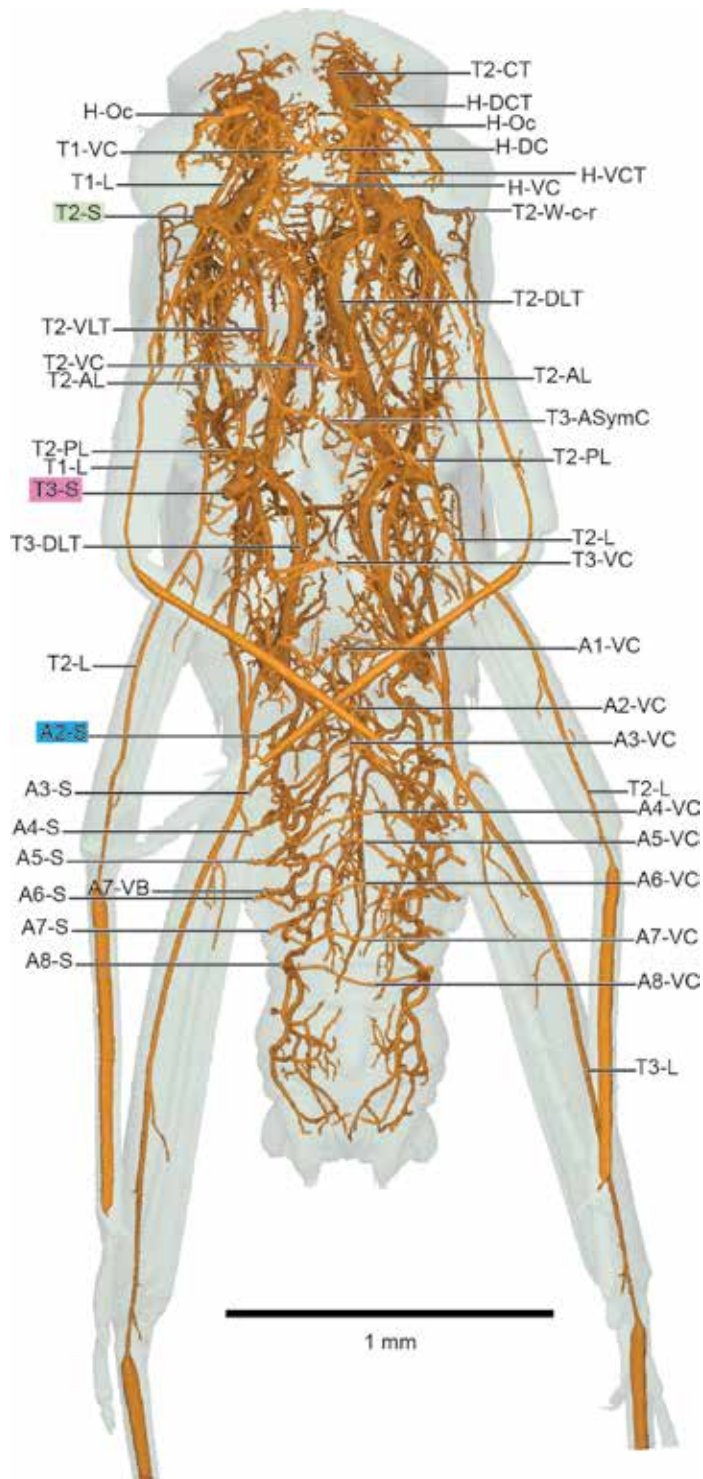


FIGURE 57. Nemouridae (Plecoptera) ventral.

(Romaleidae), *Tachycines asynamorous* (Raphidophoridae), and a *Meconema thalassinum* (Tettigoniidae). Orthoptera tracheal morphology is best represented here in the scans of *Gryllus* and *Meconema*, and these are described here in detail. Notable features are described for the remaining specimens, but they are presented in a more basic manner due to the suboptimal quality of the scan of *Tachycines* and the substantial complexity of *Romalea*.

The most comprehensive work to date on tracheal morphology of Orthoptera is by Ander (1939). His work formed the basis for many of the homology statements here, although we reinterpret some of his tracheae, in particular the supraventral (suv) in the prothorax and mesothorax. Ander indicates that the suv is absent in the metathorax in all Ensifera (his fig. 81). Interestingly, Ander cites Carpentier (1927) as the source for supraventral, where it does not go into the leg (Carpentier's figure 3). However, Ander's figure 83 details Gryllidae (fig. 81 is his overall view of Ensifera) and identifies three tracheae going into the proleg: pa, pp, and suv (supraventral), an apparent departure from Carpentier's suv. Herein, *Tn*-AL refers to Ander's pa, *Tn*-PL for pp, and *Tn*-VL for pve. (Refer to table S1 in the online supplement for all reassignments of labels and terms from previous studies.) Ander's suv, more consistent than Carpentier's, is likely T1-Cx (and even T1-PL in some taxa), designated here as such. Ander's suf (suprafurcal), lvl (lateral lateroventral), and pf (postfurcal connective, apparently absent in *Gryllus* but present in other Ensifera) tracheae were not found to be homologous outside Orthoptera. His terminology is retained for descriptions of Orthoptera for convenience.

The dorsum of the metathorax in both *Gryllus* (Gryllidae) and *Meconema* (Tettigoniidae) both possess T3-DB-Vi, paired air sacs reminiscent of a root vegetable, and ending blind (fig. 59, pl. 36). These tracheae are similar in morphology to those found in the ventral thorax of Dictyoptera for hearing, and their possible function as such should be investigated further.

FAMILY GRYLLIDAE

Gryllus sp.

"Field cricket"

Figure 58 (lateral), 59 (dorsal), 60 (ventral)

Plates 35 (lateral), 36 (dorsal), 37 (ventral)

The prothorax features a cagelike network referred to as a "pronotal rim" (prt) by Ander, which we interpret here as T1-DVi.

DESCRIPTION: HEAD: Three paired trunks extending into head: H-DCT and H-VCT present, with additional ventral H-VLT branch from prothorax. Head branches highly networked and cagelike, with multiple dorsal-ventral and lateral connections, making assessment of homology challenging. Mouthparts, H-Ant, and H-Oc determined, but remaining tracheae are highly networked and not homologized here. Readers are referred to online digital models for interactive viewing and further research.

THORAX: T2-S positioned just posterior of foreleg with split opening, typical T2-S dorsal and secondary T2-VS ventral. T2-S with four branches: H-DCT, H-VCT, T2-DB, T2-VB. H-DCT thick, extending dorsad and medially, curving anteriorly and extending into head; T1-DVi branching laterally and dorsad from H-DCT close to dorsal margin of T2-S, dividing into cagelike network of T1-DVi tracheae along pronotal wall. H-VCT with short T1-Cx running just anteriorly of spiracular opening, extending anteriorly and ventrally into forecoxa with multiple branches in a cagelike network similar to pronotum. H-VCT extends medially, curving anteriorly and extending into head; T1-AL running ventrad at this curve. T2-DB runs dorsad, curving medially and ventrad as start of T2-DLT, T2-AWL extending laterally and dorsad near this curve, bifurcating into T2-Wbr posteriorly and T2-AL ventrad, extending posteriorly toward T3-S; fanlike tracheae extend posteriorly from T2-DB, likely into flight muscles. T2-Wbr with T2-W-c-r branching dorsad into wing, while T2-Wbr continues ventrad, connecting with

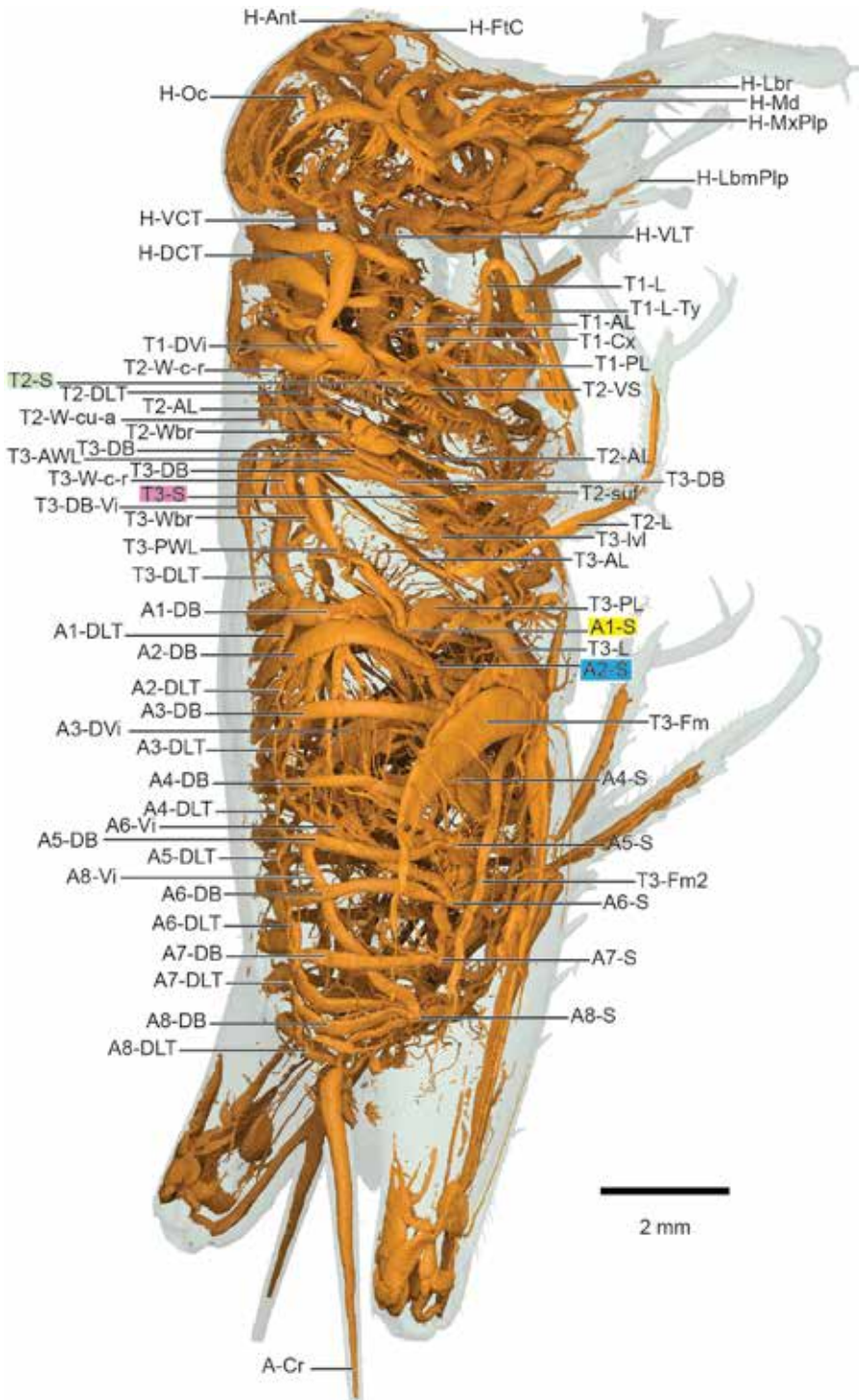


FIGURE 58. *Gryllus* sp (Orthoptera: Gryllidae), lateral view.

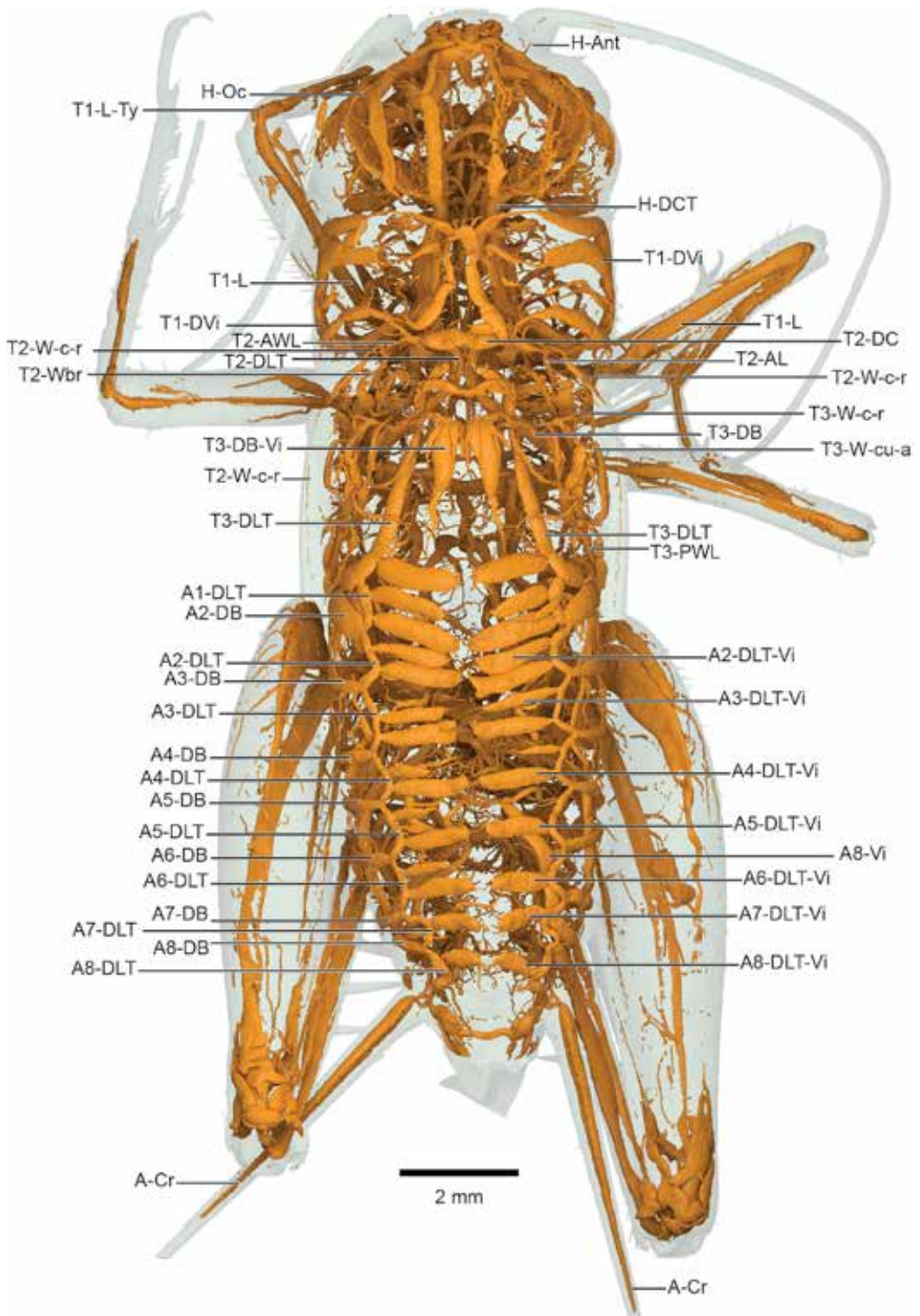


FIGURE 59. *Gryllus* sp (Orthoptera: Gryllidae), dorsal view.

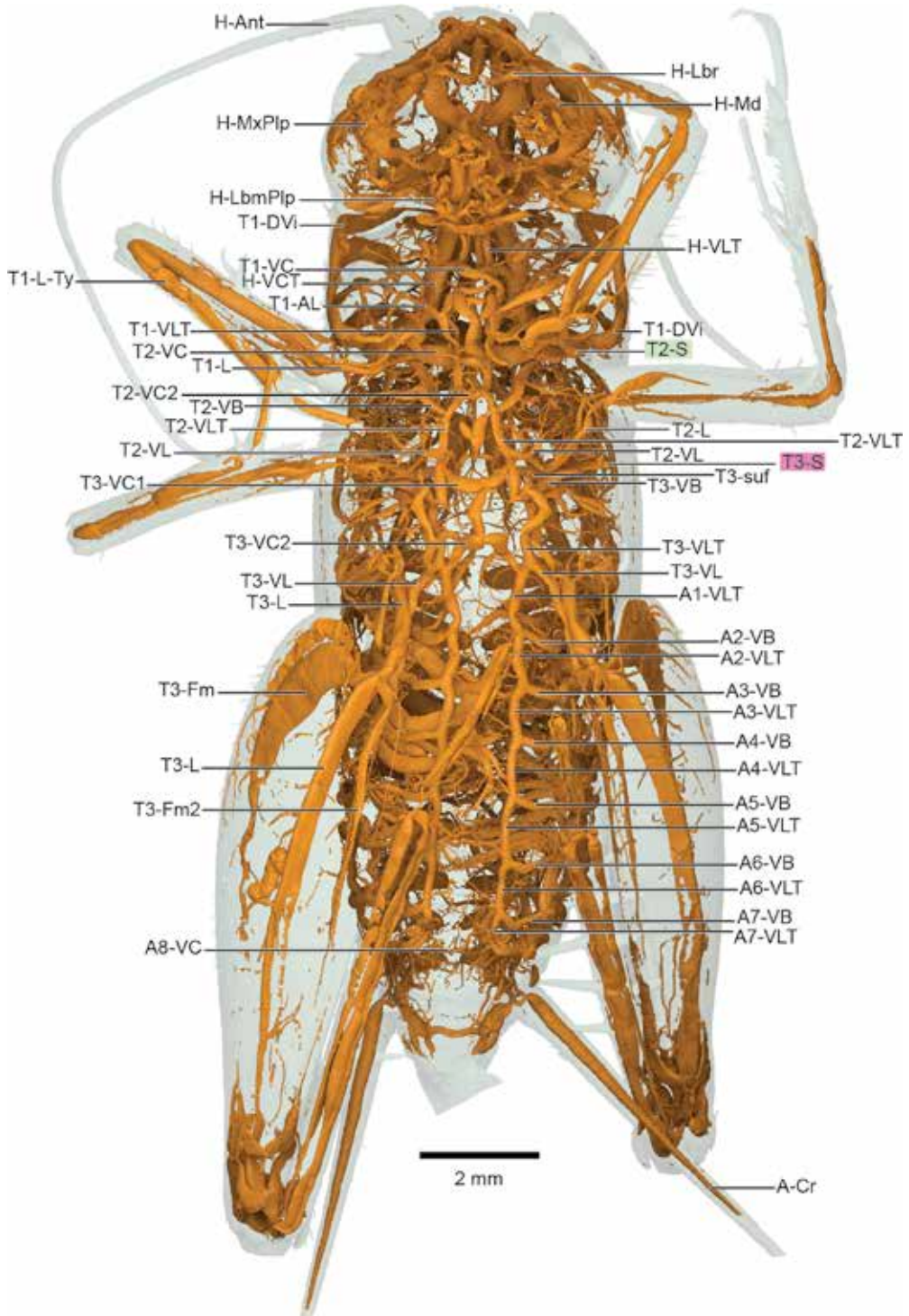


FIGURE 60. *Gryllus* sp (Orthoptera: Gryllidae), ventral view.

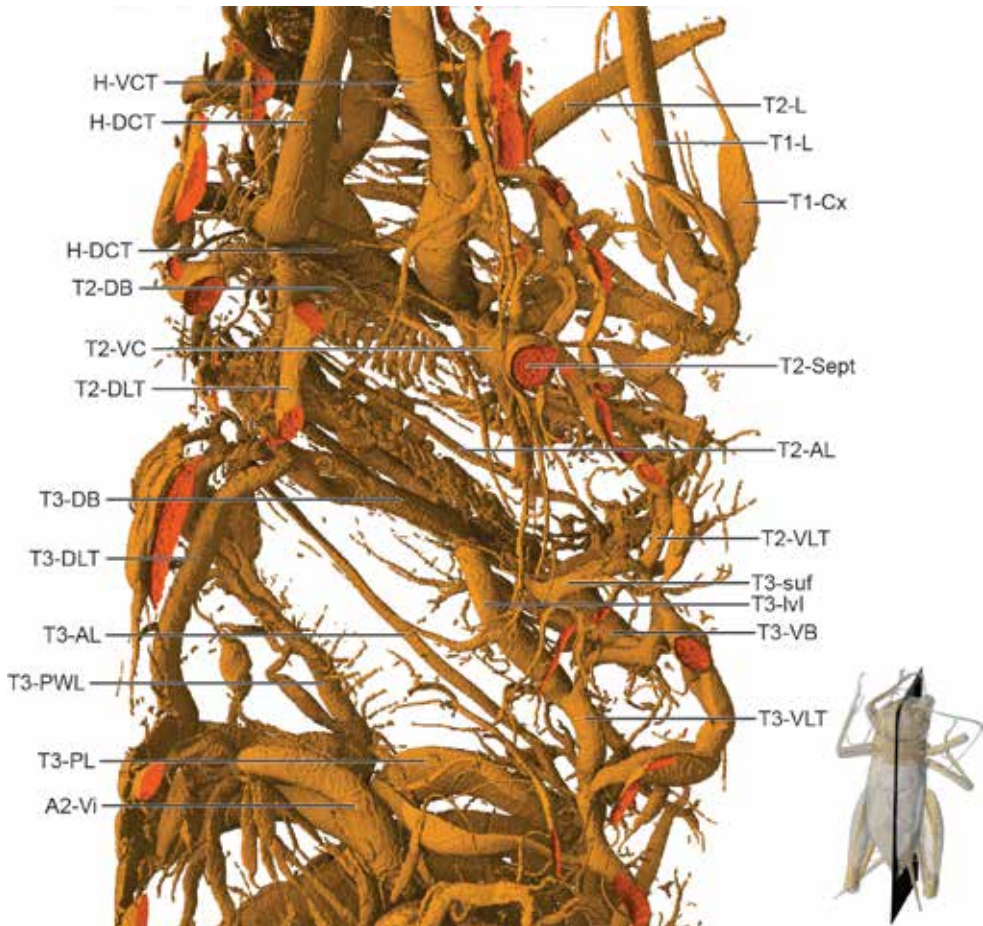


FIGURE 61. *Gryllus* sp interior left side thorax cutaway. See inset for location of cut.

T3-DB. T2-VB runs ventrad, linking with T2-VLT; similar to T2-DB, fanlike flight muscle tracheae extend posteriorly from T2-VB. T2-VLT running posteriad, with T2-VC2 possible. T1-AL with posterior branch extending into forecoxa and linking with T2-Cx network; anterior branch running dorsad into prothorax. Multiple expanded visceral tracheae along venter; T1-VC possible but networked morphology makes homologies uncertain. T2-VS thick, extending directly mediad as T2-VC, meeting at midline with circular T2-Sept present; see figure 61 for internal cut-away view showing medial septum, and figure 62 for ventral view with legs removed for clarity. Large T1-PL runs dorsad and lateral

from T2-VC, extending into foreleg as T1-L; T1-AL and T1-PL join only via smaller tracheae extending from T1-Cx network. T1-L-Ty tympanum present at proximal end of tibia. T3-S with five branches: T3-DB, T3-lvl, T3-suf, T2-PL, T3-VB. T3-DB runs dorsad, with connection to T2-Wbr just dorsal of T3-S; T3-DB continues dorsally, with T3-AWL splitting dorsad and slightly lateral; T3-DB connecting in Y-shaped junction with T2-DLT from anterior and T3-DLT posteriorly. T3-DB-Vi dorsal, extending posteriad, ending blind with several small tracheae posteriad. T3-AWL with sharp curve ventrad and laterally, with dorsal branch to T3-Wbr at apex of curve; T3-Wbr with small T3-W-c-r

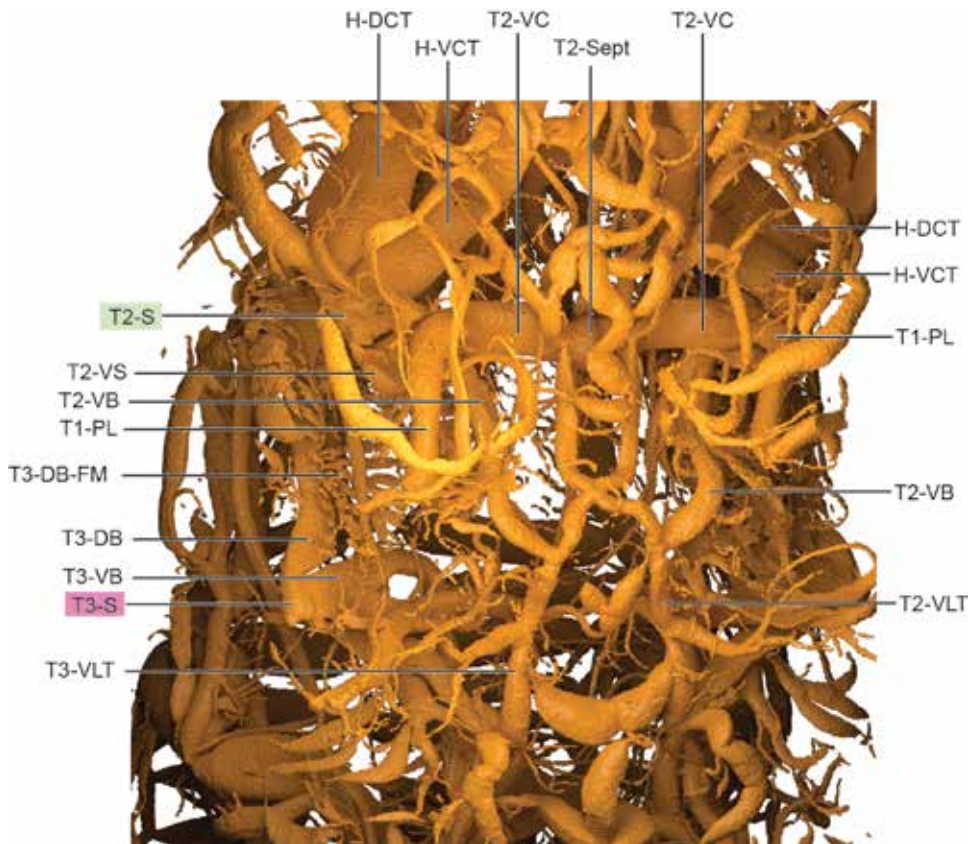


FIGURE 62. *Gryllus* sp thorax, ventral view. Leg tracheae have been removed for clarity.

branch posteriad; T3-AL thin, joining with T3-PL ventral from A1-S and continuing as very thick T3-L. Additional T3-VL branching laterally from T3-VLT, extending into hind leg, and joining in multiple-tracheae junction with T3-L; extremely large T3-Fm extending dorsad into hind femur; smaller T3-Fm2 almost linear from T3-VL along ventral part of hind leg. T3-VC1 and T3-VC2 anterior and posterior, respectively, along T3-VLT. T3-lvl proceeds medially from T3-DB for a short distance before splitting into two branches, both joining with T3-VLT, one anterior and one more posteriad. T3-suf running mediad, curving ventrally to connect with T2-VLT. T2-PL runs mediad before curving laterally, extending into midleg. T3-VB extends directly ventrad, connecting to T3-VLT near T3-suf connection.

ABDOMEN: A1..8-S present; A1..2-S modified, remaining A3..8-S all similar. A1-S with two additional connections: T3-PL, running ventrad with connection to thin T3-AWL before continuing into hind leg; and T3-PWL, connecting anteriorly from T2-S. A1..8-DB present, running directly dorsad from spiracle and leading to *An*-DLT, arcing posteriorly to link with subsequent *An*-DB. A1..4-DLT with paired *An*-DLT-Vi, wide but flattened, extending medially; anterior A3,4-DB-Vi smaller. A5..8-DLT with single *An*-DLT-Vi. A1..8-DC absent; however, a few *An*-DLT-DVi with small lateral commissure to opposite side present. A1..8-VB present, running directly ventrad and mediad, following sternite wall and connecting with straight *An*-VLT, spanning length of abdomen. *An*-VC absent. Numerous visceral tracheae extending into gut, with many

Vi spanning several segments and some connecting spiracles, including A3-Vi, linking with A6-Vi on specimen left side. Several visceral branches lie close to others, appearing to join but remaining separate, such as A3-Vi close to A8-Vi on right side. Several visceral tracheae are labeled in the plates and figures; readers are directed to the online 3D supplemental models for additional detail. Notably large A-Cr extending from A8-DB.

FAMILY ROMALEIDAE

Romalea microptera

“Eastern lubber grasshopper”

Figures 63 (lateral), 64 (dorsal, ventral)

Plates 38 (lateral), 39 (dorsal), 40 (ventral)

The tracheal structure of the lubber grasshopper *Romalea microptera* features a substantial number of air sacs, integrated into the tracheal system, and discrete air cells distributed throughout the body, especially the head and thorax. Due to the complexity of the tracheal architecture of *Romalea*, only spiracles and major tracheae are labeled in the plates. 3D models are provided in the supplementary digital data for further investigation.

FAMILY RHAPHIDOPHORIDAE

Tachycines asynamorous

“Greenhouse camel cricket”

Figures 65 (lateral), 66 (dorsal, ventral)

Plates 41 (lateral), 42 (dorsal, ventral)

A single camel cricket, *Tachycines asynamorous*, was scanned, but substantial fluid infilling of tracheae resulted in assessing homology of many branches difficult. Although of suboptimal quality, this specimen was included because of its placement within Orthoptera and the relative modifications of the mesothoracic tracheae, specifically how they relate to modifications for

sound reception. Identifiable tracheae are labeled and described here but should be considered preliminary.

Our mesothorax assessments differ from Ander (1939), particularly with H-DCT and H-VCT. Ander identifies most of the larger tracheae extending into head as multiple branches of H-VCT and the small branch as H-DCT, whereas we have determined the small dorsal branch is T2-VB, the next ventral branch is H-DCT, followed by H-VCT, which *does* have a split into H-VCT and a smaller anterior trachea that has T1-AL ventrad.

DESCRIPTION: HEAD: T1-DLT partially visible and likely extending into head capsule. H-DCT and H-VCT both thick, with dorsal-ventral connection likely but not visible. Several air spaces visible, likely preservational artifacts. H-VCT splits into two branches, large dorsal one and smaller ventral, which proceeds anteriorly with T1-AL ventrad.

THORAX: T2-S with five branches: T2-DB, T2-VB, H-DCT, H-VCT, and T1-PL. T2-DB running dorsad and anteriad, extending into head capsule after broad curve along prothorax. H-DCT thick, extending anteriad through prothorax into head capsule. H-VCT splitting into two branches: large dorsal trachea, extending anteriad into head, and a smaller ventral branch, extending anteriad into head with T1-AL ventrad. T2-VC not visible but likely present; many ventral thoracic tracheae infilled with fluid. T2-DB runs dorsad, with T2-AL branching in hairpinlike turn ventrad into T2-L. Remaining branches of T2-DB not visible. T2-VB partial, with T-shaped intersection with T2-VLT. H-DCT and H-VCT both large, of similar size, extending into head as described above. T1-PL running directly ventrad, partial, likely joining with T1-AL but not visible in this scan. T3-S branches largely infilled and difficult to differentiate, appearing to include: T3-DB, T3-VB, T3-lvl, T2-PL, and T3-suf. T3-DB partial, with T3-AWL visible, leading to T3-AL, dorsad before curving sharply ventrad and posteriorly into hind leg. T3-VB running ventrad, joining

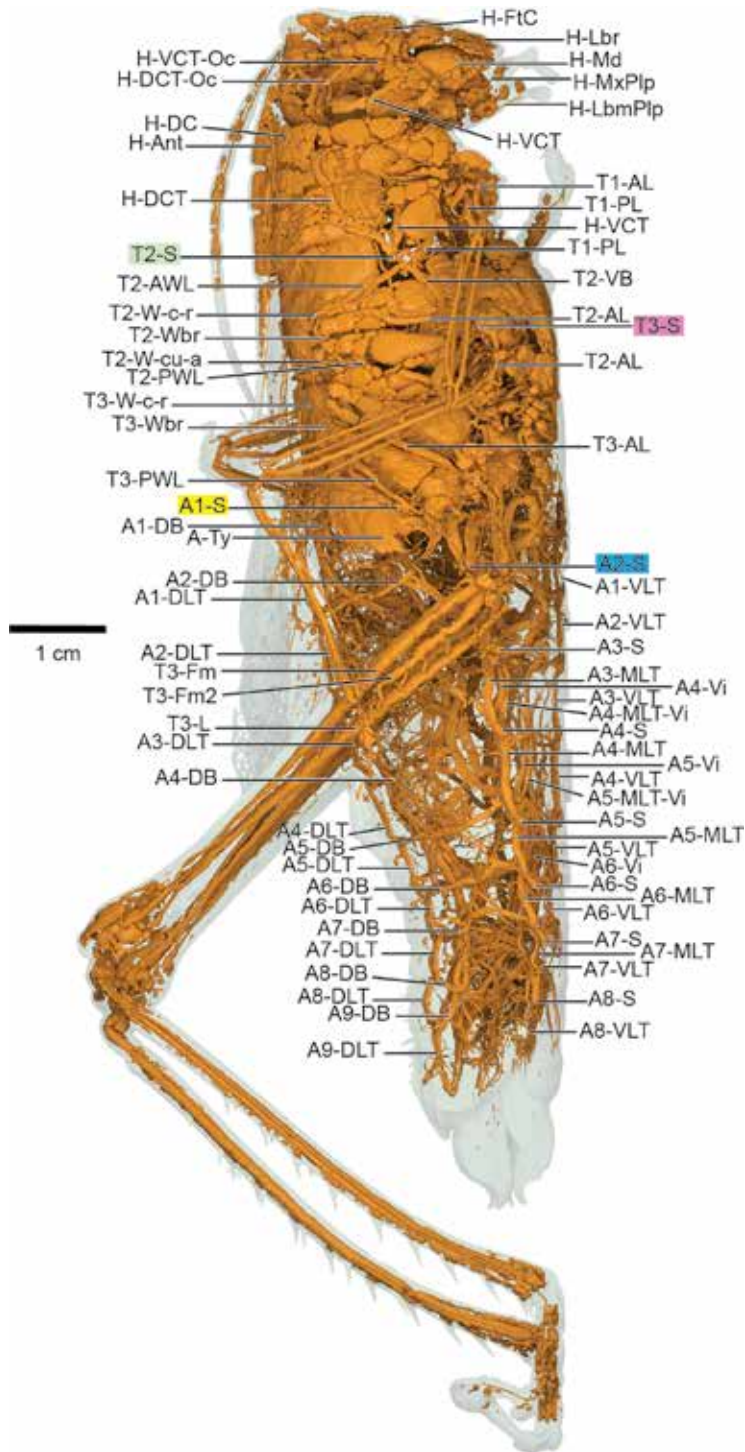


FIGURE 63. *Romalea microptera* (Orthoptera: Romaleidae) lateral view.

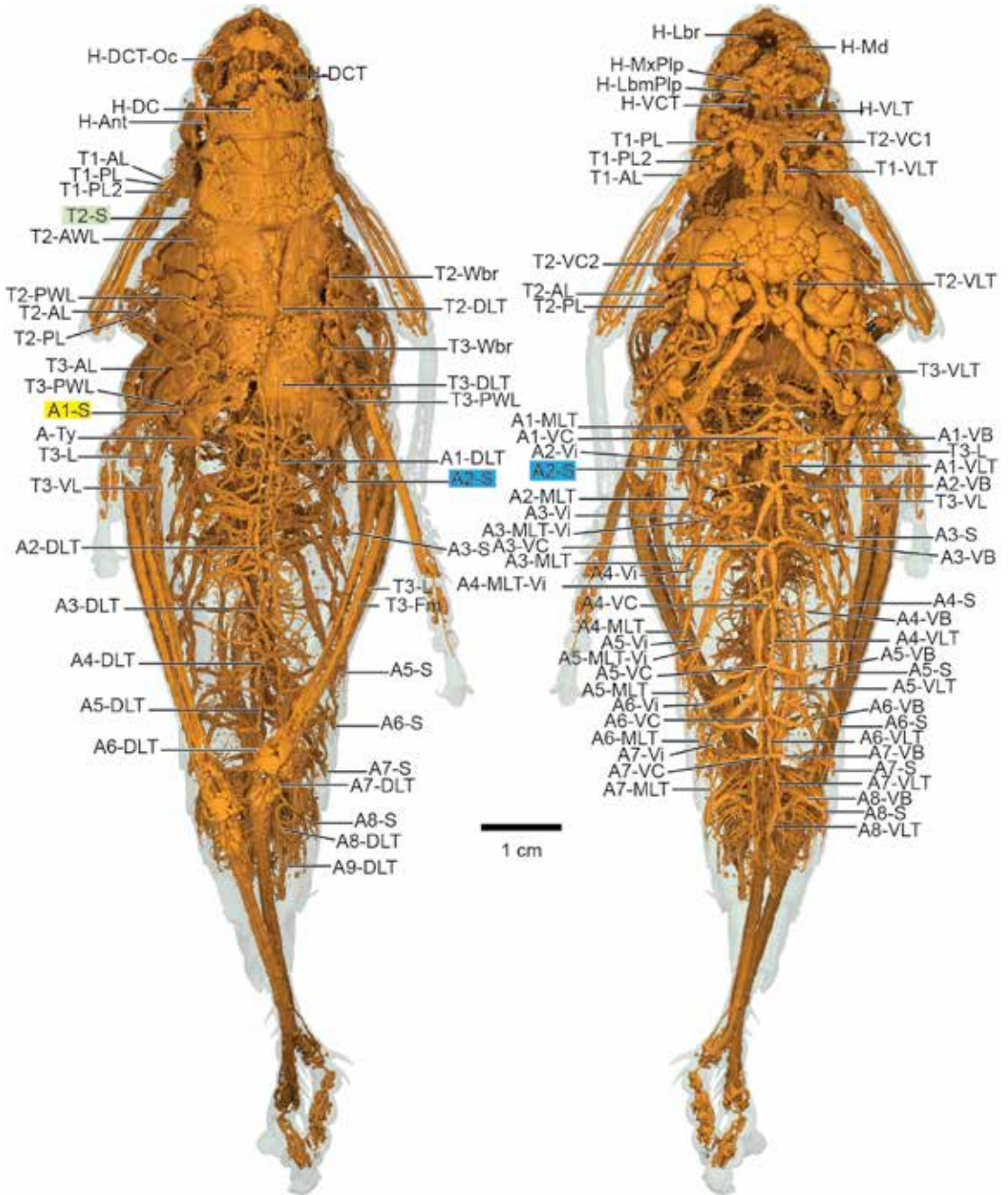


FIGURE 64. *Romalea microptera* (Orthoptera: Romaleidae) dorsal (left) and ventral (right).

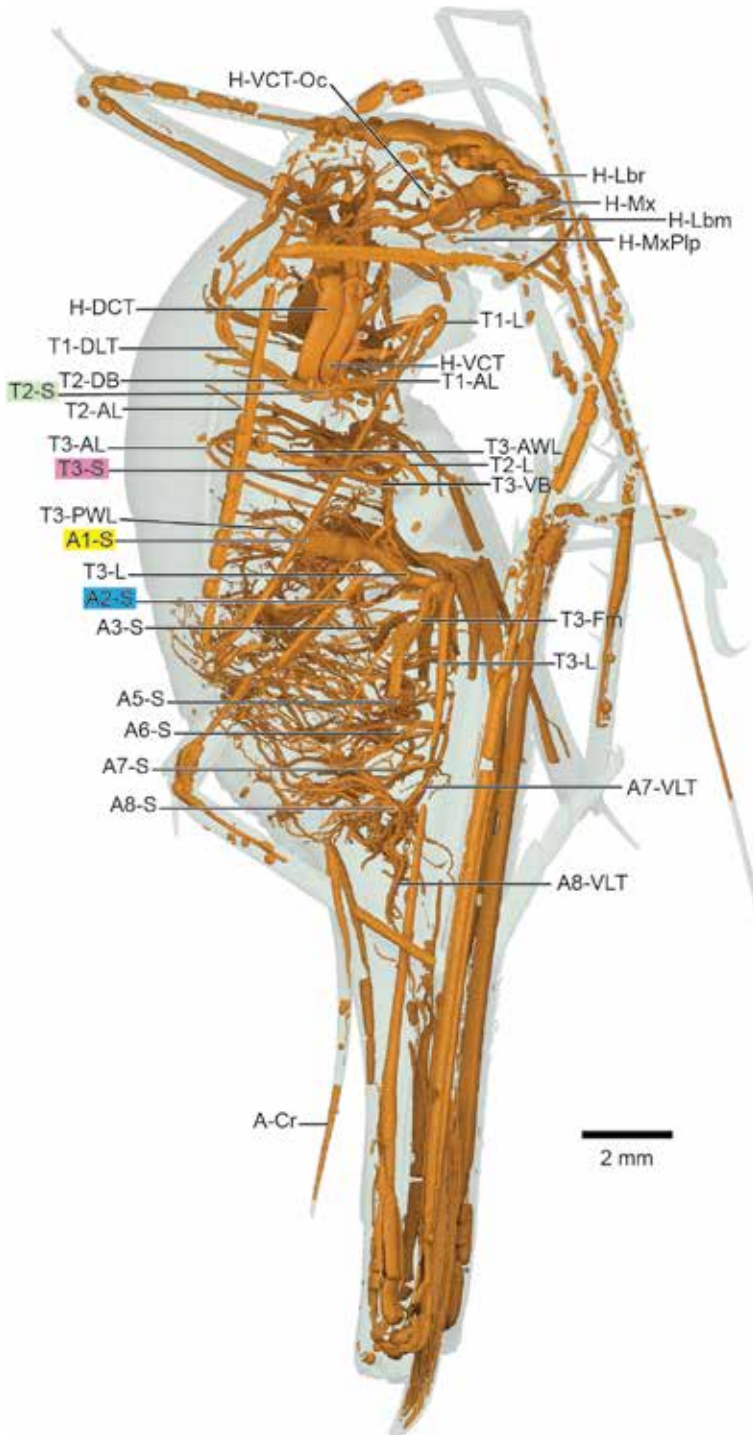


FIGURE 65. *Tachycines asynamoros* (Orthoptera: Rhaphidophoridae) lateral view.

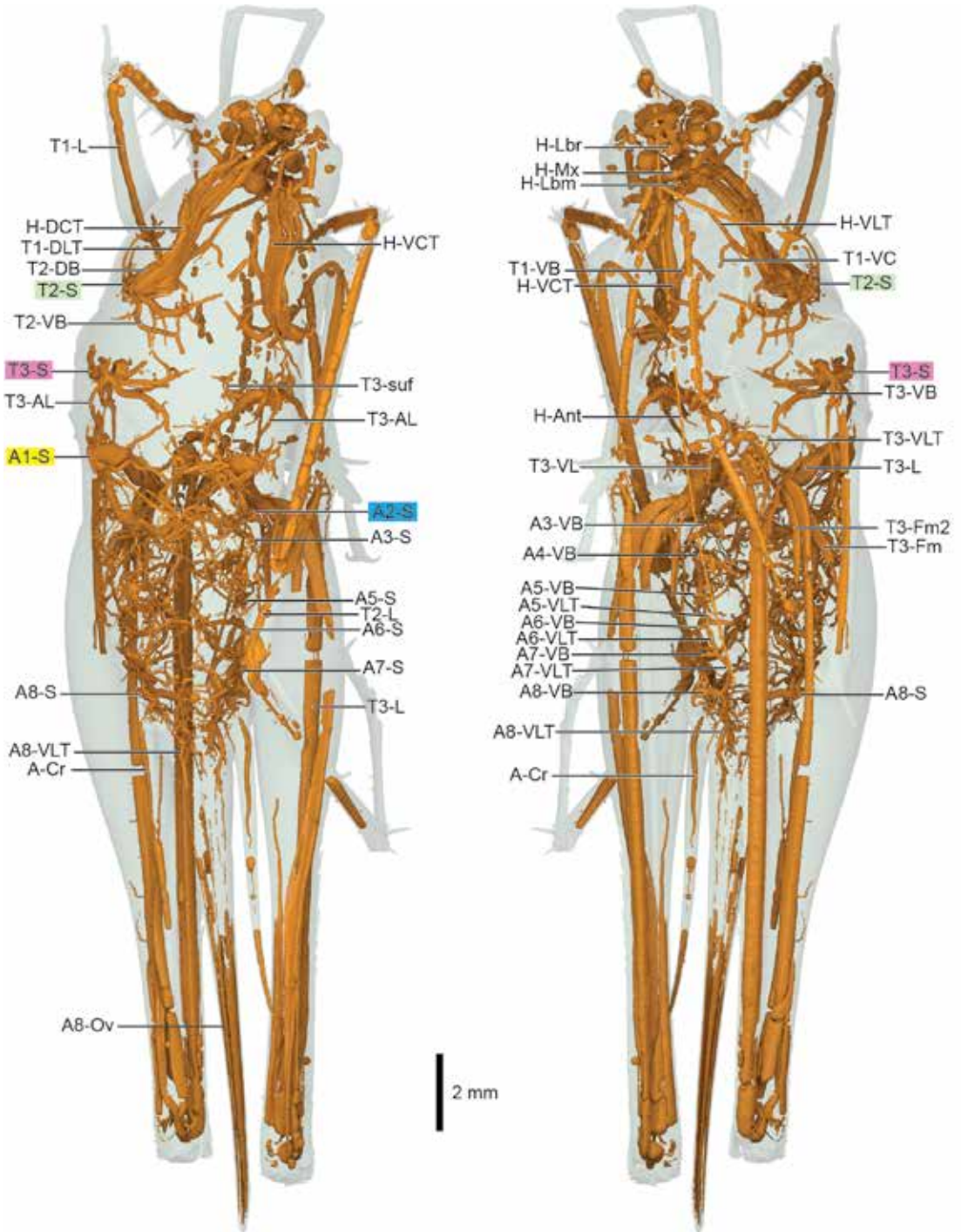


FIGURE 66. *Tachycines asynamoroux* (Orthoptera: Rhaphidophoridae) dorsal (left) and ventral (right).

with T3-VLT. T3-lvl extending mediad, joining with T3-VLT, with small branch posteriad connecting with T3-PL. T3-suf partial, extending mediad and slightly anteriorly. T3-VL possibly visible on specimen left side; T3-VL likely present but infilled.

ABDOMEN: A1..8-S present. A1-S modified from subsequent abdominal segments, with large ventral T3-PL branch. *An*-VB visible on most segments, leading to partially infilled *An*-VLT. *An*-DB likely present but infilled and not visible. *An*-DLT likewise probably present but not visible, likely infilled. Several visceral tracheae present from all *An*-S.

FAMILY TETTIGONIIDAE

Meconema thalassinum

“Drumming katydid”

Figures 67 (lateral), 68 (dorsal, ventral)

Plates 43 (lateral), 44 (dorsal, ventral)

The female drumming katydid we scanned is likely a late-stage instar due to the reduced wings. T2-DB-Vi and T3-DB-Vi each form a trapezoidal set of double dorsal commissures. It is possible that these may be homologous with sausage-like dorsal commissures seen in other taxa that might be for weight relief or could be involved in stridulatory sound dissemination.

DESCRIPTION: HEAD: Three pairs of tracheae into head: H-DCT, H-VCT, and H-VLT. Head with several interconnected dorsoventral and lateral loops; readers are encouraged to review the supplementary 3D digital models. Air space, possibly a preservational artifact, present in right side of head capsule (see fig. 69). H-DCT runs anteriorly, curving dorsally along head capsule and curving medially to connect in a loop just dorsal of eyes. H-DC present. Anteriorly of cervix, H-DCT-Oc branches ventrad, linking with H-VCT-Oc with Y-shaped junction to H-Oc-Md. Several small, visceral-like H-Oc run dorsad from H-Oc-Md; H-Oc-Md anteriorly, reconnecting to H-VCT with H-Md branching anteriorly, with lat-

eral H-FtC branch linking left and right side. H-VCT runs anteriorly with ventral curve; T1-AL running posteriad prior to H-VCT entry to head capsule. H-VCT with aforementioned H-VCT-Oc branch running anteriorly; H-VCT continuing anteriorly with ventral branch, linking with H-VLT before continuing into H-Mx and H-Lbm split.

THORAX: T2-S opening very large, positioned under pronotum; T2-S with five branches: T2-DB, T2-VB, H-DCT, H-VCT, and T1-PL. Several tracheae behind T1-DVi; see figure 70 for view rotated to see additional detail. Readers are also directed to 3D models from supplemental digital data. T2-DB and T2-VB from short dorsal spiracular branch, extending directly dorsal and ventrad, respectively. T2-DB with T2-AWL split, with T2-DB continuing dorsad, connecting with T2-DLT extending posteriorly. T2-AWL runs dorsad with sharp curve directly ventrad toward midleg; T2-W-c-r positioned posteriad at apex of curve. T2-VB runs directly ventrad from T2-DB/T2-VB split, arcing posteriad to connect with T2-VLT; several small visceral branches forming cage-like network along venter. H-DCT runs dorsad from T2-S, arcing anteriorly and continuing through prothorax into head capsule; T1-DVi branches forming cage-like morphology along inner wall of protergum, around H-DCT. H-VCT runs dorsad, arcing ventrad before turning anteriorly into head capsule, arranged along outside of enlarged T1-PL; T1-AL with ventral branch anteriorly of T1-PL. T1-PL greatly enlarged in horn-like arc, reducing in size and extending into proleg. T1-L-Ty tympanum present on foreleg tibia. T3-S much smaller than T2-S, with five branches: T3-DB, T2-PWL, T3-AWL, T3-VB, and T2-PL. T3-DB and T3-VB split dorsad and ventrad after short dorsal spiracular branch from T3-S. T3-DB running directly dorsad, with T3-AWL branching dorsad and slightly lateral; T3-DB continuing dorsad to join with T2-DLT from anterior and smaller T3-DLT posteriad. T3-AWL runs dorsad, with sharp curve ventrad and posteriad toward midleg. T3-AWL with two connections to tracheae leading to A1-S: T3-Wbr, branching

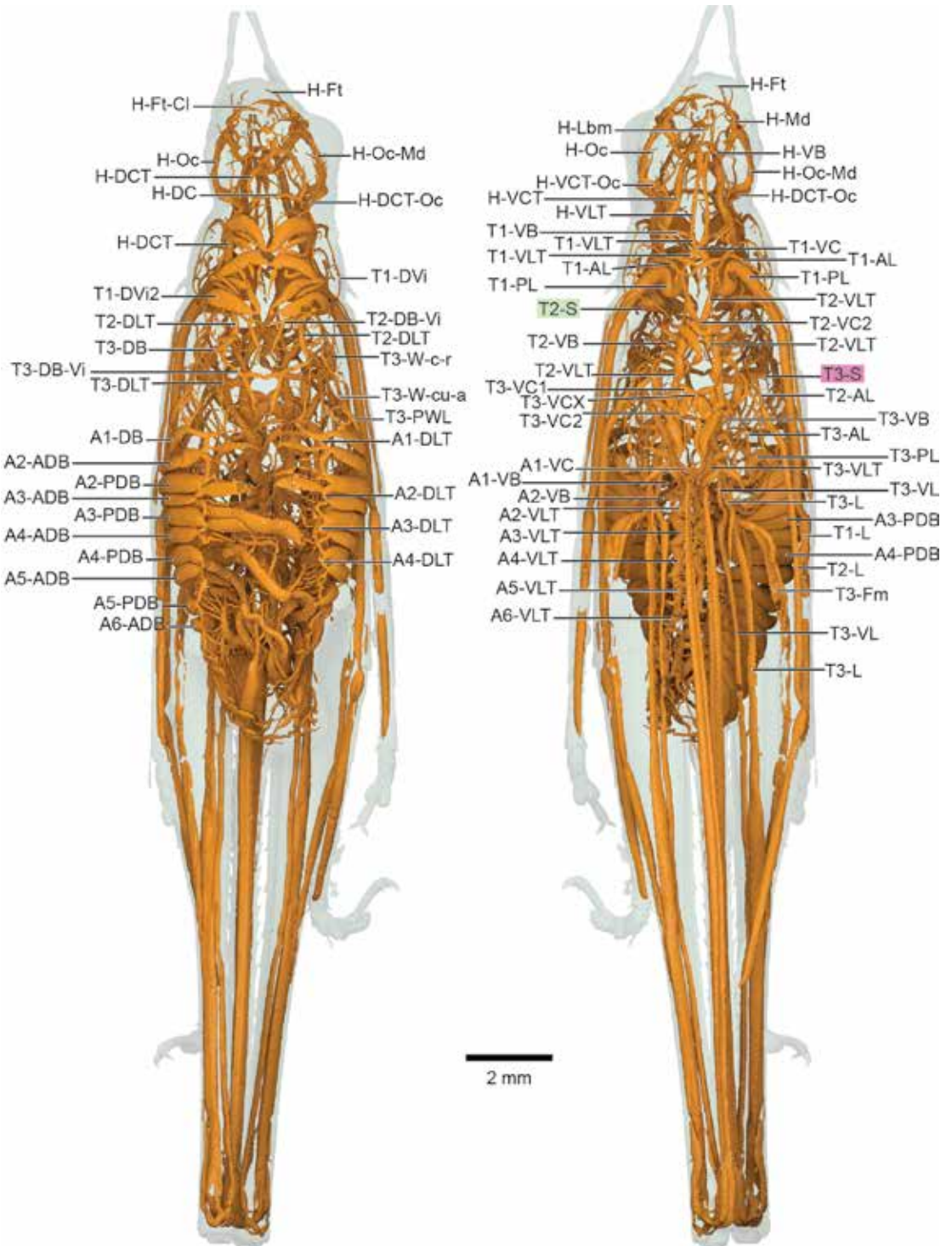


FIGURE 68. *Meconema thalassinum* (Orthoptera: Tettigoniidae) dorsal (left) and ventral (right) views.

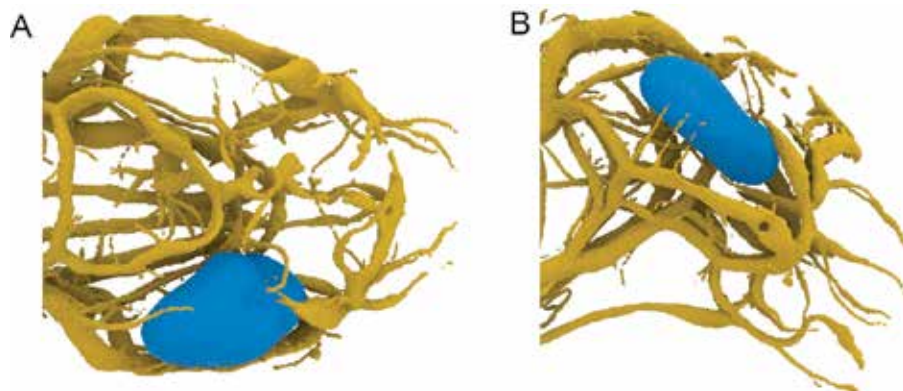


FIGURE 69. *Meconema* head, showing air space (blue) and trachea (yellow) in **A**. dorsal and **B**. lateral views. Direct screen capture from 3D Slicer.

dorsally at apex of curve, with T3-W-c-r and T3-W-cu-a dorsad; and apparent T3-PWL extension, dorsal and anterior from A1-S, connecting with T3-AWL/T3-AL. (See Discussion on Orthoptera.) T3-VB runs mediad and ventrad, connecting with T3-VLT toward posterior and T2-VLT anterior. T2-PL ventrad with curving T2-pf branch to T2-VLT; T2-PL continues into midleg, joining with T2-AL.

ABDOMEN: A1..8-S present. A1-S modified, positioned slightly dorsad relative to A2..8-S. A1-S with four connections: A1-DB, T3-PWL, A1-VB, and T3-PL. Single A1-DB runs dorsad and slightly anterior, broad and flat; intersecting with T3-DLT anterior and A1-DLT posterior. Several small visceral-type tracheae connecting with T3-PWL and likely extending into flight musculature. T3-PWL running dorsad and anterior, similar to A1-DB but smaller; T3-PWL splitting slightly dorsad into T3-Wbr anterior connection to T3-S, and smaller unnamed extension connecting to T3-AL (see THORAX, above, and Discussion section on Orthoptera). T3-PL thick, running directly ventrad from A1-S, connecting with smaller T3-AL from metathorax and extending into hind leg. T3-VL present, extending into hind leg from T3-VLT. A1-VB runs ventrad and slightly mediad, connecting with T3-VLT from anterior and A1-VLT posterior. A2..8-S similar, each with anterior and pos-

terior dorsal branches *An*-ADB and *An*-PDB, both intersecting with *An*-DLT along dorsum. *An*-VB short, running ventrad and slightly mediad, connecting directly to *An*-VLT along venter. X-shaped commissures positioned ventrad to VLT (see fig. 71). Numerous visceral tracheae present in abdomen, often spanning several segments, but none appearing to connect segments longitudinally.

ORDER GRYLLOBLATTODEA

FAMILY GRYLLOBLATTIDAE

Grylloblatta sp.

“Ice crawler”

Figures 72 (lateral), 73 (dorsal, ventral)

Plates 45 (lateral), 46 (dorsal, ventral)

Ice crawlers are remarkably active insects given their ecology, and studies have investigated their tolerance to cold (Schoville et al., 2015). *Grylloblatta* head morphology, especially musculature, was detailed by Wipfler et al. (2011) using both micro-CT and scanning electron microscopy, but tracheal morphology was notably absent from this study. As the sister group to Embioptera and Phasmatodea, the tracheal morphology of Grylloblattodea was important for assessing homology of these orders.

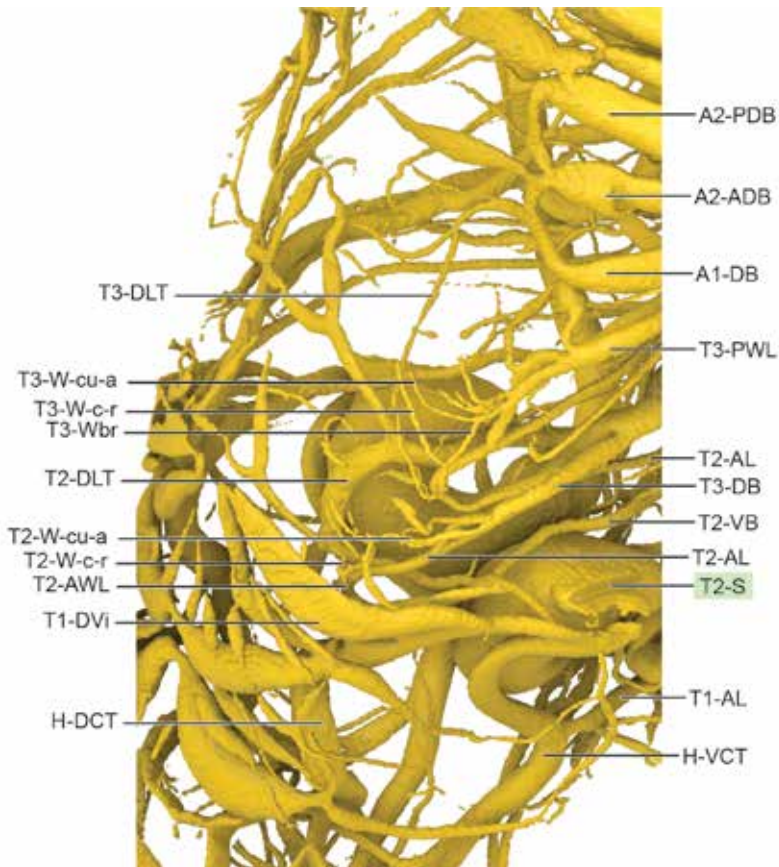


FIGURE 70. *Meconema* thorax, rotated to show mesothoracic tracheal detail; view is from specimen's left side and slightly above, looking anteriorly. Note repeated X-shaped commissures, connected longitudinally, ventral from *An-VLT*. Direct screen capture from 3D Slicer.

Several head tracheae, including H-Oc, are difficult to localize. *Grylloblattodea* have very few ommatidia (Wipfler et al., 2011), and perhaps this is why tracheation appears reduced around the eyes relative to other taxa. In the thorax, T2-DB branches off T2-L, an unusual condition, as typically T2-DB extends directly from T2-S. This branch is very likely T2-DB, as it leads to T2-DLT, T3-DLT, and successive tracheae as seen elsewhere. The branching pattern of T2,3-AWL and PWL is also notable, in that it is unclear if these tracheae branch from T2,3-DB or directly from T2,3-S. Both conditions are present in other taxa, and this could merely be an “intermediate” positioning.

DESCRIPTION: HEAD: Major tracheae indicated in plates, refer to figure 74 for head detail. Due to looping, networked 3-dimensional nature of *Grylloblatta* head tracheae, readers are encouraged to refer to digital supplemental models (see Availability of Digital Data, above). H-DCT slightly ventrad at cervix, curving dorsally on entry into head capsule; H-DCT divides into H-DCT-Vi1, H-DCT-Vi2, and H-Ant anteriorly of cervix. H-DCT-V1 lateral and anteriorly, following head capsule wall. H-Ant anteriorly, curving laterally to extend into antennae. H-DCT-Vi2 anteriorly, with each side curving anteriorly to meet in X-shaped intersection at H-DX and continuing anteriorly before arcing ventrad to connect

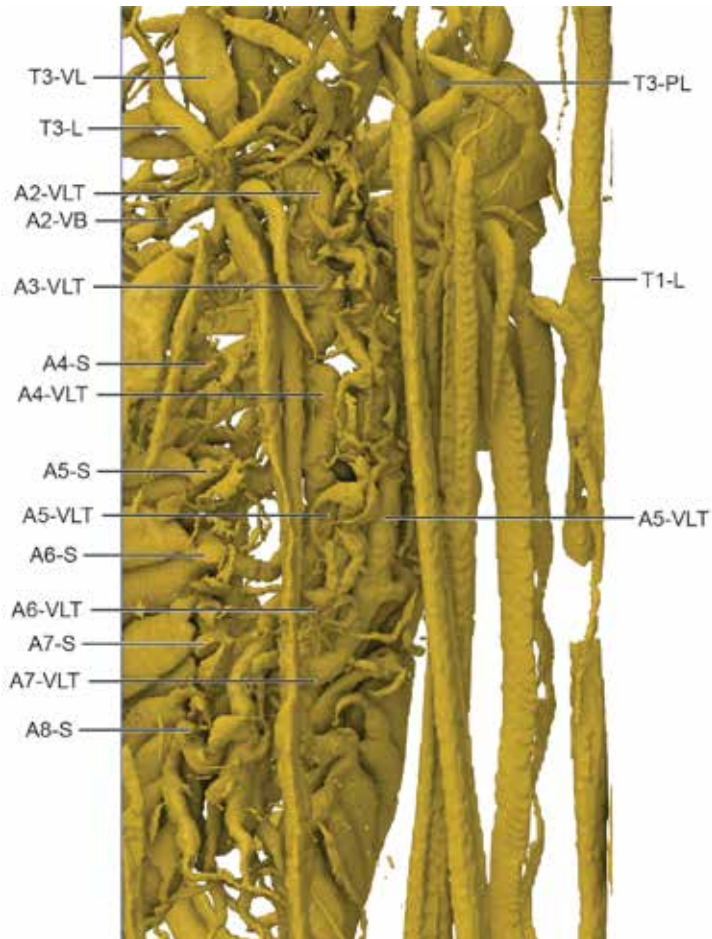


FIGURE 71. *Meconema* (Tettigoniidae) ventral view of abdomen, rotated to show detail obscured by legs. Direct screen capture from 3D Slicer, annotated in Adobe Illustrator.

with H-VCT-Loop via dorsal-ventral branch H-DVB. H-Ant on specimen left side with link to H-DVB. Just posteriad of cervix, each H-DCT with small branch extending medially, joining in Y at base of head capsule into medial branch, extending anteriorly as H-DCMedB (dorsal cephalic medial branch). H-DCMedB splits near vertex into three branches; two extend laterally, looping backward to connect with H-Ant as H-DCT-Loop; last branch directly dorsad, connecting to H-DX. H-VCT directly anteriorly, with H-Lbm branching ventrad at posterior margin of submentum. H-VCT continuing anteriorly with branches to H-Md and H-Lbr before curving

medially to join H-VCT from opposite side in dorsal two branches of X-shaped H-AX. Ventral two branches of H-AX formed by H-Lbm, which continues anteriorly before arcing dorsally to H-AX, forming H-Lbm-Loop. H-LbmPlp branching from H-Lbm-Loop near anterior curve of H-Lbm toward H-AX. H-Lbm extending anteriorly from H-AX anteriormost point; H-Md extending anteriorly from dorsal portion of H-Lbm-Loop before curving ventrad. H-DVB dorsal-ventral connection of H-DCT and H-VCT at branching off point of H-Md. Small H-VC running ventrad near anterior end of H-VCT-Loop.

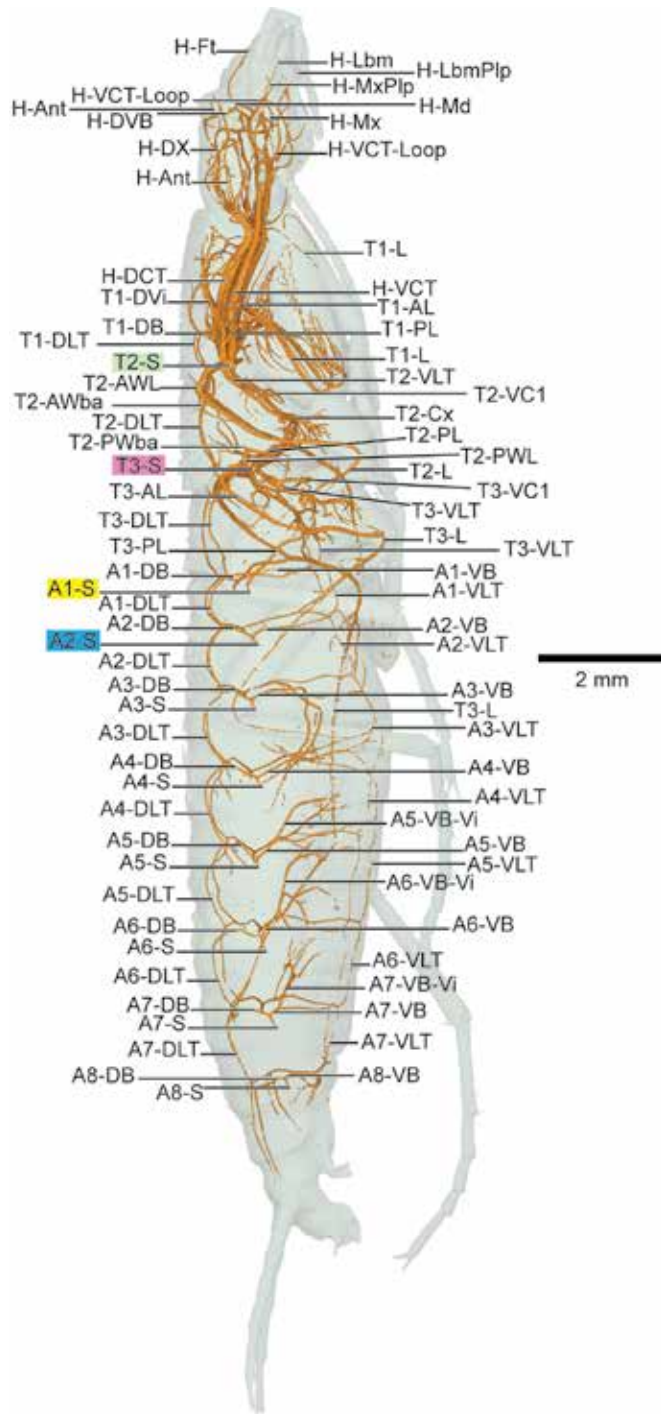


FIGURE 72. *Grylloblatta* sp. (Grylloblattodea: Grylloblattidae) lateral.

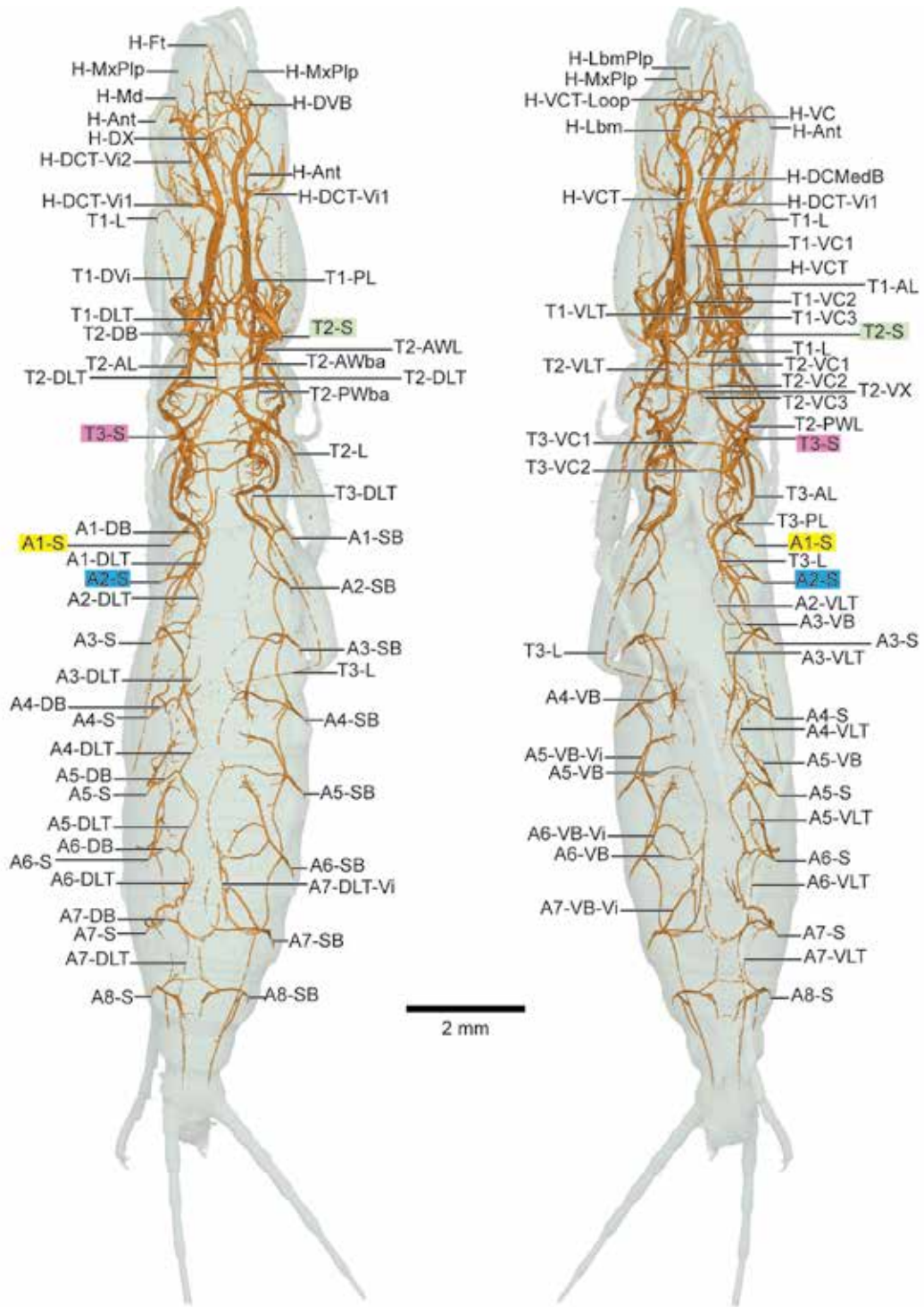


FIGURE 73. *Grylloblatta* sp. (Grylloblattodea: Grylloblattidae) dorsal (left) and ventral (right).

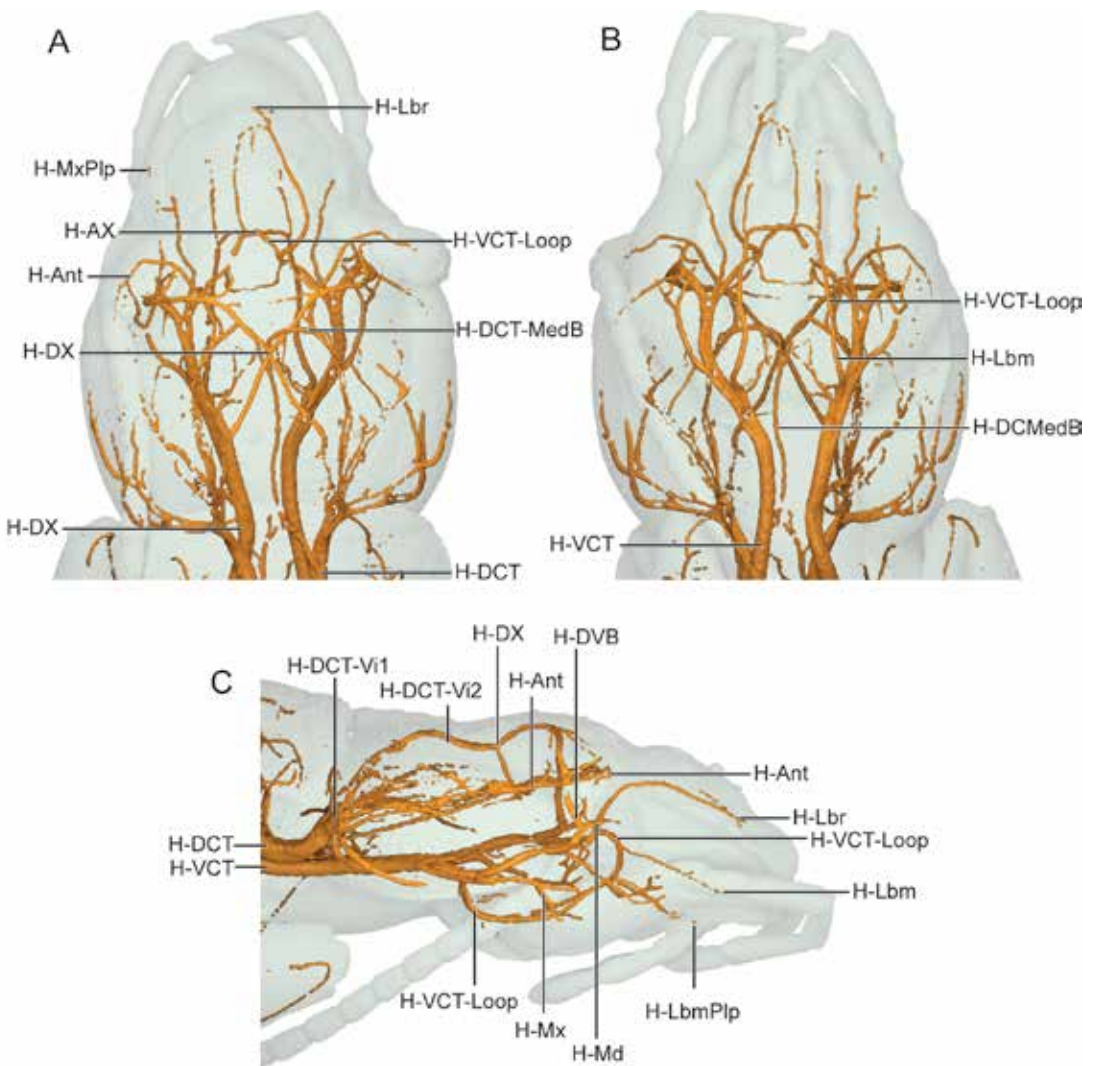


FIGURE 74. *Grylloblatta* head trachea detail in **A.** dorsal, **B.** ventral, and **C.** lateral views. Head is not in same orientation as plates and has been rotated to visualize smaller tracheae more easily.

THORAX: T2-S with four branches: H-DCT, H-VCT, T2-DB, T2-VB. T2-CT absent. H-DCT runs anteriad from T2-S with slight curve medially; branching of T1-PL and T1-Dvi at posterior margin of prothorax, with T1-PL running laterally and ventrad, proceeding into proleg and T1-Dvi directly anteriad; T1-DB beginning just anterior of this split, extending dorsad to join with T1-DLT in Y-shaped junction. H-DCT compressed laterally anterior of the split; com-

pression likely preservational artifact. H-VCT similar in size to H-DCT, with single T1-L branching directly ventrad, located mid prothorax. T2-DB running initially dorsad splitting off large T2-AWL, smaller T2-DB continues, extending medially and dorsad, arcing posteriorly to connect to T3-S via T2-DLT. T2-AWL arcing ventrally and posteriad, dividing into T2-AL and T2-Awba; T2-AL continuing posteriorly into midleg, joining with T2-PL near mesothoracic

coxa; small T2-Awba branching from T2-AWL, dorsad near apex of arc toward T2-L. T2-VB short, proceeding ventrad and medially before splitting into T1-VLT anterior and T2-VLT posterior and ventrad. T1-VLT with three ventral commissures: T1-VC1 most anterior, at the apex of a long oval loop reaching the posterior end of the cervix; T2-VC2 ventrad, joining at the opposite end of loop to forming X-shaped T1-VX; T2-VC3 near the prothoracic coxae; T1-AL-VC branching ventrad from T1-AL to connect with loop at halfway between T1-VC1 and T1-VC2. T2-VLT runs ventrad and posteriad, extending toward mesothoracic coxae before turning dorsally to join with T3-VB. T2-VLT with three ventral commissures: T2-VC1 most anterior, branching directly toward midline to join with opposite side; T2-VC2 branching inward where T2-VLT arcs dorsally; T2-VC3, branching from metathoracic portion of T2-VLT, branching medially and joining with T2-VC2 at X-shaped intersection T2-VX. T2-Cx comprised of two branches, one each extending from T2-VC2 and T2-VC3. T3-S with only two branches, short T3-DB and T3-VB. T3-DB dorsad, splitting into T2-PWL anterior and ventrad, T3-AWL arcing dorsad and posteriorly, and remaining small T3-DB continuing dorsally to link T2-DLT and T3-DLT in Y-shaped junction. T3-AWba absent; T3-AWbr absent. Short T2-PWL runs anterior, dividing into ventral T2-PL that links with T2-AL from anterior, continuing into T2-L; and small dorsal T2-PWba. T2-PWbr not present. T3-VB short, bifurcating into connection to T2-VLT from anterior and continuing as T3-VLT toward posterior. T3-VLT with two ventral commissures: T3-VC1 slightly ventrad from T2-VLT/T3-VLT intersection; T3-VC2 where T3-Cx extends into base of metacoxae. T3-VLT extends from split of T3-Cx, continuing in shallow, ventral arc to link with A1-VLT via A1-VB.

ABDOMEN: A1..8-S present. All abdominal segments similar, with notable exceptions below. Short *An-SB* present, bifurcating into *An-DB* and *An-VB*. *An-DB* runs directly dorsad, linking with *An-DLT* in Y-shaped junction; A5-DB with

short A5-DB-Vi extending mediad. *An-DLT* runs in shallow, dorsal arch along tergum; *An-DC* absent; short, mediad A4.6-DLT-Vi present; A7-DLT-Vi beginning posteriad before arcing medially and then anterior, extending past A6-S; A8-DLT extending posteriad into A-Cr. A1-SB with two tracheae ventrad: T3-L ventrad and slightly anterior, extending into hind leg, along same path as A1-SB; A1-VB smaller, extending directly ventrad. A[2,4]-VB extending directly from A[2,4]-SB with no branches. A3-VB runs directly from A3-SB, with A3-VB-Vi continuing ventrad before turning posteriorly while smaller A3-VB directly ventrad. A[5,6] similar to A3 with large A[5,6]-VB-Vi anterior and smaller A[5,6]-VB ventrad. All *An-VB-Vi* link with *An-VLT* in Y-shaped junction, similar to *An-DLT*, but with a less pronounced arch ventrad. A8-VC present, other ventral commissures not visible and likely absent. Small A9-VC visible.

ORDER EMBIOPTERA

FAMILY OLIGOTOMIDAE

Oligotoma negra

"Black webspinner"

Figures 75 (lateral), 76 (dorsal, ventral)

Plates 47 (lateral), 48 (dorsal, ventral)

The respiratory system of Embioptera remains rather understudied, with the most recent detailed analysis of tracheal anatomy by Lacombe (1958, 1971). The specimen of *Oligotoma* shown here is a male and is notable because of the air-filled alimentary canal (fig. 77). Male webspinners do not feed, and like Ephemeroptera (fig. 21), the alimentary canal is coopted as a large air space, spanning the length of the body. In this specimen, the distention of the alimentary canal compressed tracheae against the inner body wall, making determination of morphology and assessment of homology challenging (particularly in the abdomen). Some notable differences were observed

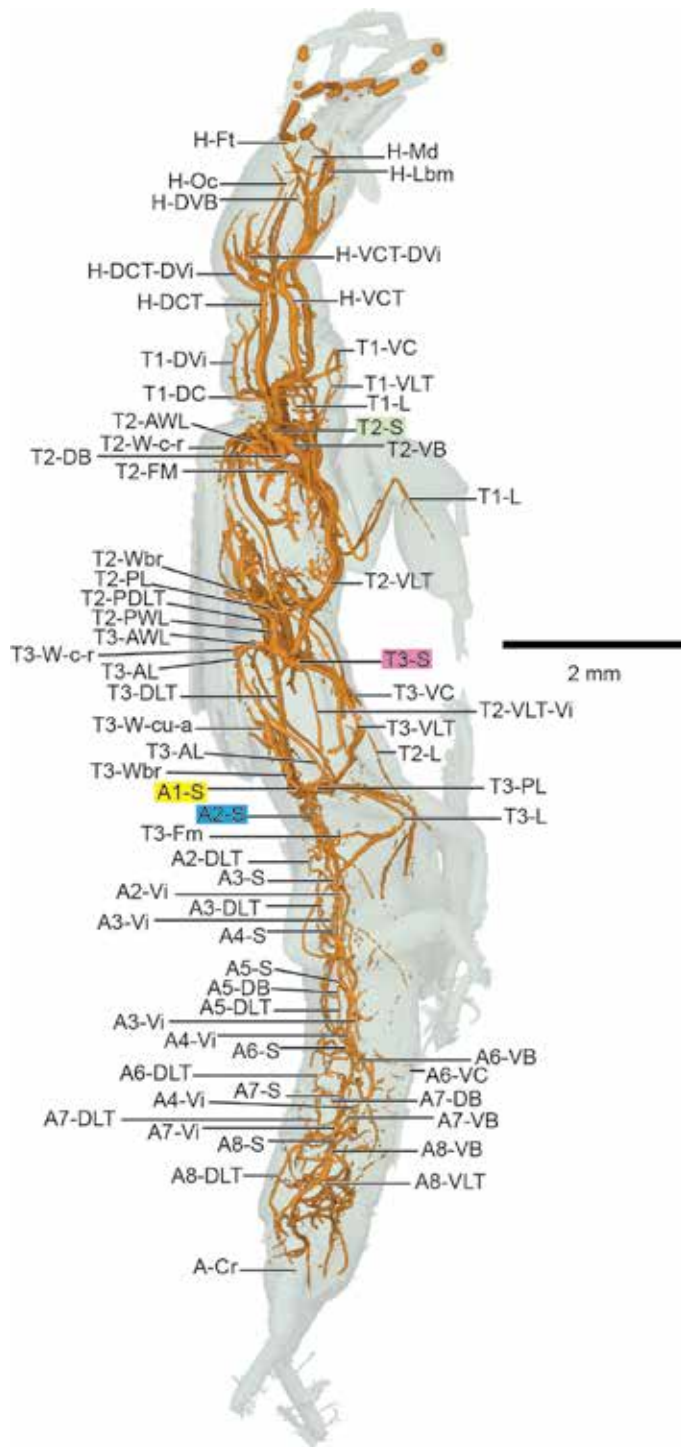


FIGURE 75. *Oligotoma negra* (Embioptera: Oligotomidae) lateral view.

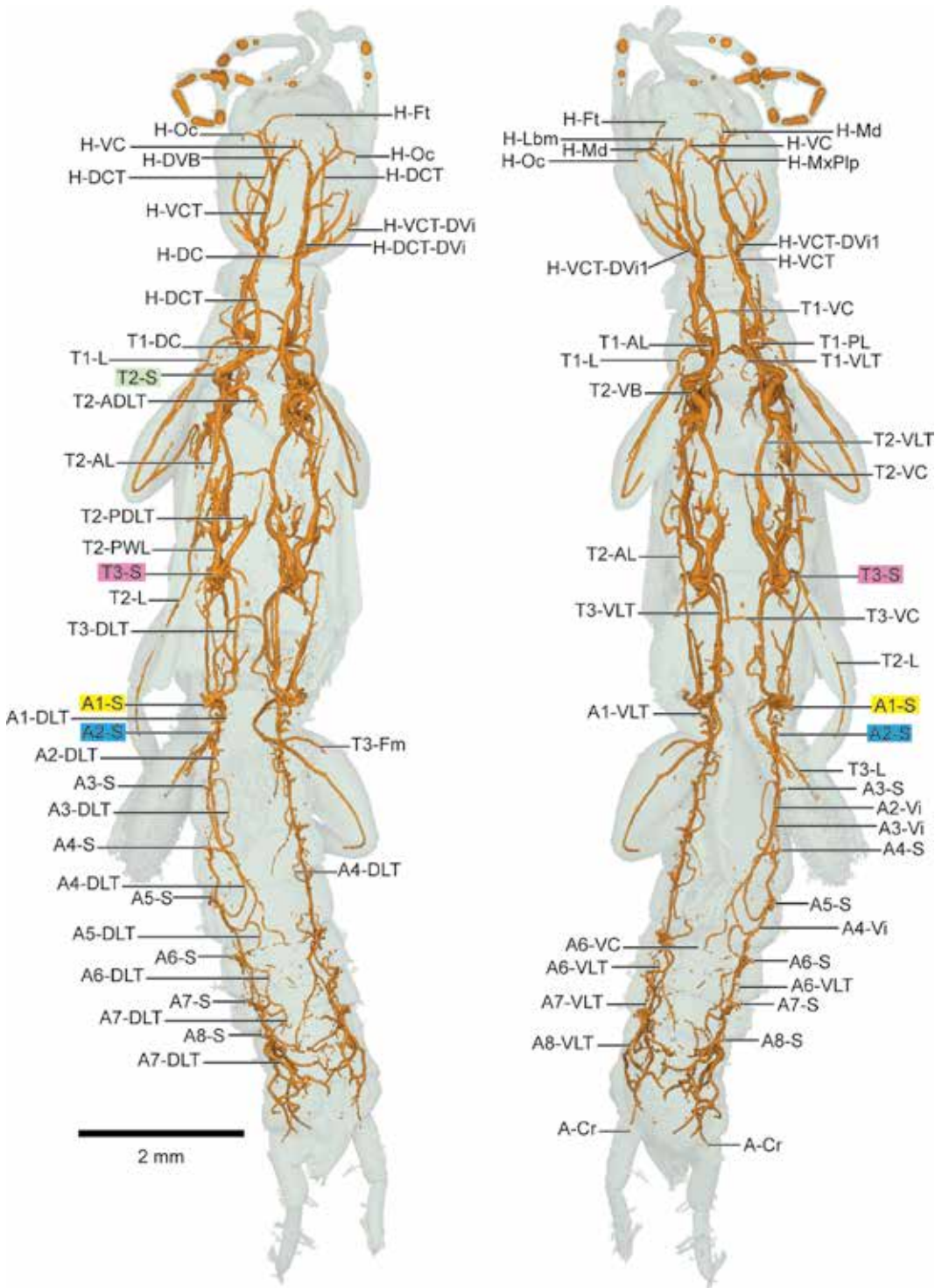


FIGURE 76. *Oligotoma negra* (Embioptera: Oligotomidae) dorsal (left) and ventral (right) views.

between Lacombe (1958) and the specimen here, particularly in the thorax, but her work was useful in mapping abdominal tracheae.

The meso- and metathoracic wing base T2,3-Wbr are likely present but partial in this scan, likely due to fluid infilling of this specimen as it was frozen to -20°C rather than -80°C .

Although a tympanal hearing organ in the femur (of pro- and mesoleg, and occasionally hind leg) of webspinners was described by Szumik et al. (2019), there is no evidence of an air space in femur of any leg (as seen here in the foretibia of *Gryllus*, for example).

DESCRIPTION: HEAD: H-DCT extending anteriad, curving laterally along head capsule; H-VCT slightly ventrad. H-DC present, slightly anterior of cervix. H-DCT with H-DCT-DVi running dorsad anterior of cervix, following head capsule. H-DCT runs directly anteriad, dividing into H-DVB ventrad and H-Ant. H-VCT with H-VCT-DVi extending dorsally, nearly in contact with H-DCT-DVi and following head capsule laterally. H-VCT continues anteriorly, with dorsal H-DVB connection to H-DCT. After short extension, H-VCT divides into H-Lbm, and subsequently into H-MxPlp, H-Md, and H-Oc. H-Lbm branch connecting mediad as H-VC. Branch leading to H-Oc continues to H-Ft.

THORAX: T2-S with four branches: H-DCT, H-VCT, T2-DB, and T2-VB. T2-CT absent. H-DCT runs directly anteriad, with T1-DVi branching dorsad before continuing dorsally along prothoracic tergum. T1-DC present, extending mediad near branching of T1-DVi. H-VCT runs anteriad, with T1-L branching ventrad just prior to a nearly 90° turn ventrad, subsequently turning anteriad along prothoracic sternite. T1-VC present, branching off T1-L. T2-VB runs posteriad and slightly ventral briefly before curving dorsad; small T2-AWL branching anteriad at apex of curve, dividing into T2-AWba dorsad and T2-AL continuing posteriorly toward midleg. T2-DB continues, curving medially with several branches, likely for flight muscle, before extending posteriad as T2-ADLT. Full DLT not visible but likely present, possibly fluid infilled; Lacombe (1958) indicates

presence of dorsal connective. T2-VB runs posteroventrad, with large T2-FM branching dorsad and laterally. T2-VB continues as T2-VLT, connecting with T3-S. T2-VC present, branching mediad approximately halfway between T2-S and T3-S. T3-S with four branches: T3-AWL, T2-PWL, T3-DB, and T3-VB. T3-AWL running dorsad, curving posteroventrad where T3-W-c-r splits dorsally and remaining branch continues as T3-L. T2-PWL connecting directly from anterior; T2-PL branching ventrally, joining with T2-AL after a short distance and continuing as T2-L; T2-Wbr continues anteriorly from T2-PWL; T2-Wbr partial likely due to fluid infilling. T3-DB runs mediad, dividing after a short distance into T2-PDLT anteriorly and T3-DLT posteriad. T3-VB runs posteroventrad, with a connection to T2-VLT very close to T3-S; T3-VB continues posteriorly as T3-VLT, linking up with A1-S. T2-VLT-Vi on right side, extending past T3-S into abdomen; unclear if T2-VLT-Vi links with an abdominal spiracle. T3-S on right side slightly different from left, possibly due to displacement of tracheae by distended alimentary canal air space; T3-S on right side with T3-VLT positioned posteriad as with right side, but with short, curving spiracular branch dorsad and anteriad, with T2-VLT connecting from anterior; branch continues dorsad to T2-AWL, T2-DB, T2-PWL split as with left side.

ABDOMEN: A1.8-S present. A1-S modified from subsequent abdominal segments; A1-S with five branches: A1-DB, T3-PWBa, T3-VLT, and T3-PL. A1-DB short and running mediad, connecting with T3-DLT from anteriad and continuing as A1-DLT posteriad. T3-WBr (also partial, likely due to fluid infilling) runs anteriad, continuing with small T3-W-cu-a into trailing edge of hind wing. T3-VLT from directly ventrad. T3-PL runs ventrad, lateral from T3-VLT, joining with T3-AL and extending into hind leg as T3-L. Segments A2..7 likely similar but morphology difficult to determine due to distention of air-filled alimentary canal. A2..7-DLT present, arcing slightly dorsad and usually sinuous. An-VLT present. A6-VC visible; other An-VC likely present but displaced against body wall, see fig-



ure 78. Several visceral tracheae visible, but difficult to determine morphology; A3-Vi and A4-Vi large and directly posteriad, spanning several segments. A-Cr visible at base of cerci.

ORDER PHASMATODEA

Tracheal architecture of stick insects has most recently been investigated by Strauss (2021), with an emphasis on the prothorax and possible adaptations for sound reception. Here, three specimens were scanned: the basal *Timema* cf. *californicum*, the popular Australian stick insect *Extatosoma tiaratum*, and the Vietnamese stick insect *Medauroidea extradentata*. Although many basal taxa exhibit synapomorphies found in sister taxa of a given monophyletic group, *Timema* exhibits numerous apomorphies and its tracheal system is quite distinct from *Extatosoma* and *Medauroidea*. *Medauroidea* appears to be more representative of the larger phasmids, with good scan quality and characters that appear to be common to *Extatosoma* (which is more complex and somewhat harder to homologize). *Timema* and *Medauroidea* are described here in detail; *Extatosoma* is covered here in a more basic fashion due to the substantial complexity in the abdomen. Future studies should focus on the unique morphology of the abdominal tracheae—resembling the jumble of dried, packaged ramen noodles—of *Extatosoma* and its possible functions.

FAMILY TIMEMATIDAE

Timema cf. *californicum*

“California timema (walkingstick)”

Figures 79, 80 (lateral, anterior, posterior); 81, 82 (dorsal, anterior, posterior); 83, 84 (ventral, anterior, posterior)

Plates 49 (lateral), 50 (dorsal), 51 (ventral)

The tracheal morphology of *Timema* is notable for the proliferation of comparatively thin

tracheae that form networks throughout the body. These networks make assessment of homology difficult especially in the thorax, where differentiating similarly networked tracheae from other taxa is unclear. Identifiable homologous tracheae are labeled here, and incorporation of data from some of the 20 or so other *Timema* species could help to resolve ambiguous structures. Notably, T2,3-DLT are absent in *Timema*, with the additional absence of the corresponding T2,3-DB; however, the networked nature of tracheae elsewhere likely compensates for the lack of dorsal longitudinal connections. Although distantly related, the *Timema* thorax is rather reminiscent of termites, with (possibly) dual ventral commissures, which may be convergent.

DESCRIPTION: HEAD: Head tracheae with several networked interconnections dorsoventrally; due to three-dimensional nature of head tracheal architecture, readers are encouraged to refer to models in supplementary digital data. Prominent H-DCT-VCT-Loop at anterior margin of prothorax, with smaller H-DCT and H-VCT branching from dorsal and ventral portions of loop. H-DCT extending anteriorly and slightly dorsad, splitting into dorsal branch to H-DX intersection near vertex; and anteriorly H-DCT-Ant branch, joining with ventral H-VCT-Ant branch and extending into H-Ant. H-DX with anteriorly branches extending laterally and ventrad, reconnecting with H-VCT-Ant as H-DX-VCT-Loop. H-VCT runs anteriorly, with H-VCT-Ant branching anterodorsally to join with H-DCT-Ant. H-VCT continues anteriorly with H-Mx branching ventrad; H-Mx with H-VC before branching to H-MxPlp. H-VCT with continued anterodorsal curve, with H-Md branching anteriorly; H-VCT joining with H-DCT via H-VCT-Ft-Loop; H-Ft-Lbr branching ventrad near anterior apex of H-VCT-Ft-Loop.

THORAX: T2-S with three branches: H-DCT, H-VCT, and T2-AWL. H-DCT runs directly

FIGURE 77. *Oligotoma* (Embiodoptera: Oligotomidae) in **A.** lateral and **B.** ventral views, showing extent of air-filled alimentary canal and effect of distention on position of tracheae. Tracheae in orange, alimentary canal in grey.

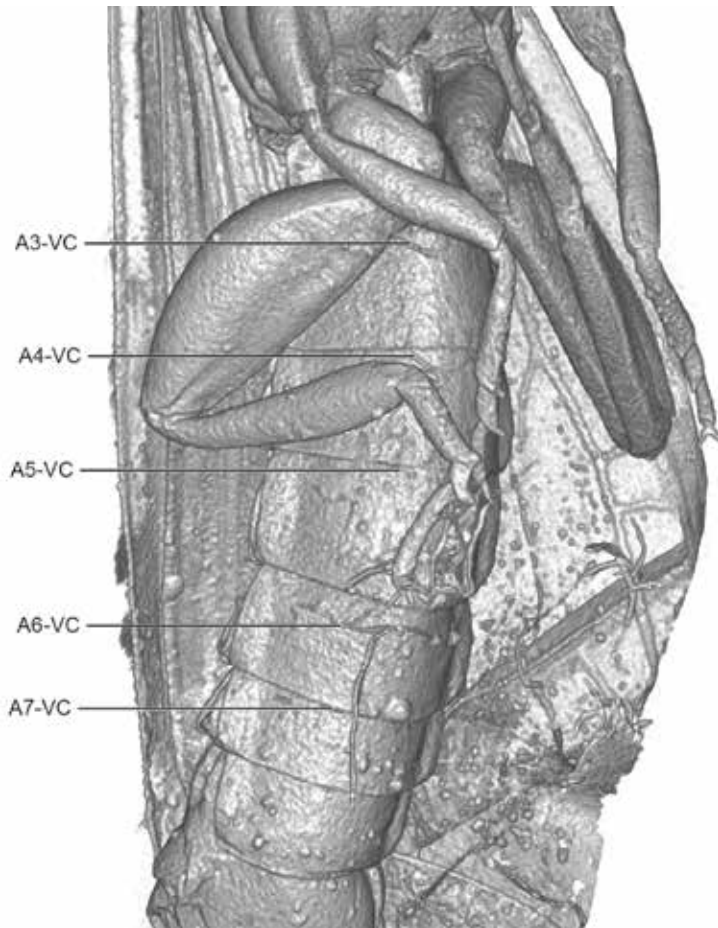


FIGURE 78. Volume rendering of *Oligotoma* (Embiopoda: Oligotomidae) venter. Volume rendering as a visualization technique can reveal small details with subtle intensity differences that are difficult to hand-segment; note apparent presence of A3..7-VC, displaced against body wall by air-filled alimentary canal.

anteriad toward head; small T1-Cx ventrad in middle of prothorax. H-VCT likewise running anteriopad, with T1-AL ventrad at posterior margin of prothorax; T1-PL not present. T1-AL with medial branch to T1-VX. T1-VX branching into three anteriopad tracheae, extending toward head as H-VLT, with right side H-VLT fusing with H-VLT-Med anteriopad of cervix. T2-AWL runs ventrad and mediad before turning dorsally and posteriad in an S-shaped curve; small T2-DB and T2-VB branching dorsad and ventrally (respectively) from T2-AWL. T2-DB linking with apparent T1-DLT anteriopad; T2-DLT not visible. T2-VB

runs ventrad at bottom of T2-AWL S-curve, bifurcating into anterior and posterior branches, both leading to network of tracheae forming numerous ventral commissures. Remainder of T2-AWL bifurcating into T2-Wbr and T2-AL; T2-Wbr directly posteriad, linking with T3-S via T2-PWL; T2-AL posteriad and ventrad, linking with T2-PL and extending into midleg. T3 with three branches: T2-PWL, T3-AWL, and T3-VB. T2-PWL runs anteriopad, splitting into T2-Wbr dorsally and T2-PL ventrad; T2-PL joining with T2-AL and extending into midleg. T3-AWL runs dorsad, curving posteriorly and splitting into

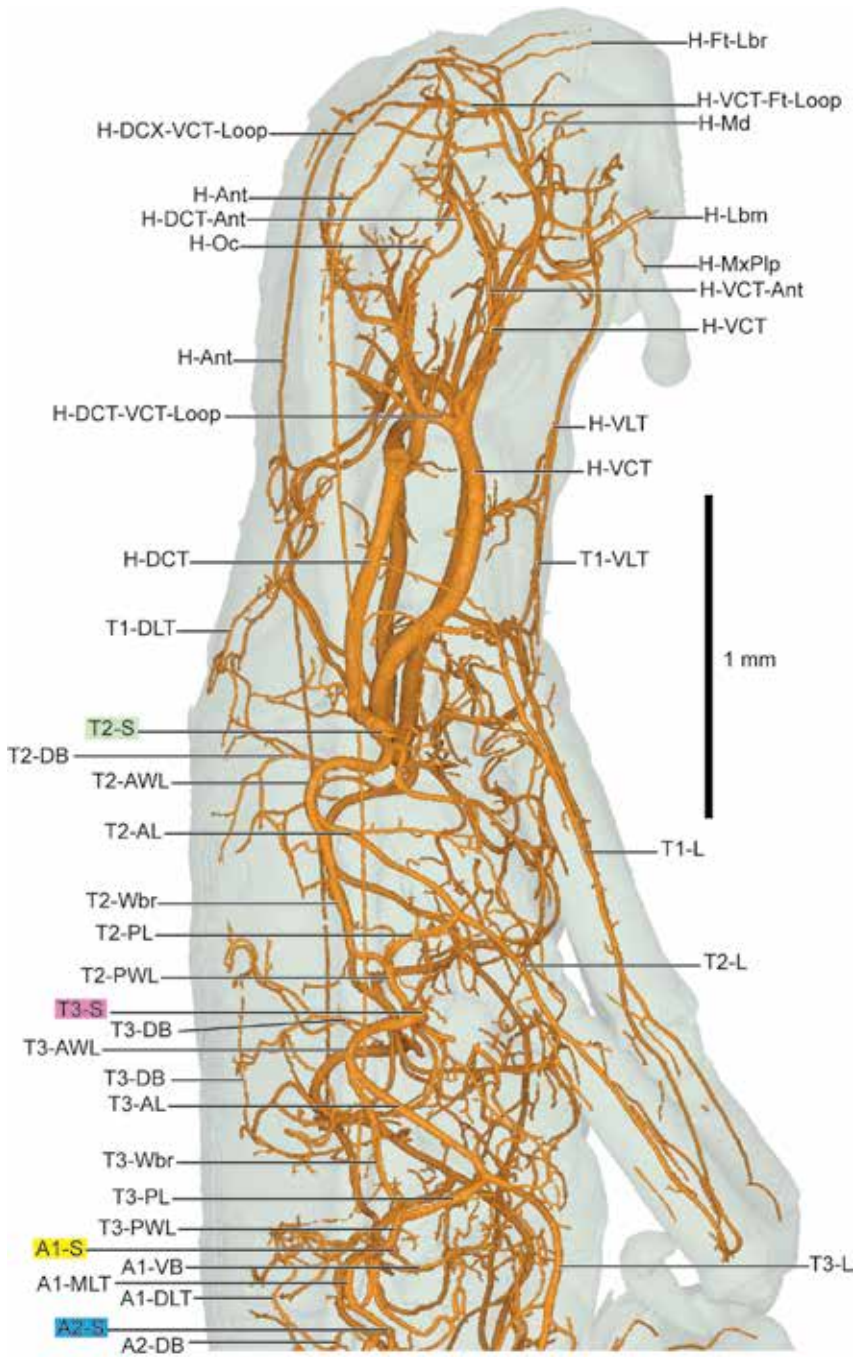


FIGURE 79. *Timema cf. californicum* (Phasmatodea: Timematidae) anterolateral view.

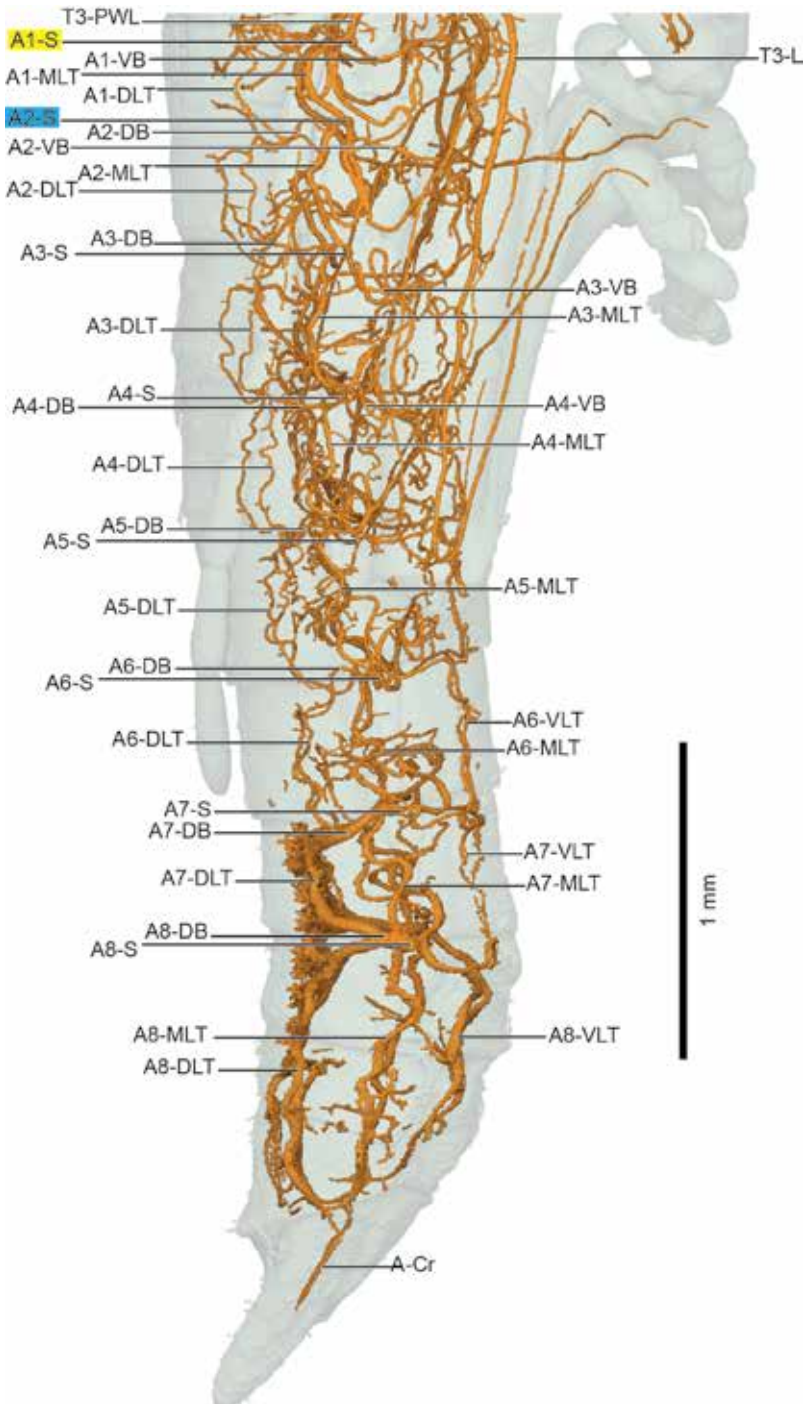


FIGURE 80. *Timema cf. californicum* (Phasmatodea: Timematidae) postero-lateral view.

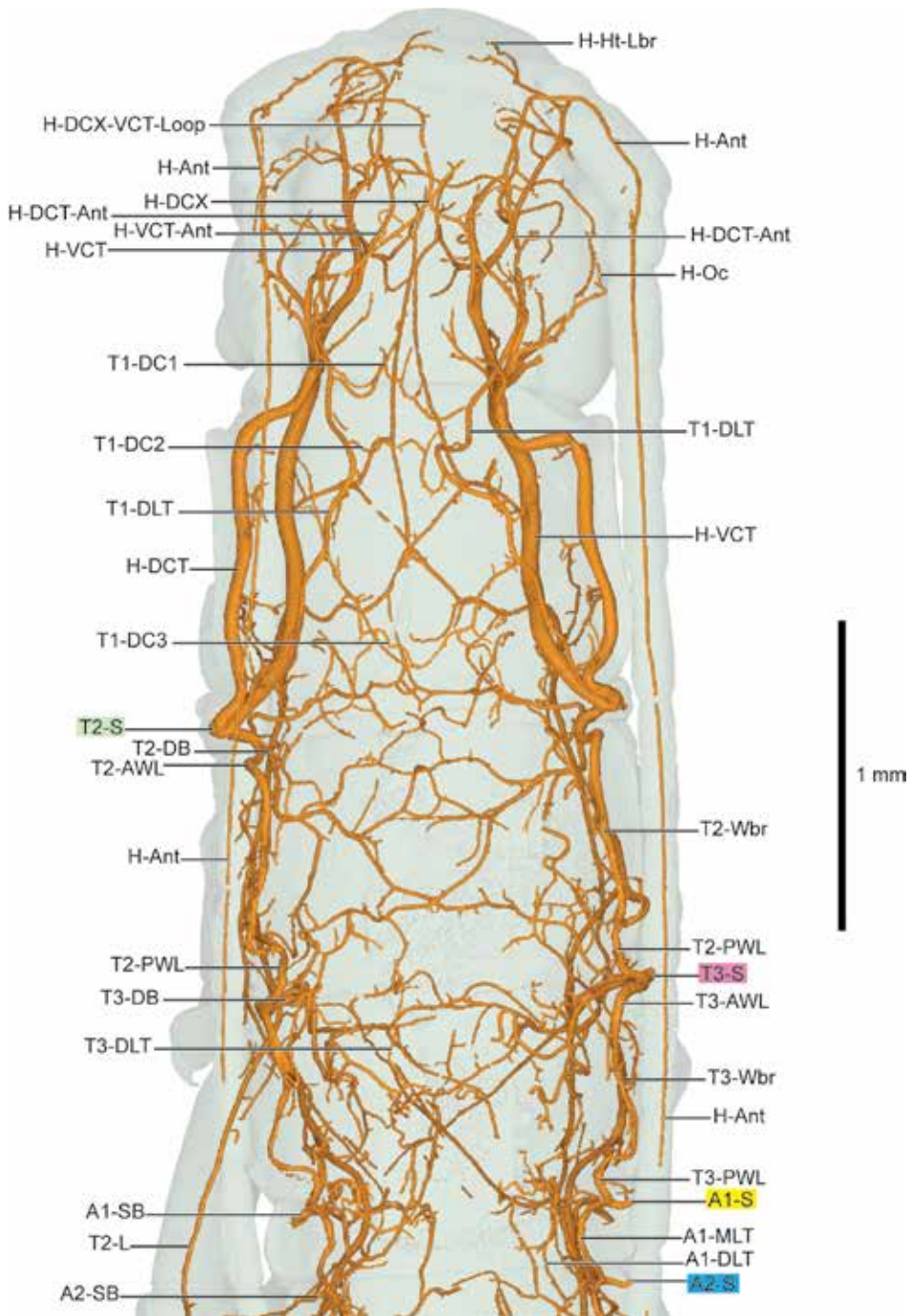


FIGURE 81. *Timema cf. californicum* (Phasmatodea: Timematidae) anterodorsal view.

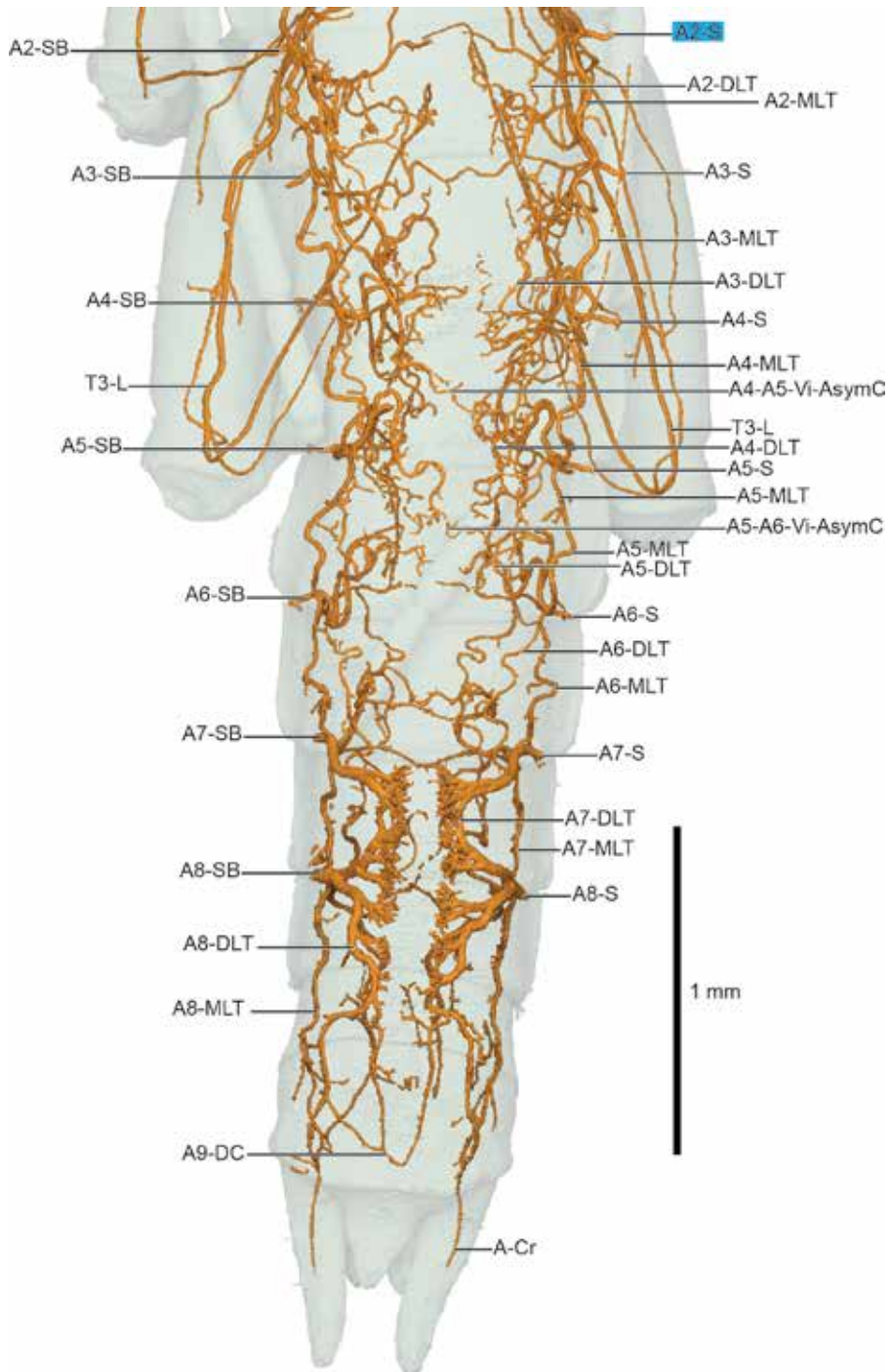


FIGURE 82. *Timema* cf. *californicum* (Phasmatodea: Timematidae) postero-dorsal view.

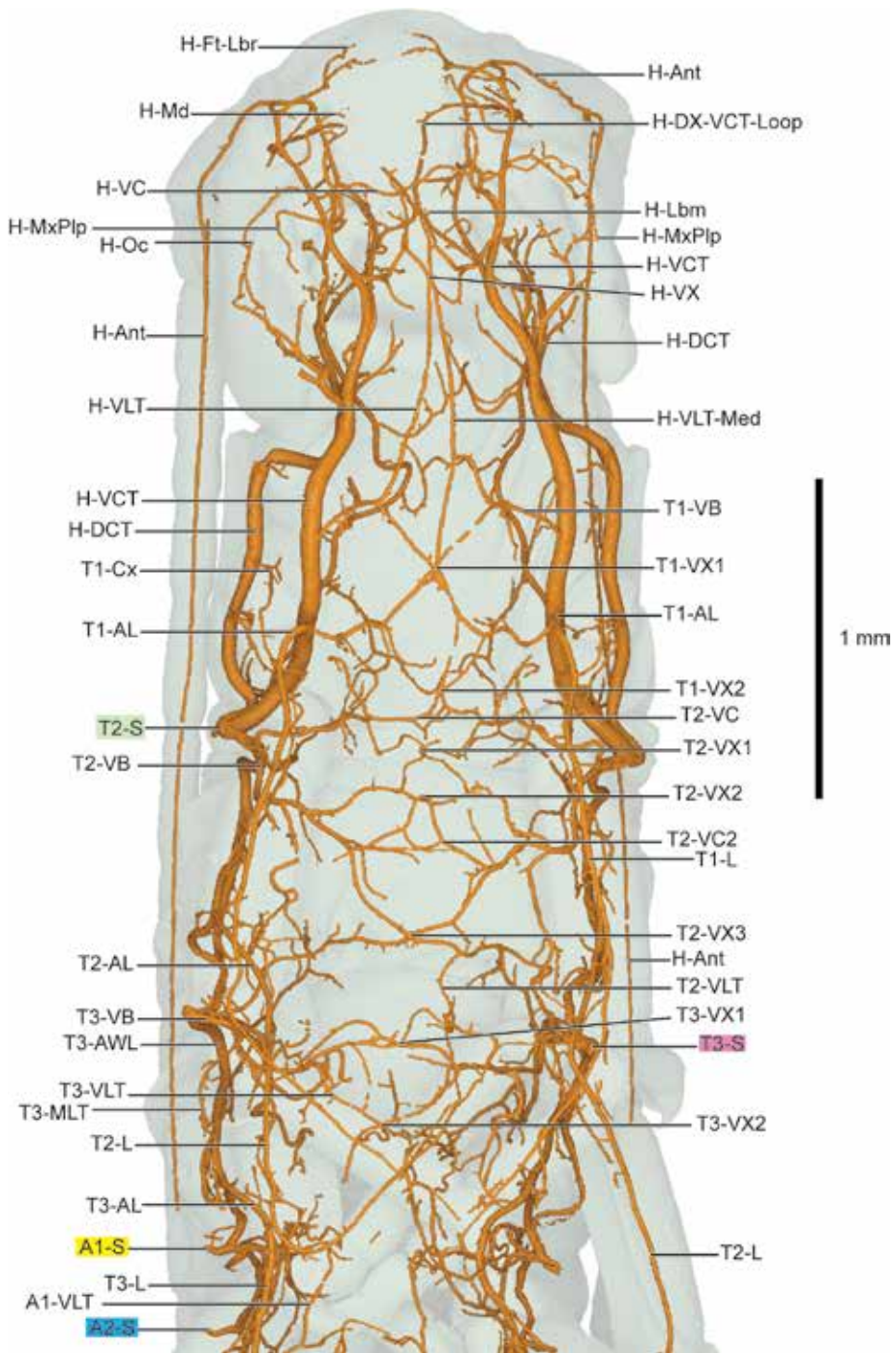


FIGURE 83. *Timema cf. californicum* (Phasmatodea: Timematidae) anteroventral view.

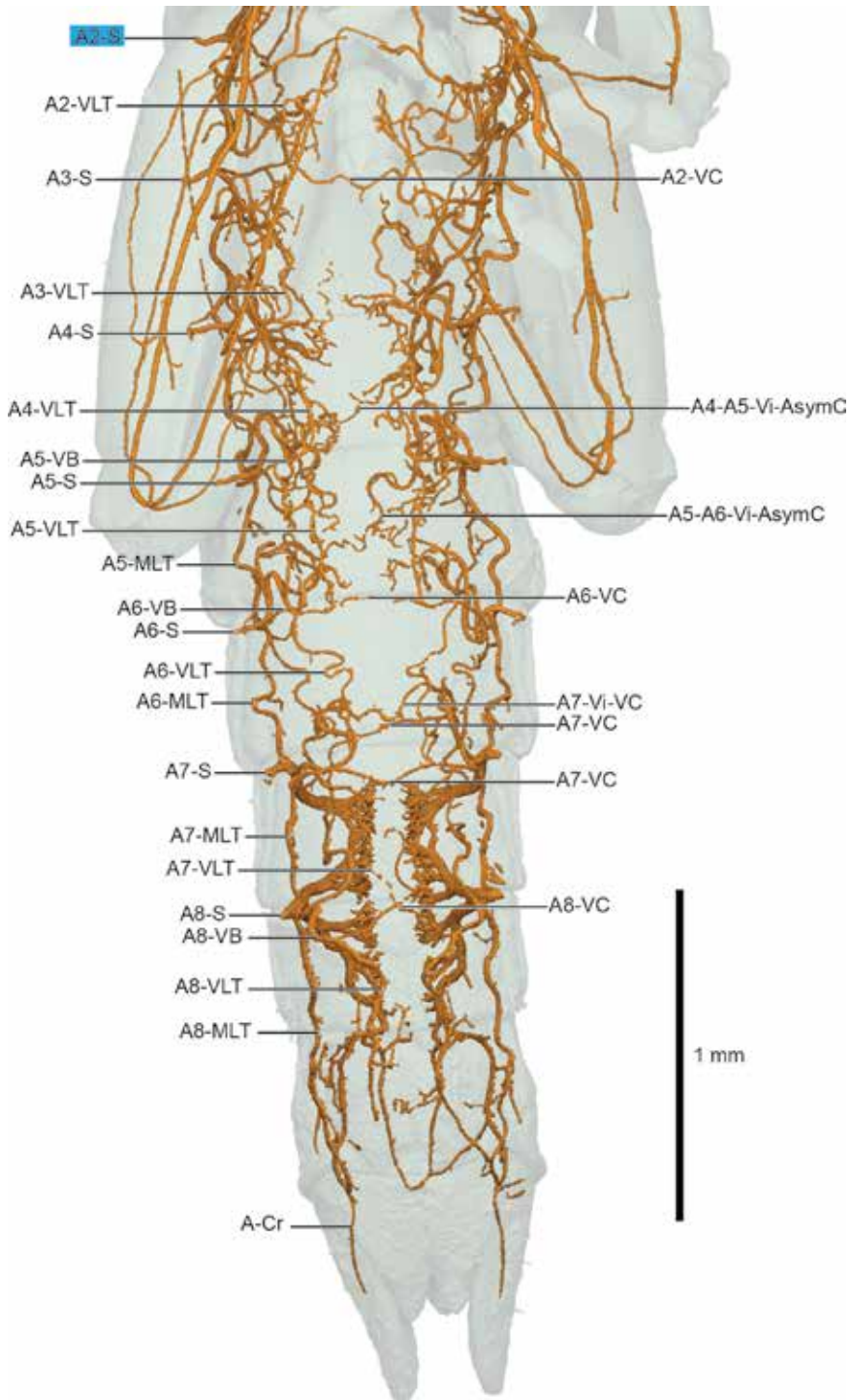


FIGURE 84. *Timema* cf. *californicum* (Phasmatodea: Timematidae) posteroventral view.

T3-Wbr posteriad and T3-AL ventrad; T3-AL joining with T3-PL and extending into hind leg. T3-VB splitting into four tracheae close to T3-S; at least two of these extending into network of ventral commissures; several X-shaped commissure intersections present.

ABDOMEN: A1.8-S present, short *An*-SB spiracular branch present on all A1.8-S. A1-S branching pattern slightly modified from remaining A2.8-S, with T3-PWL running anteriorly, splitting into T3-Wbr anteriorly and T3-PL ventrad, with T3-PL joining with T3-AL and extending into T3-L. A1.8-MLT present, with A1.5-DB branching dorsad from *An*-MLT; A6.8-DB branching directly from A6.8-SB. All A1.6-DB linking with thin, sinuous A1.6-DLT along dorsum; *An*-DC not present. A7,8-DLT substantially larger, with fanlike morphology expanding into highly tracheated hind- and midgut “appendices” (Shelomi et al., 2015). A1.8-VB present, extending to link with sinuous *An*-VLT along venter; A2,3,6,7,8-VC present; given distribution, other *An*-VC likely present but not visible. Numerous visceral tracheae, most notably forming asymmetric connectives A4-A5-Vi-AsymC and A5-A6-Vi-AsymC; A7-Vi-VC also present.

FAMILY PHASMATIDAE

Extatosoma tiaratum

“Spiny leaf insect”

Figures 85, 86 (lateral, anterior, posterior); 87, 88 (dorsal, anterior, posterior); 89, 90 (ventral, anterior, posterior)

Plates 52 (lateral), 53 (dorsal), 54 (ventral)

The spiny leaf insect *Extatosoma tiaratum* features a highly networked tracheal system with many lateral commissures and longitudinal connections. The posterior portion of the abdomen features a dense packing of noodlelike visceral tracheae that has morphological similarities to a package of dried ramen noodles, likely important for ventilation of the ovaries during the con-

tinuous egg production of adult females. *An*-DLT and *An*-VLT are discernible in regions, along with larger anatomical features such as the location of spiracles, but the complexity of the specimen calls for a more in-depth analysis than can be presented here. Interested readers are encouraged to view the 3D models in the supplementary digital data.

Medauroidea extradentata

“Vietnamese walking stick”

Figures 91, 92 (lateral, anterior, posterior); 93, 94 (dorsal, anterior, posterior); 95, 96 (ventral, anterior, posterior)

Plates 55 (lateral), 56 (dorsal), 57 (ventral)

Although Strauss (2021) conducted the most recent work on stick insect tracheae, he focused on the prothorax and prolegs, concentrating on hearing. He employed terminology from Ander (1939), also incorporated here, although he left several branches unlabeled. In the *Medauroidea* scan here, T1-AL and T1-PL remain separate, at least as far as the distal end of the foretibia. Strauss indicates foreleg (and mid- and hind leg) adaptations for hearing; these cannot be verified from this scan.

Medauroidea is a good example of assessing homology using secondary criteria (serial homology). The T2-DB branching pattern posteriorly in *Medauroidea* is somewhat ambiguous, in particular the placement of T2-AL and T2-Wbr. T2-AL and T2-Wbr could be swapped; however, the decision that the dorsal one is T2-AL is based on serial homology with T3. Additionally, the shorter DB branches, such as T3-DB and T3-VB here in *Medauroidea* (but also applicable elsewhere), could be argued to be branching directly from the spiracle. The presence or absence of a spiracular “atrium” is not specific here; these structures are most prominent in groups such as Orthoptera, where a large “cavity” sits just inside the spiracle with multiple tracheae branching in various directions. In

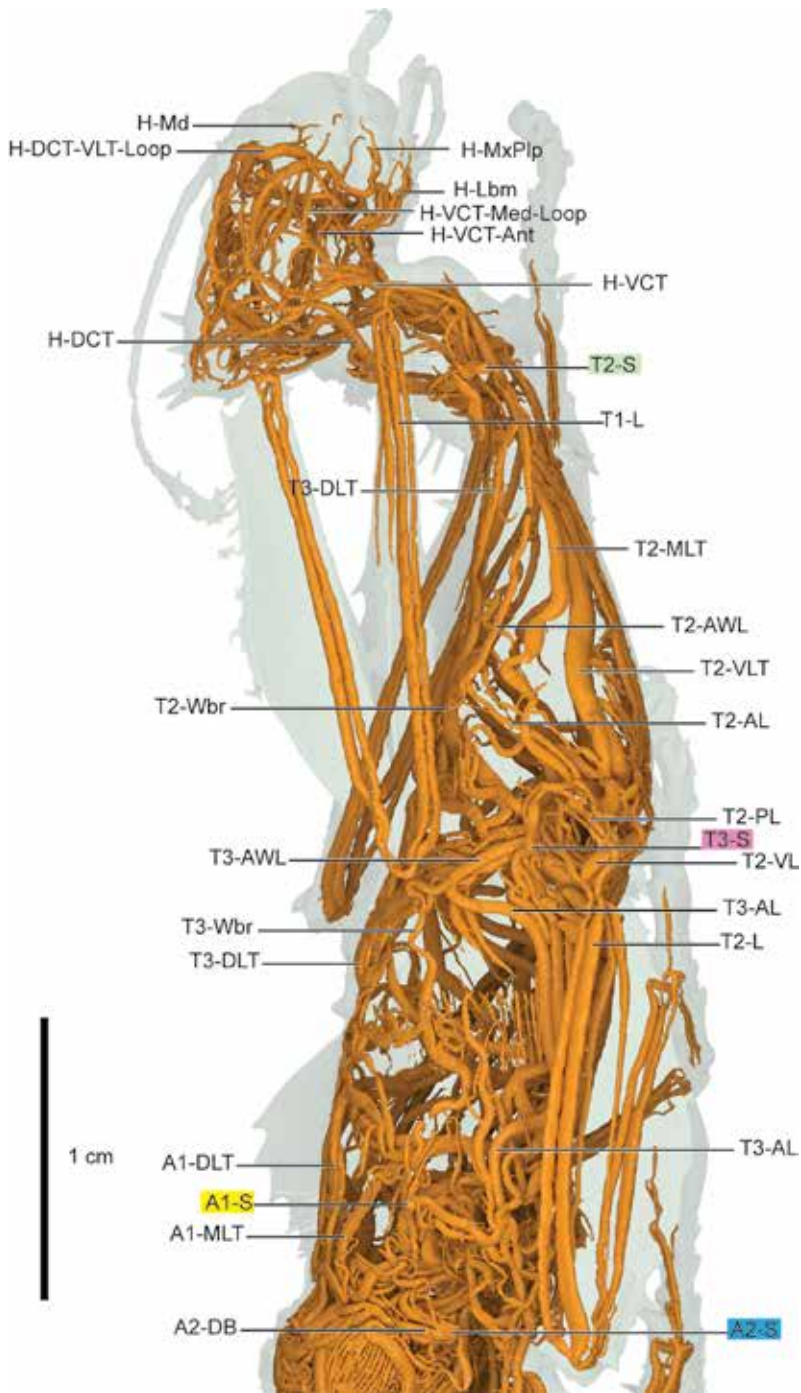


FIGURE 85. *Extatosoma tiaratum* (Phasmatodea: Phasmatidae) anterolateral view.

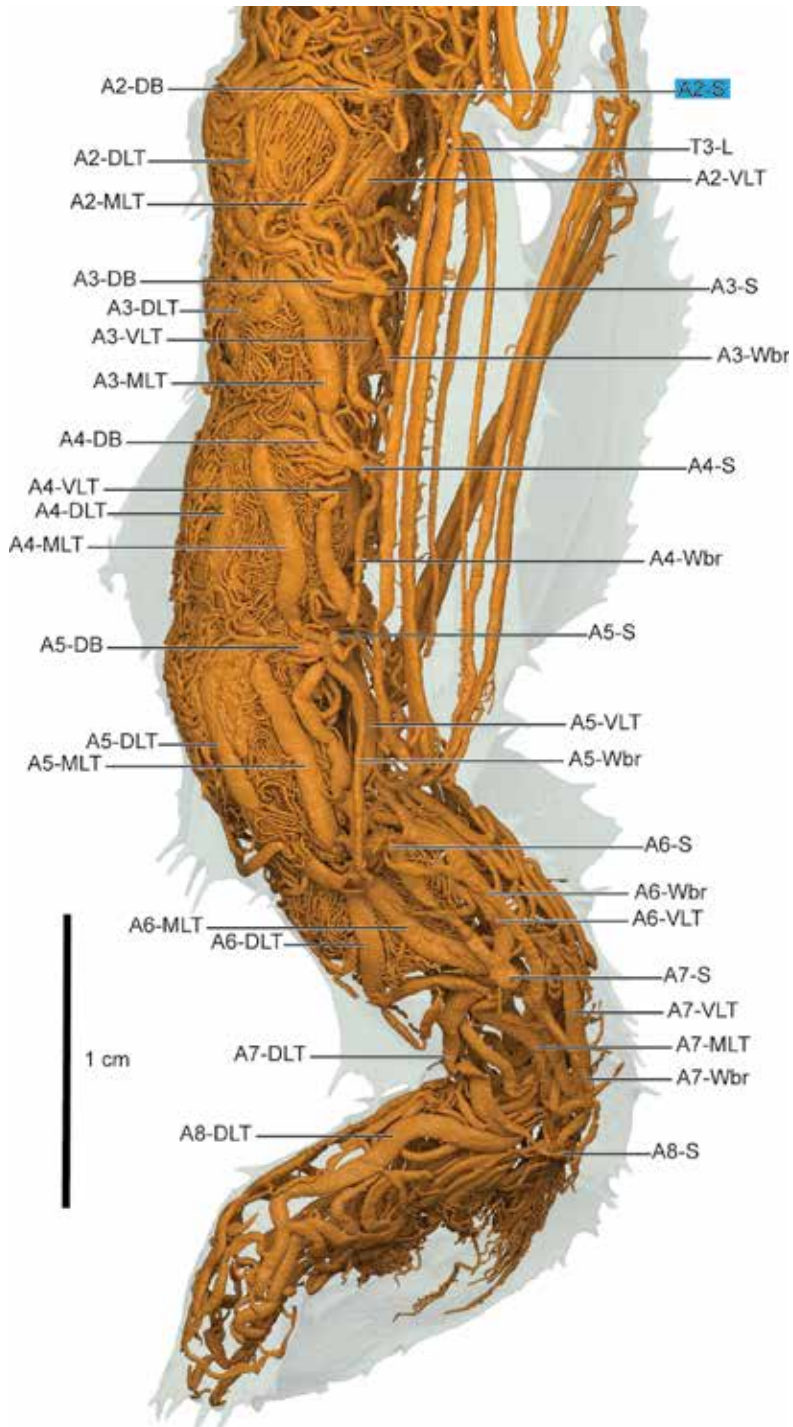


FIGURE 86. *Extatosoma tiaratum* (Phasmatodea: Phasmatidae) posterolateral view.

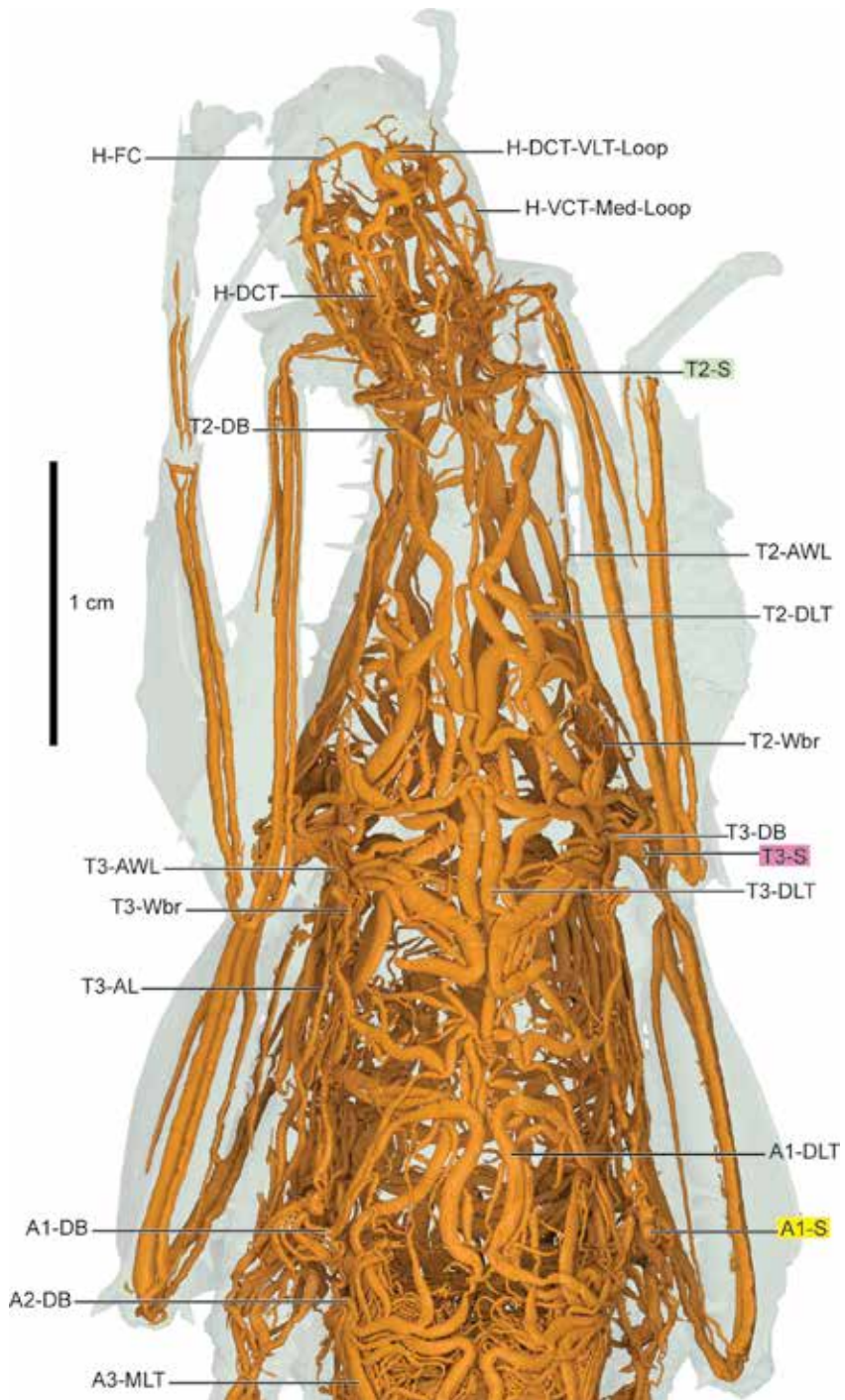


FIGURE 87. *Extatosoma tiaratum* (Phasmatodea: Phasmatidae) anterodorsal view.

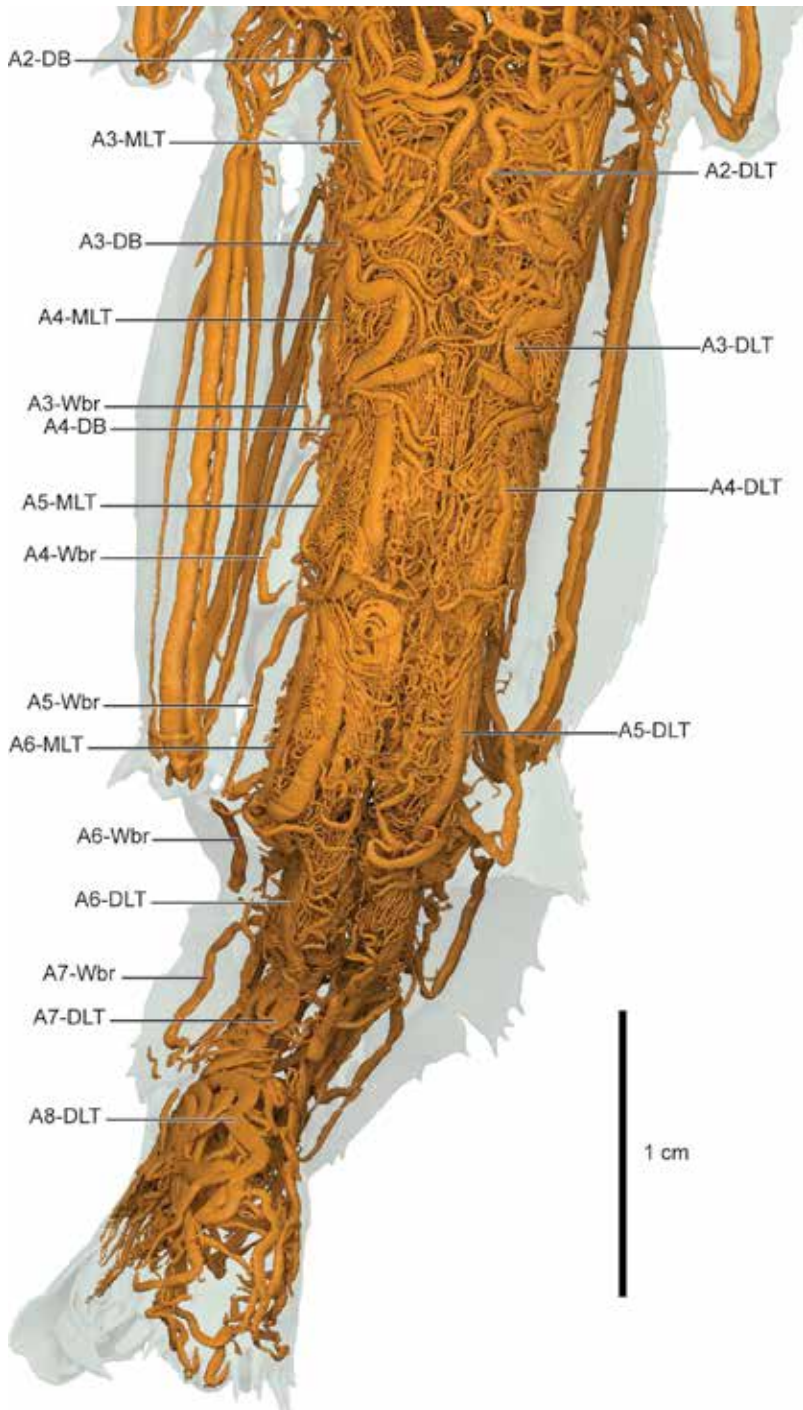


FIGURE 88. *Extatosoma tiaratum* (Phasmatoidea: Phasmatidae) posterodorsal view.

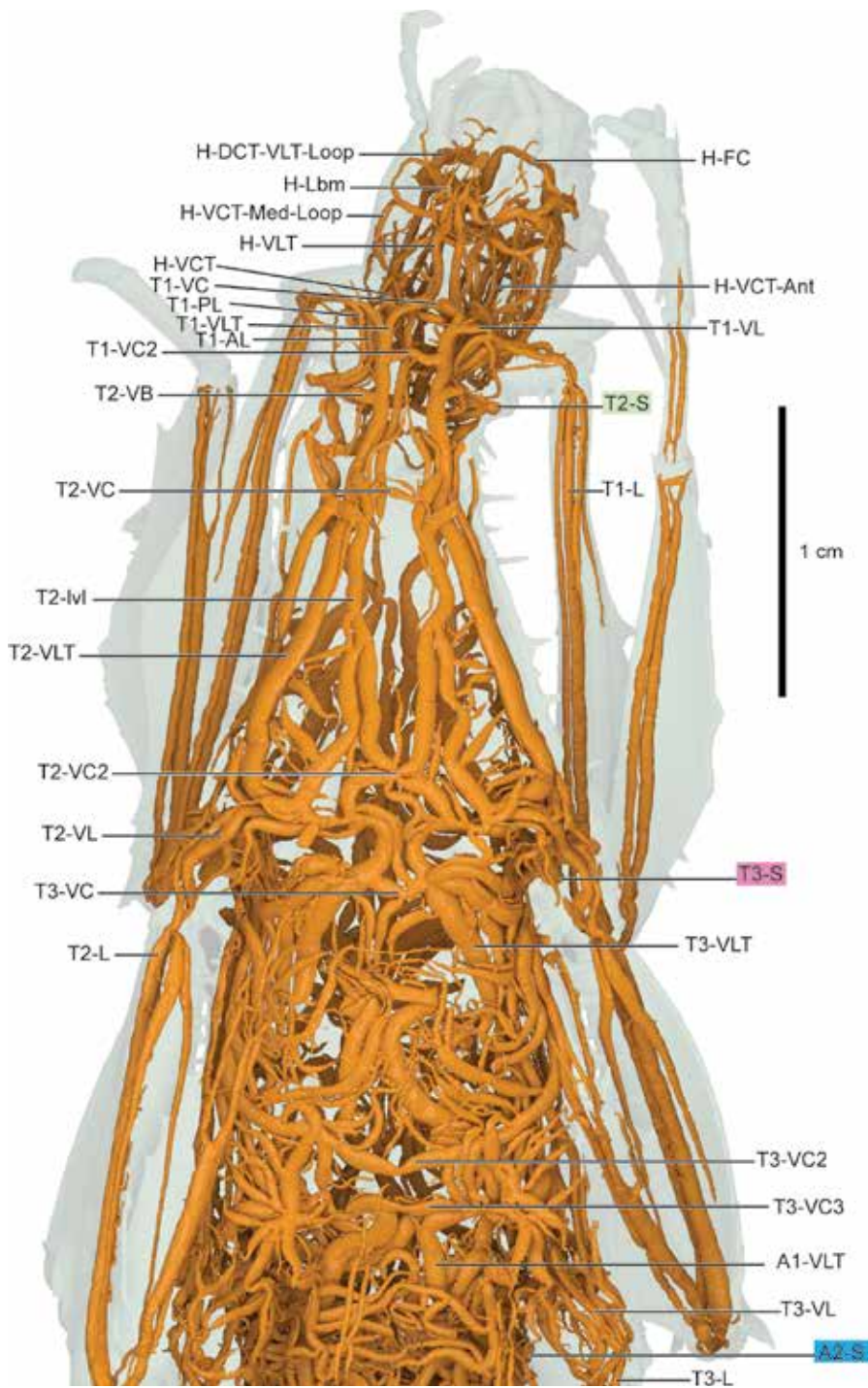


FIGURE 89. *Extatosoma tiaratum* (Phasmatodea: Phasmatidae) anteroventral view.

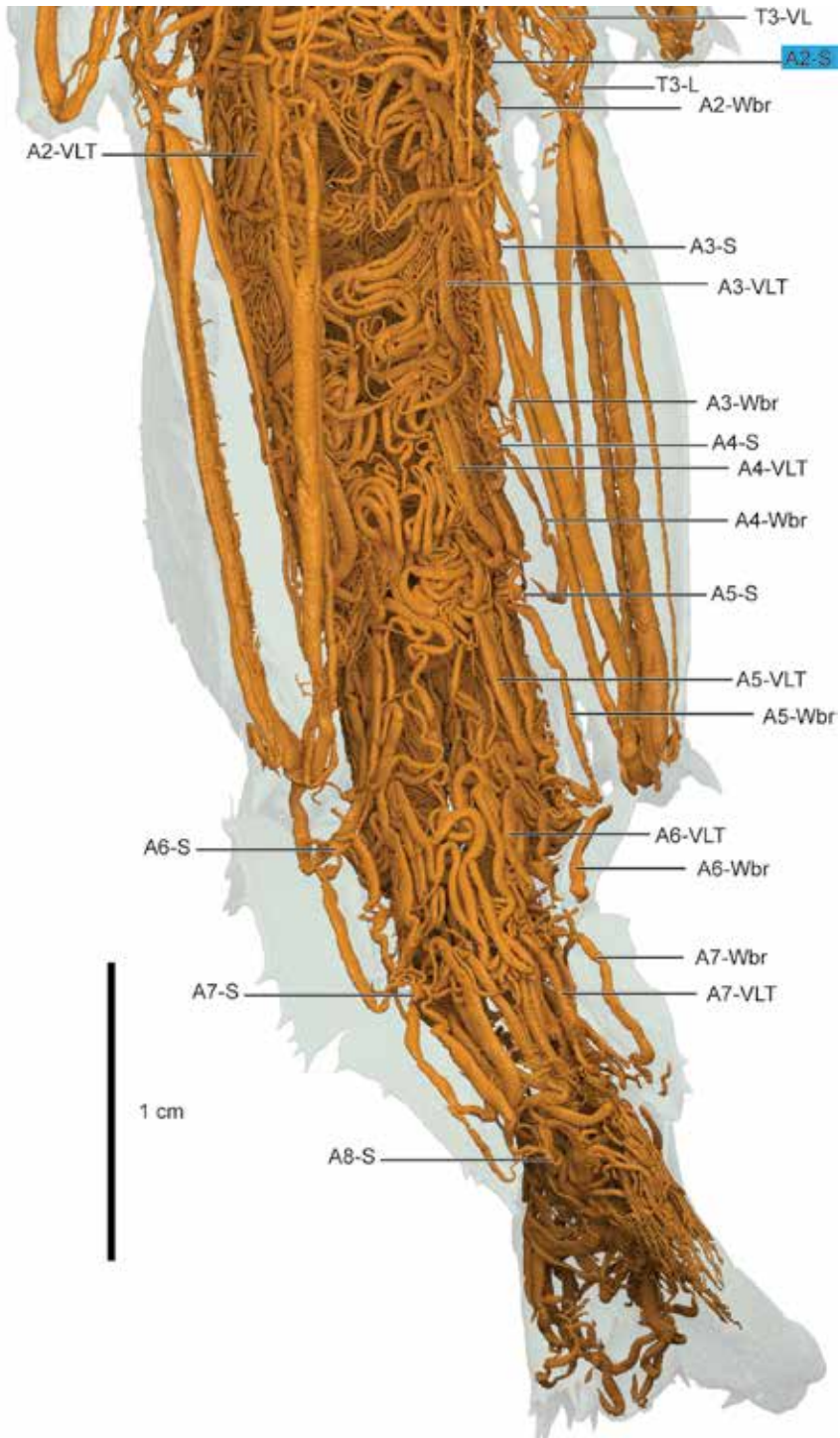


FIGURE 90. *Extatosoma tiaratum* (Phasmatodea: Phasmatidae) posteroventral view.

Medauroidea, it appears that a very short “stub” of DB or VB may have trachea branching from it. T2-CT may be present, but this stub may also be a spiracular atrium, as the closest (phylogenetically) relative with T2-CT is Plecoptera (rather distant).

The tracheal branching in first abdominal segment is very unusual and assessing its homology calls for some explanation. A1-DLT is quite clearly absent, as no tracheae arc posteriorly in the form of a DLT; T3-DLT connects directly to the dorsum of A1-S with no continuation. A1-VLT initially appears to be A1-MLT, but the ventral branch of T3-VL into the hind leg is indicative of it being a VLT, not MLT. Additionally, A1-VC branches from T3-VL, rather than A1-VB, an unusual arrangement. This branch is not a section of A1-VB, as A1-VLT connects A1-S and A2-S. The remaining branches are typical.

The second abdominal segment is also slightly modified from the remaining segments extending posteriad. A2-DB and A2-VB are basically absent—while A2-DC and A2-VC are present, they branch directly from A2-DLT and A2-VLT. The primary connection between A2-S and A1-S anteriorly is A1-VLT. A2-DC extends a little anteriorly of A2-S; A2-DC could arguably be A1-DC but the branching pattern is from A2-DLT, so homologizing based on connectivity or branching pattern seems more reasonable.

DESCRIPTION: HEAD: The head tracheal morphology of *M. extradentata* features a network of loops interconnecting both dorsoventrally and laterally. Exploration of the 3D models in the supplementary digital data is encouraged. Three sets of tracheae into head: H-DCT, H-VCT, and additional H-VLT. H-DCT dorsad, proceeding anteriorly and forming a prominent H-DCT-VLT-Loop anteriorly and ventrad, connecting directly with H-VLT. H-Lbm anteriorly from ventral apex of H-DCT-VLT-Loop. H-VCT runs anteriorly, dividing into H-Ant and two branches, one looping posteriad to connect with H-VCT, forming H-Ant-Loop; second branch looping ventrad and posteriad to join H-VLT.

THORAX: T2-S with four connections: possible T2-CT, T2-DB, T2-VB, and T1-PL. T2-CT short and running directly anteriorly, bifurcating into H-DCT and H-VCT near posterior margin of prothorax; as T2-CT absent in other Phasmatoidea, this T2-CT is possibly a deeper spiracular atrium rather than T2-CT. H-DCT runs anteriorly, extending through prothorax into head. H-VCT anteriorly, with T1-AL splitting off into foreleg; short connection to T1-VLT at this branching point. T2-DB runs posteriorly, curving slightly ventrad before splitting into two pairs: T2-DLT/T2-AL dorsal branch and T2-Wbr/T2-lvl ventral branch; T2-AWL notably absent. For dorsal T2-DLT/T2-AL pair, T2-DLT as with other specimens, positioned along dorsum with connection posteriorly to T3-DB; T2-AL extending posteriorly, connecting with T3-S via T2-PWB. Ventral T2-Wbr/T2-lvl pair with T2-AL posteriorly with shallow arc dorsad to connect with T2-PWL; T2-lvl along venter, connecting with T3-S via T2-VLT connection just anteriorly of T3-S. T2-VB short and directly ventrad, linking with T2-VLT posteriorly and T1-VLT anteriorly. Both T1-VC and T2-VC present. T1-PL runs anteriorly, linking with T1-VLT via short T1-VL; T1-PL extends into foreleg without joining T1-AL. T1-AL and T1-PL do not join and remain separate at least until the distal end of the foretibia. Two small, visceral medial A1-DVi-Med and A1-VVi-Med extend through mesothorax, originating at A1-S and extending into head. T3-S with four branches: T2-VLT, T3-DB, T3-VB, and T2-PL. T2-VLT from anterior, connecting T2-S to T3-S. T3-DB short and medially, quickly branching into T3-AL posteriorly and remaining T3-DB dorsad; T3-DB joining with T2-DLT anteriorly and T3-DLT posteriorly in Y-shaped junction, linking to T2-S and A1-S. T3-AL posteriorly, joining with T3-PL to form T3-L, extending into hindleg. T3-VB short, similar to T3-DB, quickly splitting into T3-VLT posteriorly and remaining T3-VB ventrad. T3-VLT runs directly posteriorly to A1-S; T3-DC present toward posterior margin of metathorax. T3-VB continues to T3-PVC, which forms posteriorly

segment of hexagonal network comprised of T3-VC anterior and lateral sections connected to T2-VLT. T2-PL anterior, joining T2-AL and extending into midleg. T2-VL branching from T2-VLT, also extending into midleg; T2-VL and T2-L remain separate to distal end of midleg tibia. A2-DVi-Med and A2-VVi-Med extending through metathorax, with laterally asymmetric connections: A2-DVi-Med to T2-VLT on specimen's left side, A2-DVi-Med to T2-VLT on specimen's right side.

ABDOMEN: A1..8-S present. First abdominal segment approximately half as long as remaining abdominal segments. A1-S and A2-S branching patterns highly modified from remaining abdominal segments. A1-S with four branches: T3-DLT, A1-VLT, T3-VLT, and A1-PL. A1-S with additional A2-VVi-Med connection on left side only, see description of A2-VVi-Med below. T3-DLT runs dorsad, connecting in anterior arc from T3-S; A1-DLT notably absent. A1-VLT runs directly posterior to A2-S; T3-VL directly ventrad from A1-VLT; A1-PVC branching from T3-VL. T3-VLT from anterior, with two ventral commissures A1-AVC1 and A1-AVC2. T3-PL ventrad, linking with T3-AL before arcing posterior to extend into hind leg. A2-S with seven branches: A1-VLT, A2-DVi-Med, A2-VVi-Med, A2-DLT, A2-DVi, A2-VVi, and A2-VLT. A1-VLT runs directly anterior from A1-S. A2-DVi-Med beginning as sinusoidal, looping branch, extending anteriorly and medially, each side combining in Y-shaped junction in metathorax and proceeding anteriorly along venter; A2-DVi-Med asymmetric, with sinusoidal form on both sides but only right side leading to Y-shaped join, with left side coming from A1-S. A2-VVi-Med similar, arranged along venter. A2-DLT runs dorsad and posterior in arc connecting to A3-S; A2-DC present off A2-DLT. A2-DVi and A2-VVi ventrad, connecting with A3-S. A2-VLT likewise in ventral arc, also connecting with A3-S; four tracheae connect A2-S with A3-S. Remaining A3..A8 segments similar, with varying degrees of *An-DB*; A3-DB short, A4-DB not present, etc. *An-DLT* and *An-VLT* present on all, connecting

segments longitudinally. A3..8-S with anterior visceral tracheae generally dorsad, posterior visceral tracheae generally ventrad. A4-Vi-VC present, formed from visceral tracheae and not from VLT as is typical.

SUPERORDER DICTYOPTERA

ORDER MANTODEA

The tracheal system of mantises in part has been examined in detail since the discovery of the ventrally located “cyclopean” ear by Yager and Hoy (1986). More recent investigations have used micro-CT based methods (Wipfler et al., 2012); however, a complete mapping of mantis respiratory systems has been lacking. Two specimens are included here: the common Chinese mantis *Tenodera sinensis* and the popular “Devil’s flower mantis,” *Idolomantis diabolica*. *Tenodera* is described here in detail but the somewhat more complex *Idolomantis* is covered only broadly; 3D models are included in the supplementary digital data for further research.

The morphology of H-DCT and H-VCT deserves special note here. Nominally, branching patterns starting at spiracle are judged to be more stable, as spiracles are used as the landmarks for assessing homology (as discussed above). The tissues supplied in the mantis prothorax and head, however, indicate a dorsal/ventral swap of H-DCT and H-VCT. For H-VCT in all other taxa, T1-AL branches ventrally from H-VCT in the prothorax. In Mantodea, however, this branch (H-VCT) begins dorsally at T2-S, and then flips position with the other cephalic trachea at the anterior end of the pronotum and retains the condition of T1-AL extending ventrally. The length of the prothorax in mantises likely plays a role in this dorsal-ventral reversal, but the reasons are unclear. An alternative interpretation is that one of these trunks is T2-CT and splits into H-DCT and H-VCT in the prothorax, in conjunction with dorsal-ventral connections in the head. However, this would also imply that T1-PL splits from T2-CT, a condition not encountered in any specimen.

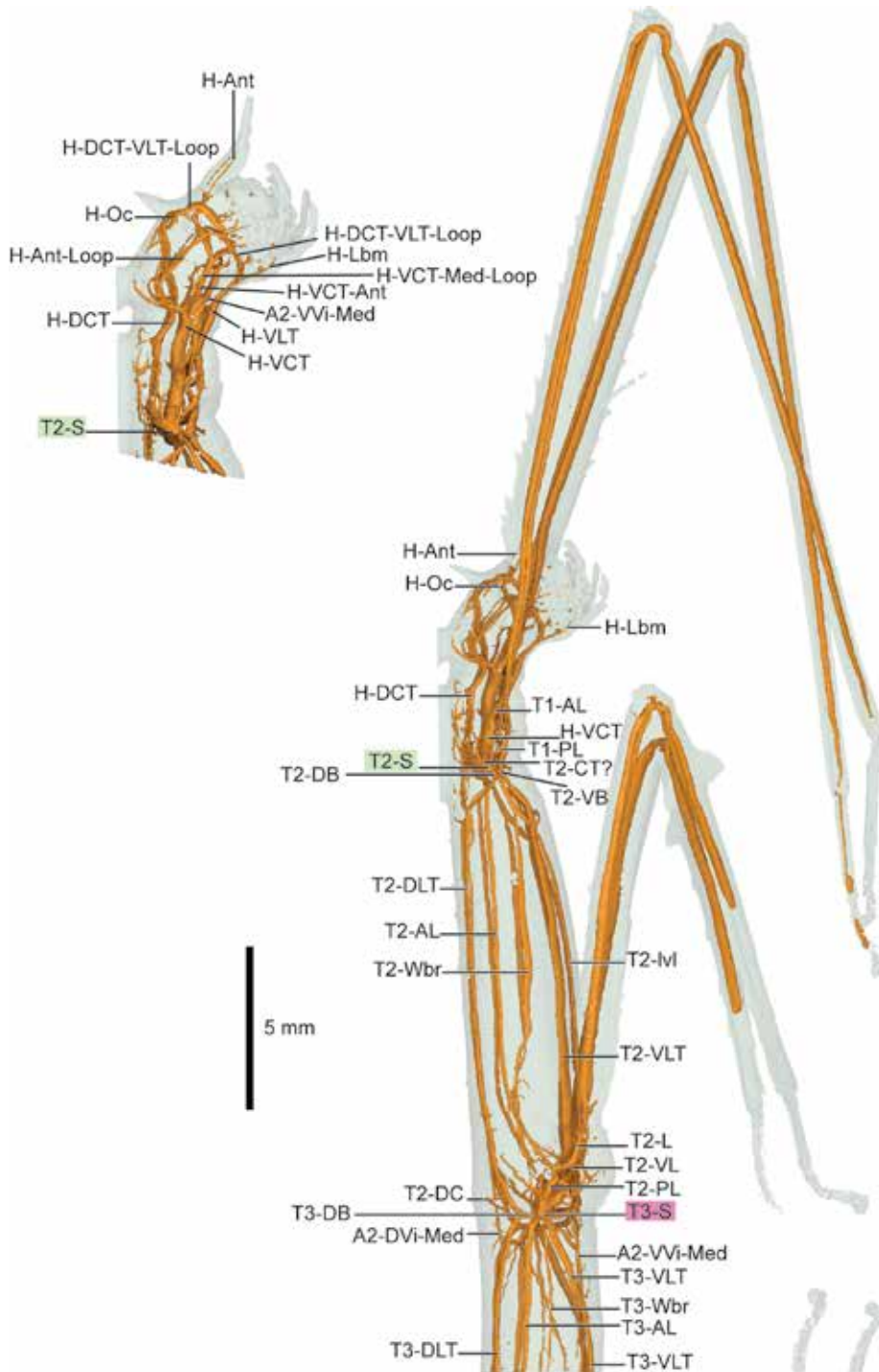


FIGURE 91. *Medauroidea extradentata* (Phasmatodea: Phasmatidae) anterolateral view.

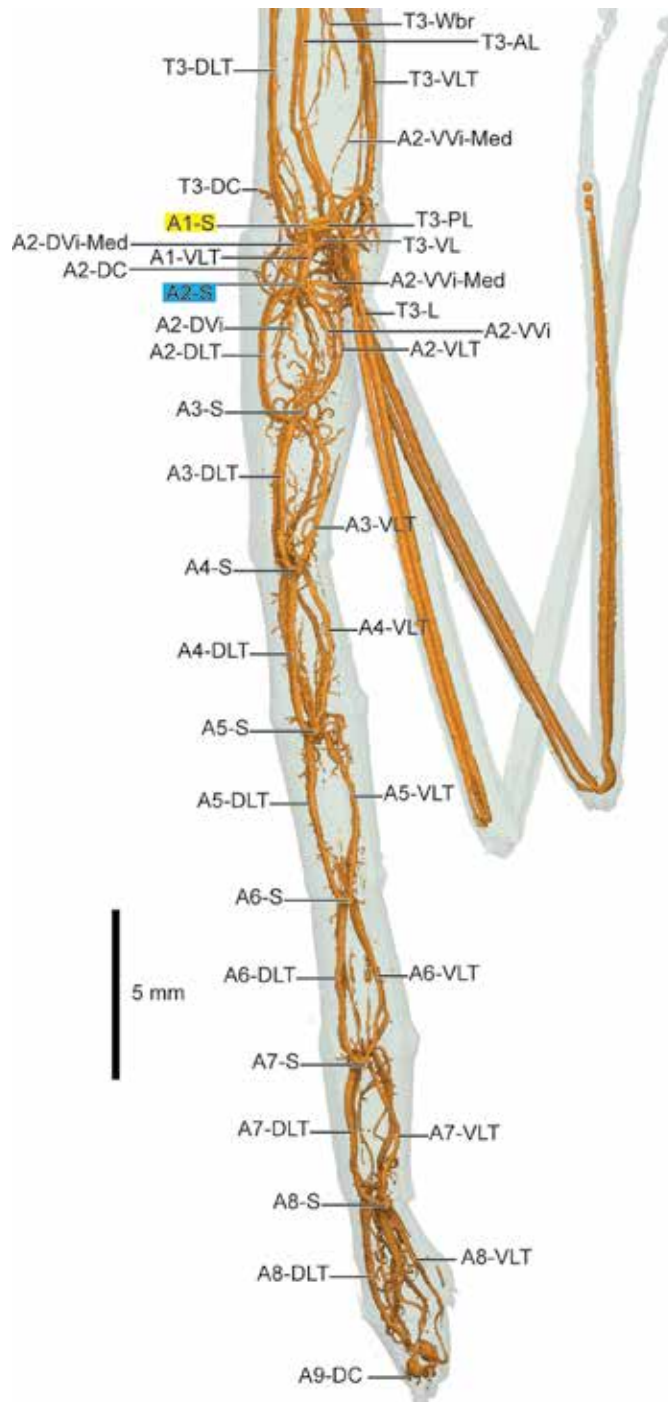


FIGURE 92. *Medauroidea extradentata* (Phasmatodea: Phasmatidae) posterolateral view.

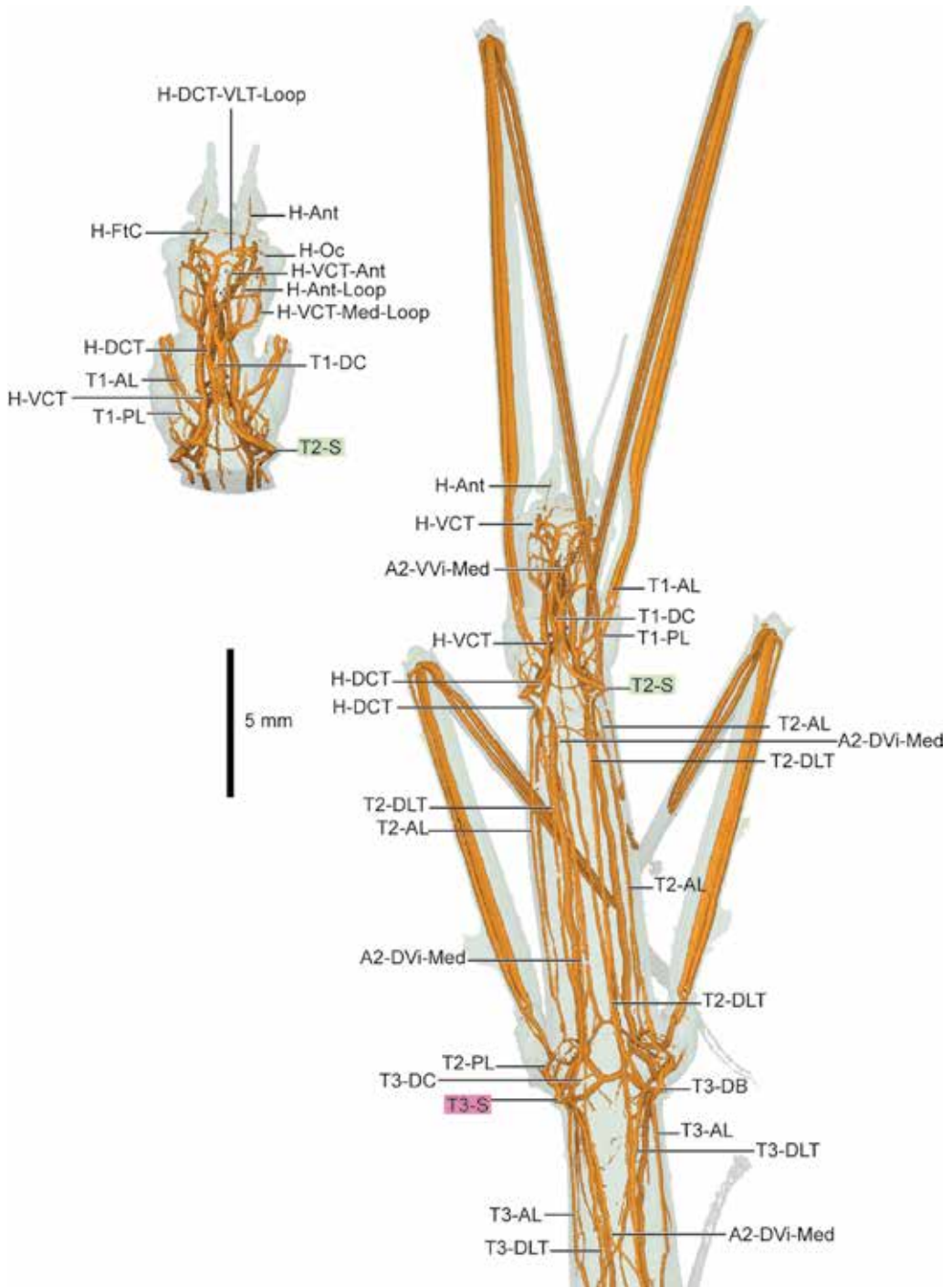


FIGURE 93. *Medauroidea extradentata* (Phasmatodea: Phasmatidae) anterodorsal view.

Looking toward the posterior end of the thorax, T3-DLT is unusual in that it skips a connection to A1-S, extending from T3-S posteriad to A2-S via A2-DB; A2-DLT continues posteriad as with other taxa. Also curious is T2-PWL branching from T2-PL and connecting with T2-AL. This is similar to what is seen in T3 in Orthoptera but appears to be present here in the midleg. The mesothorax is shorter anterior-posteriorly in Orthoptera, so perhaps this condition is either difficult to discern or simply not present. Another modified branching pattern is T3-VL branching from directly from A1-VC rather than VLT. While the origin (VLT) of T3-VL here is unusual, its extension into the leg and overall pattern appears homologous with T3-VL elsewhere.

FAMILY MANTIDAE

Tenodera sinensis

“Chinese mantis”

Figures 97, 98 (lateral, anterior, posterior); 99, 100 (dorsal, anterior, posterior); 101, 102 (ventral, anterior, posterior)

Plates 58 (lateral), 59 (dorsal), 60 (ventral)

DESCRIPTION: Pronotum, metathorax, and anterior portion of abdomen with air-filled spaces, likely alimentary canal and transient as not connected to tracheae (see fig. 103).

HEAD: Tracheae leading to appendages are labeled; however, the head of *Tenodera* features a complex network of intersecting tracheae and air sacs. Readers are encouraged to review the 3D models in the supplementary digital data.

THORAX: Thorax with numerous elongate, bandlike visceral tracheae throughout, often obscuring views. Exploration of 3D models in digital supplementary data is encouraged. T2-S positioned posterior to characteristically elongate pronotum, with four branches, crowded close together: T2-DB, T2-VB, H-DCT, H-VCT. T2-DB runs mediad and slightly dor-

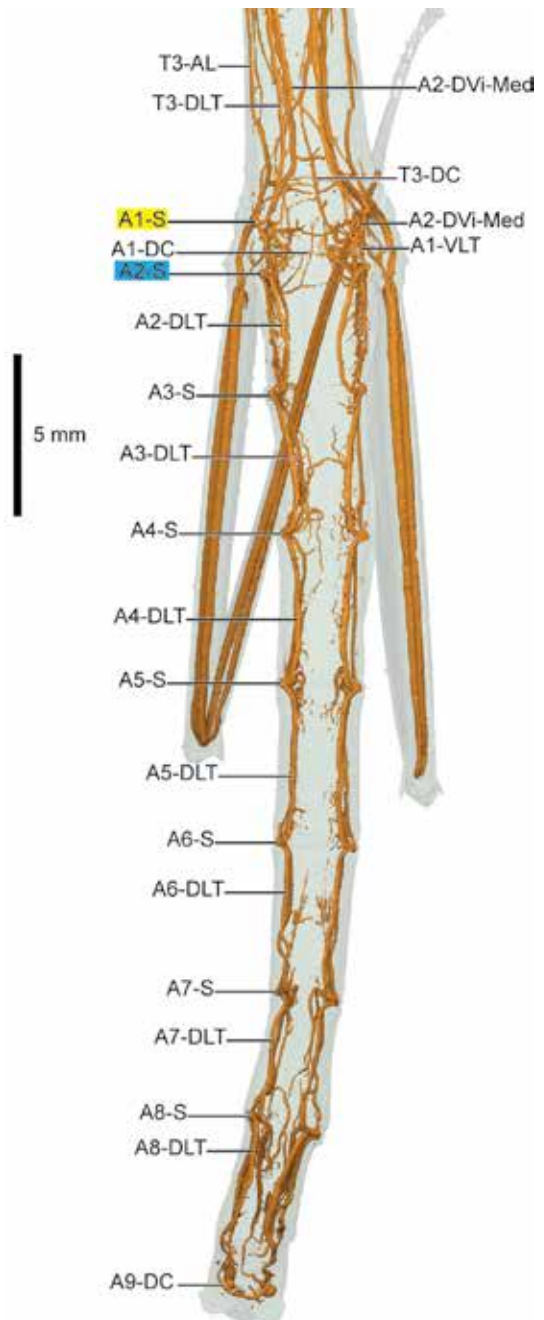


FIGURE 94. *Medauroidea extradentata* (Phasmatoidea: Phasmatidae) posterodorsal view.

sad, with split off to T2-AWL posteriad; T2-DB continues briefly before joining T1-DLT anteriorly and T2-DLT posteriad in Y-shaped junction. T2-DLT running in shallow arc ventrad, with unusual condition of linking with T3-S via connection to T2-PL. T2-AWL arcing dorsally and posteriad, with T2-Wbr branching dorsad at apex of curve; T2-AWL continues as T2-AL, extending posteriad into midleg; T2-Wbr with dorsad T2-W-c-r branch, remaining T2-Wbr connecting to T2-PWL from T3-S. T2-VB short, running directly anteriorly, bifurcating into T1-PL anteriorly and T2-VLT posteriad; T2-VC likely present off T2-VLT; T1-PL extending through mesothorax and prothorax with ventral curve into foreleg at base of forecoxa. T2-VL branching close to origin of T2-VLT, extending straight through coxa into midleg. H-DCT beginning ventrad and H-VCT dorsad, opposite of usual arrangement; both tracheae extending directly anteriorly, switching dorsoventrally to typical positions at anterior margin of mesothorax. (See Discussion section for homology assessment of these tracheae.) H-VCT with T1-AL running ventrad just anterior of dorsoventral H-DCT/H-VCT switch. T3-S with n connections: T3-DB, T3-AWL, T3-VB, T2-PWL. T3-DB mediad, curving dorsally and posteriad as T3-DLT, connecting directly to A2-S with no connection to A1-S; A1-DB absent. T3-AWL runs just lateral of T3-DB, arcing posteriad, with T3-Wbr branch; remaining T3-AWL continuing as T3-AL into hind leg. T3-Wbr with T3-W-c-r, continuing posteriad to connect to A1-S via T3-PWL. T3-VB runs ventrad and posteriad, connecting with A1-S via T3-VLT; T3-VL branching from T3-VLT close to T3-S. T2-PWL short, extending anteriorly, splitting into T3-PL ventrad and T2-Wbr anteriorly. Metathorax with several networked visceral tracheal branches, especially along venter; most notable is T3-Ty for hearing. (Additional tracheae of unknown homology enter the legs, similar to Blattodea [roaches], which require further investigation.)

ABDOMEN: A1..8-S present and functional. A1-S connections atypical from remaining spiracles; A1-S with only two connections: T3-PWL and A1-VB. A1-DB absent; A1-MLT possible but not discernible in this scan. T3-PWL runs from anterior, linking with T3-S via T3-Wbr. A1-VB ventrad, following sternite, forming A1-VC; T3-VLT joining with A1-VB, A1-VLT extending posteriad from T3-VC. T3-VL branching from A1-VC. Remaining A2..8-S connections largely similar, with *An-DB* extending dorsad, joining with *An-DLT*; *An-MLT* extending anterior-posteriorly through length of abdomen; and *An-VB* ventrad, joining with *An-VLT*. Nearly all tracheae bandlike, with visceral branches throughout abdomen. A4-S and A5-S with numerous sinusoidal visceral tracheae.

FAMILY EMPUSIDAE

Idolomantis diabolica late-stage instar

“Devil’s flower mantis”

Figures 104 (lateral), 105 (dorsal), 106 (ventral)

Plates 61 (lateral), 62 (dorsal), 63 (ventral)

The tracheal morphology of *Idolomantis* is very similar to *Tenoderella*, in particular the elongate pronotum and the dorsal-ventral switch of H-DCT and H-VCT. The curling of the abdomen over the thorax unfortunately does not lend itself well to diagramming in two dimensions; major tracheae are labeled in the figures and plates, but readers are encouraged to explore the supplementary digital data.

ORDER BLATTODEA

Three roaches were scanned during the study: the common American cockroach *Periplaneta americana*, the popular Madagascar hissing cockroach *Gromphadorhina portentosa*, and *Blattella germanica*. The tracheal system of *Gromphadorhina* has been studied via dissection to determine the physiology of its hissing behavior (Nelson, 1979; Nelson and Fraser, 1980) and was

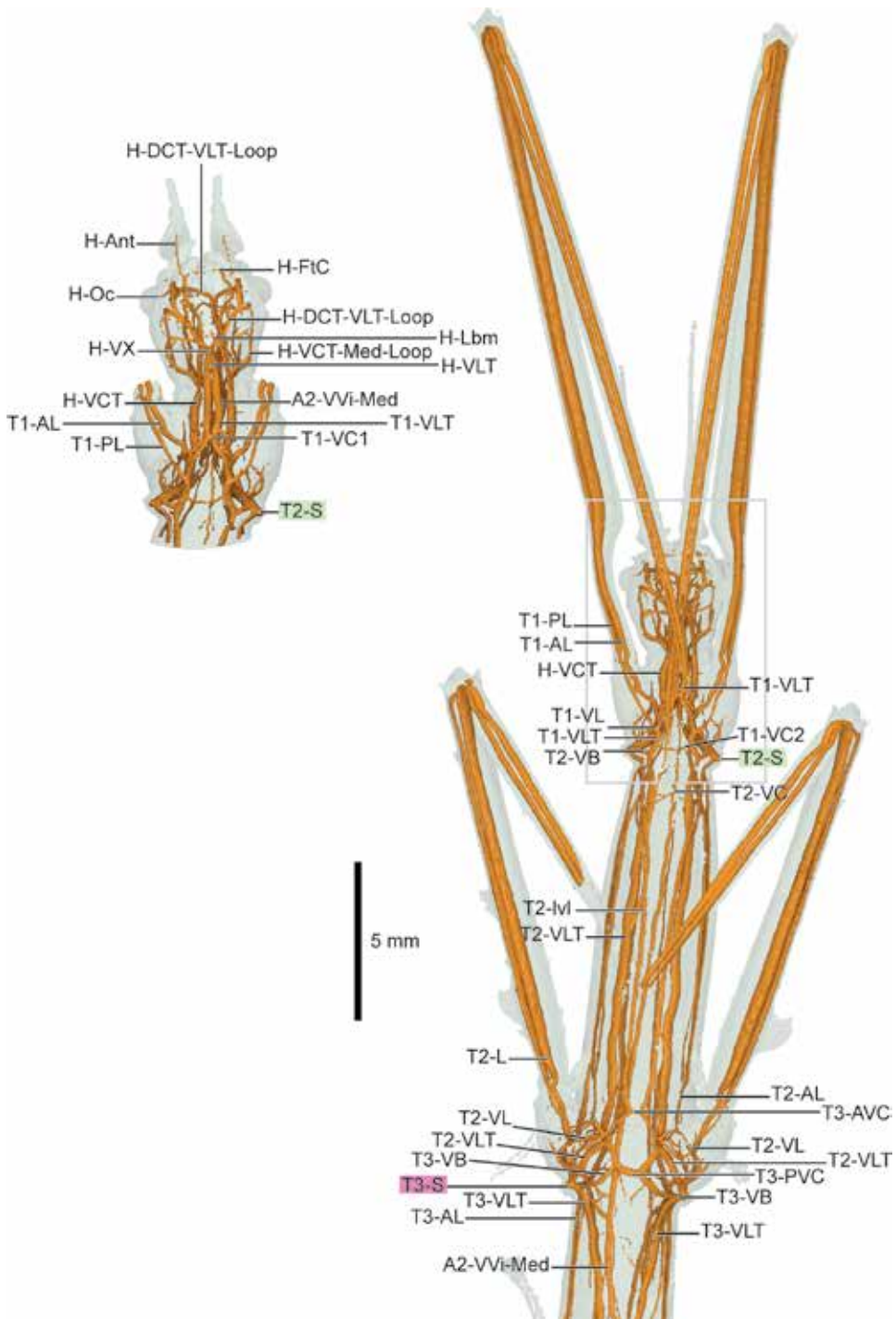


FIGURE 95. *Medauroidea extradentata* (Phasmatoidea: Phasmatidae) anteroventral view.

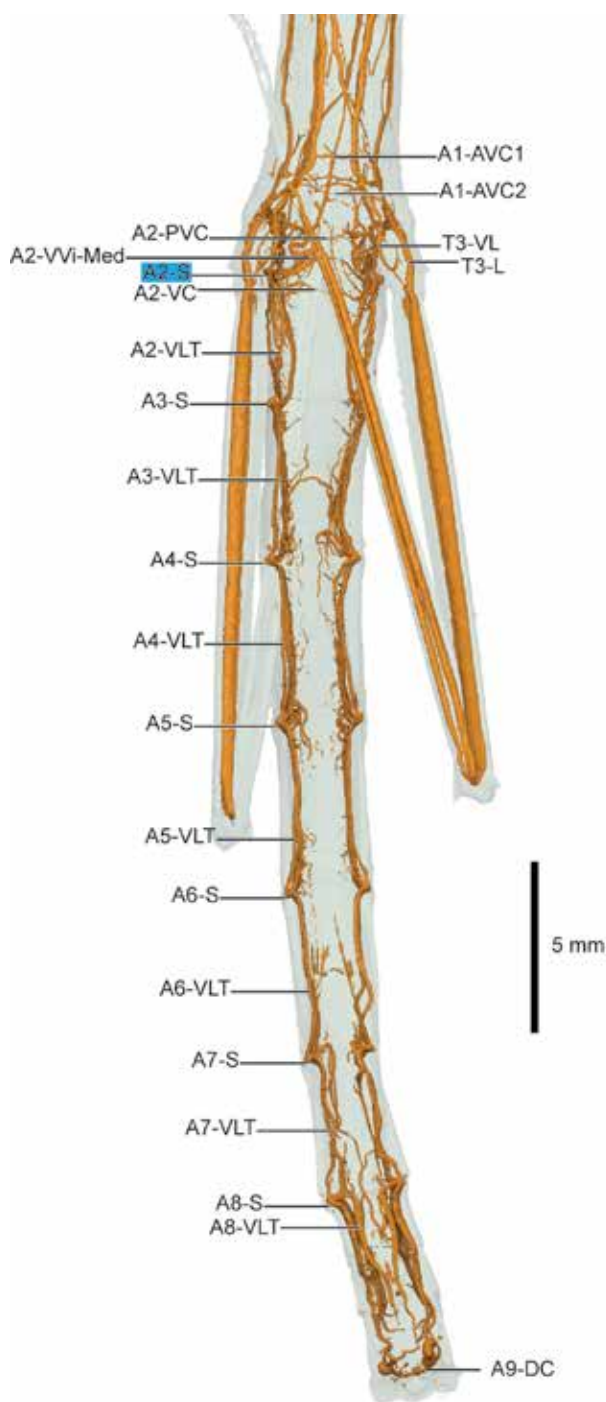


FIGURE 96. *Medauroidea extradentata* (Phasmatodea: Phasmatidae) posteroventral view.

micro-CT scanned in a demonstration of semiautomated segmentation techniques (Lösel et al., 2020). Active tracheal compression in Blattodea was studied via synchrotron imaging by Westneat et al. (2003).

Periplaneta is described here in detail. As with other complex specimens, the other two roaches, *Gromphadorhina* and *Blaptica*, are only briefly described. Readers are directed to the labeled 3D models in the supplementary digital data for further investigation.

FAMILY BLATTIDAE

Periplaneta americana

“American cockroach”

Figures 107 (lateral), 108 (dorsal), 109 (ventral)

Plates 64 (lateral), 65 (dorsal), 66 (ventral)

The *P. americana* specimen here was scanned early in the study, frozen to -20°C rather than -80°C , and at relatively coarse resolution ($38.6\ \mu\text{m}$, specimen approximately 3.5 cm in length). Some fluid infilling likely occurred due to the freezing to -20°C , but sufficient detail is present to assess homology of major tracheae and discern substantial visceral tracheal anatomy. Although not described in detail, *Blaptica* was used as a comparison to infer the likely presence of thoracic tracheae in *Periplaneta*, in particular branching patterns from the mesothoracic spiracle. The thorax features a network of bandlike visceral tracheae along the dorsum and venter, connecting in various locations throughout. This morphology, combined with the long, broad coxae reminiscent of silverfish, obscures internal thoracic tracheal structures in two-dimensional views. The hypognathous position of the head also results in ventral tracheal views of the thorax being obscured; see figure 110 for a ventral view with head and leg tracheae removed.

Periplaneta has large air spaces in the coxae, and jumping has been filmed at high speed by Smith (2022). The scan here is of relatively coarse resolution (38 μm); it is possible muscle tracheae could be observed at higher resolutions or with contrast-enhancing stains such as iodine or phosphotungstic acid (Gignac et al., 2016).

DESCRIPTION: HEAD: H-DCT and H-VCT present, branching into head capsule in highly networked cagelike arrangement. Mouthparts, H-Ant, and H-Oc determined, but networked nature of head morphology, combined with some apparent fluid infilling, makes assessing homology difficult. Readers are directed to 3D models in the supplementary digital data.

THORAX: T2-S with five branches: H-DCT, H-VCT, T2-DB, T2-AWL, and T2-VB. H-DCT and H-VCT both arteriad, curving slightly medially, with H-DCT proceeding along dorsum and H-VCT along venter. T1-AL branching ventrad off H-VCT. T2-DB short, splitting anteriorly into T2-DLT and posteriorly as network of cagelike T1-DVi along pronotum. T2-AWL posteriorly, with T2-W-c-r splitting dorsad and posteriorly; T2-AWL splits into T2-AL extending into midleg and T2-Wbr, partial in this scan but likely present between T2-S and T3-S. T2-VB likewise short, bifurcating into T2-VC directly ventrad and T2-VLT posteriorly. T2-VL branching posteriorly close to T2-S, extending into midcoxa and T2-L; T2-VLT continuing posteriorly to link with T3-S. T3-S with n branches: T2-PWL, T3-DB, T3-AWL, T2-VLT, and T3-VLT. T3-VB not visible but may be very short. T2-PWL anteriorly from T2-S, bifurcating into T2-Wbr anteriorly and curving posteriorly as T2-PL, joining with T2-AL from ante-

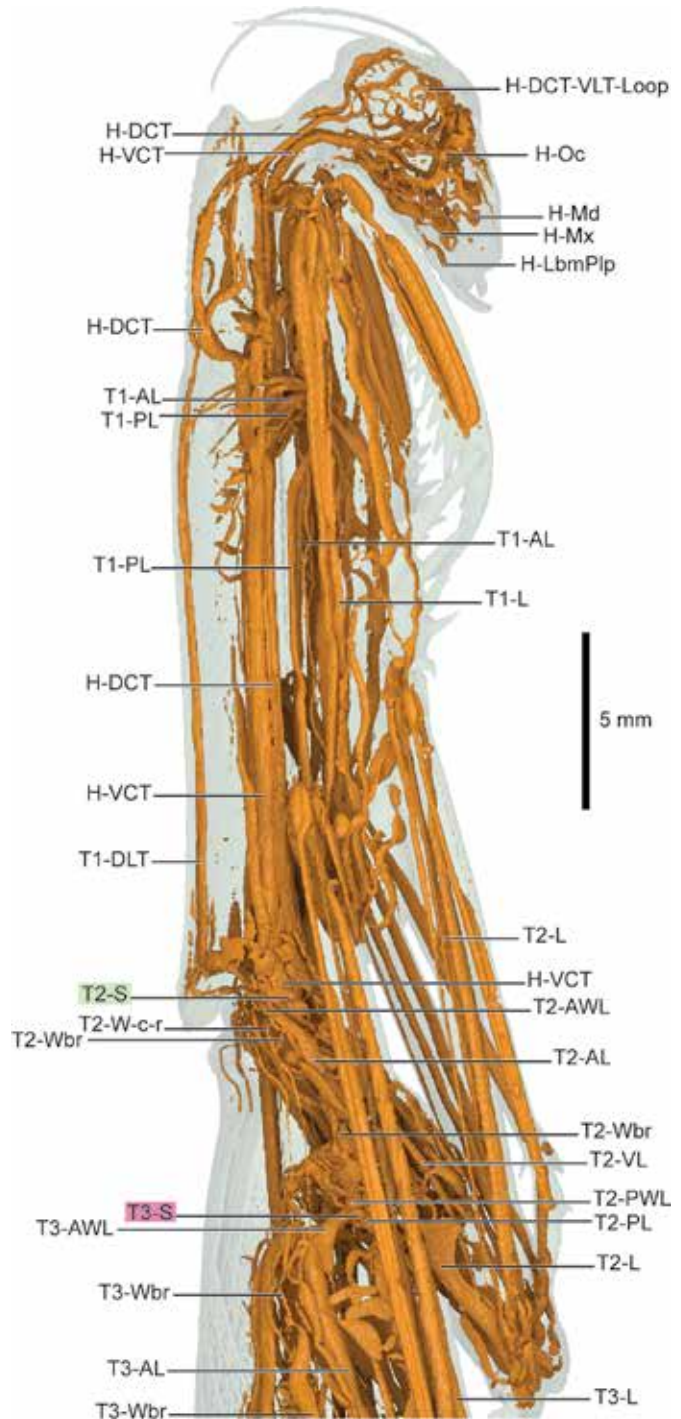


FIGURE 97. *Tenodera sinensis* (Mantoda: Mantidae) anterolateral view.

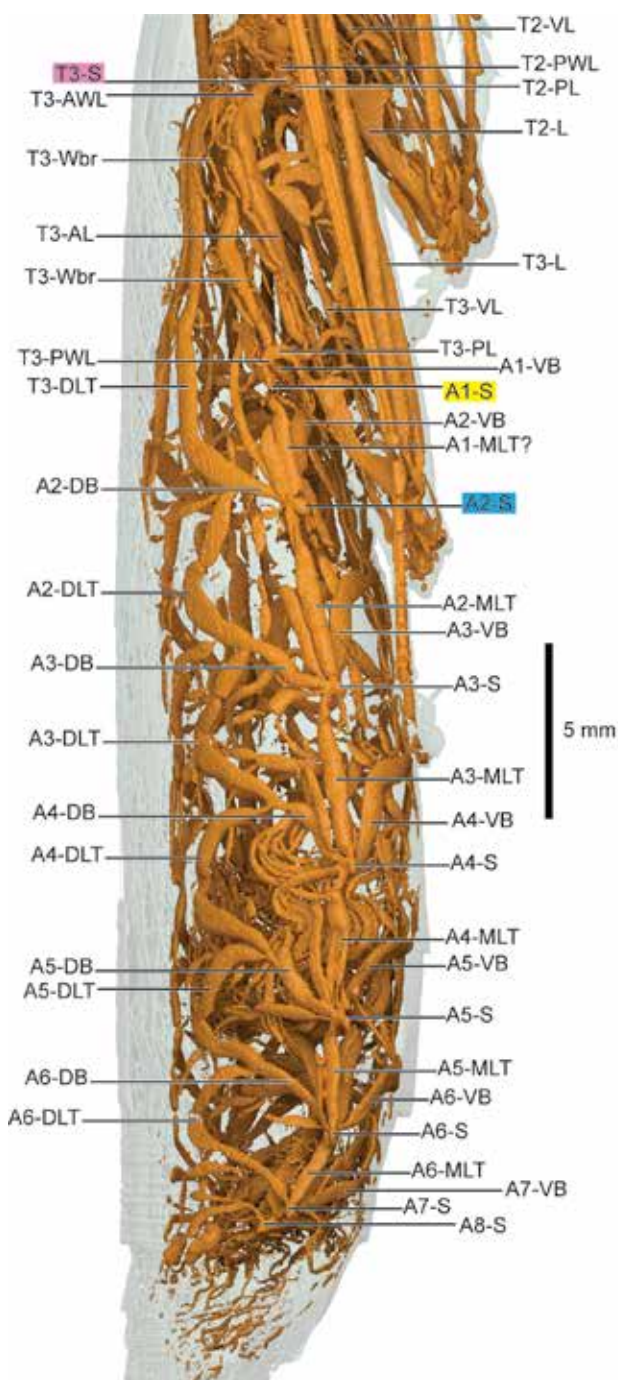


FIGURE 98. *Tenodera sinensis* (Mantoda: Mantidae) postero-lateral view.

riad and extending into mid-leg. T3-DB mediad and slightly ventrad, curving posteriorly before extending along dorsum to join with small T2-DLT anteriorad and larger T3-DLT posteriorad; T3-DC visible at this junction. T3-AWL posteriorad, with T3-W-c-r splitting dorsally; T3-AWL continues as T3-AL posteriorly and ventrad into hind leg. T2-VLT mediad, connecting anteriorly to T2-S. T3-VLT mediad and slightly posterior, connecting to A1-S via A1-VB.

ABDOMEN: Abdomen featuring numerous visceral tracheae throughout. A1..8-S present. A1-S modified from A2..8-S, with three branches: T3-PWL, A1-DB, A1-VB. T3-PWL anteriorad and slightly mediad, curving posteriorly and joining with T3-AL and extending into hind leg; T3-Wbr branching from T3-PWL at apex of curve and extending anteriorad to T3-S. A1-DB runs mediad, linking with T3-DLT anteriorad and A1-DLT posteriorad; A1-DB partial in this scan, likely due to fluid infilling (A1-DB present in *B. dubia* and *G. portentosa*). A1-VB mediad and slightly ventrad, extending along venter to A1-VC, connecting to A1-VLT posteriorad; A1-MLT posteriorad from A1-VB. *An*-MLT runs straight, extending posteriorad and much smaller than thoracic T3-VLT. A2..7-S branching all similar: *An*-DB, *An*-VB, and *An*-MLT. *An*-DB beginning small, expanding into bandlike trachea and intersecting with *An*-DLT sections anteriorly and posteriorly in Y-shaped junctions; *An*-DC absent. *An*-MLT wide and almost bulblike, connecting abdominal spiracles along lateral margin of body wall. *An*-VB much smaller and apparently fluid infilled in several spiracles, extending along venter to join with straight *An*-VLT anteriorad and posteriorad in T-shaped junction. A4..8-S with numerous visceral tracheae; readers are encouraged to view 3D models in supplementary digital data.

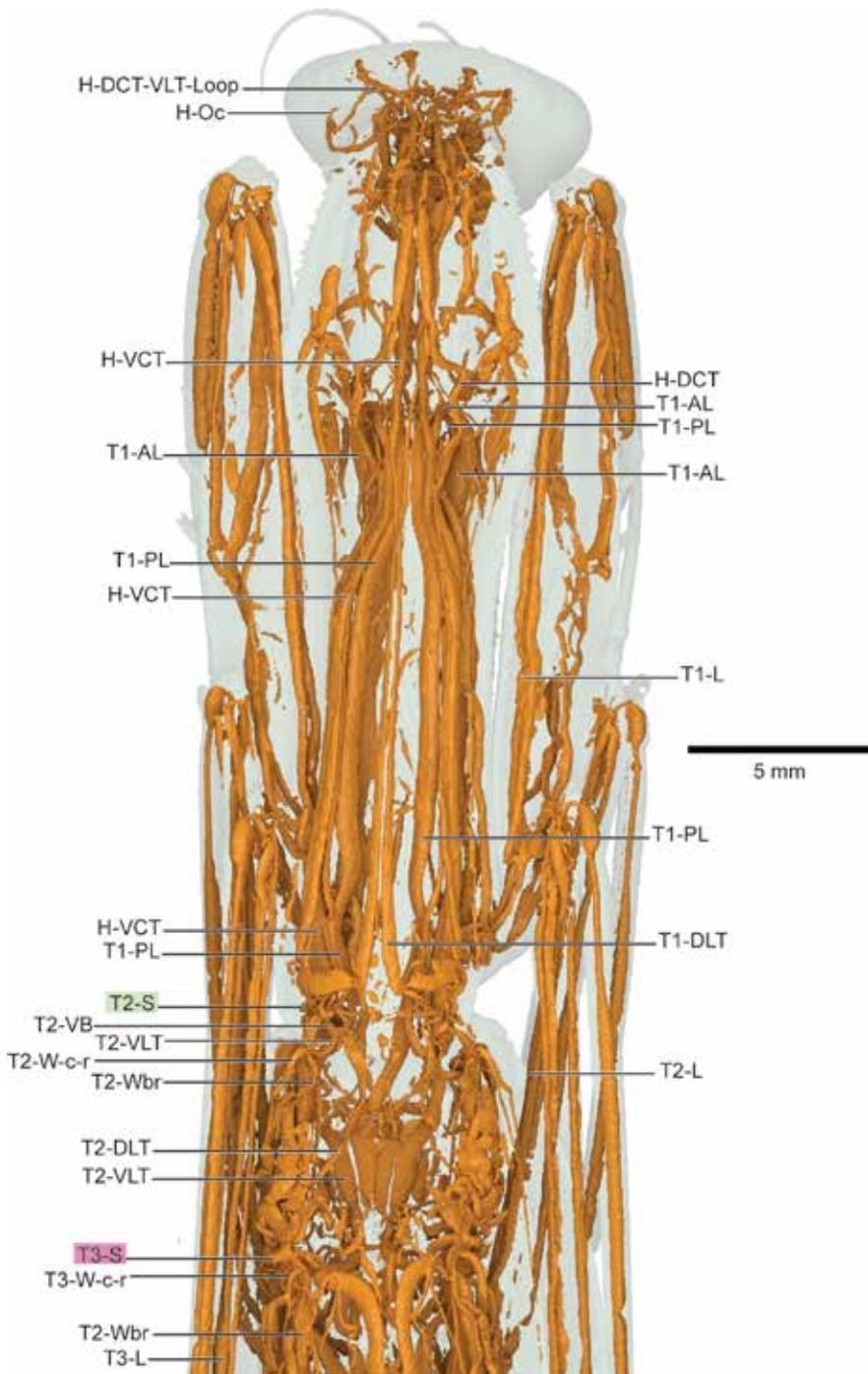


FIGURE 99. *Tenodera sinensis* (Mantoda: Mantidae) anterodorsal view.

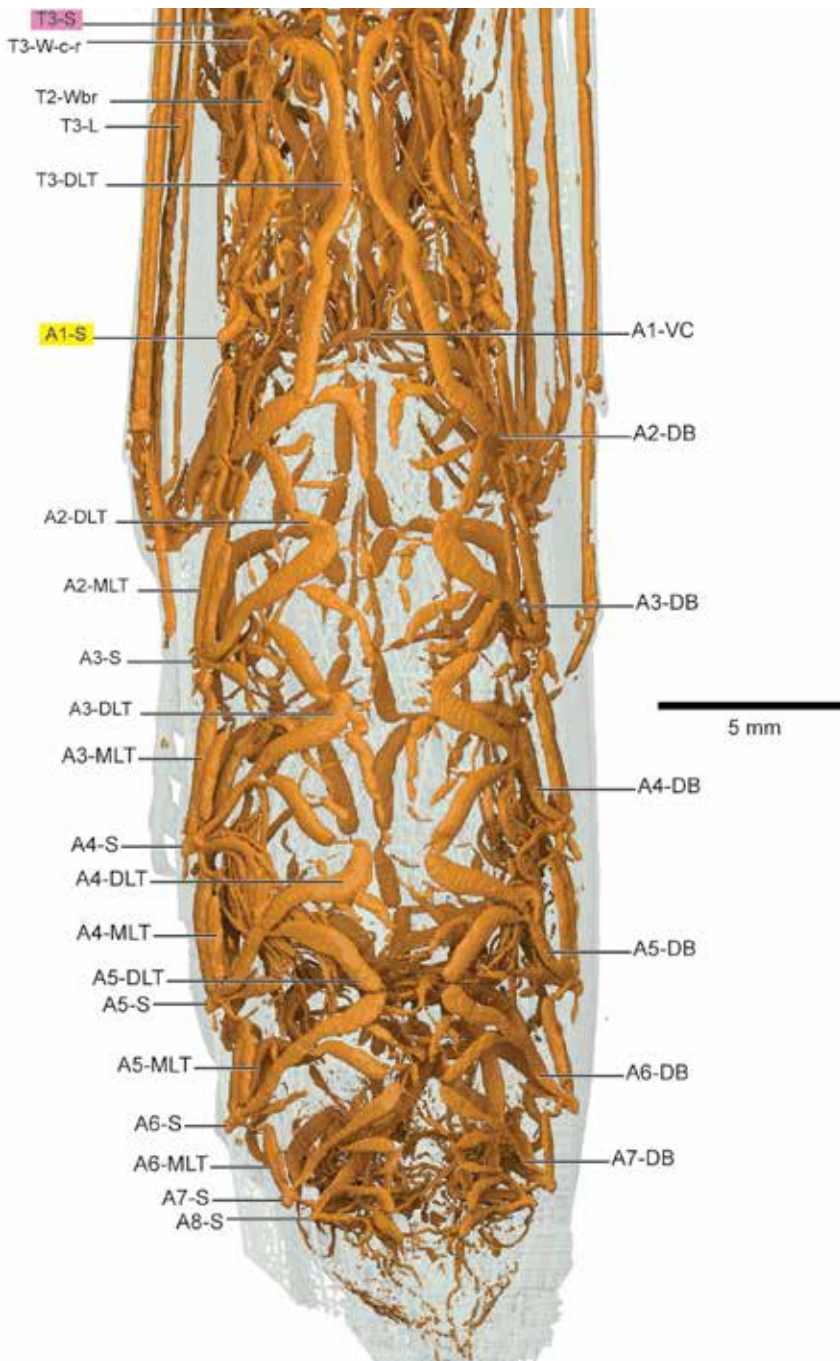


FIGURE 100. *Tenodera sinensis* (Mantoda: Mantidae) posterodorsal view.

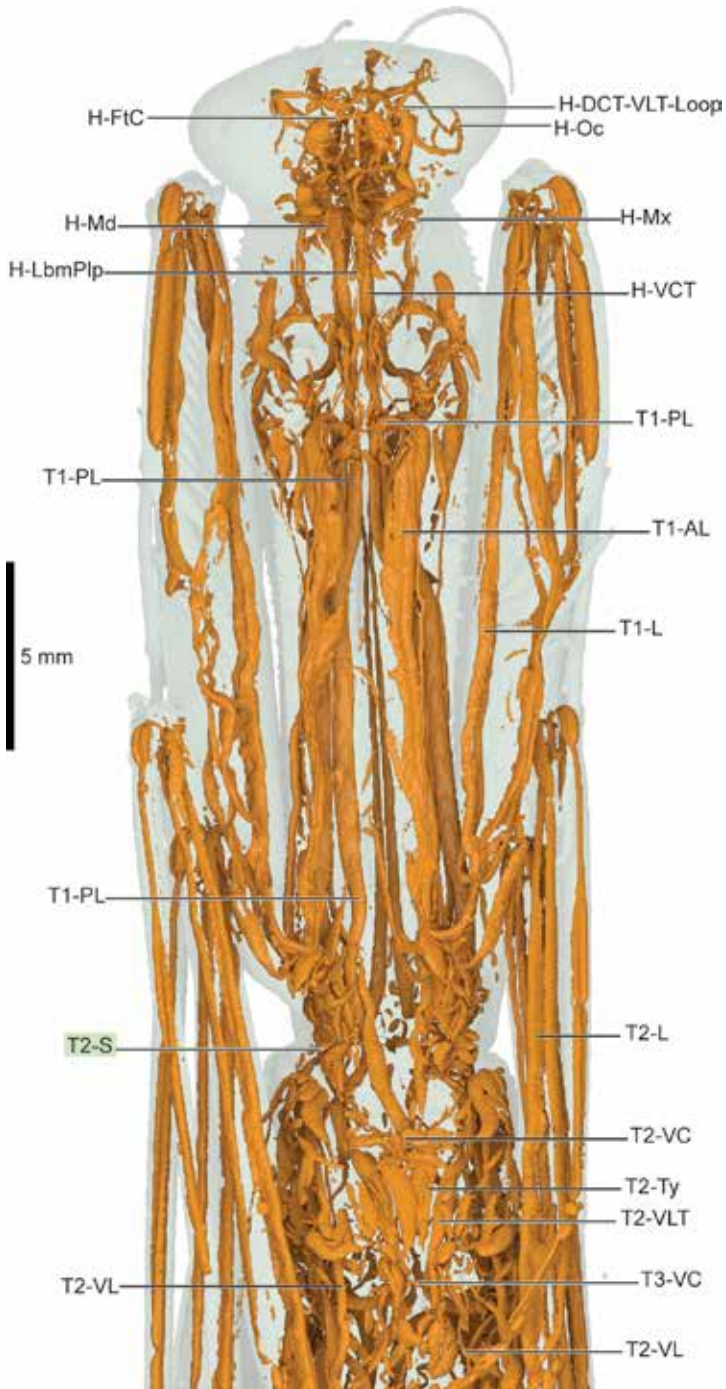


FIGURE 101. *Tenodera sinensis* (Mantoda: Mantidae) anteroventral view.

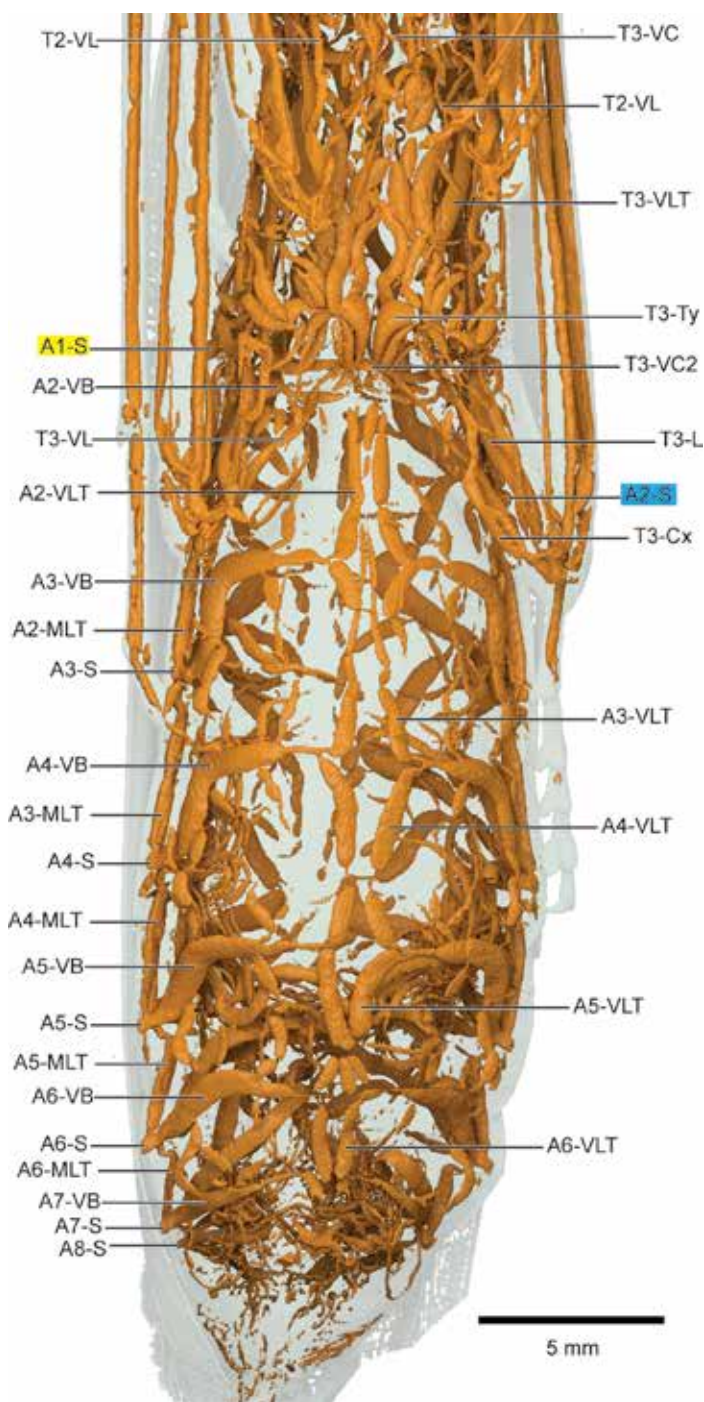


FIGURE 102. *Tenoderina sinensis* (Mantoda: Mantidae) posteroventral view.

FAMILY BLABERIDAE

Blaptica dubia

“Argentinian wood roach”

Figures 111 (lateral), 112 (dorsal), 113 (ventral)

Plates 67 (lateral), 68 (dorsal), 69 (ventral)

The tracheal architecture of *B. dubia* features wide, bandlike tracheae and numerous visceral branches throughout the body; preliminary results indicate that tracheae may comprise nearly 12% of the volume of the insect (Herhold et al., in prep.). Spiracles and a handful of major tracheae are labeled in the figures and plates; readers are encouraged to view the 3D models provided in the supplementary digital data for further investigation.

Gromphadorhina portentosa

“Madagascar hissing cockroach”

Figures 114 (lateral), 115 (dorsal), 116 (ventral)

Plates 70 (lateral), 71 (dorsal), 72 (ventral)

Easily the most popular cockroach (as far as cockroach popularity goes), the physiology of the hissing behavior of *G. portentosa* was investigated by Nelson and colleagues (Nelson, 1979; Nelson and Fraser, 1980), with the notable finding that the fourth spiracle (A2-S) is the source of the hiss. Heinrich et al. (2013) documented unidirectional airflow in *G. portentosa* resulting from spiracular valve control. As seen in the plates, the tracheal architecture of *Gromphadorhina* is

remarkably complex, so only spiracles and major tracheae are labeled here. As is common in reared *Gromphadorhina* colonies, the individual scanned was infested with mites (see fig. 117), likely *Gromphadorholaelaps schaeferi*, found to be possibly beneficial by Yoder et al. (2012).

INFRAORDER ISOPTERA

Although the respiratory physiology of termites (especially as it relates to their digestive system) has been studied for decades, micro-CT scans of respiratory architectures have been absent. The tracheal scans of the reproductive caste *Reticulitermes flavipes* and soldier caste *Zootermopsis angusticollis* shown here detail the remarkable intricacy of tracheal branches, especially in the abdomen, well known for its adaptations for digesting cellulose. Although both specimens were scanned at approximately 5 μm resolution, the worker *Reticulitermes* possesses notably smaller tracheae than the soldier *Zootermopsis*. Although the two specimens feature many similarities, notably a T1-DLT prothoracic “loop,” the differences are sufficient to describe both in detail.

Wing-leg branching patterns, referred to here as Chapman’s Triangle (see Discussion section), are evident in both termites, albeit with some minor modifications (Chapman, 1918). In *Zootermopsis*, T2-AWL branches from T2-DB rather than directly from T2-S (as in Dermaptera and others), T3-AWL is off T3-S. In *Reticulitermes*, T2-VL branches from T2-VB, rather than T2-VLT, and T3-VL branches off T3-VB. (These could be Tn-Cx and not Tn-VL.)

FAMILY ARCHOTERMOPSIDAE

Zootermopsis angusticollis Soldier caste

“Dampwood termite”

Figures 118 (lateral), 119 (dorsal), 120 (ventral)

Plates 73 (lateral), 74 (dorsal), 75 (ventral)

DESCRIPTION: HEAD: Major tracheae indicated in plates, due to networked nature of head

tracheae, readers are referred to 3D models in supplemental digital data (see “Availability of Digital Data,” above). H-Oc notably absent, as is expected in termite soldiers. H-DCT with Y-shaped branch meeting in midline as H-DCMedB, which loops posteriad to rejoin H-DCT near origin of Y-shaped branch. Two branches at anterior end of H-DCMedB-Loop: H-Ant anterior and H-DVB directly ventrad, linking with H-VCT on each side. Close to origin of Y-split, H-DV-Loop extends laterally and anterior in wide arc, following head capsule lateral wall, looping medially and posteriad near base of antenna, connecting with anterior end of H-VCT as H-DV-Loop; additional H-Ant extends from anterior end of H-DV-Loop. H-VCT runs directly anterior along floor of head capsule, with large H-DVB connecting to H-DCT and H-DCMedB-Loop. Remainder of H-VCT anterior toward mouthparts, linking with H-DV-Loop, and branches extending to H-Md, H-MxPlp, and H-Lbm along this loop. H-VLT present, extending into labium. H-VLT asymmetric in soldier caste, see figure 121 for ventral view of worker caste showing symmetric H-VLT branches.

THORAX: T2-S with four branches: H-DCT, H-VCT, T2-DB, and T2-VB. H-DCT mediad, curving anterior toward large head capsule; short T1-DLT from T2-DB connecting before curve. H-VCT like H-DCT, with ventrad T1-AL near curve toward anterior. T2-DB short, with T2-AWL branch running posteriad close to T2-S; T2-DB continues mediad with Y-shaped bifurcation of short T1-DLT anterior toward H-DCT and T2-DLT posteriad toward T3-S. T2-AWL arcing posteriad, splitting in to T2-AL and T2-Wbr at apex of arc; T2-Wbr with small T2-W-c-r and T2-W-cu-a, connecting with T2-PWL posteriorly; T2-AL posteriad and ventral, joining T2-PL and extending into midleg. T2-VB runs directly mediad, bifurcating into T2-VC1 mediad and T2-VLT arcing ventrally and posteriad along sternite. T2-VC1, the first of two mesothoracic ventral commissures, proceeding mediad with T1-PL branch directly ventrad



FIGURE 103. *Tenodera* air spaces, likely air-filled alimentary canal in gray, in A. dorsal, B. lateral, and C. ventral views.

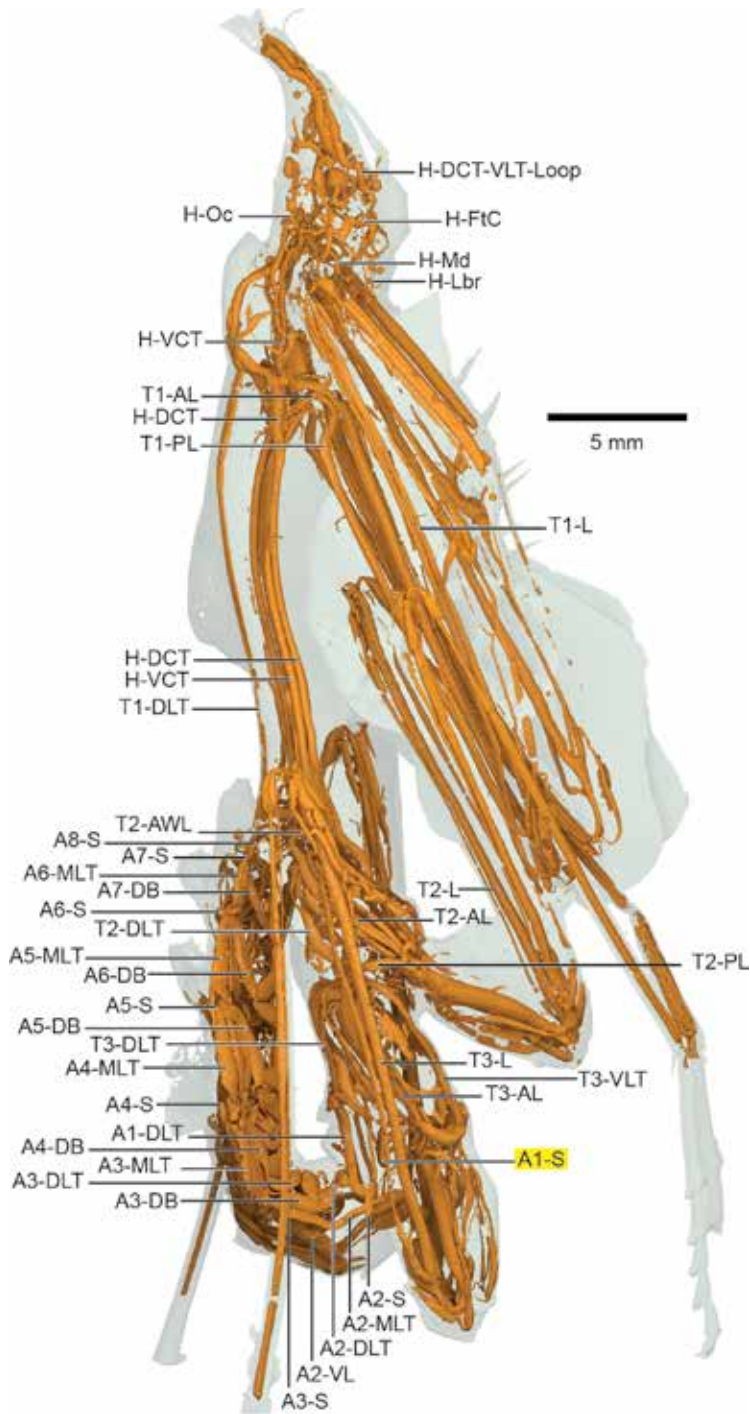


FIGURE 104. *Idolomantis diabolica* (Mantodea: Empusidae) lateral view.

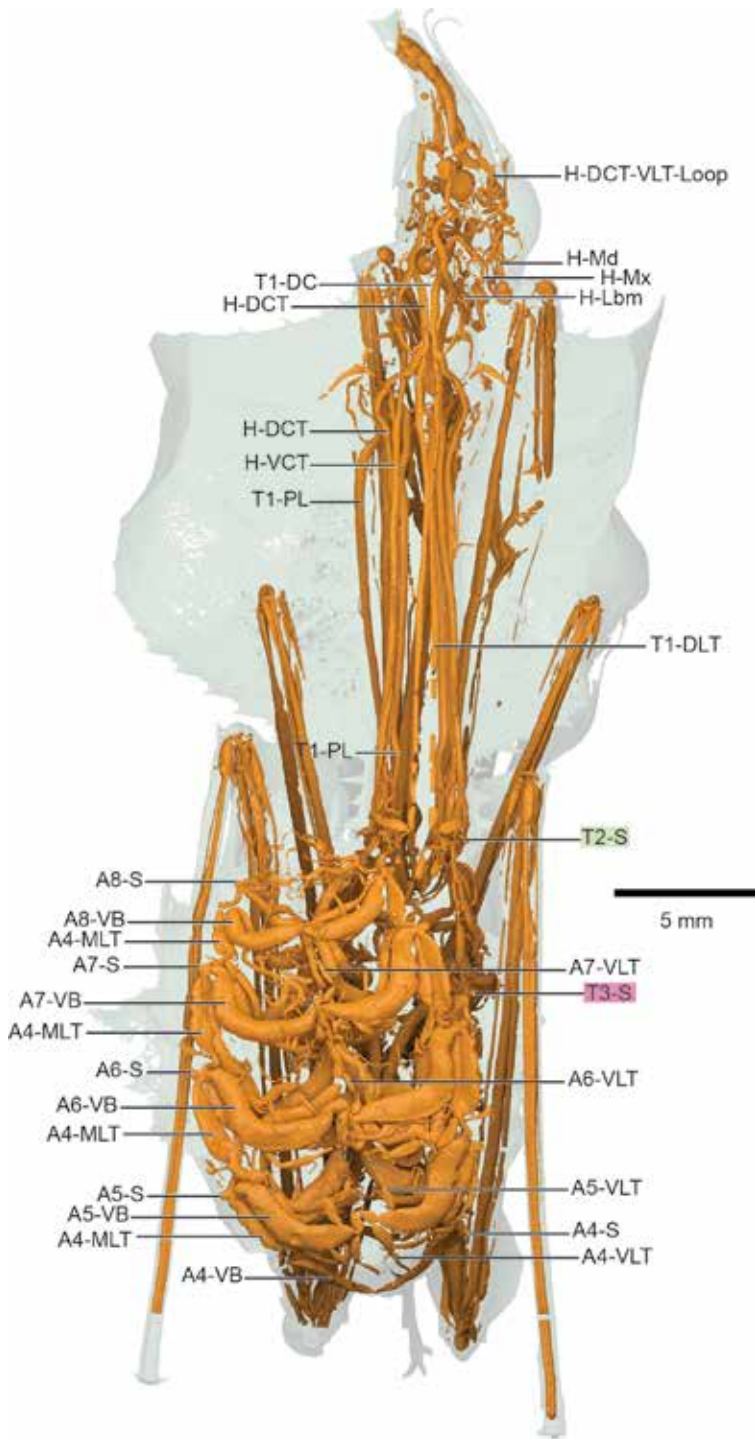


FIGURE 105. *Idolomantis diabolica* (Mantodea: Empusidae) dorsal view.

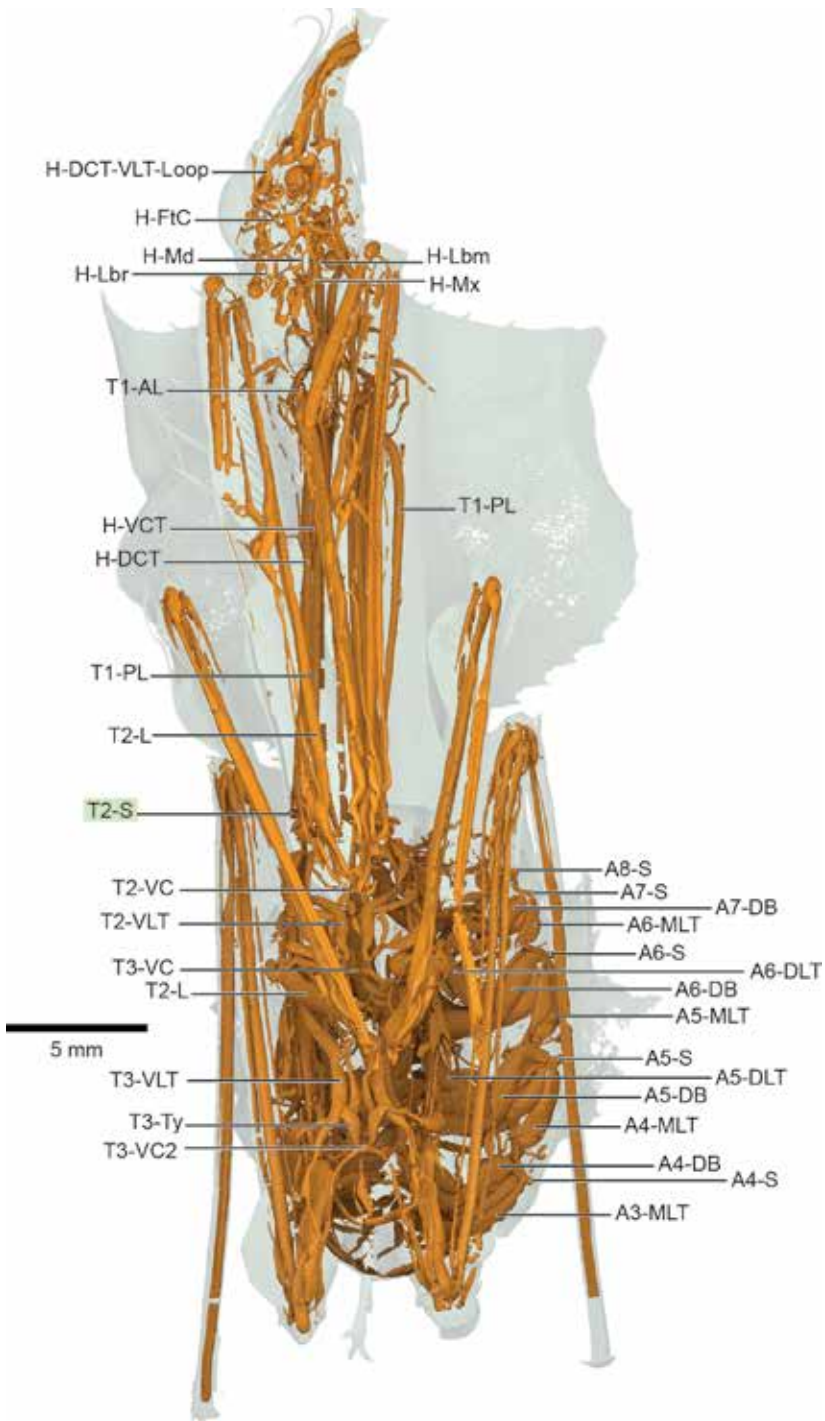


FIGURE 106. *Idolomantis diabolica* (Mantodea: Empusidae) ventral view.

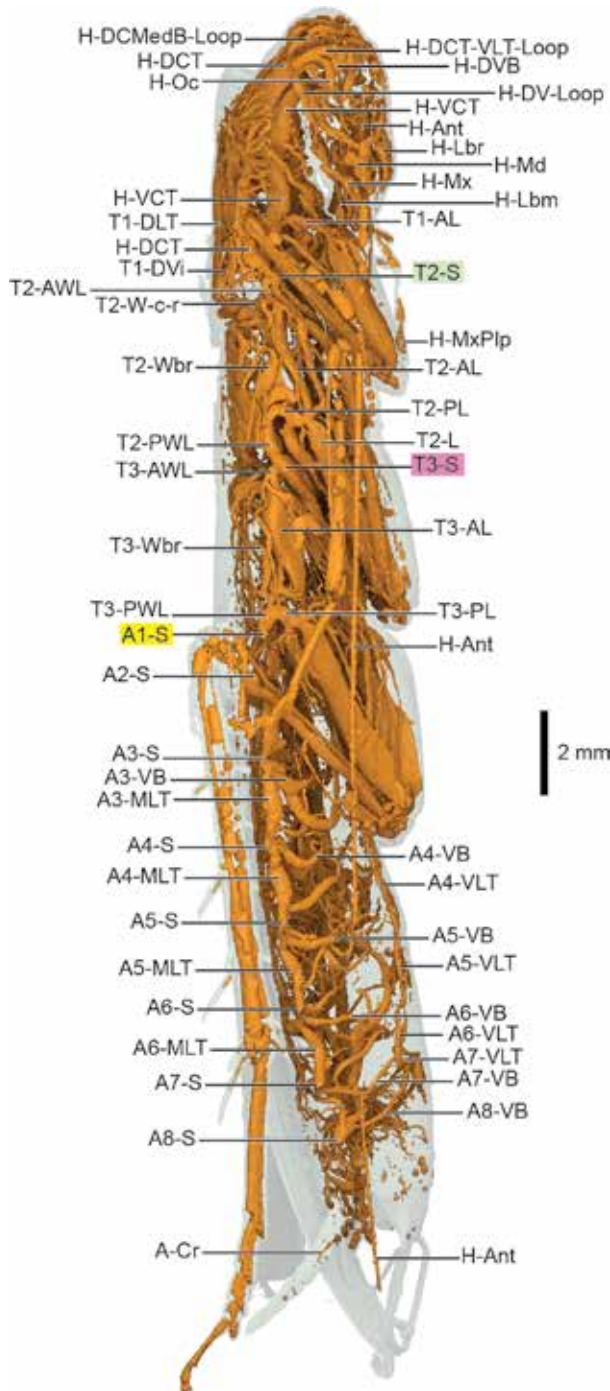


FIGURE 107. *Periplaneta americana* (Blattodea: Blattidae) lateral view.

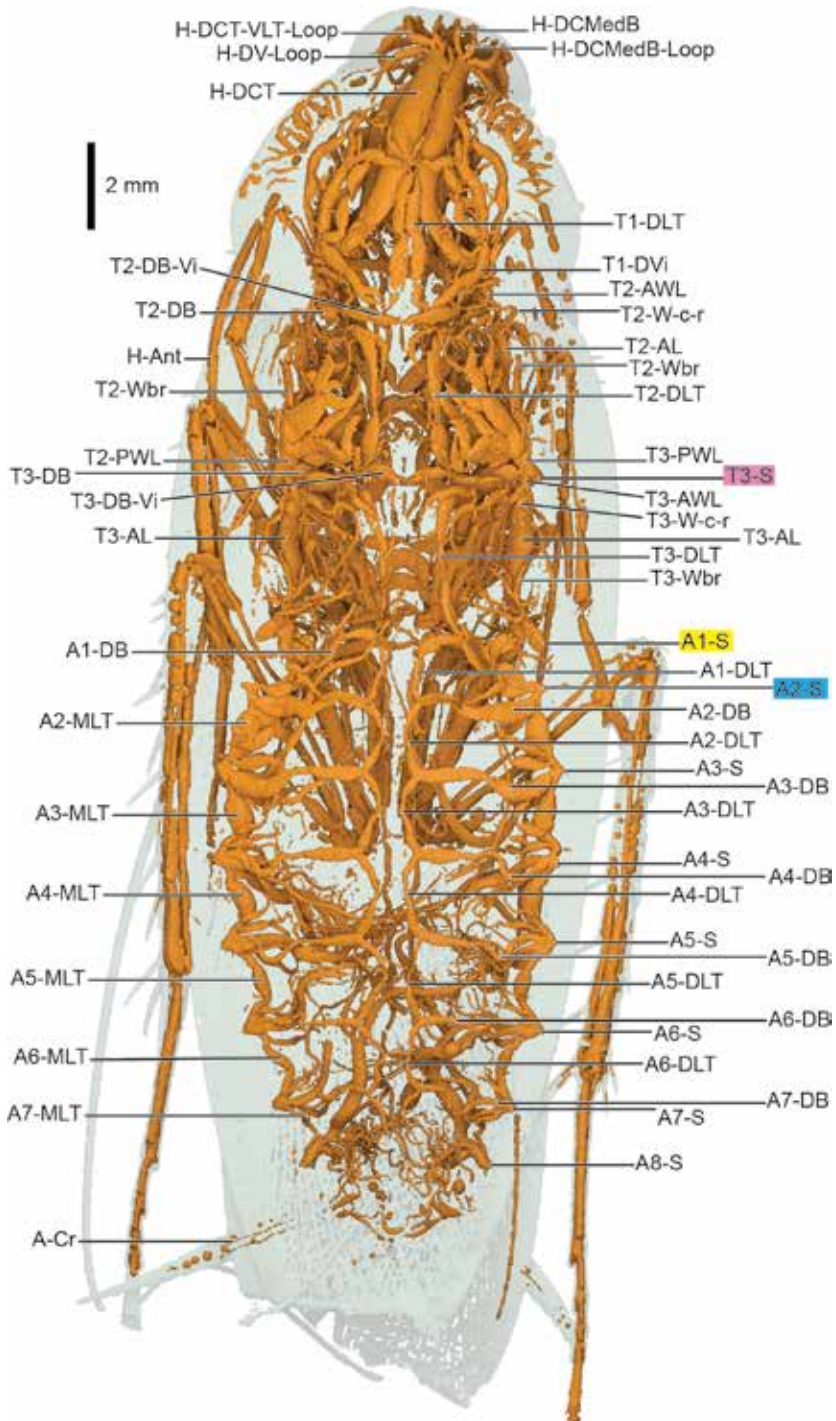


FIGURE 108. *Periplaneta americana* (Blattodea: Blattidae) dorsal view.

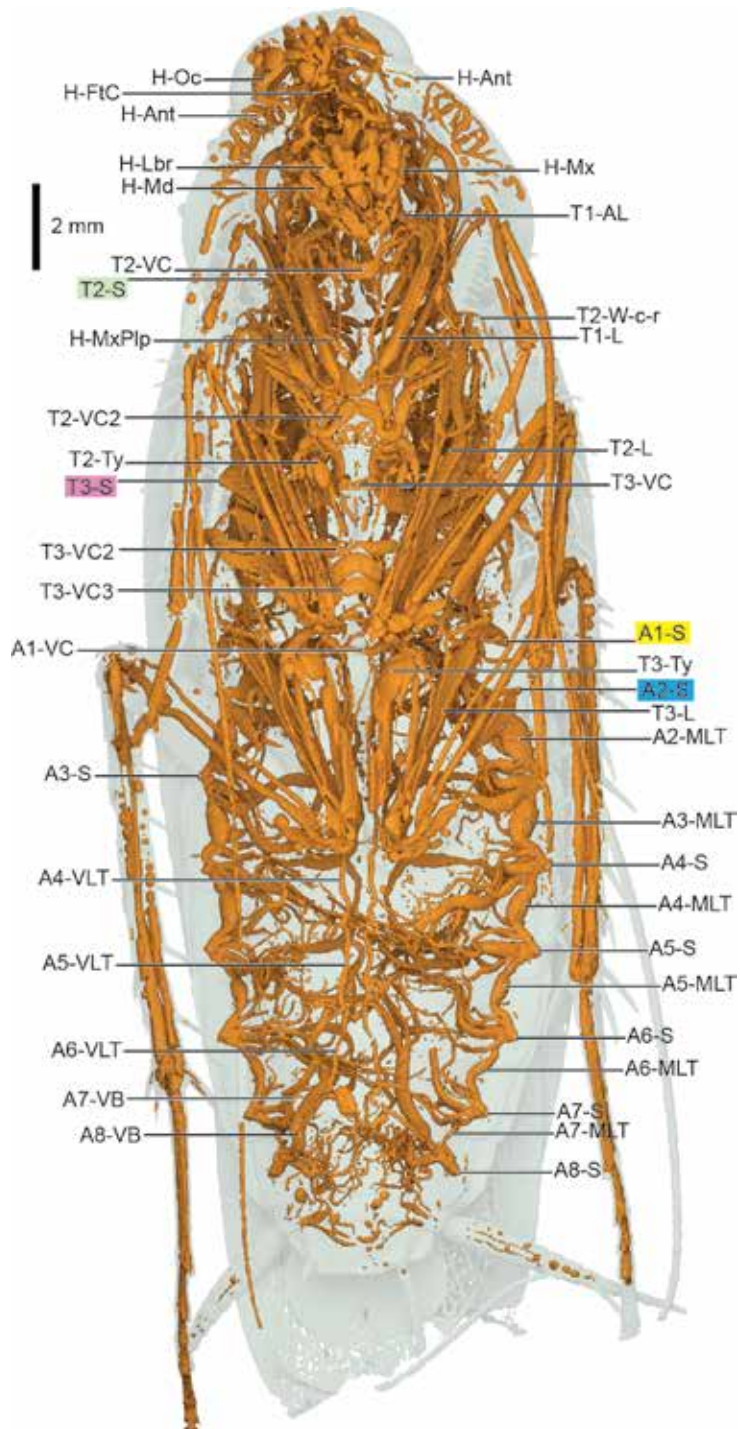


FIGURE 109. *Periplaneta americana* (Blattodea: Blattidae) ventral view.

and smaller connection anteriad to T1-VX. T1-VX with H-VCT extending anteriad into head; single branch on specimen left side but likely present on right—see T2-VC2 branching mediad from T2-VLT anteriad from T2-VLT's curve dorsad toward T3-S; T2-VLT with additional T2-Cx branch, larger on right side than on left. T3-S with four branches: T2-PWL, T3-DB, T3-AWL, and T3-VB. T2-PWL from anterior, connecting T2-PL and T2-Wbr from T2-S. T3-DB mediad, joining with T2-DLT and T3-DLT in flat Y-shaped junction. T3-AWL mediad briefly, arcing posteriad and dorsally, splitting into T3-AL ventrad into hindleg and T3-Wbr posteriad, joining with A1-S via T3-PWL. T3-Wbr with small T3-W-c-r anterior and T3-W-cu-a posterior. T3-VB runs directly ventrad, with T3-VLT splitting posteriorly just ventrad of T3-S. T3-VB continuing ventrad, with T2-VL branch ventrad and posteriad, extending into midleg; remaining T3-VB arcing medially to form T3-VC1; T2-VLT joining with T3-VB near this arc. T3-VLT ventrad, arcing posterior along sternite before continuing anteriad toward A1-S, with T3-VC2 mediad near apex of this arc. T2-VLT and T3-VLT both with two ventral commissures: posterior T2-VC2 and anterior T3-VC1 along same section of T2-VLT; posterior T3-VC2 and A1-VC both along same section of T3-VLT.

ABDOMEN: A1..8-S present. Short *An-SB* possible on several segments. A1-S with three branches: T3-PWL, A1-DB, and A1-VB; remaining A2..8-S with just *An-DB* and *An-VB* branches. For A1-S, T3-PWL from anterior, completing T3-Wbr link from T3-S. *An-DB* runs mediad and slightly dorsad, meeting *An-DLT* branches from anterior and posterior in Y-shaped junction. Large *An-DB-Vi* typical for all segments, often asymmetric and extending into various abdominal regions and occasionally spanning several segments. *An-DC* absent. *An-VB* runs ventrad, following body wall, continuing to form *An-VC*; A8-VB split into A8-VC1 anterior and A8-VC2 posterior. *An-VB* with *An-MLT* branching ventrad from *An-S*, directly posteriad toward proceeding posterior

segment, linking with *An-VB*. A5..8-MLT slightly modified, connecting nearly directly with subsequent *An-S*. As with *An-DB*, *An-VB-Vi* extend throughout abdomen; A7-VB-Vi and A8-VB-Vi extend mediad, crossing middle of body and extending anteriad past A4-S.

FAMILY RHINOTERMITIDAE

Reticulitermes flavipes

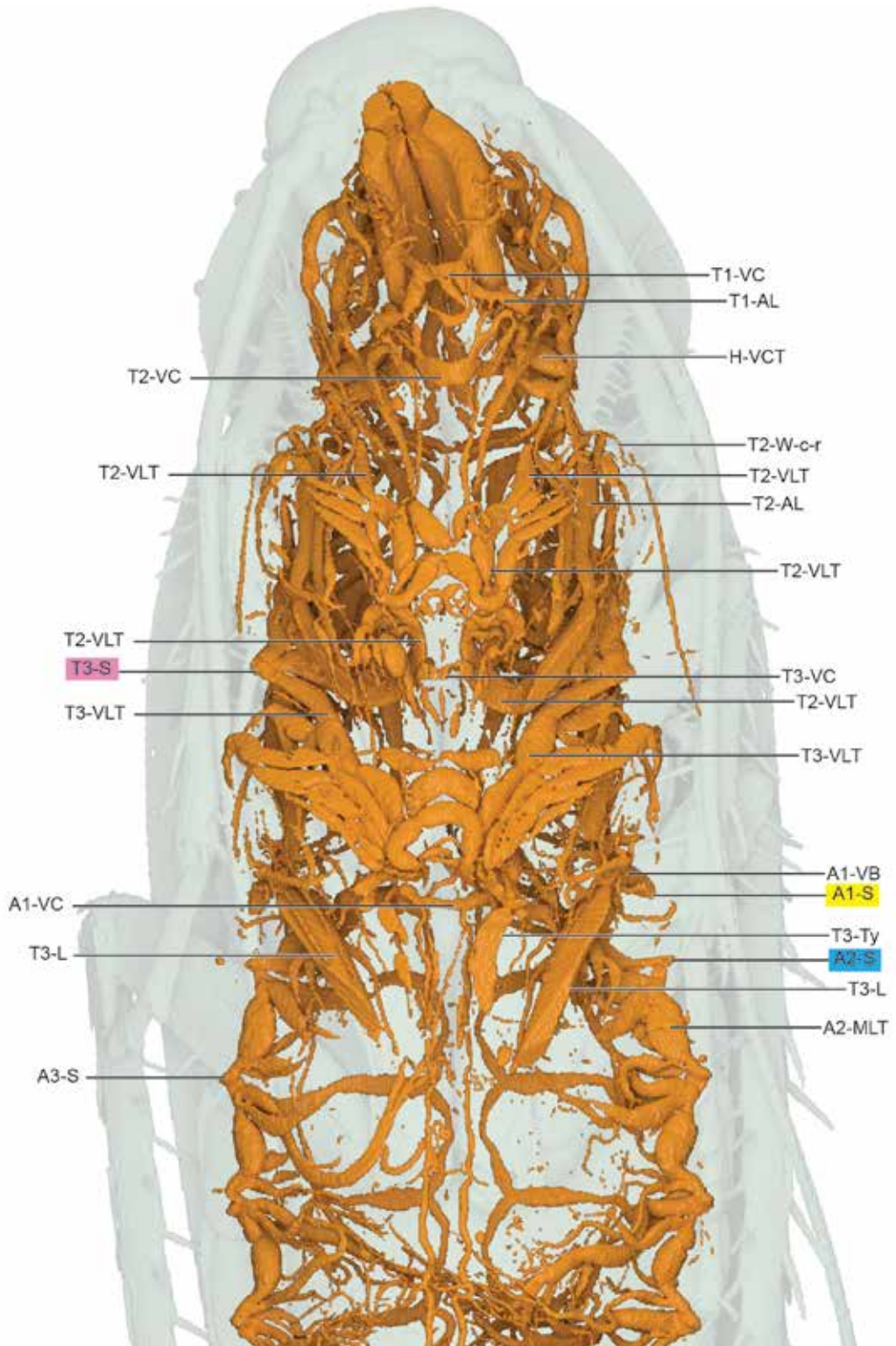
“Eastern subterranean termite”

Figures 122 (lateral), 123 (dorsal, ventral)

Plates 76 (lateral), 77 (dorsal), 78 (ventral)

DESCRIPTION: HEAD: H-Oc absent, as is typical in termite workers and soldiers. H-DCT runs slightly dorsad anterior of cervix, with visceral branches dorsad and lateral. H-DCT arcing anteriad, with H-Ant branching laterally where H-DCT meets H-DVB join with H-VCT. H-VCT running directly anteriad, with split into H-Md-Mx branch, H-Lbm, and third branch that splits into H-DVB dorsad, H-Ft anteriad, and H-VC medially. H-Md-Mx anteriad, with H-Mx dividing ventrad. H-Md runs anteriad with short branch anteriad as second H-Ant.

THORAX: T2-S with four branches: H-DCT, H-VCT, T2-DB, and T2-VB. H-DCT runs mediad, curving anteriad toward head capsule. H-VCT curving similar to H-DCT, but with single T1-L directly ventrad; T1-AL and T2-PL absent, but T1-VC present, branching from T1-L and joining medially. T2-DB short, with T2-AWL splitting dorsally and posteriad; T2-DLT continues medially, splitting into Y-shaped junction with T2-DLT posteriad and a pronounced, looping T1-DLT joining with H-DCT. T2-AWL arcing dorsad, bifurcating into T2-Wbr and T2-AL at apex of curve. T2-Wbr runs posteriad, linking with T3-S via T2-PWL; T2-AL runs ventrad, proceeding into T2-L. T2-VB short and running ventrad, splitting into anterior visceral branch and remaining T2-VB, running ventrad and toward posterior as T2-VLT. T2-Wbr with small T2-W-c-r and T2-W-cu-a present. T2-VC pres-



ent, extending off T2-VLT. T3-S with three branches: T2-PWL, T3-DB, and T3-VB. T2-PWL anteriad from T3-S, splitting into T2-Wbr toward T2-S and T2-PL running ventrad, joining with T2-AL and proceeding into midleg as T2-L. T3-DB runs directly mediad, with T3-AWL branch arcing posteriorly close to T3-S; remaining T3-DB runs further mediad, joining with T2-DLT from anterior and proceeding as T3-DLT toward posterior. T3-AWL arcing posteriorly, splitting into dorsal T3-Wbr and ventrad T3-AL. T3-W-c-r and T3-W-cu-a not visible off T3-Wbr but likely present and very small. T3-VB runs ventrad with anterior branch leading to T2-VL. T2-VB continuing ventrad, joining with T2-DLT anterior and T3-DLT posterior in Y-shaped junction. T3-VC present, branching medially off T3-DLT.

ABDOMEN: A1..8-S present. Short *An-SB* possible on several segments. Nearly all *An-DB* and *An-VB* with visceral branches that occasionally span several segments. A1-S with three branches: T3-PWL, A1-DB, and A1-VB. T3-PWL joining medially from anterior, completing link between T3-S via T3-Wbr. A1-DB runs mediad and slightly ventrad, with A1-DB-Vi branching ventrally while A1-DB, smaller, continuing medially to join T3-DLT from anterior and A1-DLT to posterior in Y-shaped join. A1-VB runs ventrad, splitting off A1-VB-Vi with A1-VB continuing ventrad with T3-VL lateral before A1-VB splits to join T3-VLT from anterior and A1-VLT to posterior; A1-VC present, branching off A1-VB. Remaining A2..8-S with just *An-DB* and *An-VB* branches. *An-DB* runs mediad and slightly ventrad, meeting *An-DLT* branches from anterior and posterior in Y-shaped junction. *An-DLT* typically small and sinuous. Large *An-DB-Vi* typical for all segments, often asymmetric and extending into various abdominal regions and occasionally spanning several segments. *An-DC* absent. *An-VB* runs ventrad, following body wall, con-

tinuing to form *An-VC*. Large *An-VB-Vi* also typical for all segments; directional notation in 3D supplemental models for visceral tracheae is to denote relative directions for clarity and not an assessment of homology. *An-VB* with small *An-MLT* branching ventrad from *An-S*, directly posteriad toward proceeding posterior segment, linking with *An-VB*. As with *An-DLT*, *An-MLT* often small and hard to distinguish, occasionally not visible on one side of the specimen but likely present.

DISCUSSION

Assessing homologies within a complex adaptation such as the insect respiratory system is best undertaken with a broad application of the comparative method, as done here. Through the examination of representatives from 13 orders, 26 families, and 29 genera, we have generated a scaffold of the tracheal architecture of insects that should serve as a guide for future endeavors.

Results sections provided above discussed patterns observed within individual orders; the following discussions highlight homologies, patterns, and features observed in a broader context, often spanning several orders.

PHYLOGENETIC PATTERNS

One would not attempt to reconstruct the phylogeny of insects based on a handful of morphological characters from the respiratory system, but mapping traits onto an established phylogeny can reveal some interesting patterns, shed some light on contentious issues, and possibly even test long-held conclusions. Based on the phylogeny from Misof et al. (2014), figure 124 maps tracheal morphology characters to be discussed here in a phylogenetic context. Refer to figure 124 for character numbers in the discussion below, and table 5 for a description of character states.

←
FIGURE 110. *Periplaneta* ventral view, head and leg tracheae removed.

TABLE 5

Character States

Letters a–e correspond to character state variations in figure 124.

Number	Description	States
1.1	Longitudinal connections between spiracles (DLT)	
1.2	VLT present	a = Tn-VLT present b = An-VLT present
1.3	MLT present	
2	Alimentary canal of adult coopted as air sac	For Embioptera, male only
3	Long, linear trunk running length of body (from T2-S)	
4	Extensive bush of tracheae from T2-FM and T3-FM, supplying flight muscles	
5	Dorsal-ventral connection between H-DCT and H-VCT in head	
6	Sausagelike tracheae in abdomen. Various forms and positions.	a = enlarged extensions off DLT b = DB enlarged c = dual, enlarged DB d = DLT enlarged e = VB enlarged
7	Wing bridge Wbr.	a = WBr present b = AWba/PWba present c = AWba only, PWba absent
8	AWL branching pattern	a = T2,3-AWL off T2,3-S b = T2,3-AWL off T2,3-DB
9	T[2,3]-VL present	a = T2-VL, V3-VL present b = T3-VL only
10	T2-CT present	
11	Asymmetric connectives in thorax	

LONGITUDINAL CONNECTIONS

Apart from *Trigoniophthalmus* (and probably all other Archaeognatha), all insect tracheal systems possess connections between spiracles of adjacent segments with at least one longitudinal trunk (paired laterally, one on the right side and one on the left). Most insects have more than one longitudinal trunk, with odonates appearing to have the highest number (four trunks). Among other hexapods, longitudinal connections have been documented in Protura and Diplura (Dittrich and Wipfler, 2021); Collembola are thought to have cuticular respiration, although a tracheal system (apparently without longitudinal connections) has been found in several families includ-

ing Sminthuridae (Davies, 1927; Dittrich and Wipfler, 2021).

Dorsal longitudinal trunks (DLT, char. 1.1) are the connection present in all orders except Archaeognatha. Ventral trunks (VLT, char. 1.2) appear in all orders except Zygantoma, Ephemeroptera, and Zoraptera. Finally, medial trunks (MLT, char. 1.3) are present in Odonata, *Timema* but not in other Phasmatodea, and all orders of Dictyoptera. The fourth trunk, *An-ViLT*, is present in Odonata and hypothesized here to be a novel trunk required in the aquatic immature tracheal system that remains in the adult, as it begins near the location of the rectal gills and proceeds anteriorly (see fig. 30).

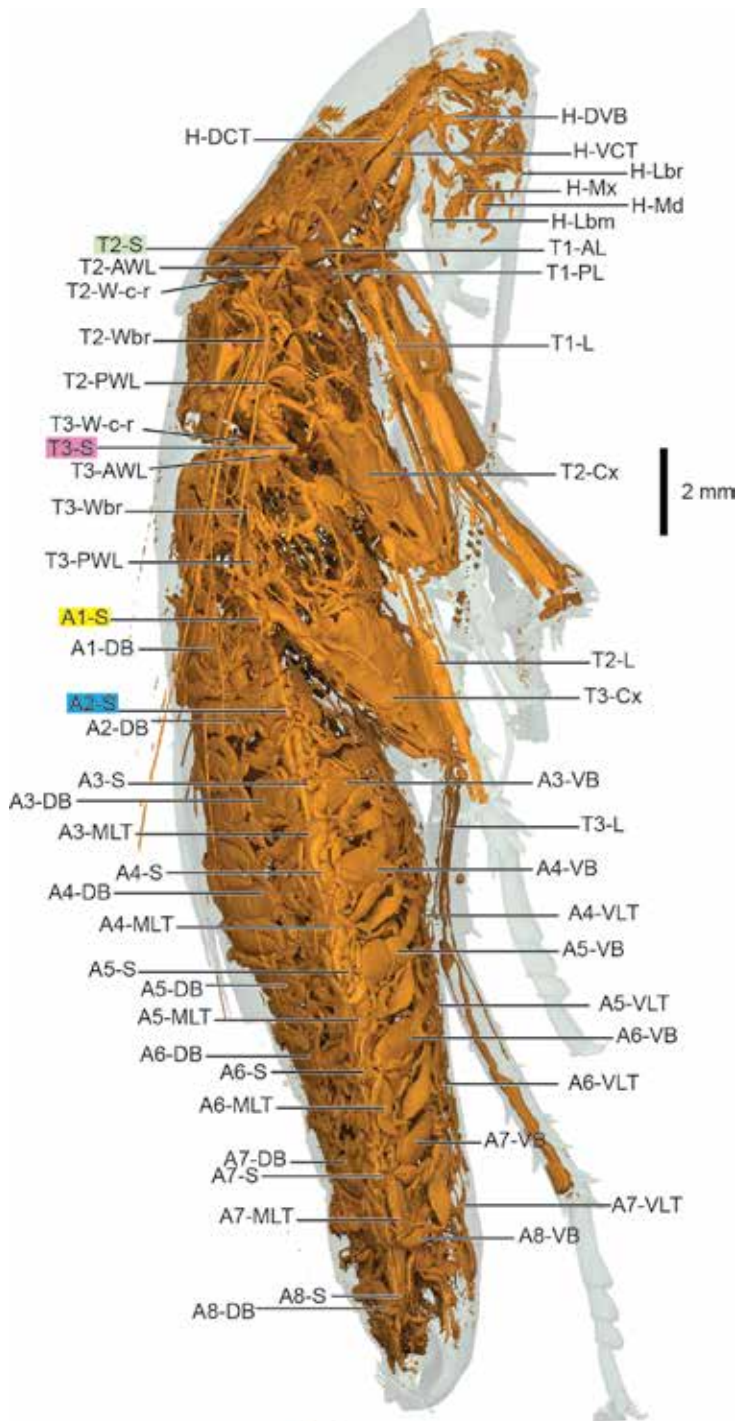


FIGURE 111. *Blaptica dubia* (Blattodea: Blaberidae) lateral.

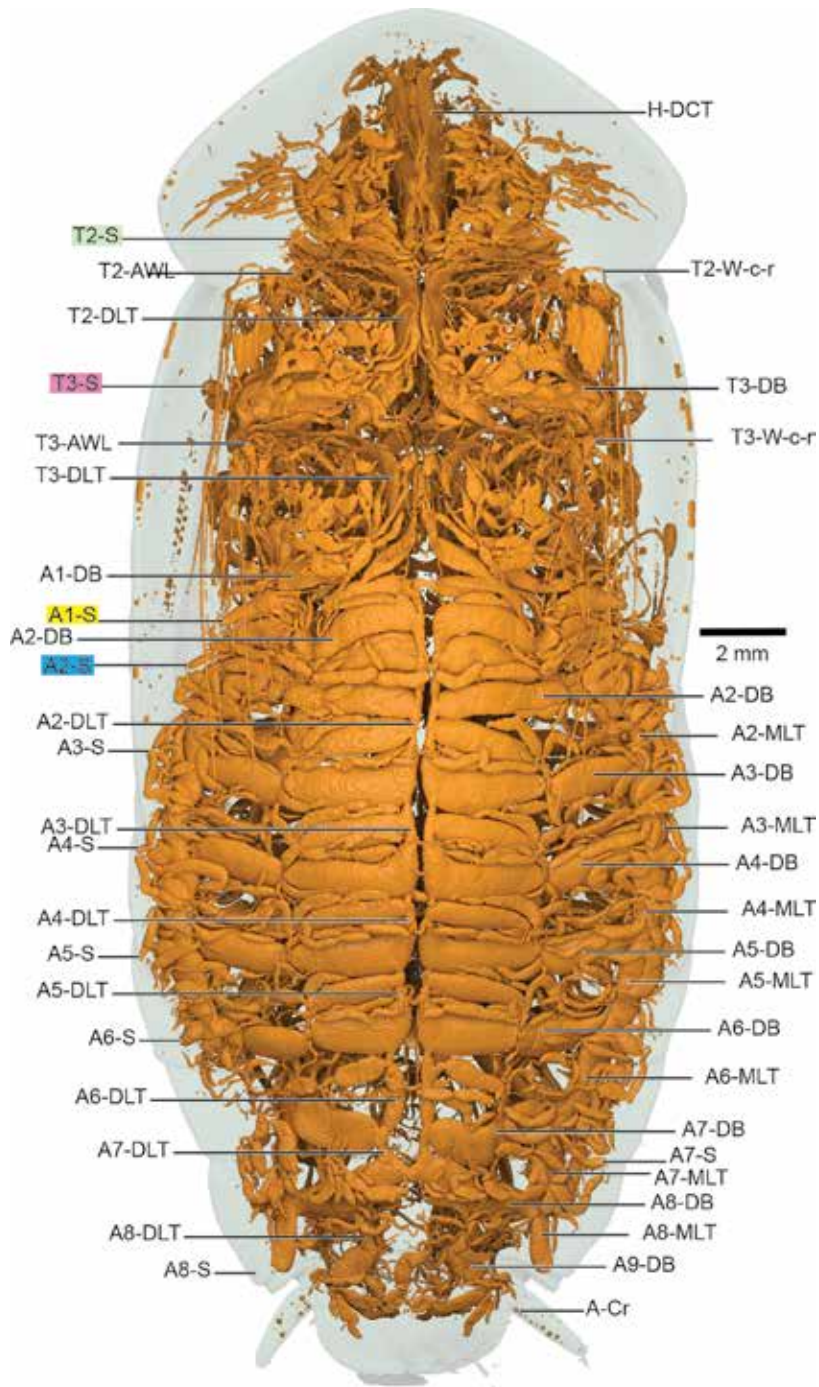


FIGURE 112. *Blaptica dubia* (Blattodea: Blaberidae) dorsal.

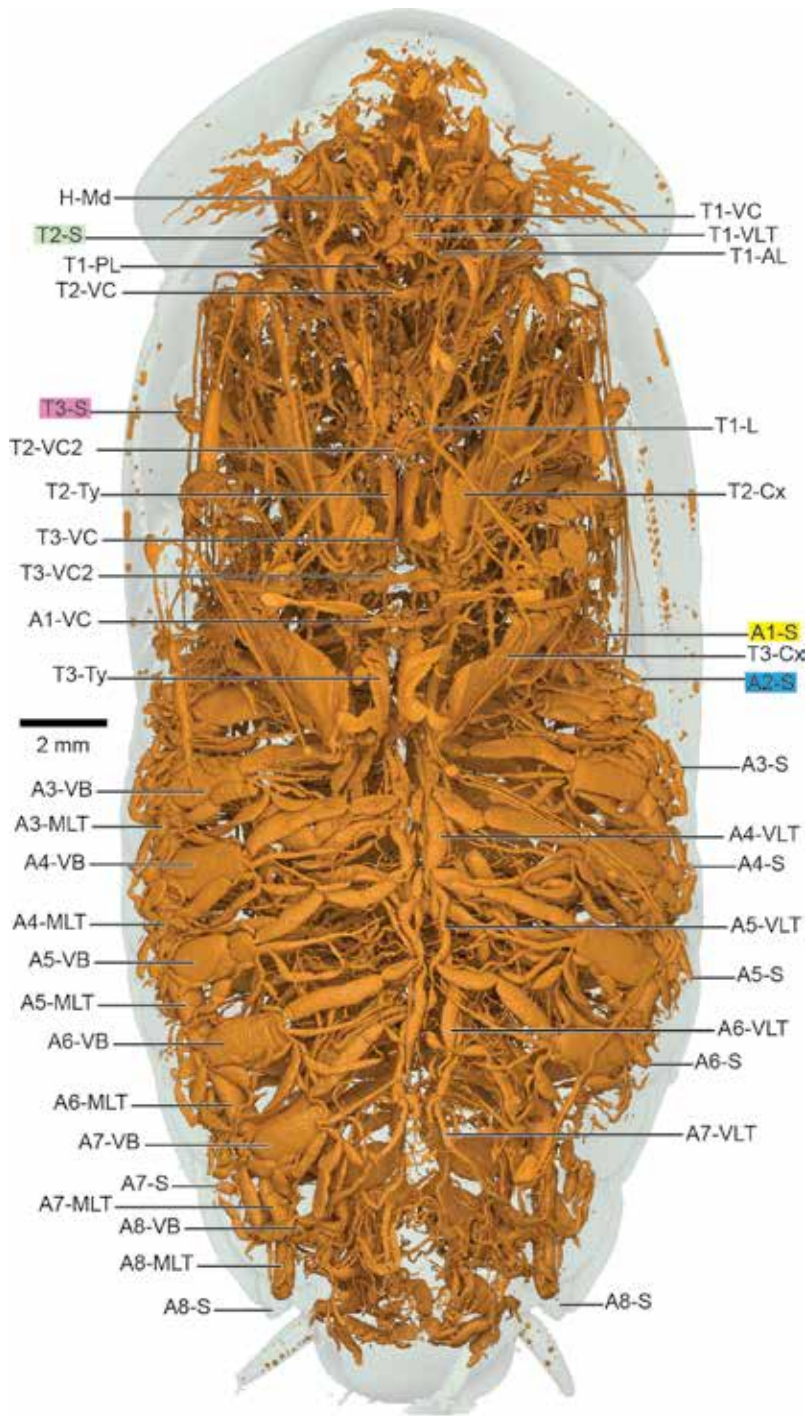


FIGURE 113. *Blattica dubia* (Blattodea: Blaberidae) ventral.

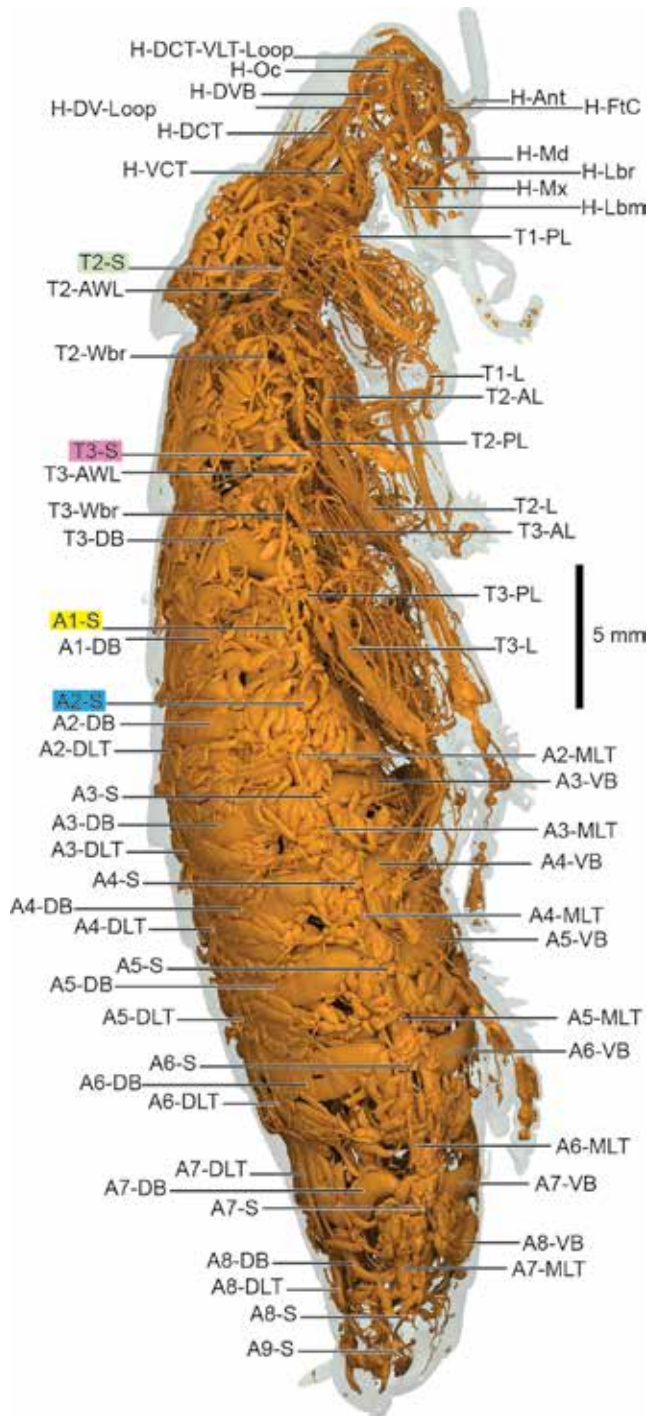


FIGURE 114. *Gromphadorhina portentosa* (Blattodea: Blaberidae) lateral view.

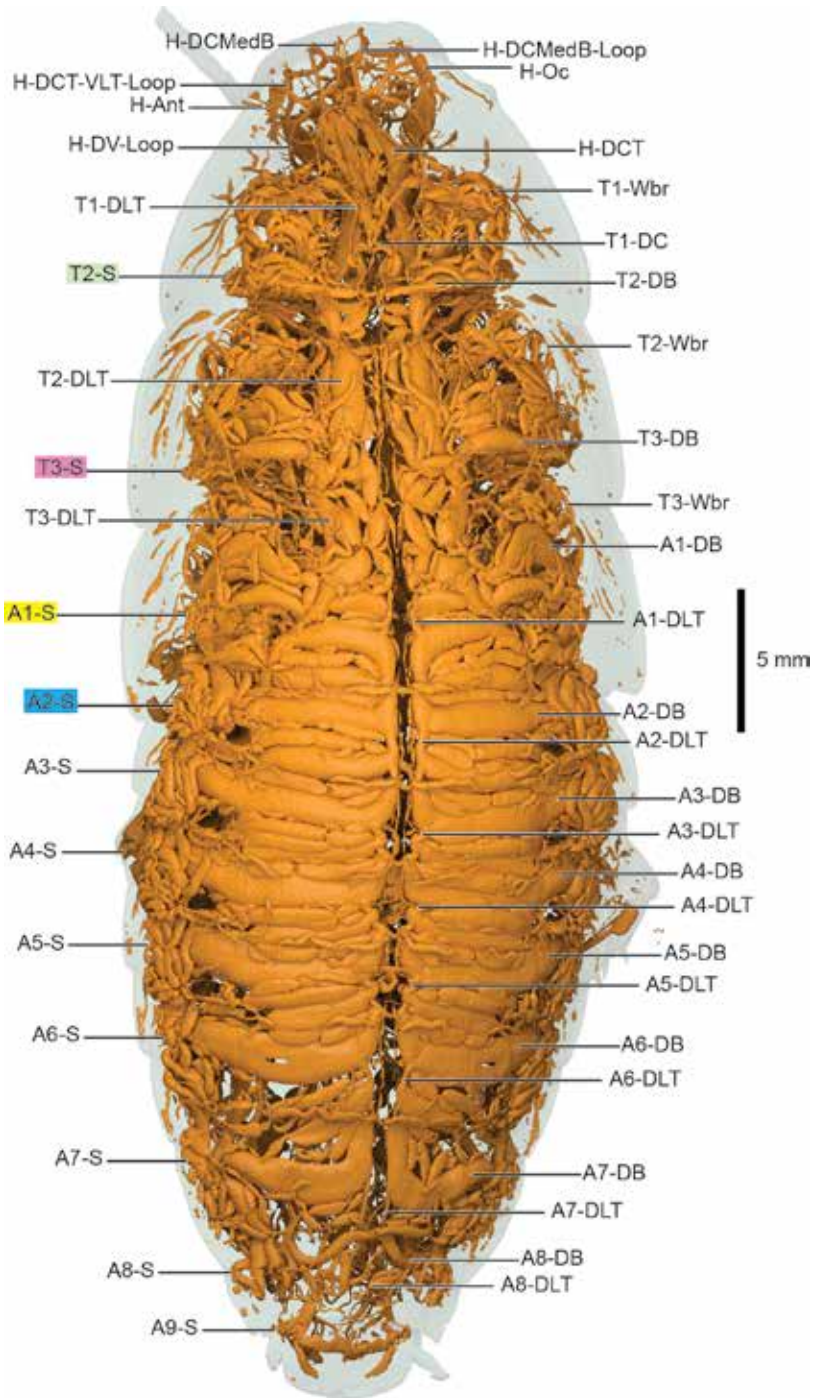


FIGURE 115. *Gromphadorhina portentosa* (Blattodea: Blaberidae) dorsal view.

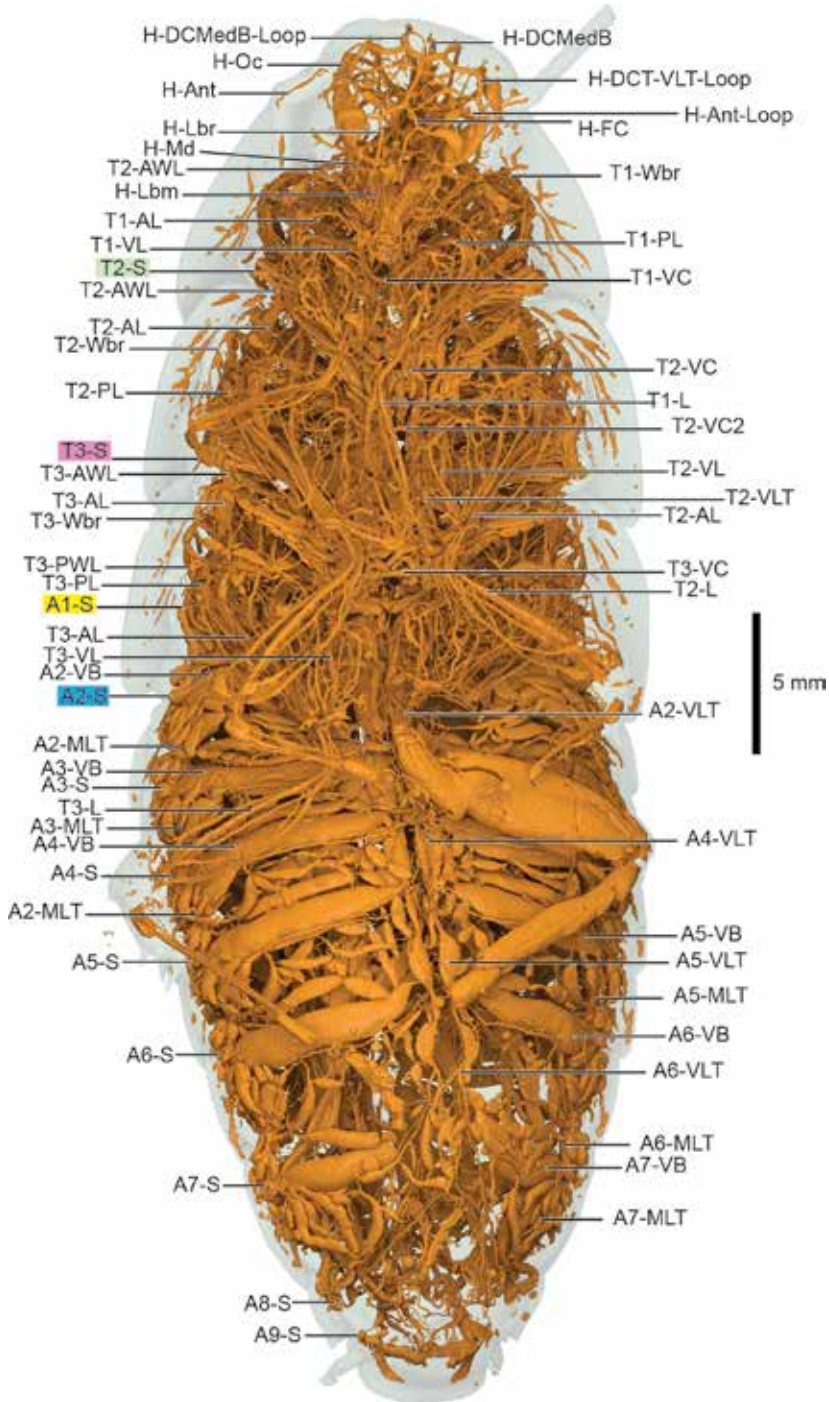


FIGURE 116. *Gromphadorhina portentosa* (Blattodea: Blaberidae) ventral view.

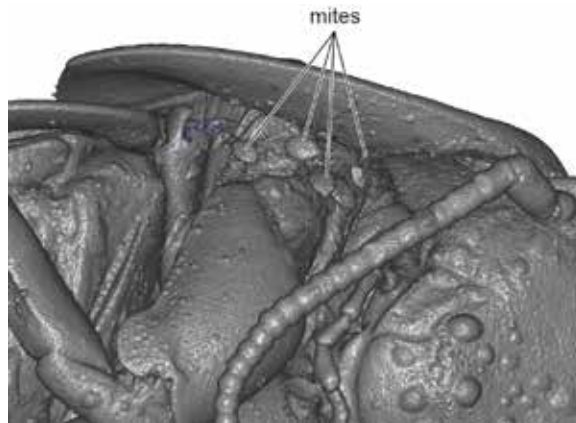


FIGURE 117. *Gromphadorhina* with *Gromphadorholaelaps schaeferi* mites, shown in iso-surfaced volume rendering of right pronotum and mesothoracic spiracle (T2-S). Direct screen capture from 3D Slicer.

WING-LEG TRACHEAE AND CHAPMAN'S TRIANGLE

Chapman's (1918) comparative work on wing and leg tracheae described what we refer to as "Chapman's Triangle," a structure consisting of *Tn-AL*, *Tn-PL*, and *Tn-Wbr* (see fig. 6, Chapman's Triangle is highlighted in blue). Chapman noted the consistency of this structure and attempted to generalize patterns based on "addition" and "subtraction" (his terms) of elements of the triangle. This early study preceded the resolution of many relationships among insect groups (and even before the invention of systematic phylogenetics), and more than a few of his hypotheses are now outdated. Regardless, the presence of this structure across Insecta does provide a scaffold for application of the comparative method in an updated phylogenetic context.

Chapman's Triangle is present in all winged orders except possibly Zoraptera (although the scan was of insufficient quality to judge presence or absence). Simpler modifications include lack (or loss) of *Tn-PWL*, seen in Ephemeroptera and discussed below, and loss of the *Tn-Wbr* connection, where *Tn-AWba* supplies the leading edge of the wing and *Tn-PWba* supplies the trailing edge. The absence of *Tn-PWL* may have implica-

tions for the basal relationships among insect groups (also discussed below).

While *Zygentoma* are apterous, *T2,3-AWL* was observed in Lepismatidae, but absent in the relict *Tricholepidion* (Lepidotrichidae). The presence of these tracheae indicates that the respiratory architecture to support flight was in place prior to the origin of wings in insects.

The ventral leg trachea *T2,3-VL*, a connection between the VLT and the leg (char. 9), is a common modification within Polyneoptera, encountered in Dermaptera, Orthoptera, Phasmatodea (but not *Timema*), and Dictyoptera. Branching patterns encountered at the base of the hind leg in conjunction with the ventral leg trachea *T3-VL* vary widely, with the most complex seen in Orthoptera. Insects with saltatorial legs would likely require more airflow for higher leg muscle metabolism, and large air spaces possibly functioning as weight relief are also seen in *Gryllus* and *Romalea*. The enlarged tracheae in Blattodea (roaches specifically) likely serve several functions as well, providing weight relief and permitting increased airflow for fast running speeds. Determining airflow through these enlarged leg tracheae would help in understanding the functions of these enlarged tracheae.

In addition to the additional *T2,3-VL* tracheae, Orthoptera also feature a range of adapta-

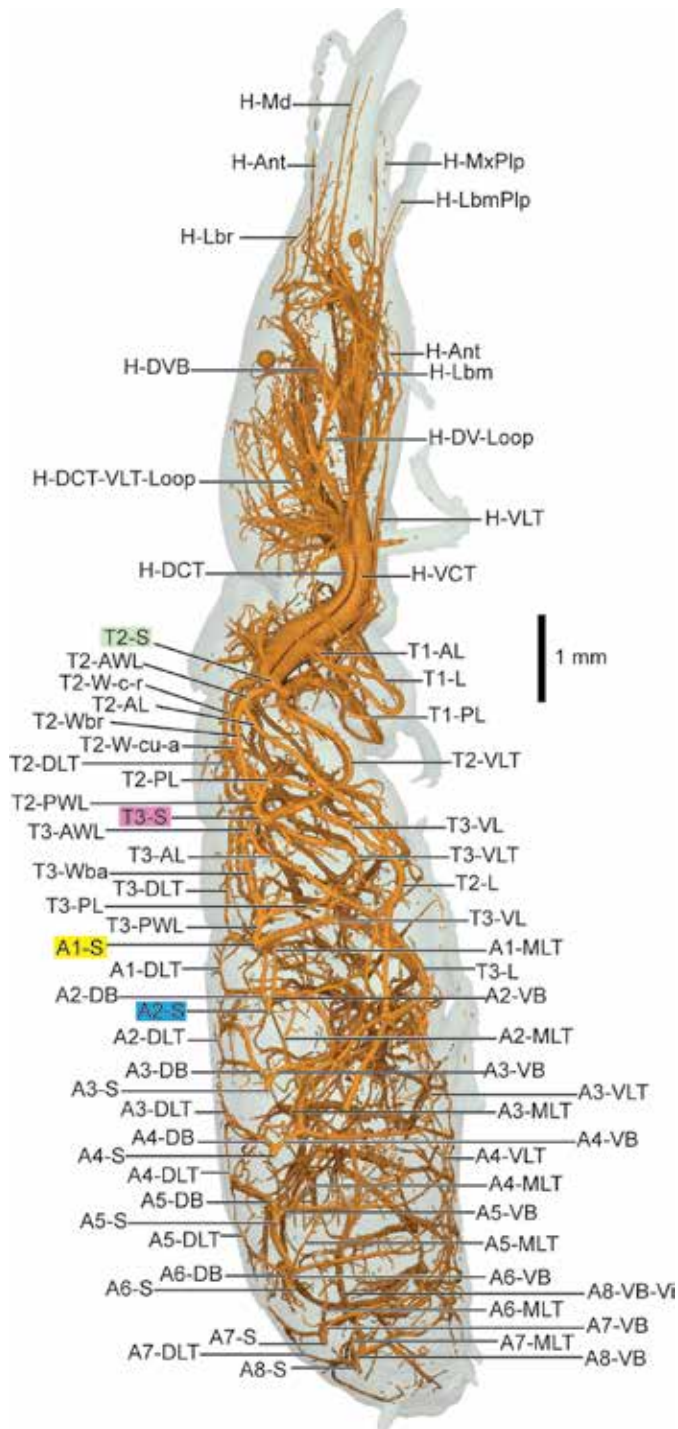


FIGURE 118. *Zootermopsis angusticollis* (Blattodea: Archotermopsidae) lateral.

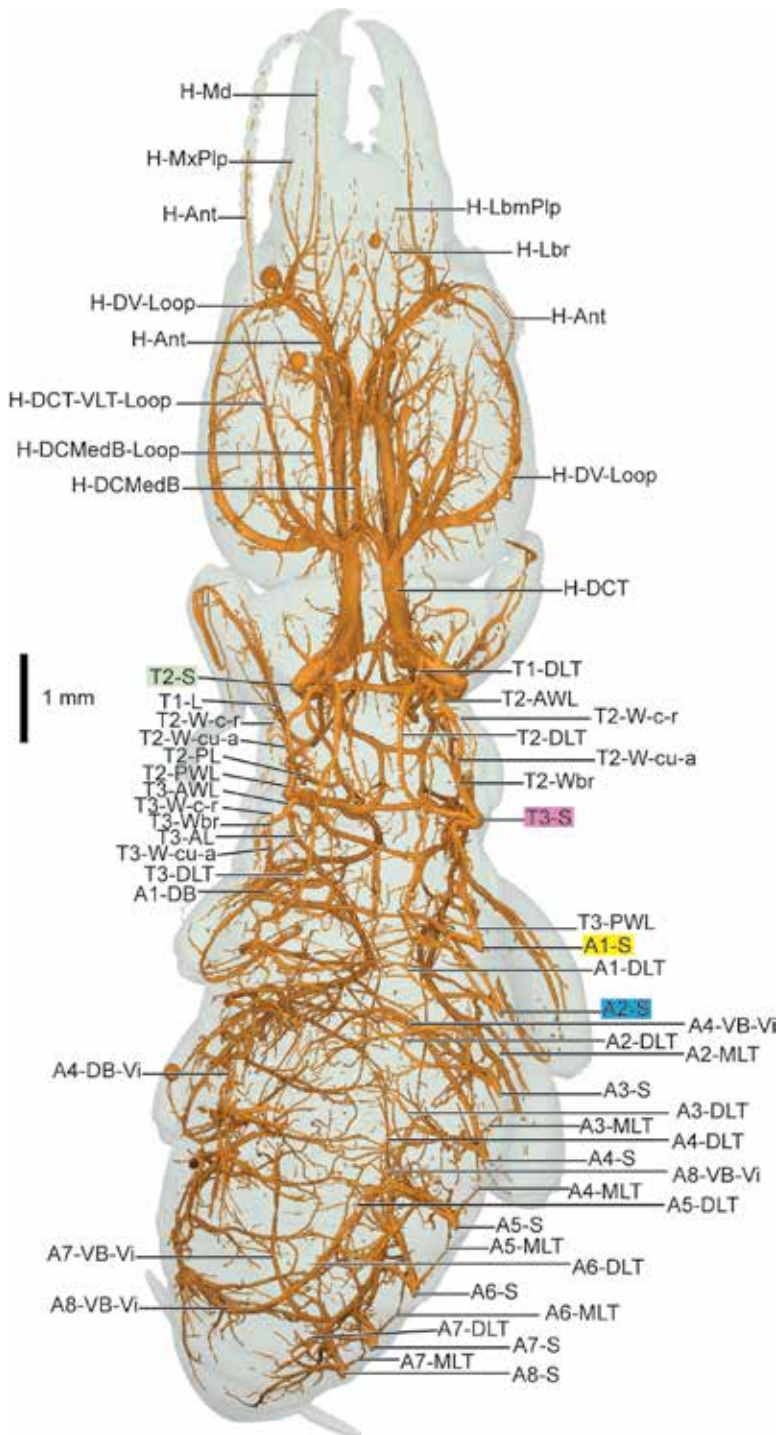


FIGURE 119. *Zootermopsis angusticollis* (Blattodea: Archotermopsidae) dorsal.

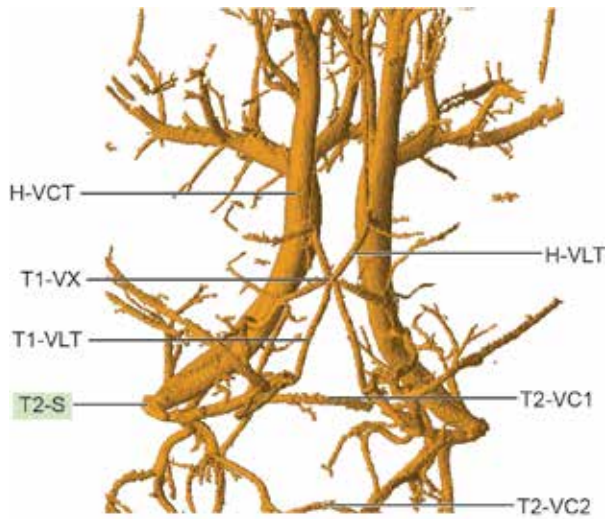


FIGURE 121. *Zootermopsis* worker caste, prothorax ventral view. Note presence of bilaterally symmetric H-VLT. Direct screen capture from 3D Slicer, annotated in Illustrator.

tions to T2,3-PWL, T2,3-Wba, and T2,3-PL, all likely due to the highly modified legs. T3-PWL extends from A1-S dorsal-anteriad and T3-AWL from T3-S posteriad, joining via T3-Wbr with T3-W-cu-a and T3-W-c-r (respectively). However, T3-PWL has an additional ventral T3-PL-like branch ventrally, joining with T3-AL and proceeding into the hind leg. This T3-PL-like/T3-AL branch then joins with a large T3-PL from A1-S, so it may be T3-PL separated from T3-PWL at A1-S. (Refer to fig. 125 for a simplified diagram of branching patterns across several taxa.) T3-PL from A1-S is notably large, so this could be another modification for saltatorial legs. A second possibility is that this T3-PL is *not* homologous with T3-PL and is an additional trachea for saltatorial legs. This would mean two additional tracheae; however, as T3-VL is already an additional trachea into the hind leg, branching off T3-VLT. Thus, either T3-PL has a different branching pattern, such that the T3-PWL separation occurs at the spiracle and leads to an additional “triangle” form in the metathorax, or there are two new tracheae in Orthoptera. Note that the descriptions in the Orthoptera section above on *Gryllus* (Gryllidae) and *Meconema* (Tettigoniidae) are written with the first hypoth-

esis in mind (that of the early split of T3-PL large and ventrad, not the additional PL hypothesis).

Polyneoptera without saltatorial legs also possess T2,3-VL, such as Dermaptera, with an active lifestyle, and Phasmatodea, which might require not only increased airflow but weight relief in very long legs. Mantises and roaches (including termites) (Dictyoptera), with disparate lifestyles, also possess T2,3-VL, indicating the likelihood of multiple functions for this trachea. While not present in *Timema* and also absent in Plecoptera, Grylloblattodea, and Embioptera, it does seem apparent that T2,3-VL is likely a trait of Polyneoptera, but is lost in these four groups. Higher quality scans of Zoraptera, as possibly basal Polyneoptera (although see Song et al. (2016)) would likely be helpful.

While not considered as part of Chapman’s Triangle, a number of variations are also seen in foreleg tracheae. T1-AL is typically seen branching ventrally from H-VCT and joining with T1-PL before extending into the leg. Occasionally, additional branches from H-DCT also appear, but may be restricted to the forecoxae. T1-PL, however, branches from a range of sites, including directly from T2-S, T2-VB, or even T2-DB (Dermaptera). At first glance these modi-

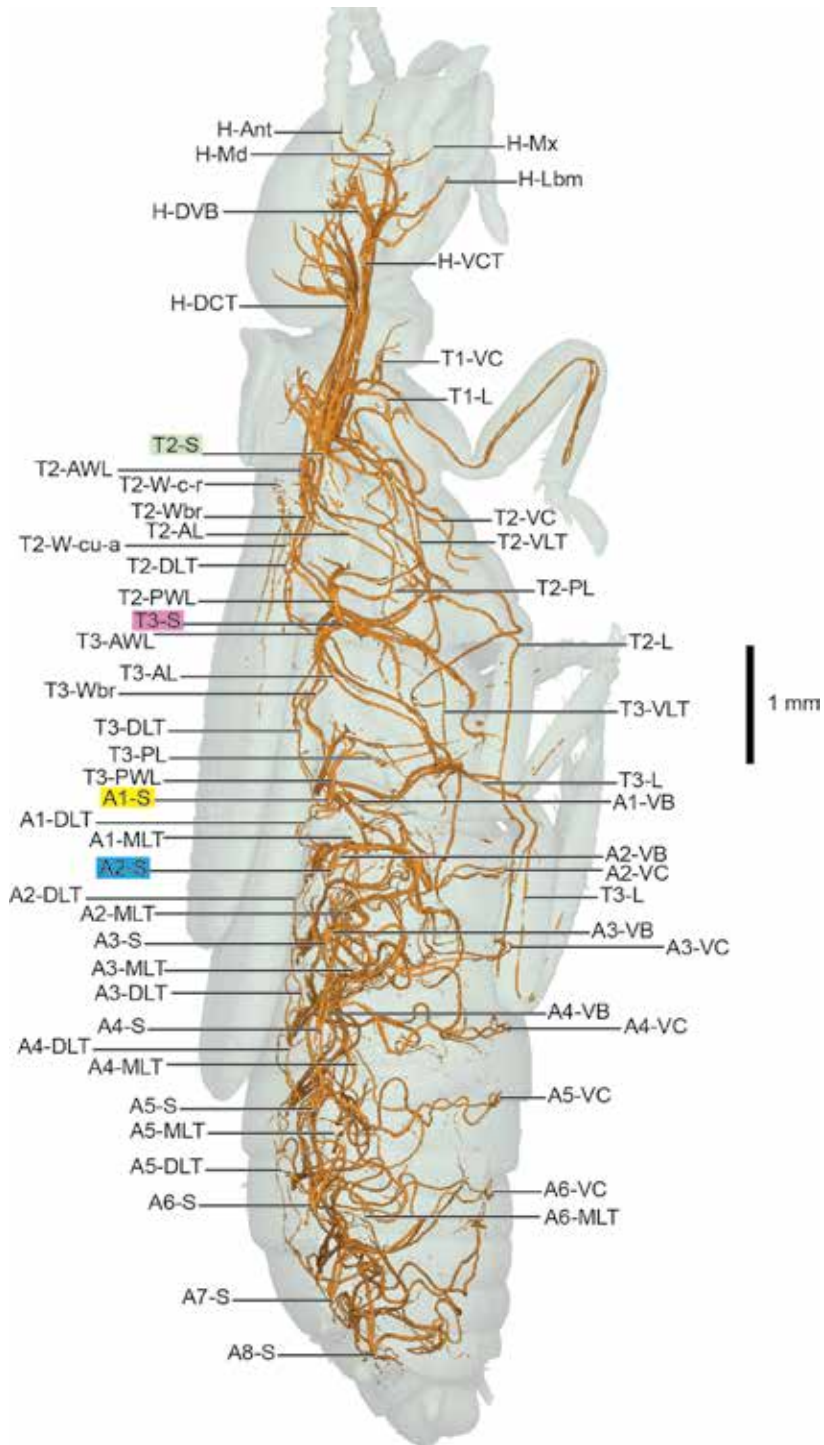


FIGURE 122. *Reticulitermes flavipes* (Blattodea: Rhinotermitidae) lateral view.

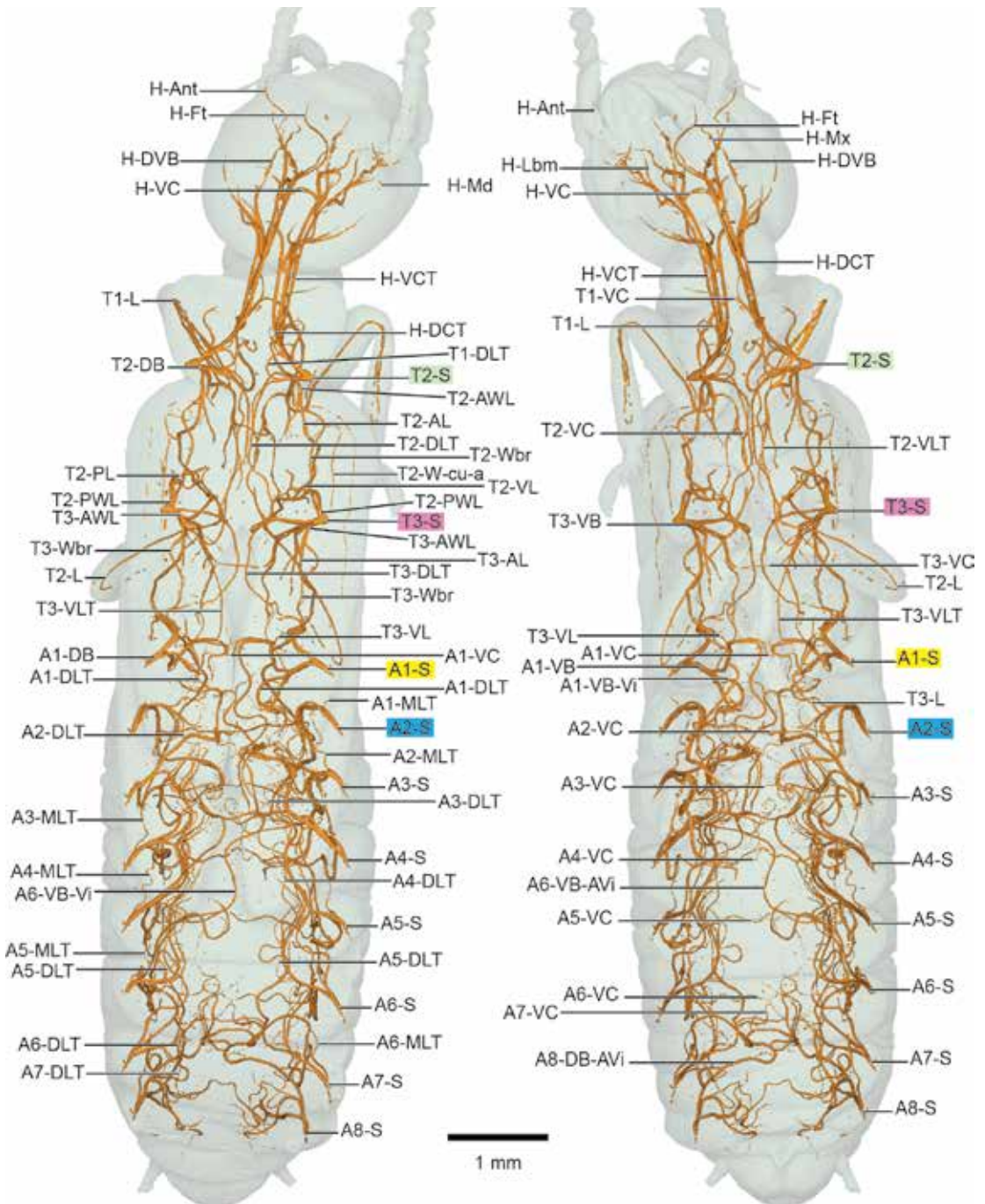


FIGURE 123. *Reticulitermes flavipes* (Blattodea: Rhinotermitidae) dorsal (left) and ventral (right).

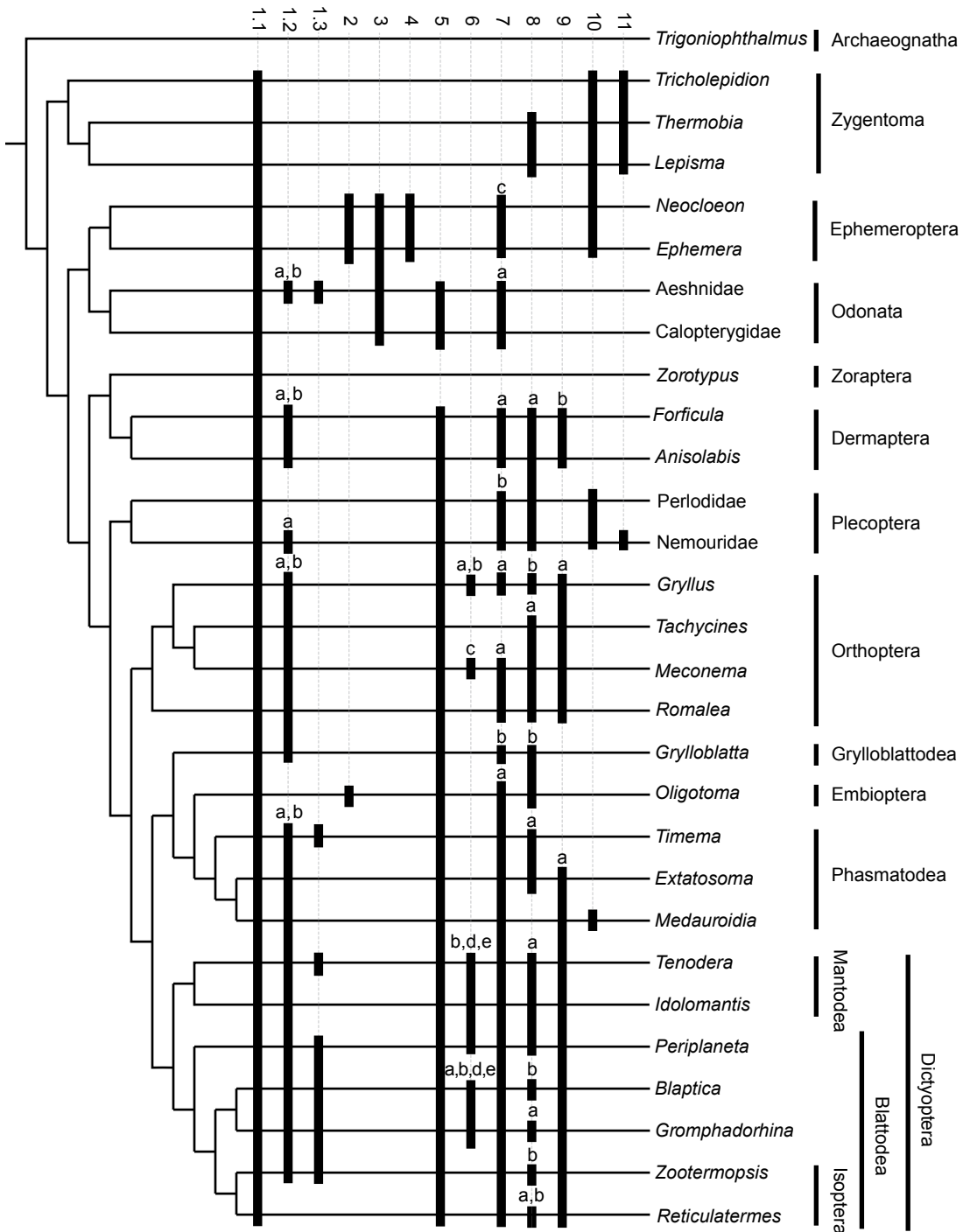


FIGURE 124. Phylogenetic tree based on Misof, et al. (2014) with tracheal characters from table 5. Letters a–e denote variations in characters; refer to table 5.

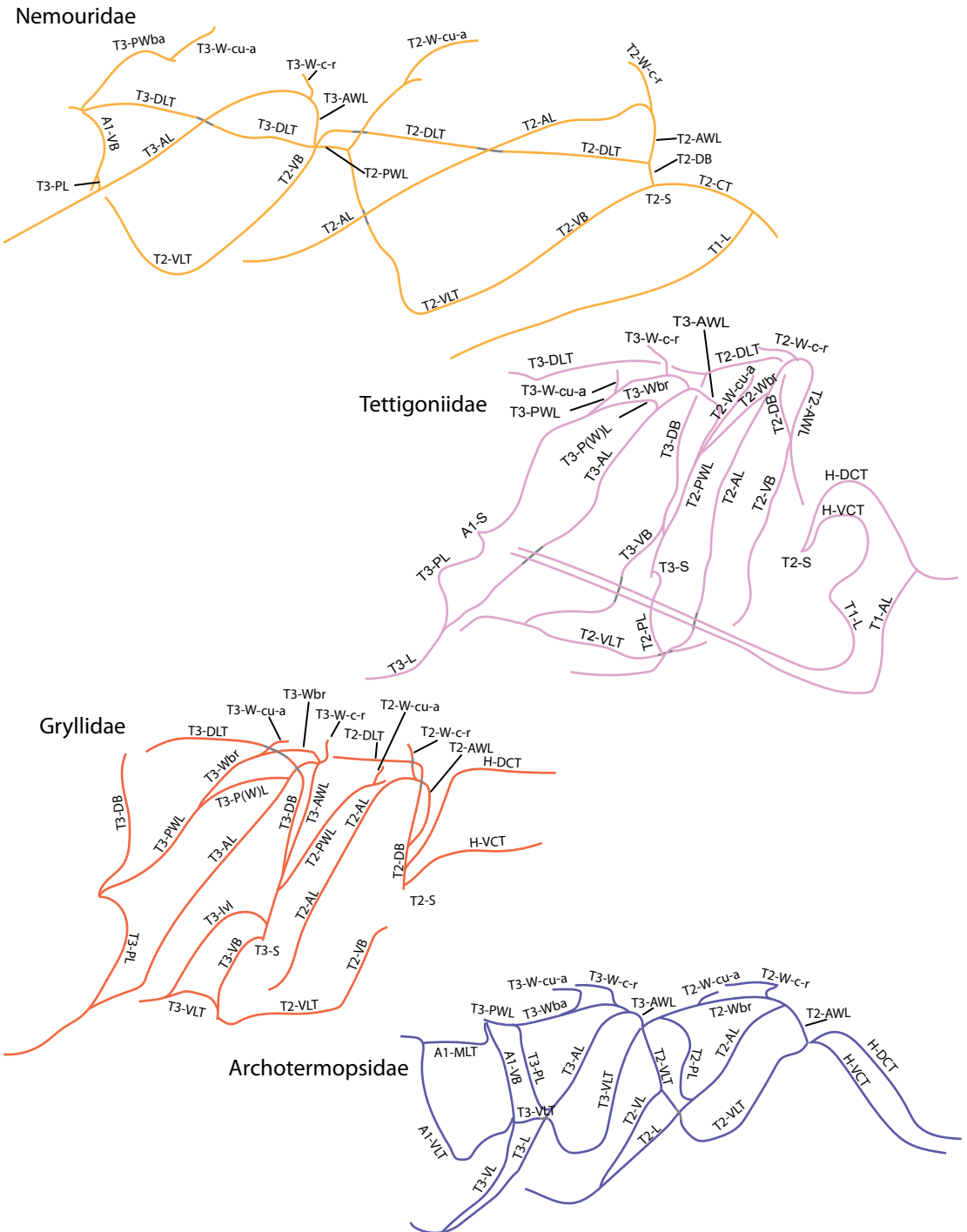


FIGURE 125. Thoracic tracheal diagrams (lateral views).

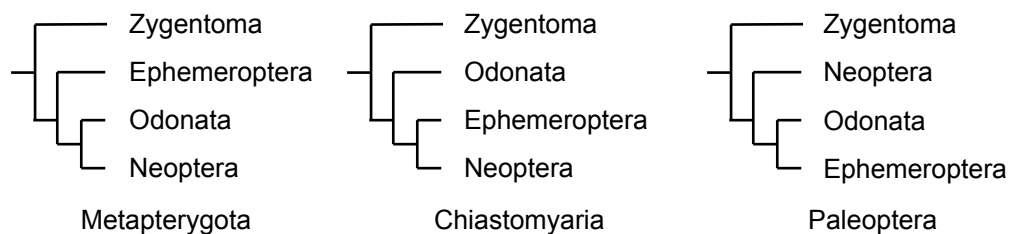


FIGURE 126. Hypothesized basal relationships of insects: Metapterygota (Odonata + Neoptera sister to Ephemeroptera), Paleoptera (Odonata + Ephemeroptera sister to Neoptera), and Chiasmomyaria (Neoptera + Ephemeroptera sister to Odonata).

fications could be attributed to the plasticity of the tracheal system, but the stability of the connectivity patterns of major trunks such as these has been established, and it is unlikely that this is ontogenetic variation (Harrison et al., 2018).

BASAL RELATIONSHIPS

The relationships between Ephemeroptera (mayflies), Odonata (damselflies and dragonflies), and all other winged insects remain unsettled (see fig. 126 for a summary of the three hypotheses of basal relationships). While molecular evidence (Misof et al., 2014) suggests a monophyletic Palaeoptera, morphological studies, some of which also incorporate molecular data (Blanke et al., 2012; Blanke et al., 2013; Thomas et al., 2013; Kjer et al., 2016; Simon et al., 2018), suggest the grouping Metapterygota (mayflies as the most basal group) or even Chiasmomyaria (dragonflies as most basal). Respiratory morphology, however, has yet to be incorporated into these analyses, and provides some interesting features.

The wing base of mayflies is notable in the complete lack of posterior wing base tracheae (T2,3-PWba). Wing tracheae are supplied only via T2,3-AWba, which extends into the wing as T2-c-r, with remaining tracheae fanning out into the wing; T2,3-PWba is absent (see char. seven in fig. 124). Chapman (1918) interpreted this as a reduction of T2,3-PWba; however, it is also possible that T2,3-PWba is truly absent in Ephemeroptera, suggesting the validity of the

group Metapterygota, in which T2,3-PWba and T2,3-Wbr are synapomorphies of odonates plus Neoptera.

Mayflies are also unique in having single, nearly linear, paired abdominal longitudinal trunks, here designated *An*-DLT. In all other taxa, *An*-DB branches dorsad from *An*-S, leading to an anterior-posterior (generally) arching *An*-DLT, but *An*-DB appears to be absent in Ephemeroptera. Numerous *An*-DV_i are present, but none of these branches connect longitudinally between segments, and if these are homologous with *An*-DLT, it would mean that Ephemeroptera would have two longitudinal trunks, *An*-DLT and *An*-MLT (or *An*-VLT). The lack of ventral branches makes this equally unlikely. Odonates have four paired longitudinal trunks in the abdomen, with the linear *An*-ViLT tracheae most similar to the ephemeropteran *An*-DLT. These are unlikely to be homologous, however, as the dragonfly *An*-ViLT does not connect to any abdominal spiracles except its A8-S source. The linear nature of these trunks, however, across these two taxa does indicate a possible convergent nature in that immatures of both taxa are aquatic. *An*-ViLT is possibly derived from the rectal gills and remains filled with air in the adult, possibly for weight relief. *An*-DLT in the mayflies retains gill attachment sites, positioned almost exactly halfway between adjacent spiracles, and the size and linear nature of the trunk is possibly for buoyancy and effective transfer of respiratory gases (although mayflies also possess an air-filled gut, discussed below). The remaining

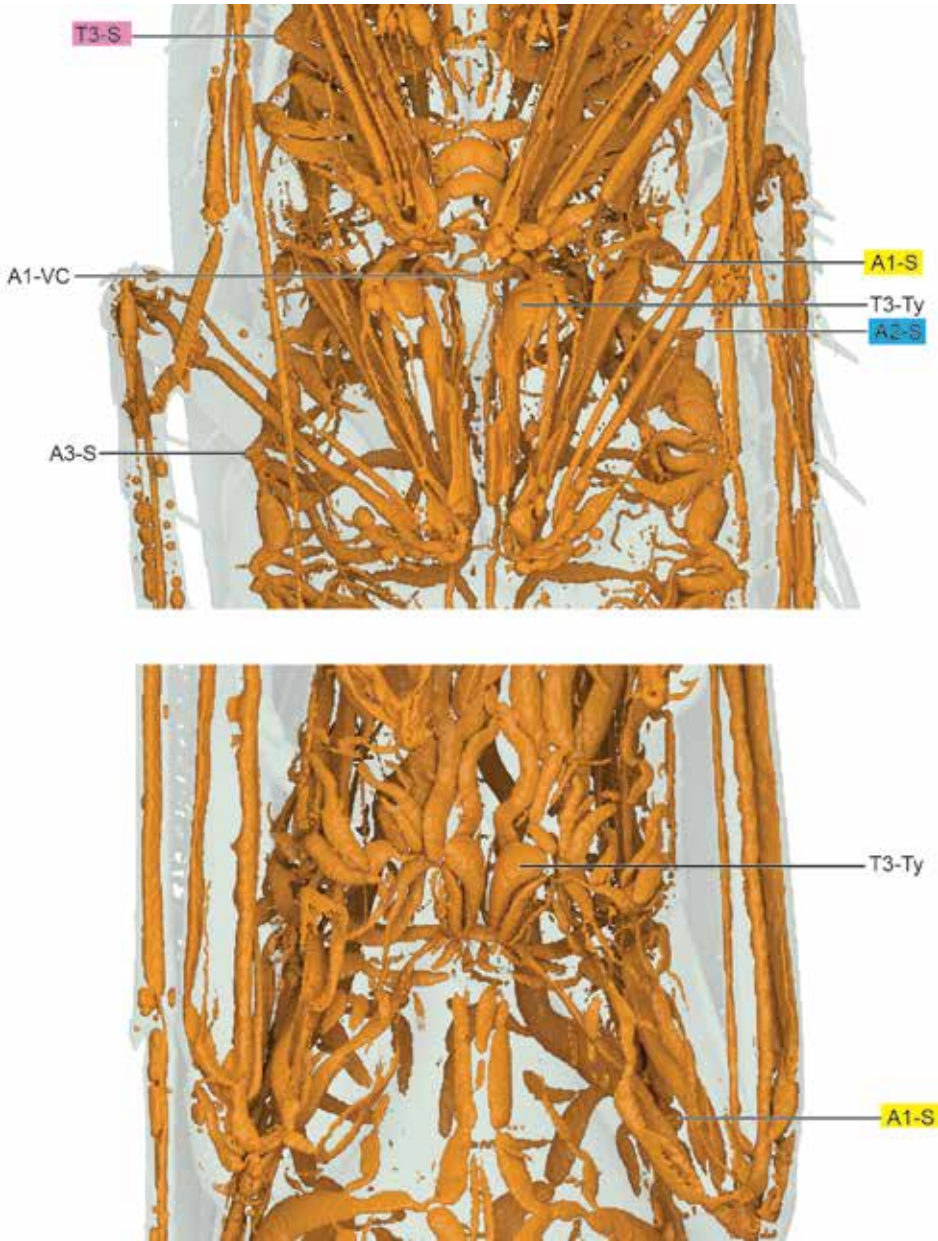


FIGURE 127. Ventral view of *Tenodera sinensis* (top) and *Periplaneta americana* (bottom, showing thoracic tympana). Specimens not presented at same scale.

longitudinal trunks in Odonata, *An*-DLT, *An*-MLT, and *An*-VLT are identified by the presence of dorsal DB and ventral VB branches leading to them, a condition common with Neoptera. While respiratory morphology alone is unlikely to resolve the basal relationships of winged insects, these data at least indicate the issue remains unsettled.

NETWORKED HEAD TRACHEAE

All insect heads are supplied primarily by paired H-DCT and H-VCT tracheae. For most species shown here, H-DCT and H-VCT connect dorsoventrally, forming a tracheal network of varying complexity. A handful of orders, however, retain simple, treelike head tracheal morphology, where H-DCT and H-VCT remain disconnected. Archaeognatha, Zygentoma, Ephemeroptera, and Zoraptera are the only orders where H-DCT and H-VCT remain independent (char. 5); all other heads feature a networked tracheal system in the head. The presence of dorsal-ventral connections between H-DCT and H-VCT in odonates and the lack in Ephemeroptera also suggests the validity of Metapterygota.

It is important to note that assessing homology in head tracheae using only tracheal architecture is challenging and is only touched upon here. Head musculature has been extensively studied in many taxa, and these data could assist greatly in correctly mapping tracheae.

HOMOPLASY

Homoplasy, or a similar trait found in groups not closely related (i.e., not found in a common ancestor), occurs in several groups for tracheal features, as seen in figure 124. While developmental plasticity is known to occur during tracheal growth, major trunks have been shown to exhibit remarkable stability, with significant variation in tracheal form and volume seen only in smaller branches such as tracheoles (Harrison et al., 2018). As such, plasticity of the tracheal sys-

tem is not considered to be a significant factor in assessing homology or homoplasy.

The alimentary canal as an air-filled space (char. 2) was mentioned previously. The T2-CT cephalic trunk (char. 10), a single branch extending anteriorly toward the head prior to bifurcating into H-DCT and H-VCT, is another interesting example. Present in Zygentoma, Ephemeroptera, and Plecoptera, its absence in Odonata also highlights the uncertainty around Ephemeroptera and Odonata. Additionally, Zygentoma have T2,3-AWba but not T2,3-PWba, similar to Ephemeroptera, further support for the group Metapterygota.

Asymmetric thoracic commissures, *Tn*-ASymC, are likewise present in Zygentoma and Plecoptera (Nemouridae). This condition appears to be rather basal, and an adaptation required in these taxa for some unidentified purpose.

Medial trunks *An*-MLT, mentioned earlier, are present in Odonata, Phasmatodea, and Dicotyoptera. The absence of these trunks in the remaining orders suggests convergence in the development of the MLT.

FLIGHT AND WING TRACHEAE

The importance of the ability to fly in the success of insects cannot be overstated. Occasionally described as a key innovation (Miller et al., 2022), numerous early adaptations (such as T2,3-AWL observed in apterous Zygentoma) were required for the successful evolution of powered flight, not the least of which is a respiratory system suitable for the supply of oxygen to flight musculature.

Flight muscles are either synchronous (one nerve impulse results in a single contraction) or asynchronous (one nerve impulse elicits multiple contractions, via stretch activation and other processes). Although all species included here possess synchronous flight muscles, a variety of tracheal structures for flight musculature is shown.

Ephemeroptera and Odonata feature flight musculature noticeably different from all other insect orders presented here. Ephemeroptera (pls. 11–17, figs. 22–27) are by far the simpler of the two, with

several large bush- or fanlike flight muscle (FM) tracheae extending dorsad from T2-SAttr, with a second smaller bundle extending ventrad from T2-DLT. T3-S is structured slightly differently, apparently without T3-SAttr, with FM tracheae extending dorsally high into the thorax and a smaller set running ventrally. Additionally, and unlike odonates, A1-S also supplies its own A1-FM, extending dorsad. As mentioned previously, mayflies lack T2,3-Wbr and T2,3-W-cu-a, a condition seen in no other pterygote order examined here.

Odonate flight musculature and the associated wing base have more in common with the remaining orders, albeit with substantial differences that call for more research. Rather than the fanlike proliferation of smaller and smaller branches seen in Ephemeroptera, dragonfly flight muscles appear to be fed by a dorsal-ventral trachea extending through the length of each direct flight muscle bundle, aligned in parallel with muscle fibers. Small finlike tracheae extend radially outward from this central trachea with a structure highly reminiscent of a heat exchanger (pl. 18, figs. 31, 35). This fanlike tracheal structure appears to be unique to dragonflies and is likely very efficient.

WEIGHT RELIEF

While the primary function of tracheae is gas exchange, structures in biological systems rarely serve a single function. Insects were the first creatures with powered flight, an achievement that required an array of adaptations and modifications. Weight is a critical factor in any flying animal, and it is likely that tracheal modifications serve as weight relief, allowing less energy expenditure during flight.

The most extreme modification is the complete conversion of the alimentary canal into an air space. As insects possess a hard, chitinous exoskeleton, reduction of body parts to reduce size is not possible—indeed, during ecdysis, insects increase in size. Consequently, when internal organs decrease in volume, either fluid, air, or other tissue must take up the space.

While air spaces in the alimentary canal and even in the hemocoel are commonly encountered in micro-CT scans, these are temporary in nature, soon to be filled during feeding. The complete conversion of the alimentary canal is seen here only in insects that do not feed as adults: mayflies, the perlotid, and male Embioptera—groups that are not closely related, highlighting the convergence of this phenomenon (see section below on Phylogenetic Patterns).

These spaces are further distinguished from tracheal air spaces by the lack of tracheal connections supplying air, leading to the question of how these spaces are filled. It is possible that the last preadult instar simply ingests large volumes of air prior to the reduction or loss of mouthparts; however, this likely incurs some advantages (the air space as an adult) and disadvantages (space normally filled with food but now taken up by air). Micro-CT scanning of a live last-stage larval instar would likely shed some light on this question.

For some odonates, including the aeshnid shown herein, half the body volume (or more) is occupied by air, with large air spaces in the head, thorax, and abdomen. This seems logical, on two fronts—air spaces in the thorax possibly provide space for presumed muscle growth (as discussed previously), and abdominal air spaces are likely for balance (as are those in the head). The length of the very long abdomen is held horizontal during flight, and air distribution can affect the balance of forces in flight.

In many species, tracheae themselves constitute a substantial portion of the body volume. Two rows of enlarged tracheae, reminiscent of a package of sausages, are located in various parts of the abdomen across Orthoptera and Dictyoptera. In addition to the large *An-DB* tracheae of *Gryllus* (figs. 58–60; plates 35–37), extending medially from *An-DLT* are (generally) paired *An-DLT-DVi* tracheae, thicker than the *DLT* and nearly as large as *An-DB*. The *An-DB* of *Mecanema* is likewise thick, but also paired (see fig. 67, pl. 43), an unusual condition noted by Ander (1939). Both mantises display enlarged *An-DB*,

An-VB, and *An-DLT* tracheae, as well as *Periplaneta*. Finally, of the remaining roaches scanned, *Blaptica* (figs. 111–113, plates 67–69) and *Gromphadorhina* (figs. 114–116, plates 70–72) have not only enlarged *An-DB*, *An-VB*, and *An-DLT*, but numerous visceral tracheae arranged in parallel along the inside of the tergal wall. While these may function as air space for supplying the hissing spiracle in *Gromphadorhina*, the morphology in *Blaptica* is remarkably similar. Bipedal running has been observed in *Periplaneta* (Full and Tu, 1991), and it is possible that the weight relief afforded by larger tracheae in the head and thorax facilitates this behavior.

AUDITORY ADAPTATIONS

Hearing and sound production in insects has evolved numerous times, with an array of adaptations for making and perceiving sounds. Non-tympanal hearing organs are known in several orders (Hoy and Yack, 2009), and are thought to occur in most insects (e.g., subgenual organs, e.g., Field and Matheson, 1998), but numerous independent evolutionary events of more advanced insect ears comprise a suite of features: a tympanal membrane, a tracheal air chamber, and a chordotonal organ. Visualization of tracheae allows the investigation of the numerous modifications of air spaces for the reception and production of sound.

Mantises are known for their hearing, even though the so-called cyclopean ear located in the thorax has only been described in detail relatively recently (Yager and Hoy, 1986, 1987). What is less known is that similar tracheal modifications are present elsewhere in Dictyoptera, namely, in roaches (Shaw, 1994; Hoy and Robert, 1996; Yager, 2005). Figure 127 ventral views of both *Periplaneta* and *Tenodera*, shows the similarities between the tympanal tracheal space. As the size of the air cavity has a direct effect on the frequency response, it is likely that the roach is sensitive to a different range of sounds than the mantis.

A particularly striking example of multiple tracheal modifications for hearing in a single

organism is *Gryllus*. In addition to the well-known tympana on the foretibia (T1-L-Ty), *Gryllus* cerci (A-Cr) are hollow (see pls. 36–38, figs. 58–60). Their elongate structure allows them to function as signal processing filters, selectively reducing background noise while they detect sound up to 1 kHz in frequency (Longley and Edwards, 1979; Mulder-Rosi et al., 2010). As mentioned in the Results section, *Gryllus* possesses yet another tracheal modification: the large T2-VC with a circular T2-Sept (fig. 61), thought to contribute to binaural hearing.

Legs typically possess thin, elongate tracheae, particularly in stick insects and mantises where weight relief is likely important. Both plecopteran specimens, however, possess tibial tracheae larger than in the femur—an unusual condition, as leg tracheae typically reduce in diameter from the coxae to the tarsi. Studies have shown that the abdominal drumming behavior of stoneflies is likely for locating mates (Stewart, 2001); however, little work has involved the morphology and physiology of hearing organs in Plecoptera. It is possible that the enlarged tibial tracheae serve as resonance chambers, amplifying substrate vibrations that are then passed to the subgenual organs. Future studies should investigate the physiology of stonefly legs and their possible contribution to hearing.

Sound is produced by vibration of a body part, by stridulation (e.g., using wings or legs in Orthoptera) or oscillation of a membrane (such as cicada or lepidopteran tymbals). Cicadas include two (laterally paired) sets of air spaces—one for sound production, behind the tymbals at the base of the abdomen, and another for sound reception, ventrally located in the second abdominal segment (Herhold et al., in prep). *Gromphadorhina portentosa*, however, has a modified abdominal spiracle designed to amplify the hissing sound caused by the expulsion of air. Commonly used as an alarm sound, Nelson and Fraser (1980) found that the hissing is also for courtship and aggression. The source of the large volume of air required for the hiss is likely from the complex network of tracheae found in the abdomen of *Gromphado-*

rhina, as no single large air sac or similar structure is present (see fig. 115, pl. 71).

DIFFERENCES IN METAMORPHIC DEVELOPMENT

While the tracheal system of larval insects has been studied in various groups, most notably in the extensive work on Diptera by Joan Whitten (1955, 1956, 1957, 1959, 1960, 1962, 1972), few studies (Lehmann et al., 2021) have addressed changes in the tracheal system during metamorphosis. Aquatic immatures have been shown to be suitable for micro-CT based analyses, as shown here, and inclusion of a broader selection of taxa would likely be very informative.

While only a single immature was scanned for this study (the aforementioned Odonata), vestiges of larval tracheal adaptations are visible in Ephemeroptera. Gill attachments, placed halfway between adjacent spiracles, are evident in all three mayfly scans. It is interesting that the gills do not attach to the spiracular openings but have their own attachments midway down the abdominal tergum. Just as interesting, an alternative scenario is that the immature gills arise from spiracles and the spiracular sites change during metamorphosis.

OTHER VARIATIONS IN TRACHEAL MORPHOLOGY

A number of variations in morphology arise in various taxa that appear to be related to a particular lifestyle and not any phylogenetic relationship. Spiracular atria, large cavities interior to the spiracular openings, are present in a range of taxa, most notably Orthoptera. Spiracular branches, possibly a modification or reduction in volume of a spiracular atrium, are also present in lineages as varied as *Zygentoma*, Odonata, Orthoptera, Plecoptera, *Grylloblatta*, and Phasmatodea.

While extant insects possess only two thoracic spiracular pairs (only Diplura are known to possess up to four pairs), ancestrally a spiracle was present on the prothorax. Early studies referred to the possible location of T1-S, and the possible incorporation of part of the prothorax into the head (Snod-

grass, 1935; Ander, 1939). Some tracheae seem to imply vestigial location of T1-S, for example the position of T1-AL. T1-AL branches ventrally from H-VCT; however, this pattern doesn't correlate with the morphology of dorsal and ventral branches extending from a spiracle as in T2-S, T3-S, and subsequent abdominal spiracles. Dorsal-ventral connections in the prothorax could be indications of a vestigial T1-S, and positioning of T1-AL posteriorly to this could be an instance of "migration" of this branch seen in other taxa. This would involve several adaptations, however, so this may not be the most parsimonious explanation.

Several taxa also have thoracic ventral commissures T2,3-VC, positioned in various locations anterior-posteriorly. It is often not clear in what segment a given commissure is placed, which leads to annotating them simply as VC1, VC2, AVC, or AVC. Assessments of homology were performed based on the source of the trachea (the spiracle) in question, even though the positioning of the trachea may extend anteriorly or posteriorly outside that segment. Ventral commissures likely serve a variety of functions, ranging from hearing (Orthoptera) to improved locomotion (Blattodea and others). Future studies should focus on airflow in these commissures and would assist in determining their correct placement and homology.

Briefly summarized above, studies of longitudinal airflow through the tracheal system were introduced in the 1960s by Miller (1966) in a range of taxa and Weis-Fogh (1964, 1967) in locusts. Recent micro-CT analyses indicate the presence of valves in Diptera (Wasserthal et al., 2018) and similar structures seen here in Odonata suggest that these pneumatic control structures may be more common than previously thought.

CONCLUSIONS AND FUTURE WORK

Using representatives from 13 orders of apterygotes, Paleoptera, and Polyneoptera, via high-resolution micro-CT scanning we have introduced a unified nomenclature of tracheal morphology based on robust assessments of homology. To facilitate further research, we have also provided

freely available three-dimensional models with labeled tracheal branches of all scanned specimens in open-source file formats.

Throughout the study, more questions were raised than answered regarding the complexity of the insect respiratory system. Ranging from the phylogenetic, where questions of the basal relationships of all insects remain unresolved; to the physiological, where the long-held assumptions of passive diffusion continue to be turned on their collective ears, we hope that this study will provide an effective platform for the continuing research into insect breathing.

ACKNOWLEDGMENTS

We are grateful to Morgan Hill Chase and Andrew Smith of the AMNH Microscopy and Imaging Facility for scanning assistance. We are especially indebted to the Black Rock Forest Consortium (Cornwall, NY) for permission to collect. Special thanks to Lou Sorkin, who provided the leaf mantid and lubber grasshopper specimens, and Megan Wilson, for the *Zootermopsis* specimens. The 3D Slicer development community, especially Andras Lasso, has been invaluable concerning all things Slicer, without which this study would not have been possible. Special thanks also to fellow “Slicers” Murat Maga, Steve Pieper, Jean Christophe Fillion Robin, and Csaba Pinter for their many comments and suggestions over the years. Sajesh Singh of AMNH Scientific Computing was a great help with storage for the digital supplemental information and high-performance computing resources for rendering plates and figures. Thanks also go to Ian Hsieh of Pixar Animation Studios for his assistance with early pre-release access to RenderMan for Blender. We are also grateful to Jake Socha and Michael Engel for their time and suggestions, which improved this manuscript. This work was supported by a AMNH Richard Gilder Graduate School Graduate Fellowship (H.W.H.). Last, but certainly not least, we thank Mary Knight, Managing Editor of AMNH scientific publications. Her support and enthusiasm for this project are greatly appreciated.

REFERENCES

- Alba-Tercedor, J., I. Alba-Alejandre, and F.E. Vega. 2019. Revealing the respiratory system of the coffee berry borer (*Hypothenemus hampei*; Coleoptera: Curculionidae: Scolytinae) using micro-computed tomography. *Scientific Reports* 9 (1): 1–17.
- Alba-Tercedor, J., W.B. Hunter, and I. Alba-Alejandre. 2021. Using micro-computed tomography to reveal the anatomy of adult *Diaphorina citri* Kuwayama (Insecta: Hemiptera, Liviidae) and how it pierces and feeds within a citrus leaf. *Scientific Reports* 11 (1): 1–30.
- Alt, W. 1912a. Über das respirationssystem von *Dytiscus marginalis* L. Ein Beitrag zur Morphologie des Insektenkörpers. *Zeitschrift für Wissenschaftliche Zoologie* 99: 357–413.
- Alt, W. 1912b. Über das respirationssystem der larve von *Lytiscus marginalis* L. *Zeitschrift für Wissenschaftliche Zoologie* 99: 414–443.
- Ander, K. 1939. Vergleichend-anatomische und phylogenetische Studien über die Ensifera (Saltatoria). *Opuscula Entomologica* (supp. 2). Lund: Entomologiska sällskapet.
- Anholt, B.R., J.H. Marden, and D.M. Jenkins. 1991. Patterns of mass gain and sexual dimorphism in adult dragonflies (Insecta: Odonata). *Canadian Journal of Zoology* 69 (5): 1156–1163.
- Barnhart, C.S. 1958. The internal anatomy of the silverfish *Ctenolepisma campbelli* Barnhart and *Lepisma saccharina* Linnaeus (Thysanura: Lepismatidae). Ph.D. dissertation, Department of Zoology and Entomology, Ohio State University, Columbus.
- Barnhart, C.S. 1961. The internal anatomy of the silverfish *Ctenolepisma campbelli* and *Lepisma saccharinum* (Thysanura: Lepismatidae). *Annals of the Entomological Society of America* 54 (2): 177–196.
- Blanke, A., et al. 2012. Revival of Palaeoptera-head characters support a monophyletic origin of Odonata and Ephemeroptera (insecta). *Cladistics* 28 (6): 560–581.
- Blanke, A., et al. 2013. The identification of concerted convergence in insect heads corroborates Palaeoptera. *Systematic Biology* 62 (2): 250–263.
- Blanke, A., M. Koch, B. Wipfler, F. Wilde, and B. Misof. 2014. Head morphology of *Tricholepidion gertschi* indicates monophyletic Zygentoma. *Frontiers in Zoology* 11 (1): 16–16.
- Brannoch, S.K., et al. 2017. Manual of praying mantis morphology, nomenclature, and practices (Insecta, Mantodea). *ZooKeys* (696): 1–100.
- Brower, A.V.Z., and V. Schwaroch. 1996. Three steps of homology assessment. *Cladistics* 12 (3): 265–272.

- Burmester, T., and T. Hankeln. 2007. The respiratory proteins of insects. *Journal of Insect Physiology* 53 (4): 285–294.
- Burrows, M. 1980. The tracheal supply to the central nervous system of the locust. *Proceedings of the Royal Society B, Biological Sciences* 207 (1166): 63–78.
- Carpentier, F. 1927. Sur les trachées de la base des pattes et des ailes de la sauterelle verte (*Phasgonura viridissima*, L.). *Annales de la Société Scientifique de Bruxelles* 47: 63–86.
- Chapman, R.F. 2013. *The insects: structure and function*, 5th ed. Cambridge University Press, Cambridge.
- Chapman, R.N. 1918. The basal connections of the tracheae of the wings of insects. *In The Wings of insects*: 27–51. Ithaca, NY: Cornell University Press.
- Crowson, R.A. 1981. Locomotion, respiration, and energetics. *In Biology of the Coleoptera*: 204–241. London: Academic Press.
- Davies, W.M. 1927. On the tracheal system of Collembola, with special reference to that of *Sminthurus viridis*, Lubb. *Journal of Cell Science* 2 (16): 15–30.
- de Pinna, M.C.C. 1991. Concepts and tests of homology in the cladistic paradigm. *Cladistics* 7: 367–394.
- Dittrich, K., and B. Wipfler. 2021. A review of the hexapod tracheal system with a focus on the apterygote groups. *Arthropod Structure and Development* 63: 101072.
- Dreher, K. 1936. Bau und Entwicklung des Atmungssystems der Honigbiene (*Apis mellifica* L.). *Zeitschrift für Morphologie und Ökologie der Tiere* 31 (4): 608–672.
- Dunn, K.N., et al. 2022. Morphological changes in the tracheal system associated with light organs of the firefly *Photinus pyralis* (Coleoptera: Lampyridae) across life stages. *PLoS One* 17 (6): e0268112.
- Engel, M.S. 2006. A note on the relic silverfish *Tricholepidion gertschi* (Zygentoma). *Transactions of the Kansas Academy of Science* 109 (3/4): 236–238.
- Fedorov, A., et al. 2012. 3D Slicer as an image computing platform for the quantitative imaging network. *Magnetic Resonance Imaging* 30 (9): 1323–1341.
- Field, L.H., and T. Matheson. 1998. Chordotonal organs of insects. *Advances in Insect Physiology* 27: 1–56, C51–C52, 57–228.
- Flannery, B.P., H.W. Deckman, W.G. Roberge, and K.L. D'Amico. 1987. Three-dimensional X-ray microtomography. *Science* 237: 1439–1444.
- Fonseca, P.J., and A.V. Popov. 1994. Sound radiation in a cicada: the role of different structures. *Journal of Comparative Physiology A* 175 (3): 349–361.
- Franz-Guess, S., and J.M. Starck. 2016. Histological and ultrastructural analysis of the respiratory tracheae of *Galeodes granti* (Chelicerata: Solifugae). *Arthropod Structure and Development* 45 (5): 452–461.
- Franz-Guess, S., B.J. Klußmann-Fricke, C.S. Wirkner, L. Prendini, and J.M. Starck. 2016. Morphology of the tracheal system of camel spiders (Chelicerata: Solifugae) based on micro-CT and 3D-reconstruction in exemplar species from three families. *Arthropod Structure and Development* 45 (5): 440–451.
- Friedrich, F., and R.G. Beutel. 2008. Micro-computer tomography and a renaissance of insect morphology. *Proceedings of SPIE* 7078, *Developments in X-ray tomography VI*: 545–550.
- Fujita, M., and R. Machida. 2017. Embryonic development of *Eucorydia yasumatsui* Asahina, with special reference to external morphology (Insecta: Blattodea, Corydiidae). *Journal of Morphology* 278 (11): 1469–1489.
- Full, R.J., and M.S. Tu. 1991. Mechanics of a rapid running insect: two-, four- and six-legged locomotion. *Journal of Experimental Biology* 156: 215–231.
- Fuller, C. 1919. The wing venation and respiratory system of certain south African termites. *Annals of the Natal Museum* 4: 19–102.
- Gignac, P.M., et al. 2016. Diffusible iodine-based contrast-enhanced computed tomography (diceCT): an emerging tool for rapid, high-resolution, 3-d imaging of metazoan soft tissues. *Journal of Anatomy* 228 (6): 889–909.
- Giribet, G., and G.D. Edgecombe. 2019. The phylogeny and evolutionary history of arthropods. *Current Biology* 29 (12): R592–R602.
- Gonzalez, V.H., G.T. Gustafson, and M.S. Engel. 2019. Morphological phylogeny of Megachilini and the evolution of leaf-cutter behavior in bees (Hymenoptera: Megachilidae). *Journal of Melittology* (85): 1–123.
- Gopfert, M.C., and R.M. Hennig. 2016. Hearing in insects. *Annual Review of Entomology* 61: 257–276.
- Grassi, B. 1885. *Morfologia delle scolopendrelle*. Turin: Ermanno Loescher.
- Greco, M., A. Jones, R. Spooner-Hart, and P. Holford. 2008. X-ray computerised microtomography (microct): a new technique for assessing external and internal morphology of bees. *Journal of Apicultural Research* 47 (4): 286–291.
- Greco, M., et al. 2014. 3-D visualisation, printing, and volume determination of the tracheal respiratory system in the adult desert locust, *Schistocerca gregaria*. *Entomologia Experimentalis et Applicata* 152 (1): 42–51.

- Greenlee, K.J., et al. 2013. Hypoxia-induced compression in the tracheal system of the tobacco hornworm caterpillar, *Manduca sexta*. *Journal of Experimental Biology* 216 (12): 2293–2301.
- Grimaldi, D.A. 2010. 400 million years on six legs: on the origin and early evolution of Hexapoda. *Arthropod Structure and Development* 39 (2-3): 191–203.
- Grimaldi, D.A., and M.S. Engel. 2005. *Evolution of the insects*. Cambridge: Cambridge University Press.
- Haas, F. 2018. Biodiversity of Dermaptera. In R.G. Footit and P.H. Adler (editors), *Insect biodiversity: science and society*: 315–334. Hoboken, NJ: John Wiley & Sons Ltd.
- Harrison, J.F., et al. 2013. How locusts breathe. *Physiology* 28 (1): 18–27.
- Harrison, J.F., et al. 2018. Developmental plasticity and stability in the tracheal networks supplying *Drosophila* flight muscle in response to rearing oxygen level. *Journal of Insect Physiology* 106 (September 2017): 189–198.
- Harrison, J.F., et al. 2020. Physiological responses to gravity in an insect. *Proceedings of the National Academy of Sciences of the United States of America* 117 (4): 2180–2186.
- Harvey, P.H., and M.D. Pagel. 1991. *The comparative method in evolutionary biology*. Oxford: Oxford University Press.
- Heinrich, B. 1976. Heat exchange in relation to blood flow between thorax and abdomen in bumblebees. *The Journal of Experimental Biology* 64 (3): 561–585.
- Heinrich, E.C., M.J. McHenry, and T.J. Bradley. 2013. Coordinated ventilation and spiracle activity produce unidirectional airflow in the hissing cockroach, *Gromphadorhina portentosa*. *Journal of Experimental Biology* 216 (23): 4473–4482.
- Herhold, H.W., S.R. Davis, C.S. Smith, M.S. Engel, and D.A. Grimaldi. 2019. Unique metasomal musculature in sweat bees (Hymenoptera: Apoidea: Halictidae) revealed by micro-CT scanning. *American Museum Novitates* 3920: 1–28.
- Herhold, H.W., S.R. Davis, and D.A. Grimaldi. 2020. Transcriptomes reveal expression of hemoglobins throughout insects and other Hexapoda. *PLoS One* 15 (6): e0234272–e0234272.
- Hilken, G., et al. 2021. The tracheal system of scutigromorph centipedes and the evolution of respiratory systems of myriapods. *Arthropod Structure and Development* 60: 101006.
- Hochgraf, J.S., J.S. Waters, and J.J. Socha. 2018. Patterns of tracheal compression in the thorax of the ground beetle, *Platynus decentis*. *Yale Journal of Biology and Medicine* 91: 409–430.
- Hoy, R.R., and D. Robert. 1996. Tympanal hearing in insects. *Annual Review of Entomology* 41: 433–450.
- Hoy, R., and J. Yack. 2009. Hearing. In Resh, V.H., and R.T. Cardé (editors), *Encyclopedia of insects*: 440–446. London: Academic Press.
- Inder, I.M., and F.D. Duncan. 2015. Gas exchange pattern transitions in the workers of the harvester termite. *Journal of Insect Physiology* 75: 47–53.
- Iwan, D., M.J. Kamiński, and M. Raś. 2015. The last breath: a μ CT-based method for investigating the tracheal system in hexapoda. *Arthropod Structure and Development* 44: 218–227.
- Kaiser, A., et al. 2007. Increase in tracheal investment with beetle size supports hypothesis of oxygen limitation on insect gigantism. *Proceedings of the National Academy of Sciences of the United States of America* 104 (32): 13198–13203.
- Keilin, D. 1944. Respiratory systems and respiratory adaptations in larvae and pupae of Diptera. *Parasitology* 36 (1&2): 1–66.
- Kennedy, C.H. 1922. The homologies of the tracheal branches in the respiratory system of insects. *Ohio Journal of Science* 22 (3): 84–90.
- Kerry, C.J., and P.J. Mill. 1997. An anatomical study of the abdominal muscular, nervous and respiratory systems of the praying mantid, *Hierodula membranacea* (Burmeister). *Proceedings of the Royal Society of London B, Biological Sciences* 229 (1257): 415–438.
- Kjer, K.M., C. Simon, M. Yavorskaya, and R.G. Beutel. 2016. Progress, pitfalls and parallel universes: a history of insect phylogenetics. *Journal of the Royal Society Interface* 13 (121).
- Klass, K.-D., O. Zompro, N.P. Kristensen, and J. Adis. 2002. Mantophasmatodea: a new insect order with extant members in the afrotropics. *Science* 296: 1456–1459.
- Klowden, M.J. 2013. *Physiological systems in insects*, 3rd ed. London: Academic Press.
- Koenemann, S., R.A. Jenner, M. Hoenemann, T. Stemme, and B.M. von Reumont. 2010. Arthropod phylogeny revisited, with a focus on crustacean relationships. *Arthropod Structure and Development* 39 (2-3): 88–110.
- Kondo, T., P.J. Gullan, and D.J. Williams. 2008. Coccidology. The study of scale insects (Hemiptera: Sternorrhyncha: Coccoidea). *Revista Corpoica* 9 (2): 55–61.
- Lacombe, D. 1958. Contribuição ao estudo dos Embiidae. III. Aparelho respiratório de *Embolynta batesi*

- Mac Lachlan, 1877 (Embiidina). *Studia Entomologica* 1 (1): 177–195.
- Lacombe, D. 1971. Anatomy and histology of *Embolynta batesi* MacLachlan, 1877 (Embiidina). *Memórias do Instituto Oswaldo Cruz* 69 (3): 331–396.
- Landa, V. 1948. Contributions to the anatomy of ephemeropterid larvae. I. Topography and anatomy of tracheal system. *Vestník Československé zoologické společnosti* 12: 25–82.
- Landa, V. 1969. Comparative anatomy of mayfly larvae (Ephemeroptera). *Acta Entomologica Bohemoslovaca* 66: 289–316.
- Lee, M.O. 1929. Respiration in the insects. *Quarterly Review of Biology* 4 (2): 213–232.
- Lehmann, F.E. 1925. Zur Kenntnis der Anatomie und Entwicklungsgeschichte von *Carausius morosus* Br. Ph.D. thesis, Universität Zürich. Jena: Gustav Fischer.
- Lehmann, P., M. Javal, A.D. Plessis, and J.S. Terblanche. 2021. Using microCT in live larvae of a large wood-boring beetle to study tracheal oxygen supply during development. *Journal of Insect Physiology* 130: 104199.
- Lighton, J.R.B. 1996. Discontinuous gas exchange in insects. *Annual Review of Entomology* 41: 309–324.
- Longley, A., and J.S. Edwards. 1979. Tracheation of abdominal ganglia and cerci in the house cricket *Acheta domestica* (Orthoptera, Gryllidae). *Journal of Morphology* 159 (2): 233–243.
- Lösel, P.D., et al. 2020. Introducing Biomedisa as an open-source online platform for biomedical image segmentation. *Nature Communications* 11 (5577): 1–14.
- Malpighi, M. 1669. *Dissertatio epistolica de bombyce*. London: Joannem Martyn & Jacobum Allestry.
- Marden, J.H. 1989. Bodybuilding dragonflies: costs and benefits of maximizing flight muscle. *Physiological Zoology* 62 (2): 505–521.
- Marden, J.H. 2000. Variability in the size, composition, and function of insect flight muscles. *Annual Review of Physiology* 62: 157–178.
- Miller, A.H., J.T. Stroud, and J.B. Losos. 2022. The ecology and evolution of key innovations. *Trends in Ecology & Evolution* [<https://doi.org/10.1016/j.tree.2022.09.005>].
- Miller, P.L. 1960a. Respiration in the desert locust: I. The control of ventilation. *Journal of Experimental Biology* 37 (2): 224–236.
- Miller, P.L. 1960b. Respiration in the desert locust: II. The control of the spiracles. *Journal of Experimental Biology* 37 (2): 237–263.
- Miller, P.L. 1960c. Respiration in the desert locust: III. Ventilation and the spiracles during flight. *Journal of Experimental Biology* 37 (2): 264–278.
- Miller, P.L. 1966. The regulation of breathing in insects. *In Advances in Insect Physiology* 3: 279–354.
- Misof, B., et al. 2014. Phylogenomics resolves the timing and pattern of insect evolution. *Science* 346: 763–767.
- Mokso, R., et al. 2015. Four-dimensional in vivo x-ray microscopy with projection-guided gating. *Scientific Reports* 5: 8727.
- Mulder-Rosi, J., G.I. Cummins, and J.P. Miller. 2010. The cricket cercal system implements delay-line processing. *Journal of Neurophysiology* 103 (4): 1823–1832.
- Müller, G.H. 1985. The development of thought on the respiration of insects. *History and Philosophy of the Life Sciences* 7 (2): 301–314.
- Needham, J.G., Y.-C. Hsu, and J.R. Traver. 1935. *The biology of mayflies, with a systematic account of North American species*. Ithaca, NY: Comstock Publishing.
- Nelson, C.H., and J.F. Hanson. 1968. The external anatomy of *Pteronarcys (Allonarcys) proteus* Newman and *Pteronarcys (Allonarcys) biloba* Newman (Plecoptera: Pteronarcidae). *Transactions of the American Entomological Society* 94 (4): 429–472.
- Nelson, M.C. 1979. Sound production in the cockroach, *Gromphadorhina portentosa*: the sound-producing apparatus. *Journal of Comparative Physiology A* 132 (1): 27–38.
- Nelson, M.C., and J. Fraser. 1980. Sound production in the cockroach, *Gromphadorhina portentosa*: evidence for communication by hissing. *Behavioral Ecology and Sociobiology* 6 (4): 305–314.
- Neubert, D., S. Simon, R.G. Beutel, and B. Wipfler. 2017. The head of the earwig *Forficula auricularia* (Dermaptera) and its evolutionary implications. *Arthropod Systematics and Phylogeny* 75 (1): 99–124.
- Newport, G. 1836. XXIV. On the respiration of insects. *Philosophical Transactions of the Royal Society of London* 126: 529–566.
- Nikam, T.B., and V.V. Khole. 1989. *Insect spiracular systems*. Chichester, England: Ellis Horwood Limited.
- Palmén, J.A. 1877. *Zur Morphologie des Tracheensystems*. Leipzig: Wilhelm Engelmann.
- Pendar, H., M.C. Kenny, and J.J. Socha. 2015. Tracheal compression in pupae of the beetle *Zophobas morio*. *Biology Letters* 11 (6): 20150259.

- Pendar, H., J. Aviles, K. Adjerid, C. Schoenewald, and J.J. Socha. 2019. Functional compartmentalization in the hemocoel of insects. *Scientific Reports* 9 (1): 6075.
- Preibisch, S., S. Saalfeld, and P. Tomancak. 2009. Globally optimal stitching of tiled 3D microscopic image acquisitions. *Bioinformatics* 25 (11): 1463–1465.
- Raś, M., D. Iwan, and M.J. Kamiński. 2018. The tracheal system in post-embryonic development of holometabolous insects: a case study using the mealworm beetle. *Journal of Anatomy* 232 (6): 997–1015.
- Remane, A. 1952. *Die Grundlagen des natürlichen Systems, der vergleichenden Anatomie und der Phylogenetik*. Leipzig: Geest & Portig.
- Richard, D., M.E. Colin, and M. Lhomme. 1990. Anatomical organization of the tracheal system of *Varroa jacobsoni* (Acari: Varroidae). *Experimental and Applied Acarology* 9 (1-2): 63–72.
- Robertson, C.H. 1962. The anatomy of the respiratory system of the passalus beetle, *Popilius disjunctus* (Illiger). *American Midland Naturalist* 68 (2): 376–393.
- Rössler, W. 1992. Functional morphology and development of tibial organs in the legs i, ii and iii of the bushcricket *Ephippiger ephippiger* (Insecta, Ensifera). *Zoomorphology* 112 (3): 181–188.
- Ruan, Y., et al. 2018. Visualisation of insect tracheal systems by lactic acid immersion. *Journal of Microscopy* 271 (2): 230–236.
- Schindelin, J., et al. 2012. FIJI: an open-source platform for biological-image analysis. *Nature Methods* 9 (7): 676–676.
- Schmidt, C., and J.W. Wägele. 2001. Morphology and evolution of respiratory structures in the pleopod exopodites of terrestrial Isopoda (Crustacea, Isopoda, Oniscidea). *Acta Zoologica* 82 (4): 315–330.
- Schmitz, A., and S.F. Perry. 1999. Stereological determination of tracheal volume and diffusing capacity of the tracheal walls in the stick insect *Carausius morosus* (Phasmatodea, Lonchodidae). *Physiological and Biochemical Zoology* 72 (2): 205–218.
- Schoville, S.D., R.A. Slatyer, J.C. Bergdahl, and G.A. Valdez. 2015. Conserved and narrow temperature limits in alpine insects: thermal tolerance and supercooling points of the ice-crawlers, *Grylloblatta* (Insecta: Grylloblattodea: Grylloblattidae). *Journal of Insect Physiology* 78: 55–61.
- Scott, G.G. 1905. The distribution of tracheae in the nymph of *Plathemis lydia*. *Biological Bulletin* 9 (6): 341–354.
- Shaha, R.K., J.R. Vogt, C.S. Han, and M.E. Dillon. 2013. A micro-CT approach for determination of insect respiratory volume. *Arthropod Structure and Development* 42 (5): 437–442.
- Shaw, S. 1994. Detection of airborne sound by a cockroach ‘vibration detector’: a possible missing link in insect auditory evolution. *Journal of Experimental Biology* 193 (1): 13–47.
- Shelomi, M., I.R. Sitepu, K.L. Boundy-Mills, and L.S. Kimsey. 2015. Review of the gross anatomy and microbiology of the Phasmatodea digestive tract. *Journal of Orthoptera Research* 24 (1): 29–40.
- Simon, S., A. Blanke, and K. Meusemann. 2018. Reanalyzing the Palaeoptera problem – the origin of insect flight remains obscure. *Arthropod Structure & Development* 47 (4): 328–338.
- Smith, A. 2022. Cockroaches can jump & fly?! In slow mo, it’s awesome. Online resource (<https://www.youtube.com/watch?v=bnPWU-mqGL8>), accessed 21 March 2022.
- Snodgrass, R.E. 1935. *Principles of insect morphology*. Ithaca, NY: Cornell University Press.
- Snodgrass, R.E. 1936. *Anatomy of the honey bee*. Ithaca, NY: Comstock Publishing Associates.
- Socha, J.J., and F. De Carlo. 2008. Use of synchrotron tomography to image naturalistic anatomy in insects. *Proceedings of SPIE 7078, Developments in X-Ray Tomography VI*: 70780A.
- Socha, J.J., et al. 2008. Correlated patterns of tracheal compression and convective gas exchange in a carabid beetle. *Journal of Experimental Biology* 211 (21): 3409–3420.
- Socha, J.J., T.D. Förster, and K.J. Greenlee. 2010. Issues of convection in insect respiration: insights from synchrotron X-ray imaging and beyond. *Respiratory Physiology and Neurobiology* 173 (suppl.): S65–S73.
- Soldán, T. 1979. Internal anatomy of *Dolania americana* (Ephemeroptera: Behningiidae). *Annals of the Entomological Society of America* 72: 636–641.
- Song, N., H. Li, F. Song, and W. Cai. 2016. Molecular phylogeny of Polyneoptera (Insecta) inferred from expanded mitogenomic data. *Scientific Reports* 6: 36175.
- Steiner, L.F. 1929. Homologies of tracheal branches in the nymph of *Anax junius* based on their correlation with the muscles they supply. *Annals of the Entomological Society of America* 22 (2): 297–309.
- Stewart, K.W. 2001. Vibrational communication (drumming) and mate-searching behavior of stoneflies (Plecoptera); evolutionary considerations. In Dominguez, E. (editor) *Trends in Research in Ephemeroptera and Plecoptera*: 217–215. New York: Kluwer/Academic Plenum.

- Strauss, J. 2021. The tracheal system in the stick insect prothorax and prothoracic legs: homologies to Orthoptera and relations to mechanosensory functions. *Arthropod Structure & Development* 63: 101074.
- Šulc, K. 1912. Über respiraion, tracheensystem und schaumproduktion der schaumcikadenlarven (Aphrophorinae-Homoptera). *Zeitschrift für Wissenschaftliche Zoologie* 99: 147–188.
- Šulc, K. 1927. Vzdusnicova soustava lepismy (Thysanura) a puvid kridlateho hmyzu. *Acta Societatis Scientiarum Naturalium Moraviae* 4 (7): 1–108.
- Swammerdam, J. 1737. *Bybel der natuure*. Leyden: Isaak Severinus, Boudewyn van der Aa, Pieter van der Aa.
- Szumik, C., M.L. Juárez, M.J. Ramirez, P. Goloboff, and V.V. Pereyra. 2019. Implications of the tympanal hearing organ and ultrastructure of chaetotaxy for the higher classification of Embioptera. *American Museum Novitates* 3933: 1–32.
- Thomas, J.A., J.W. Trueman, A. Rambaut, and J.J. Welch. 2013. Relaxed phylogenetics and the Palaeoptera problem: resolving deep ancestral splits in the insect phylogeny. *Systematic Biology* 62 (2): 285–297.
- Tilgner, E.H., T.G. Kiselyova, and J.V. McHugh. 2008. A morphological study of *Timema cristinae* Vickery with implications for the phylogenetics of Phasmida. *Deutsche Entomologische Zeitschrift* 46 (2): 149–162.
- Tillyard, R.J. 1914. On some problems regarding the development of the wing-venation of Odonata. *Proceedings of the Linnean Society of New South Wales* 39: 163–216.
- Tillyard, R.J. 1917. *The biology of dragonflies (Odonata or Paraneuroptera)*. London: Cambridge University Press.
- Tonapi, G.T. 1977. Some adaptive features in the respiratory system of *Dineutes indicus* Aubé (Coleoptera, Gyrinidae). *Zoologica Scripta* 6 (2): 107–112.
- Tsai, Y.L., et al. 2014. Firefly light flashing: oxygen supply mechanism. *Physical Review Letters* 113 (25): 1–5.
- Vats, L.K. 1972. Tracheal system in the larvae of the Bruchidae (Coleoptera: Bruchidae). *Journal of the New York Entomological Society* 80: 12–17.
- Vinal, S.C. 1919. The respiratory system of the Carolina locust (*Dissostertia carolina* Linne). *Journal of the New York Entomological Society* 27 (1): 19–32.
- Walker, S.M., et al. 2014. In vivo time-resolved microtomography reveals the mechanics of the blowfly flight motor. *PLOS Biology* 12 (3): e1001823.
- Wasserthal, L.T. 1996. Interaction of circulation and tracheal ventilation in holometabolous insects. *In Advances in Insect Physiology* 26: 297–351.
- Wasserthal, L.T. 2015. Flight-motor-driven respiratory airflow increases tracheal oxygen to nearly atmospheric level in blowflies (*Calliphora vicina*). *Journal of Experimental Biology* 218 (14): 2201–2210.
- Wasserthal, L.T., and A.S. Frohlich. 2017. Structure of the thoracic spiracular valves and their contribution to unidirectional gas exchange in flying blowflies *Calliphora vicina*. *Journal of Experimental Biology* 220 (2): 208–219.
- Wasserthal, L.T., P. Cloetens, R.H. Fink, and L.K. Wasserthal. 2018. X-ray computed tomography study of the flight-adapted tracheal system in the blowfly *Calliphora vicina*, analysing the ventilation mechanism and flow-directing valves. *Journal of Experimental Biology* 221: 1–12.
- Waters, J.S., W.K. Lee, M.W. Westneat, and J.J. Socha. 2013. Dynamics of tracheal compression in the horned *Passalus* beetle. *American Journal of Physiology – Regulatory Integrative and Comparative Physiology* 304 (8): 621–627.
- Weber, H. 1933. Die atmungsorgane. *In Lehrbuch der Entomologie*: 421–461. Jena: Gustav Fischer.
- Weis-Fogh, T. 1956a. Biology and physics of locust flight. ii. Flight performance of the desert locust (*Schistocerca gregaria*). *Philosophical Transactions of the Royal Society of London B – Biological Sciences* 239 (667): 459–510.
- Weis-Fogh, T. 1956b. Biology and physics of locust flight. IV. Notes on sensory mechanisms in locust flight. *Philosophical Transactions of the Royal Society of London B – Biological Sciences* 239 (667): 553–584.
- Weis-Fogh, T. 1964. Functional design of the tracheal system of flying insects as compared with the avian lung. *Journal of Experimental Biology* 41 (2): 207–227.
- Weis-Fogh, T. 1967. Respiration and tracheal ventilation in locusts and other flying insects. *Journal of Experimental Biology* 47: 561–587.
- Weis-Fogh, T., and M. Jensen. 1956. Biology and physics of locust flight. I. Basic principles in insect flight. A critical review. *Philosophical Transactions of the Royal Society of London B – Biological Sciences* 239 (667): 415–458.
- Weiss, H.B. 1929. The entomology of aristotle. *Journal of the New York Entomological Society* 37 (2): 101–109.
- Westneat, M.W., et al. 2003. Tracheal respiration in insects visualized with synchrotron X-ray imaging. *Science* 299: 558–560.

- Whitten, J.M. 1955. A comparative morphological study of the tracheal system in larval diptera. Part I. Quarterly Journal of Microscopical Science 96: 257–278.
- Whitten, J.M. 1956. The tracheal system of the larva of *Lonchoptera lutea* Panzer (Diptera. Lonchopteridae). Proceedings of the Royal Entomological Society of London. Series A, General Entomology 31: 105–108.
- Whitten, J.M. 1957. The post-embryonic development of the tracheal system in *Drosophila melanogaster*. Quarterly Journal of Microscopical Science 98: 123–150.
- Whitten, J.M. 1959. The tracheal system as a systematic character in larval diptera. Systematic Zoology 8 (3): 130–139.
- Whitten, J.M. 1960. The tracheal pattern in selected Diptera Nematocera. Journal of Morphology 1–7 (3): 233–257.
- Whitten, J.M. 1962. Homology and development of insect wing tracheae. Annals of the Entomological Society of America 55 (3): 288–295.
- Whitten, J.M. 1972. Comparative anatomy of the tracheal system. Annual Review of Entomology 17 (1): 373–402.
- Wigglesworth, V.B. 1963. Entomology – a further function of air sacs in some insects. Nature 198 (487): 106.
- Wigglesworth, V.B. 1972. The principles of insect physiology, 7th ed. London: Chapman and Hall, Ltd..
- Wipfler, B., R. Machida, B. Müller, and R.G. Beutel. 2011. On the head morphology of Grylloblattodea (Insecta) and the systematic position of the order, with a new nomenclature for the head muscles of Dicondylia. Systematic Entomology 36 (2): 241–266.
- Wipfler, B., F. Wieland, F. DeCarlo, and T. Hornschemeyer. 2012. Cephalic morphology of *Hymenopus coronatus* (Insecta: Mantodea) and its phylogenetic implications. Arthropod Structure & Development 41 (1): 87–100.
- Wipfler, B., et al. 2015. The thorax of Mantophasmatoidea, the morphology of flightlessness, and the evolution of the neopteran insects. Cladistics 31: 50–70.
- Wipfler, B., et al. 2019. Evolutionary history of Polyneoptera and its implications for our understanding of early winged insects. Proceedings of the National Academy of Sciences of the United States of America 116 (8): 3024–3029.
- Wipfler, B., et al. 2020. Phylogenomics changes our understanding about earwig evolution. Systematic Entomology 45 (3): 516–526.
- Yager, D.D. 1999. Structure, development, and evolution of insect auditory systems. Microscopy Research and Technique 47 (6): 380–400.
- Yager, D.D. 2005. Cockroach homologs of praying mantis peripheral auditory system components. Journal of Morphology 265 (1): 120–139.
- Yager, D.D., and R.R. Hoy. 1986. The cyclopean ear: a new sense for the praying mantis. Science 231 (4739): 727–729.
- Yager, D.D., and R.R. Hoy. 1987. The midline metathoracic ear of the praying mantis, *Mantis religiosa*. Cell and Tissue Research 250 (3): 531–541.
- Yoder, J.A., J.B. Benoit, B.Z. Hedges, A.J. Jajack, and L.W. Zettler. 2012. Madagascar hissing cockroach mite, *Gromphadorholaelaps schaeferi*, prevents fungal infection in its cockroach host: evidence for a mutualistic symbiosis. International Journal of Acarology 38 (5): 427–435.
- Zukić, D., et al. 2016. ND morphological contour interpolation. Insight Journal (8). [<https://doi.org/10.54294/achtrg>]

LIST OF PLATES

Plate 1. *Trigoniophthalmus alternatus* (Archaeognatha: Machilidae) lateral view.

Plate 2. *Trigoniophthalmus alternatus* (Archaeognatha: Machilidae) dorsal view.

Plate 3. *Trigoniophthalmus alternatus* (Archaeognatha: Machilidae) ventral view.

Plate 4. *Tricholepidion gertschi* (Zygentoma: Machilidae) lateral view.

Plate 5. *Tricholepidion gertschi* (Zygentoma: Machilidae) dorsal (left) and ventral (right) view.

Plate 6. *Thermobia domestica* (Zygentoma: Lepismatidae) lateral view.

Plate 7. *Thermobia domestica* (Zygentoma: Lepismatidae) dorsal (left) and ventral (right) view.

Plate 8. *Lepisma saccharinum* (Zygentoma: Lepismatidae) lateral view.

Plate 9. *Lepisma saccharinum* (Zygentoma: Lepismatidae) dorsal view.

Plate 10. *Lepisma saccharinum* (Zygentoma: Lepismatidae) ventral view.

Plate 11. *Ephemera* sp. (Ephemeroptera: Ephemeridae) lateral view.

Plate 12. *Ephemera* sp. (Ephemeroptera: Ephemeridae) dorsal view.

Plate 13. *Ephemera* sp. (Ephemeroptera: Ephemeridae) ventral view.

Plate 14. *Neocloeon triangulifer* (Ephemeroptera: Baetidae) subimago lateral view.

Plate 15. *Neocloeon triangulifer* (Ephemeroptera: Baetidae) subimago dorsal (left) and ventral (right) views.

Plate 16. *Neocloeon triangulifer* (Ephemeroptera: Baetidae) adult lateral view.

Plate 17. *Neocloeon triangulifer* (Ephemeroptera: Baetidae) adult dorsal (left) and ventral (right) views.

Plate 18. Dragonfly (Aeshnidae: Odonata) lateral view.

Plate 19. Dragonfly (Aeshnidae: Odonata) dorsal view.

Plate 20. Dragonfly (Aeshnidae: Odonata) ventral view.

Plate 21. Damselfly (Calopterygidae: Odonata) lateral view.

Plate 22. Damselfly (Calopterygidae: Odonata) dorsal view.

Plate 23. Damselfly (Calopterygidae: Odonata) ventral view.

Plate 24. *Anisolabis maritima* (Dermaptera: Anisolabidae) lateral view.

Plate 25. *Anisolabis maritima* (Dermaptera: Anisolabidae) dorsal (left) and ventral (right) view.

Plate 26. *Forficula auriculara* (Dermaptera: Forficulidae) lateral view.

Plate 27. *Forficula auriculara* (Dermaptera: Forficulidae) dorsal view.

Plate 28. *Forficula auriculara* (Dermaptera: Forficulidae) ventral view.

Plate 29. Stonefly (Plecoptera: Perlodidae) lateral view.

Plate 30. Stonefly (Plecoptera: Perlodidae) dorsal view.

Plate 31. Stonefly (Plecoptera: Perlodidae) ventral view.

Plate 32. Stonefly (Plecoptera: Nemouridae) lateral view.

Plate 33. Stonefly (Plecoptera: Nemouridae) dorsal view.

Plate 34. Stonefly (Plecoptera: Nemouridae) ventral view.

Plate 35. *Gryllus* sp. (Orthoptera: Gryllidae) lateral view.

Plate 36. *Gryllus* sp. (Orthoptera: Gryllidae) dorsal view.

Plate 37. *Gryllus* sp. (Orthoptera: Gryllidae) ventral view.

Plate 38. *Romalea microptera* (Orthoptera: Romaleidae) lateral view.

Plate 39. *Romalea microptera* (Orthoptera: Romaleidae) dorsal view.

Plate 40. *Romalea microptera* (Orthoptera: Romaleidae) ventral view.

Plate 41. *Tachycines asynamoros* (Orthoptera: Rhaphidophoridae) lateral view.

Plate 42. *Tachycines asynamorous* (Orthoptera: Rhaphidophoridae) dorsal (left) and ventral (right) view.

Plate 43. *Meconema thalassinum* (Orthoptera: Tettigoniidae) lateral view.

Plate 44. *Meconema thalassinum* (Orthoptera: Tettigoniidae) dorsal (left) and ventral (right) views.

Plate 45. *Grylloblatta* sp. (Grylloblattodea: Grylloblattidae) lateral view.

Plate 46. *Grylloblatta* sp. (Grylloblattodea: Grylloblattidae) dorsal (left) and ventral (right) views.

Plate 47. *Oligotoma negra* (Embioptera: Oligotomidae) lateral view.

Plate 48. *Oligotoma negra* (Embioptera: Oligotomidae) dorsal (left) and lateral (right) views.

Plate 49. *Timema* cf. *californicum* (Phasmatodea: Timematidae) lateral view.

Plate 50. *Timema* cf. *californicum* (Phasmatodea: Timematidae) dorsal view.

Plate 51. *Timema* cf. *californicum* (Phasmatodea: Timematidae) ventral view.

Plate 52. *Extatosoma tiaratum* (Phasmatodea: Phasmatidae) lateral view.

Plate 53. *Extatosoma tiaratum* (Phasmatodea: Phasmatidae) dorsal view.

Plate 54. *Extatosoma tiaratum* (Phasmatodea: Phasmatidae) ventral view.

Plate 55. *Medauroidea extradentata* (Phasmatodea: Phasmatidae) lateral view.

Plate 56. *Medauroidea extradentata* (Phasmatodea: Phasmatidae) dorsal view.

Plate 57. *Medauroidea extradentata* (Phasmatodea: Phasmatidae) ventral view.

Plate 58. *Tenodera sinensis* (Mantodea: Mantidae) lateral view.

Plate 59. *Tenodera sinensis* (Mantodea: Mantidae) dorsal view.

Plate 60. *Tenodera sinensis* (Mantodea: Mantidae) ventral view.

Plate 61. *Idolomantis diabolica* (Mantodea: Empusidae) lateral view.

Plate 62. *Idolomantis diabolica* (Mantodea: Empusidae) dorsal view.

Plate 63. *Idolomantis diabolica* (Mantodea: Empusidae) ventral view.

Plate 64. *Periplaneta americana* (Blattodea: Blattellidae) lateral view.

Plate 65. *Periplaneta americana* (Blattodea: Blattellidae) dorsal view.

Plate 66. *Periplaneta americana* (Blattodea: Blattellidae) ventral view.

Plate 67. *Blaptica dubia* (Blattodea: Blaberidae) lateral view.

Plate 68. *Blaptica dubia* (Blattodea: Blaberidae) dorsal view.

Plate 69. *Blaptica dubia* (Blattodea: Blaberidae) ventral view.

Plate 70. *Gromphadorhina portentosa* (Blattodea: Blaberidae) lateral view.

Plate 71. *Gromphadorhina portentosa* (Blattodea: Blaberidae) dorsal view.

Plate 72. *Gromphadorhina portentosa* (Blattodea: Blaberidae) ventral view.

Plate 73. *Zootermopsis angusticollis* (Isoptera: Archotermopsidae) lateral view.

Plate 74. *Zootermopsis angusticollis* (Isoptera: Archotermopsidae) dorsal view.

Plate 75. *Zootermopsis angusticollis* (Isoptera: Archotermopsidae) ventral view.

Plate 76. *Reticulitermes flavipes* (Isoptera: Rhinotermitidae) lateral view.

Plate 77. *Reticulitermes flavipes* (Isoptera: Rhinotermitidae) dorsal view.

Plate 78. *Reticulitermes flavipes* (Isoptera: Rhinotermitidae) ventral view.